1969

THE FORMATION AND REACTIVITY OF SOME NITRIDES

JAYAWAERA, SHANATH ANARASIRI ARUABADA

http://hdl.handle.net/10026.1/2128

http://dx.doi.org/10.24382/3777
University of Plymouth

THE FORMATION AND REACTIVITY OF BORON NITRIDES

A Thesis Presented for the Degree of

Doctor of Philosophy

of the

University of London

by

Shanath Amarasiri Arunabadu Jayaweera

Department of Chemistry,
College of Technology,
Plymouth.

September, 1969.

ABSTRACT

Nitrides are reviewed generally with respect to their bonding, production (including thermodynamics and kinetics of formation) and reactivity. This is followed by a summary of the studies by previous workers on the formation and reactivity of the particular nitrides, which are the subject of the present investigation.

This thesis embodies further studies on various aspects of the formation and reactivity of nitrides of some Group II - IV elements. They include nitrides of more active metals such as calcium and magnesium, and of less active ones such as titanium and zirconium. The former may be considered to be intermediate products in the indirect corrosion of metals; the latter are important as refractories and hard materials.

Films of metallic calcium, magnesium, zinc and cadmium have been prepared by vapour deposition and their nitridation investigated on the electron microscope. The electron diffraction patterns of the films are correlated with their microcrystalline uniformity.

The hydrolyses of calcium and magnesium nitrides under various conditions are studied by X-ray powder diffraction, electron microscopy and gas sorption measurements. The changes in crystallite size and shape of the resulting hydroxides are followed, and comparisons made with the hydroxides produced by other methods. The reactivity of nitrides towards water (vapour and liquid) at different temperatures are correlated with the changes in crystal structure and particle size.

The calcination of calcium, magnesium, boron, titanium and zirconium nitrides is investigated by methods similar to the above. The reaction between lime and urea, which are intermediate products in the hydrolysis of the analogous calcium cyanamide, is studied also. The solubilities of zinc and cadmium oxides in ammonium hydroxide have been determined.

The results are discussed in the light of the general principles summarised earlier, and also in relation to the investigations of earlier workers.

ACKNOWLEDGEMENTS

The author wishes to express his very sincere thanks to Dr. D.R. Glasson for his helpful advice and guidance during the course of this work.

He is grateful to Dr. A.B. Meggy for allowing time and facilities for these studies to be carried out. His thanks are also due to Margaret Sheppard for her technical assistance.

CONTENTS

Chapter 1

LITERATURE SURVEY AND REVIEW

Nitrides are compounds formed between nitrogen and other elements, but the term is more commonly applied to the compounds of nitrogen with more electropositive elements.

The importance of nitrides is two-fold. First, the nitridation of metals followed by hydrolysis constitutes indirect corrosion, especially for more active metals such as calcium and magnesium. Secondly, nitrides are becoming increasingly important as high temperature refractories, especially the nitrides of less active elements, e.g., Si, Ti, Zr. Moreover, interstitial nitrides are widely used as hard materials and extensive studies have been made of the hardness and strength of nitrogen alloys, in particular steels.

In the past, corrosion has been studied chiefly as the direct oxidation of metals, and also oxides have been more widely used as refractories. The formation and reactivity of oxides has therefore been studied in great detail (e.g., Gleason, 1956, 1959a-b, 1960, 1961a-b, 1963a-b, 1969; Gleason & Sheppard, 1968). Similar studies on nitrides have been less extensive, especially on surface nitridation of metals and hydrolysis or oxidation of nitrides. In this thesis, selected nitrides of elements in Groups II - IV of the Periodic Table have been studied.

where relevant, comparisons have been made with the corresponding oxides (or hydroxides).

1.1 Classification of Nitrides

Nitrides are classified (Brown, 1966, p.150) as ionic, covalent and interstitial (or metallic), according to the nature of their bonding; see also Moore (1962). The atomic number of nitrogen is 7, and its electronic configuration in the ground state is, therefore, $(1s)^2,(2s)^2,(2p)^3$; the three 2p electrons occupy different space orbitals in accordance with Hund's Rules. In order to attain electronic stability, nitrogen may either form the nitride ion, N^{3-}, as in ionic compounds, or form covalent compounds by the overlapping of its singly-occupied orbitals with similar orbitals of other atoms. (Electronic stability can also be achieved by the overlapping of some of the singly-occupied orbitals with electron gain, as in nitriles, cyanides, etc.). In the interstitial nitrides, formed mainly by transition metals, small nitrogen atoms (radius 0.70Å) occupy some or all of the interstices in the metallic lattices, which are generally close-packed.

The rigid division of compounds into ionic, covalent and interstitial is unsatisfactory, because their bonding is a combination of ionic, covalent and metallic forces, of which one type may predominate. However, a classification of nitrides according to their properties is practically convenient. Thus nitrides, which readily hydrolyse forming

[illegible], are considered ionic. Accordingly, elements forming ionic nitrides are Li, Mg, Ca, Sr, Ba, Zn, Cd and Hg. They lie in Groups I and II of the Periodic Table.

The covalent character of the nitrides of a group of metals decreases with increasing atomic number; e.g., comparisons of the molecular susceptibilities of Mg, Zn and Cd nitrides show that the polarising action of the metal ion decreases from Mg to Zn to Cd (Fronte et al., 1971).

Metals having high ionic charge and small ionic radius tend to form covalent nitrides. These elements lie in Groups III and IV of the Periodic Table, and include B, Al, Ga, Si, Ge and Th.

Interstitial nitrides are generally nitrogen-deficient, nonstoichiometric compounds, which retain properties such as lustre, hardness, conductivity and high melting point of the parent metal. There are variations in the number of nitrogen-occupied sites and their type (tetrahedral or octahedral) in the close-packed metal lattice. Ranges of homogeneity vary; UN is an extreme example, having a stoichiometric composition. This may be attributed to the large radius (1.42Å) of the uranium atom, giving rise to large interstitial sites, thereby facilitating their occupation by nitrogen atoms.

1.2 Ionic Nitrides

1.2.1 Heats of Formation

The relative stabilities of various compounds are related to their heats of formation. Agreement between the

experimentally observed values and those calculated from the Born - Haber cycle is good for the alkali halides, but not quite so good for other compounds. This is partly due to the inaccuracies of the data used in the calculation, and partly to the simplifying assumptions made therein. One of the important factors of the latter category is the neglect of interionic forces other than electrical, i.e., the deviation from ionic character.

For a series of compounds having common anions or cations, it is more meaningful to compare the heats of formation per g.-equivalent. In the subsequent discussion, the term, "heat of formation", refers to the value per g.-equivalent of the compound, unless otherwise stated.

The heats of formation of simple binary compounds generally increase with increasing cationic radii and decreasing anionic radii and cationic and anionic charge. Also compounds containing ions with non-noble gas electronic structures have lower heats of formation than those without such ions (cf. Fajan's Rules). Those variations can be explained by a consideration of the terms in the Born - Haber cycle (van Arkel, 1956, p.74ff.).

1.2.2 Variation of Heat of Formation with Anionic Charge

The variation in the heats of formation with anionic charge can be illustrated by considering the fluoride, oxide and nitride of lithium. Since the radii of the ions, F^-, O^{2-} and N^{3-} are similar (1.36, 1.40 and 1.71 respectively) the differences in the heats of formation will depend mainly on

Table 1.1 Heats of Formation at 298°K

of Binary Compounds in kcal./g.-eq.

LiF	Li_2O	Li_3N
146	71	16
NaF	Na_2O	Na_3N
136	50	- *
MgF_2	MgO	Mg_3N_2
132	72	13
CaF_2	CaO	Ca_3N_2
145	76	16
AlF_3	Al_2O_3	AlN
115	67	21 **

Note: (1) Values quoted from Sicha & Block (1963).

* (2) The formation of sodium nitride is reported by Brown (1964, p.194) and Moody & Thomas (1966). The latter quote an estimated value of 12 kcal./g.-eq. for its heat of formation.

** (3) Values for AlN quoted by different authors vary from 19 to 27 kcal./g.-eq.: see, e.g., Samsonov (1964a, p.79), Shaffer (1964, p.263), van Arkel (1956, p.41).

---

the negative ion charge. The effect of this charge is to be found in the electron affinity of the nonmetal and the crystal energy (lattice energy) of the compound. The electron affinity is expected to predominate only in compounds with large positive ions of low charge, to which category the lithium ion (radius 0.60 Å) does not belong. Thus, the heat of formation decreases with increasing anionic charge, Table 1.1.

The smaller decrease from NaF to Na_3N suggests a very low value for Na_3N, which is evidently unstable at room temperature and has so far not been prepared in the pure condition. (See note (2) to Table 1.1).

The Madelung constant is significant in that it is high for LiF and unfavourable for Li_3N. Hence the decrease in heat of formation from LiF to Li_3N is much greater than in the Group III series, AlF_3, Al_2O_3, AlN, where the nitride has the higher Madelung constant compared with Al_2O_3. (In general, the Madelung constant per g.-equivalent, and hence the heat of formation, decreases with increasing anion : cation ratio).

The variation of the heat of formation with other proportion of the anion and cation can be explained similarly (van Arkel, 1956, p.7ff.).

1.2 Interstitial Nitrides

Interstitial nitrides are extremely hard, possess high melting points (higher than those of the parent metal), and have electrical and thermal conductivities comparable with those of metals. Such compounds are classified as "hard metals" (Schwarzkopf, 1950; Schwarzkopf & Kieffer, 1953, pp.3-4; Hägg, 1951) or "metal-like" refractory compounds (Sandle, 1946; Samsonov, 1964a, 1964b, 1965). Because they combine the electrical and thermal properties of metals with hardness and high melting points, they are of great industrial importance and find wide applications as refractories (Kieffer & Benesovsky, 1963; Schwarzkopf &

Kieffer, 1953, p.[illegible]ff., Samsonov, 1964a, pp.[illegible]).

The metallic components of "hard metals" include the transition and inner transition elements and aluminium; the nonmetallic components are light nonmetals of short periods, e.g., N, C, B, O, Si, P, S. In the following subsections is given a summary of some of the attempts to explain the bonding and properties of refractory compounds. The nitrides of metals of the first transition series are reviewed by Juza (1966).

1.[illegible].1 Hägg's Rule of Limiting Radius Ratio

Hägg (1930, 1931a-b, 1953) suggested that if the radius ratio of the nonmetal to metal atom of binary compounds of transition metals is less than 0.59, their structures are simple or "normal" with the nonmetal atom occupying the interstices of the original metal lattice. When the radius ratio exceeds this figure, the structures become more complex, but still exhibit metallic characteristics.

1.[illegible].2 Pauling - Ewald Theory

Ewald (1940) observed that many interstitial carbides and nitrides have the NaCl structure irrespective of the lattice of the parent metal. Indeed, in most cases, the lattice of the parent metal is different from that of its interstitial compounds. Thus, Hägg's idea of limiting radius ratio applies strictly only to carbides. According to Ewald, nitrides and carbides of formula, MX, are electro-neutral structures with covalent bonds. He applied Pauling's theory of metals, which embodies the concept of

resonance of four covalent bonds amongst six positions (Pauling, 1938, 1945, 1947, 1948, 1949; Pauling & Ewing, 1949). The idea of half-bonds is introduced, where an electron pair in an atomic orbital is used to form two bonds.

In Rundle's theory the nonmetal atom can achieve an octahedral configuration in two ways: (a) two equivalent sp hybrid orbitals form electron pair bonds and hybridise with four half-bonds formed by the two remaining p orbitals; (b) the three pp orbitals form six half-bonds, and an electron pair occupies the ss orbital. In each case, the resulting six bonds have an octahedral configuration, which explains the NaCl structure of the compounds. The directional nature of the bonds explains the brittleness and hardness of the compounds.

Rundle notes that the metal - metal distances in refractory compounds are much higher than those in the parent metal. Therefore, in forming a compound electrons are drawn from metal - metal bonds to form metal - nonmetal bonds, weakening the former. The high strengths of the latter type of bonds accounts for the low volatility of the compounds.

Hume-Rothery (1949) critically discusses Pauling's theory of metals; he also challenges Rundle's theory. According to Hume-Rothery (1953), the occupation of the octahedral sites by the nonmetal would be equally valid in a hexagonal close-packed lattice. However, the face-centred cubic structure is adopted because in this the metal too has

mutually perpendicular covalent bonds to its six neighbouring nonmetal atoms, a situation not found in the hexagonal structure. (In the latter, the octahedral sites around a metal atom form a triangular prism.)

1.[illegible] Importance of Bonding in Interstitial Compounds

Schwarzkopf (1950) and Schwarzkopf & Kieffer (1953, p.[illegible]ff.) consider the metallic character of interstitial phases more important than their crystal structures. Thus, the bonding in such compounds is important. On this basis the silicides also can be included among "hard metals" because of the large atomic radius of silicon (1.[illegible]Å), Hägg's critical radius ratio is exceeded by all transition metal silicides, yet the metallic character of these compounds is well established. Moreover, most borides do not form "normal" structures, although they are metallic in character and the radius ratios of many of them are within Hägg's limiting value. This deviation has been ascribed by Kiessling (1950) to the tendency of boron atoms to form chains, sheets or three dimensional networks. In the light of the above, Schwarzkopf & Kieffer suggest that the electronic structure of the parent metal may be more important than other factors. They also question whether the relationship, if any, between crystal structure and radius ratio are fundamental.

Brewer & Krikorian (1956) observe that the heats of sublimation of transition metals and the bond energies of their interstitial compounds calculated from thermodynamic

data vary in the same manner with the atomic number of the metal, suggesting a similarity in their bonding: see also Brikorian (1955). In contrast the bond energies of the corresponding dioxides, difluorides and dichlorides vary in a different manner because, in these compounds the bonding is ionic.

Goodenough (1963, pp.266-267) describes refractory compounds having the rock salt structure as "ionic compounds with metallic conductivity", and in particular, related to the oxides. The bond is partly ionic because of the electronegativity difference between the metal and nitrogen, and partly covalent. In contrast, nitrides such as Sc_3N and Mn_3N having the perovskite structure, are less ionic and better described as interstitial alloys. According to Goodenough (1963), in the metallic bond in transition elements and their compounds, the electron distribution between localised and more delocalised bonding states is determined by a critical interatomic separation of 2.9Å. Above this separation the electrons are localised, but below it they are present as "collective" electrons.

1.3.4 Ubbelohde - Samsonov Theory

Ubbelohde (1932, 1937) presented evidence for and developed the theory that in the interstitial dissolution of hydrogen in palladium, the former is ionised and is in the metallic state. The electrons of hydrogen fill the vacant levels of the metal. Thus, the metal is the acceptor and hydrogen the donor. Ivanskii (1943) extended this to

cover other hydrides and also carbides and nitrides. This is compatible with the fact that the ionization energies of carbon and nitrogen are comparable with that of hydrogen. Further support for this theory is provided by Seith & Kubaschewski (1935) and Frosvirin (1937) who demonstrated the ionic character of dissolved carbon and nitrogen in iron; also by Jack (1948) and Clarke & Jack (1951), who interpret the structure of the nitrides, carbides and carbonitrides of iron and cobalt on the basis of electron transfer from the interstitial carbon and nitrogen to the metal lattice. Hägglund (1950) makes a similar conclusion from a study of borides. According to him (Hägglund, 1954, 1959) the ability of the nonmetal to donate electrons increases in the order, C, N, O, B, Si. Hägglund (1957) emphasizes also the importance of bond lengths in these compounds. One of the necessary requirements for metallic bond formation is that the metal atoms should not be too far apart. This explains why small nonmetal atoms only may form interstitial compounds with transition metals.

Following Kubelohde and Graneki, Samsonov (1955a, 1956a-c, 1956b, 1965) developed the theory that the bonding between the transition metal and the nonmetal in refractory compounds is essentially metallic in character; see also Kempter (1964), Samsonov et al. (1965)[a]. This bonding involves not only the outer s and p electrons of the two elements but also the d and f electrons of the inner incomplete level of the metal. The degree of nonfilling of

these d and f electron shells influence the character of the bonding. This theory has been extended to compounds of the alkaline earth metals with light nonmetals (B, C, N and Si). Although these metals in their isolated states do not have incomplete levels of d and f electrons, in their compounds with nonmetals they may have energy states corresponding to such levels (Samsonov & Drozdnetsyn, 1956).

Samsonov defined the quantity "acceptor ability" of the metal as equal to 1/Zn, where Z is the principal quantum number of the incomplete shell of d electrons and n is the number of such electrons. A high acceptor ability favours a high electron concentration in the crystal lattice, i.e., greater metallic character. This is confirmed by the fact that the heats of formation, lattice energies, hardness and electrical conductivities of compounds increase with increasing acceptor abilities, e.g., Markisov (1954), Samsonov (1956b-c), Naughton (1955), Samsonov et al. (1961b). Similar variations are observed for other physical properties (see Samsonov, 1956a; Samsonov & Drozdnetsyn, 1956; Samsonov & Neshpor, 1958; Samsonov et al., 1957, 1958a). Also for transition metals in the latter part of a period in the Periodic Table, the metal - nonmetal bond strength diminishes with increasing atomic number of the metal, i.e., with decreasing number of d shell vacancies (Sa[illegible] & Nieszalin, 1958-1959). The interaction of the nonmetal electrons with the d shell of the transition metal leads to a reduction in the magnetic moment (Weiner & Berger, 1959).

The second important factor, which influences the nature of the bonding, is the ability of the nonmetal to give up its valency electrons, i.e., its ionisation energy (Samsonov, 1953b). This quantity decreases in the order, N, O, C, B, Si. A higher ionisation energy favours a larger proportion of ionic bonding and a correspondingly less metallic character. Thus, the nitrides and oxides are the most ionic and the silicides the least.

1.4 Production of Nitrides

1.4.1 Methods of Production

Nitrides of metals can be prepared by heating the metal in a nitrogen, ammonia or nitrogen + hydrogen atmosphere (Mellor, 1927, p.97; Brown, 1964, p.150; Suna, 1966). Variations of these methods include heating the metal amalgam, metal oxide, metal oxide + aluminium or magnesium, metal oxide + carbon, metal carbide, metal hydride, a metal salt such as the halide, phosphide, arsenide or nitrate, in a suitable nitrogenous atmosphere. Sometimes, however, heating the metal carbide in nitrogen produces carbonitrides such as cyanides and cyanamides, e.g., in the case of Ti, Zr (Portnoi & Levinskii, 1963), Ca, Sr, Ba. An advantage of using ammonia (or nitrogen + hydrogen mixtures) over nitrogen is that the reaction is carried out in a reducing atmosphere and therefore the formation of oxide impurities is minimised. The reaction between a metal oxide and ammonia to form the nitride is the reversal of the hydrolysis of the nitride. Ammonia has also been used in the liquid state and in aqueous

solution (Brown, Boveric & Cie, 1960). Interstitial nitrides have been produced in plasma flames too (Stokes & Knipe, 1960; Opfermann, 1964; SIMA, 1966; Hayashi et al., 1968).

Nitrides may be obtained also by decomposing metal amides or imides, heating an ammonium metallate in ammonia, using a molten salt bath based most commonly on cyanides and cyanates, the action of cyanogen gas or dinitrogen trioxide on the metal, the reaction between a metal salt in liquid ammonia and a reducing metal, and by double decomposition with another nitride.

Besides conventional heating techniques, high frequency induction heating has been used in nitride production. In the ionitriding process an electric glow discharge is utilised in splitting up molecular nitrogen (Reisswanger, 1959; Bernhard Berghaus, 1961; Laplanche, 1963; Sterling & Gunn, 1965; Sterling et al., 1966). An exploding wire technique also has been described (Joncich et al., 1966). Molten salt bath nitriding is used widely industrially to obtain thin protective nitride coatings. The bath usually contains a cyanide or cyanate of an alkali metal. Vapour phase deposition using a volatile metal salt such as the chloride with ammonia or nitrogen + hydrogen is also a widespread method of industrial nitridation (Campbell et al., 1949, 1952; Powell et al., 1966); a thin coating of nitride on machine parts improves hardness and other mechanical properties. This method produces a uniform nitride film on the finished article irrespective of its shape, and is used especially with transition metal nitrides.

A summary of nitride production methods is given in Table 1.2, which contains also a selection of references to methods of producing metal nitrides.

Table 1.2 Methods of Nitride Production

Method	Examples of metals nitrided	References
1) Action of nitrogen (or air) on:-		
(a) metal	Li, Mg, Ca, Sr, B, Al, Si, Ti, Zr, V, U, Cr, Mn, rare earth metals, Nb, Ta, V, Te, Th, Co	Samsonov et al. (1959b, 1961a); Kirchovskii & Chazanova (1960); Lyntsyn & Samsonov (1964); Campbell et al. (1949); Evans (1965)
(b) metal analogue	Ga, In, Tl, Pb	
(c) oxide	Zr, Al	
(d) oxide + Al or Mg	Ce, Ta, Nb, Zr, U, Ca, Cr, Ba, Al, Sr	
(e) oxide + C	Si, Mg, Ti, Sc, Al, B, Di, V	Lyntsyn & Samsonov (1964)
(f) carbide	Al	von Stackelberg et al. (1933)
(g) hydride	Ti, Si, Ca, Na, Sr, Mg, Li, V, U, Pu	Gunter et al. (1962); Anselin & Pascard (1963)
(h) boride	Mo, Cr, Fe	Samsonov (1964a, pp.312-314)
(i) silicide	Mg	David & Long (1965)
2) Action of ammonia or nitrogen + hydrogen mixture on:-		
(a) metal	Na, Mg, Mn, Cd, B, Al, Ti, Si, Sn, La, Ce, Li, Nb, Mn, Fe, Co, Ni, U, Cu, Th, Cr, Co	Lyntsyn & Samsonov (1964); Hougebauer et al. (1955); Coroch & Philippot (1963); Gautier et al. (1962); Mooley (1964)
(b) metal analogue	Re, Mn	

Table 1.2 (continued)

Method	Examples of metals nitrided	References
(c) oxide	Mg, B, Ti, In, W, Cu, Cb, Ga	Neugebauer et al. (1959); Lyntsyu & Samsonov (1964); Lorentz & Dinkowski (1962)
(d) carbide	Th	
(e) halide	Li, Ti, Cr, Di, Fe, V, Nb, Mo, B, Al, Ga, In, Be, Th, Cr, Mo, W, U, Cb, Ta, Hf	Hahn & Konrad (1951); Ruppert & Schwedler (1958); Hennor (1959); Sowa (1952); Campbell et al. (1949)
(f) phosphide or arsenide	Al, Ga	Addamiano (1961)
(g) hydride	Li	Sterling & Swann (1965); Sterling et al. (1966)
(h) boride	Cr, Fe, [illegible]	Kiessling & Liu (1951)
(i) metal salt + reducing metal with liquid ammonia	Na, In, Tl, Zn, Cd, Hg, Cu, Ag, Au, Fe, Co, Ni, Ru, Rh, Pd, Os, Ir, Pt	Schneider et al. (1963)
(j) nitrate (with liquid ammonia)	Cu	
(k) ammonium metallate	Al, U, Nb, Ta, Cr, Fe, Mo, W	Samsonov et al. (1961a); Funk & Koehland (1964); Hahn & Konrad (1951); Neugebauer et al. (1951)
3) Action of cyanides and cyanates on metal (or alloy)	Fe and its alloys: see Holler (1927, p. 7) for examples of other metals	Mitchell & Lawes (1964); Minkevich (1964); Albrecht & Mueller (1963); Mueller (1959); Deutsche Gold-und-Silber-Scheideanstalt (1963)
4. Decomposition of amides or imides	Sr, Ba, Cd, Zn, B, Cu	Ariya & Prokof'eva (1953)
5) Action of N_2O_3 on metal	Li	
6) Double decomposition with other nitrides	Cu	

1.4.2 Thermodynamics of Nitride Formation

The stability of nitrides and their production at various temperatures are related to their standard free energies of formation, ΔG_f^o; more negative values indicate thermodynamically more stable compounds. In Figure 1.1 the values of ΔG_f^o are compared for a selection of nitrides on an Ellingham (1944) diagram, using data compiled by Hicks & Block (1969); see also Pearson & Ende (1953) and Gletto & Ancey-Moret (1968). Transition metal nitrides of Groups IV and V have the greatest stability. This progressively decreases for nitrides in the lower groups and of transition metals in Groups VI to VIII. The iron nitrides, Fe_2N and Fe_4N, are relatively unstable, having positive ΔG_f^o values for a fairly wide temperature range. By comparison, ammonia is less stable than most nitrides.

From Figure 1.1 the standard free energy changes for the reaction of metal with ammonia (to form the nitride and hydrogen) can also be compared for different metals. Thus, for calcium nitride, the value of ΔG_f^o for the reaction,

$$\frac{1}{3}Ca + \frac{1}{3}NH_3 = \frac{1}{6}Ca_3N_2 + \frac{1}{2}H_2$$

is the difference between the values for the reactions:-

$$\frac{1}{3}Ca + \frac{1}{6}N_2 = \frac{1}{6}Ca_3N_2$$

and

$$\frac{1}{2}H_2 + \frac{1}{6}N_2 = \frac{1}{3}NH_3$$

Hence the difference between the graphs for $\frac{1}{6}Ca_3N_2$ and $\frac{1}{3}NH_3$ in Figure 1.1 indicates the relative ease of calcium

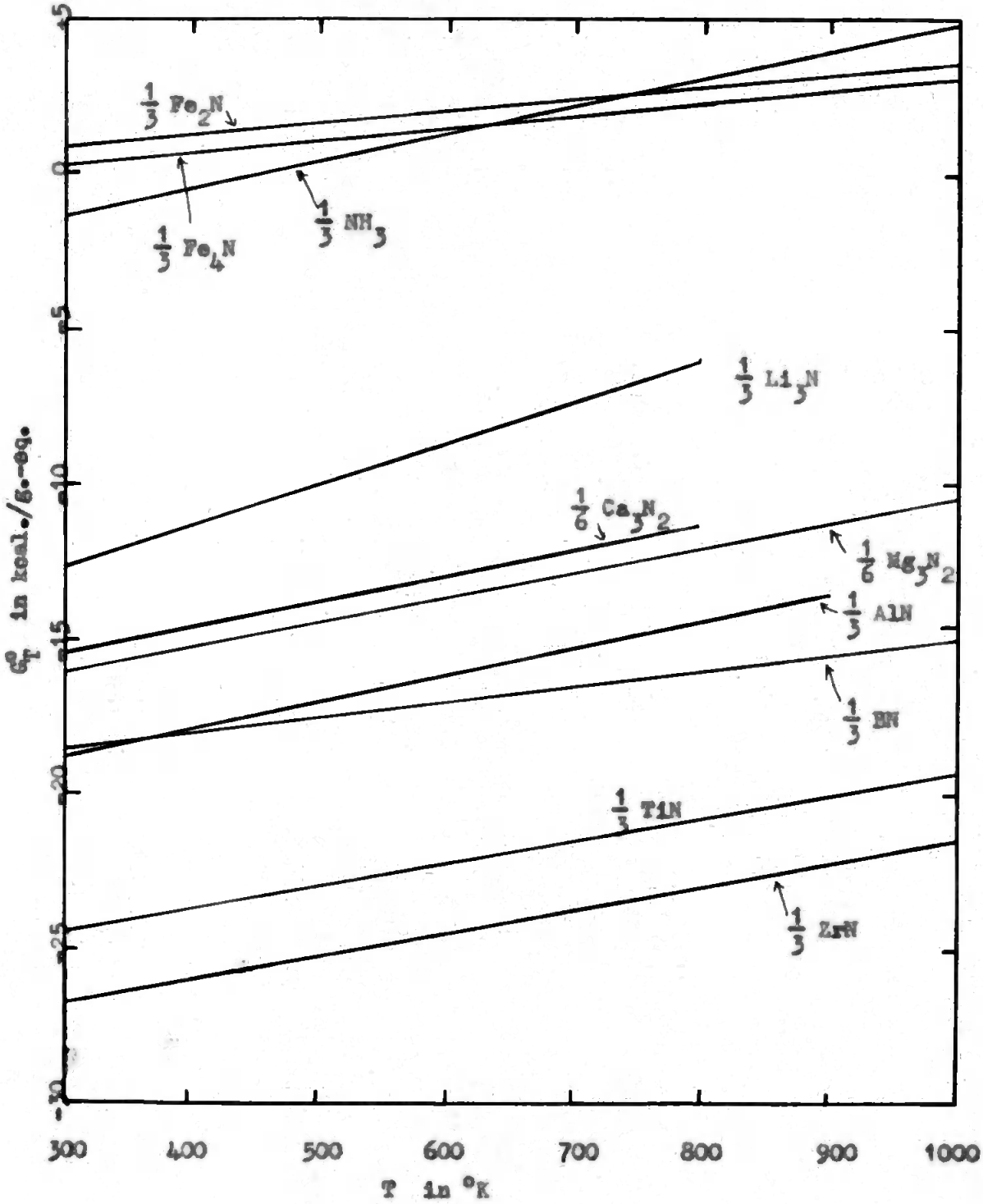

Fig. 1.1 Free Energy of Formation of Nitrides

nitride formation from the metal + ammonia, when the materials are in their standard states. From the thermochemical data, it can be seen that all the metal nitrides can be formed from the metal and ammonia, except Fe_2N and Fe_4N at lower temperatures. However, although energetically feasible, these reactions may be kinetically unfavourable. This applies especially to solid state reactions, where the number of variable factors is high, e.g., solubility of the gases in the various solid phases, formation of ternary compounds, adherence of compound layer onto the metal, etc. The last of these factors is important in the kinetics of the reaction and is discussed later, Section 1.3.2.

A plot of free energy data for the carbide, nitride, oxide and fluoride of the same metal, Figure 1.2, shows that generally the compounds are in the order of increasing stability, cf. heats of formation, Section 1.2.2 and Table 1.1.

1.3 Kinetics of Metal Nitridation

1.3.1 Rate of Nitridation

Metal nitridation is expected to conform to the same principles applying to oxide film growth (Dubnechewski & Hopkins, 1962). A number of relationships are known, which relate the extent of nitridation (or oxidation) with time. They give the weight increase per unit surface area, $\underline{m}$, as a function of time, $\underline{t}$.

The simplest relationship is the linear one, namely,

$$m = k't$$

where $\underline{k'}$ is a constant. Since the weight increase per unit

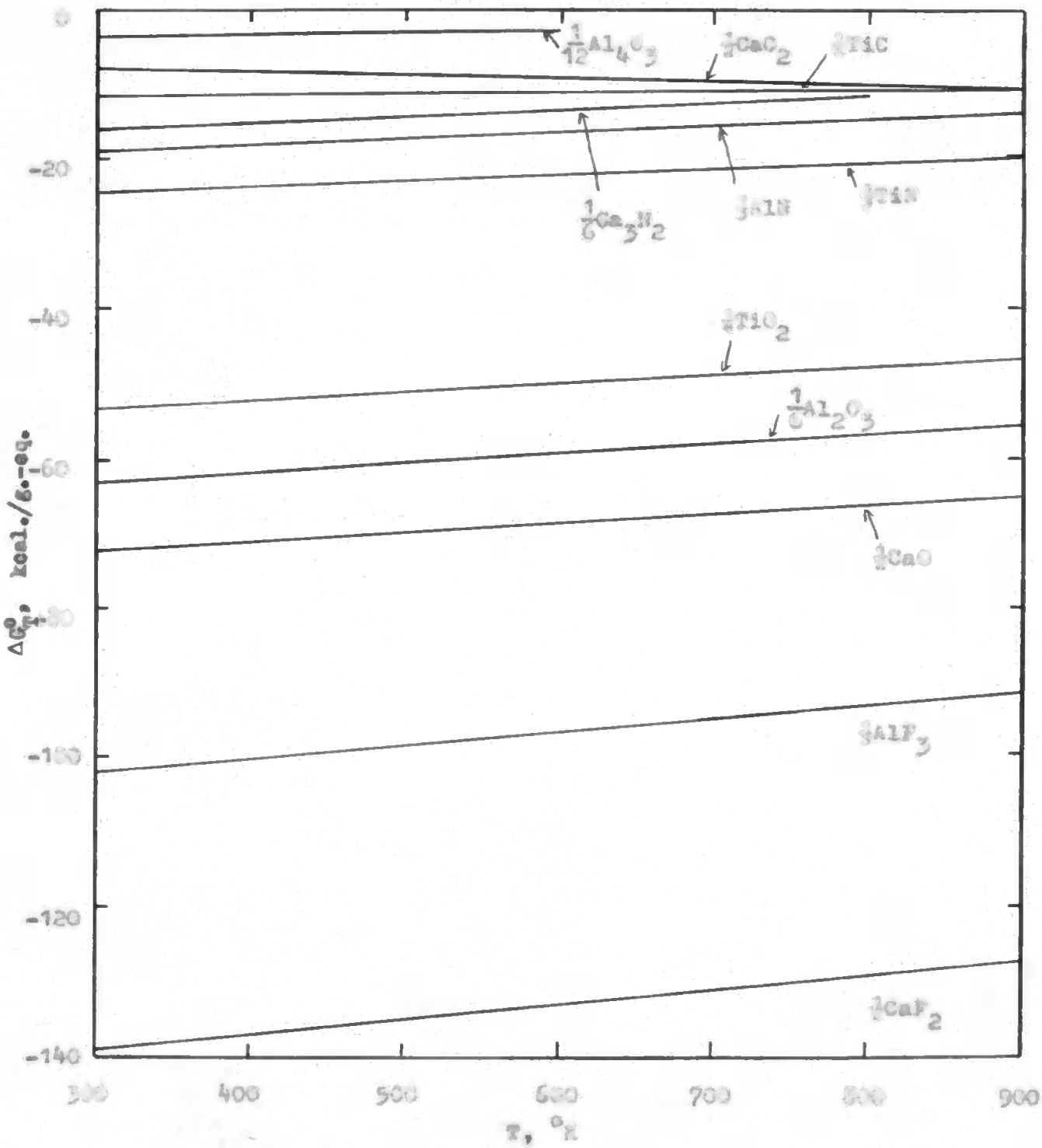

Figure 1.2 Free energy of formation of carbides, nitrides, oxides and fluorides

area is proportional to the thickness of the nitride (or oxide) film, Y, and this in turn is proportional to the decrease in thickness of the metal, y, the above equation can be written as,

$$y = kt$$

where k is a constant.

The parabolic law,

$$y^2 = kt + C$$

gives a straight line when the square of the weight increase is plotted against time, a non-zero value of C implying an initial induction period. Also reported are cubic, logarithmic and inverse logarithmic relationships.

A single nitridation curve may have combinations of two or more of the above relationships, e.g., the nitridation of a metal or alloy may begin parabolically and continue linearly. This is called a parallinear relationship.

1.9.2 Factors Affecting the Rate of Reaction

In the direct nitridation of metals a nitride layer is formed between the metal and its gaseous environment. The reactants have to pass through this barrier if the reaction is to continue and the nitride layer to grow. The overall rate of reaction may be governed by one or more of the following rates:-

(a) supply of reacting gas to the outer surface of the nitride layer;

(b) transport of reactants through nitride layer;

(c) reaction between metal and nitrogen forming nitride.

Each of the above rates is governed by factors such as temperature, external gas pressure, defects in the nitride structure, etc. The slowest of the above rates is the rate-determining step.

The mechanical stability of the nitride film is also important in determining the rate and extent of reaction. The strength of the film on the metal depends on the differences in molecular volume and type of crystal lattice of the product layer compared with the original metal (Pilling & Bedworth, 1923), and also on the rate of nitride sintering. Table 1.3 summarises molecular volume and crystal lattice changes accompanying the nitridations of some metals. The calculations are based on X-ray data compiled by Taylor & Kagle (1963), and checked experimentally. Volume changes are expressed as fractions of the original metal volume, allowing for weight increases during nitridation; expansions and contractions are indicated by + and - signs respectively. Those small decreases in unit cell size are caused by sintering of the newly-formed nitride, the lowest limiting value is recorded, e.g., for Ca_3N_2, a falls from 11.42 to 11.30Å on sintering.

1.5.3 Ion Diffusion: Parabolic Relationship

The commonest mechanism of diffusion of the reactants through the nitride layer involves the movement of cations from the metal - nitride interface towards the nitride - chemisorbed nitrogen interface. Anion diffusion is slower because of larger size, but is not always unimportant.

Table 1.3 Fractional Volume and Crystal Lattice Changes on Nitridation

Nitride	Frac. vol. change	Element		Nitride	
		Crystal lattice	Lattice constants in Å	Crystal lattice	Lattice constants in Å
Mg_3N_2	-0.11	h.c.p.	a = 3.21 c = 5.27	cubic, anti-Mn_2O_3	a = 9.99
Ca_3N_2*	-0.31	b.c.c. (γ)	a = 4.32	cubic, anti-Mn_2O_3	a = 11.32
Sr_3N_2	+0.07	h.c.p.	a = 2.06 c = 4.95	cubic, anti-Mn_2O_3	a = 9.74
Ba_3N_2	+0.22	h.c.p.	a = 2.98 c = 5.62	cubic, anti-Mn_2O_3	a = 10.10
BN	+0.17	tetragonal	a = 2.73 c = 5.03	hexagonal	a = 2.50 c = 6.66
TiN**	+0.05 +0.03	b.c.c. (β) h.c.p. (α)	a = 3.31 a = 2.95 c = 4.68	cubic, NaCl	a = 4.24
ZrN**	0.00 +0.02	b.c.c. (β) h.c.p. (α)	a = 3.61 a = 3.23 c = 5.15	cubic, NaCl	a = 4.56

* high temperature form
** low temperature form

Simultaneous movement of anions and cations also is known to be significant in mechanisms of reactions.

Cation migration is possible because of vacant cation lattice sites in the nitride layer. Such migration is favoured therefore by a high degree of nonstoicheiometry and by a large number of cation defects in the nitride lattice. The overall effect is thus a flow of cation vacancies through the nitride layer towards the metal - nitride interface or

cations in the opposite direction, i.e., an electric current through the nitride layer. According to the thin film theory of Cabrera & Mott (1949) the ions move under the potential difference set up between the anions and cations on the respective interfaces. The cations are formed by the migration of electrons through the film by the "tunnel effect" followed by reaction with gas molecules adsorbed on the outer surface of the film. The accumulation of vacancies at the nitride - metal interface leads to the formation of cavities.

The parabolic law is common for many nitridation and oxidation reactions. A simplified derivation of the law is as follows (Hilton, 1968, p.5). If ion (and electron) migration is the rate-determining step, the reaction rate, i.e., the rate of growth of product layer, is proportional to the conductance of the layer or inversely proportional to its thickness, Y. Therefore,

$$\frac{dY}{dt} = \frac{k}{Y}$$

Rearranging and integrating the above equation gives,

$$Y^2 = 2kt + C$$

where k and C are constants. In the Cabrera - Mott theory, the constants are related to the ionic diffusion coefficient and other constants.

1.5.4 Linear Relationship

The above derivation of the parabolic law assumes that the product layer remains adhered to the metal during the reaction and keeps it completely protected from direct attack by reacting gas. This is not so if stresses within the layer

are great enough to cause its breakdown when its thickness reaches a critical value, or if its surface area is less than that of the metal originally. The mechanical stability of the product layer is governed by, inter alia, the molecular volume changes accompanying the reaction. Larger volume changes, especially negative ones, enhance quicker break-up of the layer. Film rupture exposes fresh metal surface to the reacting gas, and the ensuing reaction follows a new parabola. More nitride is then produced in contact with the metal and after a similar time interval, disruption of the film again takes place. The net result is to produce a nitridation curve consisting of a series of parabolas, Figure 1.3. When film breakdown takes place very quickly the number of parabolas increases and their size decreases. The resulting curve then approximates to a straight line, i.e., corresponds to a linear rate of reaction.

A simplified derivation of the linear law is as follows. If there is no adhering nitride layer, the metal surface is

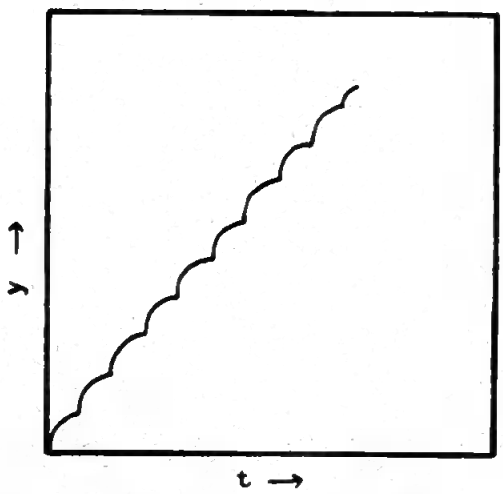

Figure 1.3 Linear Law of Nitridation

always exposed to the reacting gas and the reaction rate is independent of the amount of metal already reacted (i.e., of the decrease in its thickness, y), under a given set of conditions. Therefore,

$$\frac{dy}{dt} = k$$

whence,

$$y = kt + C$$

where k and C are constants.

The linear law is applicable whenever the rate of reaction is independent of film thickness, whether there is a coherent film of nitride on the metal or not. Thus, if the nitridation is linear, ionic migration cannot be the rate-determining step.

More comprehensive treatments of reaction rates applicable to thin films are summarised by Rubanchewski & Hopkins (1962, p. 71).

1.5.5 Nitride Scaling on Metals

For the formation of thick oxide (or nitride) layers, i.e., scaling, Wagner (1933) has provided a satisfactory theory (Rubanchewski & Hopkins, 1962, p. 4). In this, the mechanism is controlled by diffusion due to a concentration gradient. The parabolic law applies when the scale is uniform.

For the formation of non-uniform (i.e., porous or cracked) scales, the Pilling - Bedworth Rule is probably less significant if the scales grow by outward migration of matter (Vernilyea, 1957). It is more important when diffusion is from the surface towards the metal - scale interface. If the molecular volume change accompanying the reaction is negative,

the metal surface may not be completely covered with the product and therefore be exposed to direct attack by gas. Reaction then follows the linear law and is related to the pressure of reacting gas.

1.9.6 Effect of Pressure

When the rate-determining step involves the dissociation of the attacking diatomic gas (oxygen or nitrogen), the reaction rate is expected to be proportional to the square root of the pressure. In this case the direct reaction at the solid - gas interface is the rate-determining step.

When gases dissolve in metals, Henry's law is applicable; also the gas molecules dissociate into atoms (or ions) on dissociation. Hence, the solubility of a diatomic gas in a metal would be expected also to vary as the square root of gas pressure. The diffusion of gas atoms through a metal also requires a square root relationship with pressure when the metal surface is directly exposed to the gas (Kanner, 1961, p.140). A nitride (or oxide) film, however thin, can completely change these relationships.

When the diffusion process in the product layer contributes to the reaction rate, deviations occur from the square root relationship between gas pressure and reaction rate. Various empirical relationships have been reported. Another complicating factor is the sintering of the product at higher temperatures. This is further discussed in the following section.

1.6 Reactivity of Nitrides

General accounts of active solids together with

references to the original literature are given by Gregg (1951, 1958).

The reactivity of solids is governed by several factors, of which particle size is an important one. An increase in activity is usually traceable to an increase in the specific surface (i.e., the surface area per unit mass) of the substance, and often additionally, to imperfections in the lattice itself.

A substance consisting of small particles possesses high surface energy. Also lattice imperfections represent a high level of "bulk" potential energy. Thus, an active solid is in a metastable condition and tends to revert spontaneously to a more stable state. This loss of activity takes place on mere standing at room temperature, usually very slowly, and is called "ageing". Ageing results in the formation of large crystallites with less imperfections.

Ageing is enhanced by increasing temperature, which results in a decrease of both external and internal energy. The increased thermal agitation of the constituent atoms or ions facilitate their movement into positions of minimum potential energy. Also, high temperatures favour the aggregation of solid particles, a phenomenon called "sintering". Sintering is enhanced by high pressure and leads to an increase in the lump density of the substance (Spriggs & Atterans, 1966). It is also affected by additives (e.g., Glasson, 1967). Thus gas-producing contaminants such as carbonates and hydroxides delay the extent of sintering (Rice, 1966, 1969; Livery et al., 1966; Wheat & Carruthers, 1967). Hence, vacuum hot pressing is often preferred (Chiotti, 1952). These factors are important in ceramic fabrication science (Cooper, 1969).

The rate of sintering of a solid markedly increases within a narrow range of temperature near $0.5T_m$ °K, where T_m °K is the melting point of the solid. At this temperature, called the Tammann temperature, the vacancies in the solid are no longer "frozen", so that ionic migration through the bulk of the solid ("lattice" or "volume" diffusion) becomes extensive. At lower temperatures, e.g., in the region of about $0.3T_m$ °K, "surface" diffusion along grain and crystallite boundaries is the more important factor.

Methods of preparing active solids include grinding, calcination, sublimation and precipitation. In the first, the mechanical breaking up of the particles is opposed to some extent by the tendency of the fine particles to adhere together under the joint action of surface forces and the mechanical pressure of the mill.

Calcination is based on chemical reactions of the type:-

$$\text{Solid A} \longrightarrow \text{Solid B} + \text{Gas C}$$

e.g., the decomposition of hydroxides and carbonates (Glasson, 1956, 1959a, 1961b, 1963a; Glasson & Sheppard, 1960; Gregg, 1959). The specific surface of B is considerably greater than that of A, if the two solid phases possess different lattices and if there is a large volume change between them, cf. Pilling & Bedworth (1923) Rule for metal oxidations. The mechanism of the activation process involves the transformation of a crystallite of A into one of B, which is in the form of a pseudo-lattice of A. Recrystallization of the metastable pseudo-lattice soon sets in, proceeding from nuclei. The

average number of such nuclei per crystallite of A is the factor by which the number of crystallites increases in the course of the reaction. This factor is related to, and can be calculated from, the surface area and molecular volume changes accompanying the reaction (Glasson, 1959b). The development of surface will thus tend to lag behind the extent of reaction, e.g., the decomposition of calcium hydroxide (Glasson, 1956).

The above remarks also apply to other related types of reactions involving solids and gases, e.g.,

Solid A + Gas B ⟶ Solid D

Solid A + Gas B ⟶ Solid B + Gas D.

Examples of the former type are the "dry" hydrations of oxides (Glasson, 1959b, 1963b) and of the latter type the calcination of nitrides in air. The general considerations can be extended to "wet" hydrations of oxides too (Glasson, 1963, 1963b).

The rate of a reaction involving solids (and gases) is governed by several factors, which may be complex to express mathematically (Sulbrandsen & Andrew, 1951). These include changes in surface heterogeneity, specific surface, local surface temperature due to heat of reaction, solubility effects, impurity concentrations and phase composition, as the reaction proceeds.

Sublimation and precipitation are "condensation" methods of preparing active solids, whereas grinding and calcination are "disintegration" methods. The preparation of evaporated metal films is an example of a sublimation method. This is usually carried out under high vacuum. Films of calcium, magnesium,

zinc and cadmium investigated in the present work were prepared in this way, Sections 3.1 and 4.1.

The average particle size of a precipitated solid is governed by the conditions of precipitation, (e.g., Glasson, 1962a-b, Glasson & O'Neill, 1967). Ageing of the product is enhanced by elevated temperatures and by high solubility, for these facilitate the rapid movement of ions and a high concentration of them in solution.

The chemical reactivities of refractory nitrides have been summarised by Shaffer (1964) and Samsonov (1964a). These nitrides are less readily hydrolysed compared with ionic nitrides. However, some of them are transformed into oxides on calcination in air.

This thesis embodies further studies carried out by the author on a selection of nitrides of elements in Groups II - IV of the Periodic Table. They include so-called ionic (Mg, Ca, Zn and Cd), covalent (B) and interstitial (Si and Zr) nitrides. In the following sections of this chapter are summarised the studies by other workers on the formation and reactivity of the above nitrides.

1.7 Magnesium Nitride, Mg_3N_2

The methods of production of magnesium nitride are summarised by Mellor (1927, p.104) and Brown (1964, p.157). Laffite & Grandadam (1935) report that nitride formation by magnesium in an atmosphere of nitrogen or ammonia begins at 300° and is autocatalytic. Equilibrium pressure data for the magnesium - nitrogen system also support nitride formation

(Laffite et al., 1936). From thermochemical studies Mitchell (1949) deduces that there are three forms of magnesium nitride. However, this has not been confirmed by other workers, e.g., Bradley et al. (1966), who observe the one cubic form only of the compound (von Stackelberg & Paulus, 1933).

Sthapitanonda & Margrave (1956) studied the nitridation of magnesium as a function of time, temperature, pressure of nitrogen gas and metal surface properties, and made comparisons with the oxidation. A typical nitridation course consists of three distinct periods, viz., (a) initiation, then, (b) steady reaction at a linear rate, followed by (c) a decrease in the rate of reaction due to evaporation of the sample. The linear rate of reaction and its decrease on evaporation of metal are due to the lack of a protective nitride film on the metal. This is consistent with the Pilling - Bedworth (1923) rule, since the molar volume ratio of nitride to metal is 0.88.

Murugolescu & Cismaru (1969) found that in the nitridation of magnesium with nitrogen at one atmosphere pressure, the reaction rate is parabolic in the temperature range 300 - 400°; from 400 to 500°, it is linear, and in the range 500 - 580° it again approaches a parabolic law. In the nitridation with ammonia, the rate is linear from 490 to 530°; at 550 - 575° it approaches and then obeys a parabolic law. The effect of temperature on the reaction rate is less for ammonia than for nitrogen.

The results of Sthapitanonda & Margrave also indicate that the reaction rate increases with temperature over the

range 415 - 465°. Evaporation of metal sets an upper limit for obtaining consistent results. The lower limit of temperature when nitridation begins is about 300°. Below 415° the reaction stops after a film of certain thickness is formed. Sifferlen (1964) claims a much higher temperature up to which the nitride layer protects the metal, the particular temperature being a function of nitrogen pressure; e.g., below 555° nitrogen at one bar prevents corrosion, but at 590° a pressure of 19 bars is needed. Such a claim is also made by Subovik et al. (1964), according to whom the rate of nitridation is a maximum at 750 - 800° and falls off at higher temperatures. They also report that ammonia is less suitable than nitrogen. According to Belin (1962a,c) nitridation begins at 529° and is a maximum at 625°, the reaction being inhibited by a surface layer of oxide impurity. Belin (1962b,d) reports also that the weight of nitrogen fixed per unit area of metal shows first a linear dependence with temperature, followed by an exponential region. The period of acceleration extends over a temperature interval, which is more important than in the case of oxidation; see, e.g., Pepen (1943a-b).

A study of magnesium nitridation at various pressures, by Chapitaunenda & Margrave, indicates that the rate of reaction increases with nitrogen gas pressure, but the effect is not very great. The nature of the metal surface affects only the initial nitridation, this being faster for abraded than for unabraded samples. Comparison of the nitridation of magnesium with its oxidation shows that at comparatively low temperatures

nitridation is the faster reaction. However, because the activation energy of the oxidation is more than twice that of the nitridation, the rate of oxidation increases much faster with temperature. At 400° the rates are equal after which oxidation is faster. This is consistent with the observation of Belin (1962c, 1964), who correlates the initial surface state of the metal with the rate of reaction.

Gregg & Bickley (1966) made a gravimetric study of magnesium nitridation. They found that electropolished magnesium experiences a weight loss in nitrogen gas at 500° and 10 cm. mercury pressure. At lower temperatures there are weight increases. However at higher pressures there are "breakaways", i.e., sudden increases in weight gain.

These variations in the rate of magnesium nitridation are accounted for in terms of metal evaporation (which results in weight loss) accompanying nitridation (leading to weight gain). The net result on the weight of the sample is governed by which of these two opposing factors predominate. Evaporation is promoted by traces of water vapour but inhibited by oxygen and by an uneven surface. This inhibition is attributed to a growth in the nitride film, and the promotion to film rupture.

The above results can be explained in terms of the formation and growth of cavities at the metal - nitride interface, together with rupture of the film covering the cavity. When a crack appears on the film, a flow of nitrgen inwards to the cavity or of magnesium vapour outwards may occur. At comparatively low temperatures (500°) the vapour

pressure of the metal is not sufficiently high to oppose the inward flow of nitrogen gas. Reaction then proceeds leading to nitride formation and weight gain. However at higher temperatures metal evaporation will predominate: and if the film is thin at rupture, magnesium vapour will escape; but if it is thick, the vapour will react with the gas within the cracks to form the nitride. Thus, very pure magnesium nitride is manufactured by heating magnesium above its sublimation point but below its melting point (Davis, 1949). A limited amount of nitrogen (or ammonia) gas is admitted to initiate surface nitriding. The reaction is completed at a temperature sufficient for the sublimed metal to break through the nitride coating, whilst gradually admitting additional amounts of gas: see also Mitchell (1949) and Byrne (1950). The preparation of magnesium nitride at temperatures above the melting point of the metal have been reported also (Porter, 1949; Revzin & Ma'yasov, 1961).

Magnesium nitride, a typical ionic nitride, hydrolyses readily in water forming the hydroxide and ammonia (Mellor, 1967, p.105). The resultant changes in molecular volume and crystal lattice account for the destabilisation of the product layer. This is investigated further, Section 3.3.

Coates et al. (1951), Schumb & O'Malley (1964) and Shamir & Simonboyn (1966) report the results of fluorination experiments on magnesium nitride. With silicon nitride it forms a double nitride (David & Lang, 1965).

1.8 Calcium Nitride and Calcium Cyanamide

1.8.1 Calcium Nitride, Ca_3N_2

The studies by early workers on the formation of calcium nitride have been summarised by Mellor (1927, p.191) and Brown (1964, p.158). Information on the calcium - nitrogen system has been compiled by Hansen & Anderko (1958). They report two forms of calcium nitride, viz., a pseudohexagonal form when prepared at 300° and a cubic form when prepared at 800°. The transition from the pseudo-hexagonal to the cubic form is irreversible. An orthorhombic phase of Ca_3N_2 is also reported to be formed at high temperatures and pressures (Bradley et al., 1966).

According to von Antropoff & Hermann (1928) the reaction between calcium and nitrogen at 400 - 440° takes place in three stages; namely, first, (a) a fast surface reaction involving calcium atoms only, then, (b) a very slow reaction involving atoms below the surface layer of nitride, followed by, (c) another fast reaction after the nitride layer has grown to a definite thickness. The nitridation is inhibited by oxygen but once an initial nitride layer is formed, it protects the metal against further inhibition by oxygen and the reaction proceeds: see also Alexander (1949c). Alkali metals promote the reaction. Indeed it is claimed that the reaction between the pure elements at 400° stops very soon because of the formation of an initial protective layer of nitride (Hartmann & Fröhlich, 1934). It has also been suggested that the pure metal does not react with nitrogen; impurities such as sodium and

lithium present in commercial calcium catalyse the reaction, which is further complicated by the transition in the metal from the α- to the β-form (Franck & Sodea, 1951).

According to Soliman (1951) the rate of nitridation of calcium is a maximum at 425° and is accelerated by high pressure. However, Shushunov & Baryshnikov (1955), working with freshly distilled metal film, quote 500° as the temperature of maximum rate, and a temperature of 430° below which the reaction is autocatalytic. The induction period is inversely proportional to pressure and also falls off rapidly with temperature.

Roberts & Tompkins (1959, 1960) investigated the kinetics of nitridation of sintered calcium films in the temperature range 25 - 200°. Their results are in agreement with those of von Antropoff & Germann at higher temperatures. The period of initiation consists of nitridation at special sites on the surface, probably lattice defects. The results indicate that: (a) the reaction rate is a linear function of nitrogen pressure suggesting a reversible adsorption to form a "surface complex", N_2^-; (b) the Cabrera & Mott (1948) theory of thin film formation is applicable, i.e., the reaction rate is governed by the rate of diffusion of metal ions through the nitride layer under the influence of the electric field set up between the metal - nitride interface and the chemisorbed nitrogen species on the outer nitride surface, cf. nitridation of lithium (McFarlane & Tompkins, 1962); (c) below a critical temperature of 162° the films grow to a maximum thickness;

(d) above this temperature the reaction proceeds until all the metal has been used up.

Chamberlain & Margrave (1961) studied the kinetics of nitridation of large pieces of calcium and found that unlike with metal films, the reaction rates are very slow even up to 900°. An increase in pressure in the early stages of reaction was a common observation, suggesting vapourisation of metal, cf. magnesium nitridation. It was not possible to make definite conclusions from the results, because of their poor reproducibility, which was further complicated by the phase transition of the nitride in the temperature range considered. The nitridation contrasts with the oxidation, where below 350° the rates are slow and linear, but above this temperature are more nearly exponential functions of time.

According to Aubry & Streiff (1966), the nitridation of calcium changes from a parabolic law to a linear one at 650° with increasing temperature. The change is due to the allotropic transformation in the nitride at that temperature.

Calcium nitride is a typical ionic nitride and is similar to magnesium nitride in its behaviour towards water (Mellor, 1967, p.103). The nitride layers are destabilised by hydrolysis (with water vapour or liquid) when the nitride ions are replaced by hydroxyl ions; since each N^{3-} is replaced by $3OH^-$, the films become very weak and rupture whilst very thin. At higher temperatures decomposition of the hydroxide to the oxide causes further fragmentation (Ellason, 1961a).

Calcium nitride is reported to form ternary phases with

silicon nitride (Lang & Latrent, 1963; Crosley et al., 1966). With halogen fluorides it forms nitrogen fluorides (Emeléus & Sheppard, 1960).

Further studies on the formation and reactivity of calcium nitride have been carried out and are reported in Chapter 2.

1.2.4 Calcium Cyanamide, $CaCN_2$

Nitridation of calcium carbide produces the analogous calcium cyanamide (Jacobson, 1948, p.74). Calcium nitride is reported as an intermediate product (Polzenius, 1907; Krase & Yee, 1924), but this is disputed by Franck & Bolam (1931). The reaction is catalysed by various additives, such as calcium chloride and fluoride; (see, e.g., Gol'dberg & Smusenkii, 1956, 1958, 1962; Abe, 1959, 1960a-d; Simonsen et al., 1961a-c; Chearyan, 1964). The kinetics and mechanism of the reaction has been investigated by several of the above authors. A general review of the process is given by Roach (1964a-b).

Equilibrium in the system $CaC_2 - N_2 - C - CaCN_2$ at 1220 - 1350° is divariant, and is determined by the concentration of a solution of CaC_2 in $CaCN_2$, which is the true reactant (Rociat, 1937). The reaction,

$$CaC_2 + N_2 \rightleftharpoons CaCN_2 + C$$

is completely reversible up to 1325°.

Calcium cyanamide is formed from lime and hydrocyanic acid also (Franck & Heimann, 1931). The reaction is only slight at room temperature; at 150° the product contains up to [illegible]

calcium cyanide, which decomposes at higher temperatures forming the cyanamide.

At 1120 - 1130° calcium cyanamide is more stable under a nitrogen pressure of one atmosphere. With increasing temperature, decomposition takes place with a decrease in the nitrogen content. At 1400° the decomposition is accompanied by loss of calcium too.

Like the nitride, the cyanamide is hydrolysed by steam (as in the process for nitrogen fixation) or more slowly by moisture in the soil (when used as a fertilizer) (Jacobson, 1940, p.44). The overall hydrolysis is represented by the equation,

$$CaCN_2 + 3H_2O \longrightarrow CaCO_3 + 2NH_3$$

but initially CN_2^- is replaced by OH^- to form $Ca(OH)_2$ as an intermediate, e.g., Franke (1913), Jacob et al. (1924). Urea formed from the hydrolysis of the cyanamide ion reacts with the hydrated lime to produce the carbonate. These changes have been further investigated by studying the products of the reaction between hydrated lime and urea solution, Section 3.4.

1.2 Nitrides of Zinc and Cadmium

1.2.1 Zinc Nitride, Zn_3N_2

Mellor (1927, p.196) has summarised the methods of preparation of zinc nitride. The direct reaction between zinc and nitrogen takes place only in the presence of an electric arc. Brown (1934, p.150) reports that the passage of ammonia gas through molten zinc at 600° results in only traces of nitride. Maffitt & Grandadam (1939) also report the absence of

nitride formation with ammonia in the temperature range 0 - 400°. However, nitride formation is reported at higher temperatures (Mellor, 1927, p.106; Juza et al., 1938; Revzin & Kus'yanov, 1961). The most satisfactory method of preparing zinc nitride appears to be the action of heat on zinc amide, $Zn(NH_2)_2$.

The chemical properties of zinc nitride are summarised by Brown (1964, p.160). Zinc nitride, when prepared from the amide and heated in oxygen, begins to oxidise at 400°, the reaction completing at 730°. When the nitride is heated in hydrogen, ammonia formation begins at 400° and is rapid at 600°. The nitride decomposes in ammonia above 600° and in nitrogen at lower temperatures (Juza et al., 1938), and reacts with water, acids and alkalis evolving ammonia. The hydrolysis of the nitride is enhanced, particularly at lower temperatures by the increase in solubility of the hydroxide in ammonia. A complex, $Zn(NH_3)_x(OH)_2$, is formed, where $x \leq 4$ (Sillén & Martell, 1964), cf. mercury, where $x \leq 2$ (Claesson, 1949; Sillén & Martell, 1964).

Zinc nitride has the anti-Mn_2O_3 structure; thus, it is isomorphous with the nitrides of magnesium and calcium.

1.9.2 Cadmium Nitride, Cd_3N_2

The chemistry of cadmium nitride is very similar to that of zinc nitride (Mellor, 1927, p.107; Brown, 1964, p.161). Cadmium nitride is prepared by methods analogous to those used for the zinc compound; the reactions of the two nitrides with water, acids and alkalis are also similar. The structure

of cadmium nitride is isomorphous with that of zinc nitride.

Further studies relating to the formation and reactivity of zinc and cadmium nitrides have been carried out and are described in Chapter 5.

1.12 Boron Nitride, BN

Mellor (1927, p.1[illegible]) and Samsonov et al. (1960, p.214; 1962a, p.223) have summarised the methods of boron nitride production. These methods involve the action of nitrogen compounds such as ammonia, cyanides and amino compounds, on boron and its compounds, chiefly borax and boric oxide; see also Saito & Ushio (1959). The action of ammonia on borides has also been used (Kiessling & Liu, 1951). The above reactions are the basis of several patents for boron nitride production, e.g., May et al. (1958, 1960), Hamlet (1958), Lanzan (1960), Lubarsff et al. (1960). Vapour phase deposition using boron trichloride is a widely used industrial method; see also Patterson (1967).

The kinetics of nitridation of boron has been studied by Samsonov & Gloptsov (1959, 1960). At [illegible] - 1300°, the reaction rate is parabolic; at higher temperatures this changes first to a linear law, and later to a logarithmic one.

Boron nitride has a hexagonal layer type structure (Bensc, 1950). A cubic form having a structure analogous to sphalerite has been made at higher temperatures and pressures (Wentorf, 1957, 1960); see also Vereshchagin et al. (1[illegible]). An apparently amorphous form, somewhat more reactive than the crystalline one, is also reported (Moeller, 1952, p.75[illegible]).

The chemical properties of boron nitride have been investigated by, inter alia, Taylor (1955), and are summarised by Mellor (1927, p.110), Samsonov et al. (1960, p.210; 1962a, p.216), Samsonov (1964a, p.236, p.269, p.307) and Shaffer (1964, p.264). The hot pressed material has a greater chemical resistance than the powdered one. The reaction of boron nitride with alkali to form ammonia is quantitative, and is used as a method of estimating nitrogen in the compound.(Minenko et al., 1965).

Boron nitrides forms borides when heated with transition metals or their carbides (Schwarzkopf & Glaser, 1953). When reacted with fluorine, boron nitride yields boron trifluoride and nitrogen together with small amounts of nitrgen fluorides (Coates et al., 1952; Schumb & O'Malley, 1964); with compounds of fluorine the yield of nitrogen fluorides is higher (Shamir & Binenboym, 1966). From a mass spectroscopic study of boron nitride vapour, Akishin & Khodeev (1962) deduced that the decomposition of the compound begins at 1600°; see also Drager et al. (1962). Under pressure of nitrogen, boron nitride melts without decomposition at 3000° (Campbell et al., 1949).

Boron nitride powder oxidises appreciably above 800° in air, the rate depending on the calcination temperature (Zagyanskii & Samsonov, 1952). The hot pressed material has a greater thermal stability (Taylor, 1955, 1956). Further studies of this reaction are described in Chapter 5.

The chemical resistance of boron nitride at high temperatures finds many applications for it as a refractory material (Taylor, 1955, 1956; Samsonov et al., 1960, p.219;

1962a, p.225; Samsonov, 1964a, p.342).

1.11 Titanium Nitride, TiN

1.11.1 Formation

Methods of production of titanium nitride are summarised by Heller (1927, p.119) and Brown (1964, p.187). The direct combination of the elements has been carried out at temperatures ranging from 400 to 1200° (Agte & Moers, 1931; Ehrlich, 1949; Ghiotti, 1952; Samsonov et al., 1959b, 1961a; Cuthill et al., 1960; Clair, 1960; Arai et al., 1962; Ordina et al., 1962). Ammonia or mixtures of hydrogen + nitrogen also have been used in the nitridation of the metal (Schomate, 1945; Naylor, 1946; Ghiotti, 1952; Wyatt & Grant, 1954, 1957; Sato & Yamane, 1955; Minkevich et al., 1956; Samsonov et al., 1961a; Arai et al., 1962). In the method patented by Alexander (1949a) titanium dioxide is first reduced to the metal, which is then nitrided.

Vapour phase deposition from a mixture of titanium chloride and ammonia or nitrogen + hydrogen is another widespread method of titanium nitride production. Thus, van Arkel & de Boer (1925), who pioneered this method, and Moers (1931) had their mixtures hold over a heated tungsten filament; see also van Arkel (1934) and Brager (1939a). Pollard & Woodward (194) and Pollard & Powlen (1952) quote the conditions required for the continuous flow method. Suchet (1960) claims to have prepared the nitride, Ti_3N_4, by passing a high frequency discharge through the mixture of vapours. Two step methods for producing the nitride coating on a metal substrate such as iron (Münster & Ruppert, 1952, 1953b, 1954; Ruppert, 1953a-b) and a single step

process for preparing the nitride with a uniform particle size (Hughes & Harris, 1957) are also reported. Other workers, e.g., Niederhauna (1962), have produced the nitride via the formation of an intermediate ammoniated complex. In the method patented by Rupert & Schweiler (1958, 1959) the temperature should be kept high enough (>600°, preferably, 900 - 1200°) to avoid complex formation. Lowe (1962) assigns the formula, $(NH_3)_6TiCl_4$, to the complex. According to Breger (1959b) there are two forms of the intermediate complex, α- and β-$TiCl_4.4NH_3$. The thermodynamics of the reactions has been discussed by Münster & Rupert (1959a); see also Münster, Rinck & Rupert (1956).

An advantage of the vapour deposition process is that a uniformly thin coating of nitride can be prepared on the surface of an object, whatever its shape, and also the reaction can be controlled accurately. The method, therefore, is used very widely in industry to improve mechanical and other properties of articles by coating them with titanium nitride and other refractory materials, e.g., see Löhberg et al. (1958) and Münster & Weber (1958).

Douglass et al. (1961) prepared titanium nitride by heating the oxide in ammonia + argon mixtures. Stepwise reduction gave a series of oxides of decreasing oxygen content and finally the nitride. No oxynitrides were detected.

Titanium carbide reacts with nitrogen to form the nitride. Solid solutions of TiC - TiN are reported to be formed at 1500 - 1800° during the reaction (Kellman & Covarita, 1950). According to these workers a nitrogen pressure greater than one

atmosphere is necessary for complete nitridation of the carbide. Agte & Moers (1931) report that TiN and TiC form mixed crystals. Portnoi & Levinskii (1963) also report the formation of solid solutions of TiC - TiN at 1900°. They failed to nitride the carbide completely. However, when metallic titanium is heated with a mixture of carbon and nitrogen, only the nitride is obtained. Similar results are given when titanium oxides are heated with carbon in the presence of nitrogen (Tacazu, 1931; Samsonov & Petrash, 1955). These observations are explained by the greater diffusion rate of nitrogen than of carbon. According to Blum (1962) titanium nitride can be sintered on a graphite support without being attacked. Other methods of titanium nitride production involving the nitridation of the carbide have been patented by Lapenchied (1959) and Société Belge du Titane (1953). The relative reactivities of titanium with nitrogen and carbon are consistent with the thermodynamic data of the carbide and nitride, Figure 1.2; see also Münster & Ruppert (1953a).

Starting materials for other methods of titanium nitride production include the hydride, sulphide, carbosulphide and reduced titanium halides (Duwez & Odell, 1950; Foster, 1952; National Lead Co., 1956; Jacobson, 1954).

1.11.2 The Titanium - Nitrogen System

A comprehensive summary of the titanium - nitrogen phase diagram studies is given by Brown (1964, p.160). Metallic titanium undergoes a phase change at 880° from a hexagonal close-packed lattice at lower temperatures to a cubic body-

centred one. Also reported is a second form of nitride, ϵ-titanium nitride, which has a tetragonal lattice.

Titanium nitride has a fairly wide region of solid solutions around the stoicheiometric composition (Münster & Sagel, 1953) extending to the compositions, $TiN_{0.42}$ (Ehrlich, 1949) and $TiN_{0.6}$ (Holmberg, 1962).

Holmberg (1962) reports the preparation of Ti_2N, which he considers to be the phase designated as the ϵ-nitride by Palty et al. (1954). Olsen (1947) assigns the formula, Ti_3N_4, to the compound he prepared. However, Schwarzkopf & Kieffer (1953, p.230) consider that the only nitride of titanium existing is TiN.

1.12.3 Kinetics of Nitridation

Kinetic studies on the nitridation of titanium have been carried out by several workers and are summarised by Brown (1964, p.172). The reaction follows a parabolic law, but initially there are deviations from it, the rate being almost linear for short reaction times (Pasilowski & Kohl, 1954). The rate-determining step in the parabolic reaction is considered to be the diffusion of nitrogen into the metal in the presence of a thin, permeable nitride film (Gulbransen & Andrew, 1949b,c). At 700 and 1000° the rate of reaction is not sensitive to the nitrogen pressure (up to 0.8 atmosphere) and is very much less than that of oxidation (Carpenter & Roswell, 1948; Gulbransen & Andrew, 1949c; Richardson & Grant, 1954). The difference can be interpreted on the basis of the relative stabilities of the oxide and nitride films on the metal surface.

The former flake off easily, whereas the latter do not. These observations are consistent with the Pilling & Bedworth (1923) Rule, Section 1.5.2.

According to Takaoura (1960), for the nitridation of titanium to proceed deep into the metal, it is favourable to have the temperature high but not above the transition point of the metal. The most practical nitriding temperature is about 900°. Smirnov & Kachinov (1960) report that the nitridation is deeper if conducted with nitrogen + argon mixtures. This is ascribed to the absence of a nitride layer at a reduced partial pressure of nitrogen. When the partial pressure of nitrogen is 0.[illegible] atmos., the nitrided layer consists of only a solution of nitrogen in α-titanium. On increasing the nitrogen partial pressure, nitride inclusions appear.

The high initial rate of nitriding of titanium has been attributed to the presence of small quantities of oxygen, which reacts about 50 times as fast as nitrogen. Wasilewski & Kehl (1954), however, from a study of the absorption of nitrogen in the temperature range 900 - 1170°, account for the initial deviation from the parabolic rate by postulating rupture of the surface layer of nitride. Above 950°, they observed two surface layers, an outer one of nitride and an inner one of α-titanium surrounding the core of the β-phase, cf. oxidation products of titanium (Jenkins, 1954). Below 950°, yet another phase, thought to be the ε-nitride, was observed. The ε-phase was observed at 1000° also by Turai & Someno (1966).

The foregoing authors suggest that the rate-controlling

process is the diffusion of atomic nitrogen through the nitride layer and the diffusion layer. The latter consists of a solid solution of nitrogen in α-titanium. Diffusion through the latter layer is more important during the initial reaction.

Wyatt & Grant (1954) studied the nitridation of titanium with ammonia and obtained similar results at times and temperatures lower than those required to get comparable results with nitrogen. However, this observation conflicts with that of Samsonov et al. (1961a).

1.11.4 Reactivity

The chemical properties of titanium nitride are summarised by Mellor (1927, p.119), Münster (1957), Brown (1964, p.167), Samsonov (1964a, p.236ff.), Shaffer (1964, p.232) and Juza (1966). Unlike ionic nitrides such as those of calcium and magnesium, titanium nitride is comparatively unreactive towards ordinary chemical reagents, especially at low temperatures. This is typical of interstitial nitrides, which therefore find wide applications as refractories, e.g., Pokorny (1965); see also Section 1.3. Schumb & O'Malley (1964) and Shamir & Rinenbcym (1966) report the results of the fluorination of titanium nitride.

According to Pollard & Woodward (1950) titanium nitride decomposes in a vacuum above 1000°. They also report that the compound oxidises rapidly in air at 1200°. However, Wasilewski & Kehl (1954) observe no decomposition in vacuo up to 1400°. From mass spectroscopic studies, Akishin & Khodeev (1962) deduce that the decomposition begins at 1700°. According to Roch et al. (1959), when titanium nitride vapourises, gaseous titanium and nitrogen

are formed.

The kinetics of titanium nitride oxidation have been studied by Samsonov & Goluteva (1956), Münster & Schlamp (1957a-c), Münster (1959) and Fedoseev & Nenkova (1962). The oxidation is governed by parabolic kinetics, and between 625 - 1075° gives scales consisting of rutile and possibly thin films of TiO - TiN solid solutions adjacent to the nitride. Platinum marker experiments show that the oxide - nitride interface moves away from the oxide - gas interface indicating that the diffusion of oxygen rather than that of titanium is rate-determining.

The chemical resistance of titanium nitride finds many applications for it as a refractory (Münster, 1957; Samsonov, 1964a, p.339).

Further studies on the oxidation of titanium nitride by calcining in air are reported in Chapter 6.

1.12 Zirconium Nitride, ZrN

1.12.1 Formation

Zirconium nitride can be produced by methods similar to those for titanium nitride (Mellor, 1927, p.120; Brown, 1964, p.177). In the direct nitridation of the metal, temperatures varying from 700 to 2 000° have been used (Agte & Moers, 1931; Glaunsing, 1932; Fujiwara, 1950; Chiotti, 1952; Clair, 1960; Samsonov et al., 1961a; Kough, 1962; Salibekov et al., 1964). The nitridation has also been effected with ammonia gas (Chiotti, 1952; Wyatt & Grant, 1957). Samsonov et al. (1961a) found that the reaction is slower with ammonia.

The van Arkel - de Boer (1925) method of depositing the nitride from the chloride in the vapour phase is also applicable (Moers, 1931; Campbell et al., 1949). Other starting materials for zirconium nitride production include the bromide, hydride and oxide (Schneider et al., 1953; Foster, 1952; Sauer & Odell, 1950; Alexander, 1949b). According to Portnoi & Levinskii (1963), zirconium, like titanium, reacts preferentially with nitrogen rather than with carbon, because of the greater diffusion rate of the former. Blum (1962) found that zirconium nitride, unlike titanium nitride, is attacked by carbon at high temperatures forming the carbide. These observations can be correlated with the thermodynamic data of the compound, cf. titanium nitride.

1.12.2 The Zirconium - Nitrogen System

Phase diagram studies of the Zr - N system are summarised by Brown (1964, p.178); see also Domagala et al. (1956). Two forms of metallic zirconium are reported, an α-form having a hexagonal close-packed structure stable up to 862° and a β-form with a cubic body-centred structure above this temperature. Metallic zirconium dissolves nitrogen up to an atomic percentage of 20 (de Boer & Fast, 1936; Jaffe & Campbell, 1949). Above this limit the nitride is formed. The absorption of nitrogen, like that of oxygen, raises the transition point of the metal. Zirconium nitride has a homogeneity range varying from $ZrN_{0.46}$ at 1555° to ZrN below 650°. According to Ishii (1943) and Ishii & Wada (1943) there are two modifications of ZrN, but this has not been confirmed by other workers.

1.12.3 Kinetics of Nitridation

The kinetics of nitridation of zirconium has been investigated by various workers (Brown, 1964, p.179). Sultranoen & Andrew (1949a,c) report that the reaction is much slower than the corresponding one with oxygen or hydrogen. They observed that the rate is independent of nitrogen pressure in the temperature range 400 - 800°, and ascribe this to the formation of a surface nitride layer. This observation was made also by Kravnieks (1958) at higher temperatures. From a study of the reaction at 900 - 1100°, Baliet et al. (1953, 1954) report the formation of a β-solid solution and a thin layer of α-solid solution surrounded by zirconium nitride. The rate of diffusion of nitrogen into zirconium is much lower than that of oxygen. Near the transition point there is a marked increase in the absorption of both gases (Guldner & Cooten, 1960; Meyer & Robertson, 1960). Salibekov et al. (1964) studied the nitridation of zirconium at 1400 - 1700°. They observed the formation of an outer layer of nitride, a second layer of α-solid solution, and a base mixture of β-solid solution with some α-solid solution precipitated as a result of cooling. According to all the above workers the reaction rate is parabolic. Their results suggest that the rate-controlling process is the diffusion of nitrogen into the metal.

1.12.4 Reactivity

The chemical properties of zirconium nitride are summarised by Keller (1927, p.120), Samsonov (1964a, p.2[illegible] ff.) and Chaffee (1964, p.3[illegible]5). These properties are similar to

those of titanium nitride, Section 1.11.4. The use of zirconium nitride as a refractory material is based on these properties (Münster & Weber, 1958; Samsonov, 1964a, p.340).

Shaffer (1964, p.309) reports that zirconium nitride melts without decomposition. However, from mass spectroscopic data, Akishin & Khodeev (1962) deduce that decomposition begins at 1800°. According to Hoch et al. (1959), zirconium nitride decomposes to solid zirconium and nitrogen, cf. titanium nitride.

When heated in air zirconium nitride oxidises rapidly, especially at high temperatures (Hayes & Robertson, 1949). This reaction has been investigated further in the present work, Chapter 6.

Chapter 2

EXPERIMENTAL TECHNIQUES

The experimental techniques used in this work, including the principles underlying them and a description of the apparatus, are summarised in this chapter.

2.1 X-ray Diffraction

A comprehensive summary of the theory and practice of X-ray diffraction techniques is given by Weiser et al. (1960, pp.87-322).

2.1.1 Theory of X-ray Diffraction

A crystal consists of a regular three-dimensional arrangement of atoms in space. Points having identical surroundings in the structure are called lattice points, and a collection of such points in space forms the crystal lattice. If neighbouring lattice points are joined together one obtains the unit cell, i.e., the smallest repeating unit of the structure. Sometimes it is more convenient to choose a larger repeating unit, i.e., a centred cell. In general the shape of the unit cell is a parallelepiped, but in some cases, depending on the symmetry of the crystal, it can have a more regular shape, e.g., a rectangular box, or in the extreme case, a cube. The shape of the unit cell is completely described by the lengths of its three edges or axes and the angles between them. Conventionally, the axes are named $\underline{x}$, $\underline{y}$, $\underline{z}$ or $\underline{a}$, $\underline{b}$, $\underline{c}$ and the angles α, β, γ; the angle between $\underline{y}$ and $\underline{z}$ is α, etc.

Crystals are classified into seven classes according to their symmetry. The unit cell dimensions of a crystal obey

Table 2.1 Classification of Crystals

Crystal Class	Conditions Limiting Cell Dimensions	Minimum Symmetry
Triclinic	$a \neq b \neq c$ $\alpha \neq \beta \neq \gamma \neq 90^\circ$	-
Monoclinic	$a \neq b \neq c$ $\alpha = \gamma = 90^\circ \neq \beta$	One 2-fold axis or one plane of symmetry
Orthorhombic	$a \neq b \neq c$ $\alpha = \beta = \gamma = 90^\circ$	Two perpendicular 2-fold axes or two perpendicular planes of symmetry
Tetragonal	$a = b \neq c$ $\alpha = \beta = \gamma = 90^\circ$	One 4-fold axis
Hexagonal	$a = b \neq c$ $\alpha = \beta = 90^\circ$, $\gamma = 120^\circ$	One 6-fold axis
Trigonal	$a = b = c$ $\alpha = \beta = \gamma \neq 90^\circ$	One 3-fold axis
Cubic	$a = b = c$ $\alpha = \beta = \gamma = 90^\circ$	Four 3-fold axes

certain relationships depending on the crystal class. These are set out in Table 2.1.

Various sets of parallel planes can be drawn through the lattice points of a crystal. Each set of planes is identified by a set of three integers, namely, the Miller indices, h, k, l, corresponding to the three axes a, b, c, respectively. The index, h, is the reciprocal of the fractional value of the intercept made by the set of planes on the a axis, and so on.

When a crystal interacts with an incident beam of X-rays, the lattice acts as a diffraction grating, because its dimensions are of the same order of magnitude as the wavelength of X-rays. A diffracted beam emerges from a particular set of lattice planes when their scattering is in phase. This is governed by Bragg's law:

$$\lambda = 2d \sin \theta$$

where λ = wavelength of X-rays

d = interplanar spacing

θ = angle of incidence = angle of diffraction.

d is related to the unit cell dimensions of the crystal and the Miller indices of the set of planes. Thus, the measurement of Bragg angles can lead to the determination of lattice constants.

When the crystal is large, i.e., there are a large number of lattice planes in each set, the diffracted beam appears at a sharp angle. However, with sufficiently small crystals, diffraction takes place over a range of Bragg angle. Thus, X-ray line broadening provides information on crystallite size.

If a single crystal of a substance is rotated in a beam of monochromatic X-rays, the diffraction pattern forms a series of spots on a photographic film. However, if the sample is in the form of a powder with the crystallites in random orientation, the diffracted beams lie along the surfaces of a set of coaxial cones. The pattern can then be recorded photographically in a powder camera, or by a rotating Geiger counter as in a diffractometer.

The distribution with respect to Bragg angles and intensities of the diffracted beams is characteristic of a particular structure and can be used therefore as a means of identification. The X-ray powder diffraction patterns of most crystalline substances are recorded in the ASTM Tables which can be used to identify "unknown" substances. The powder

pattern of a mixture of crystalline substances consists of the superimposed patterns of the individual structures. Therefore, the method can be used to identify the different components of a mixture also.

An unknown crystal structure can, in principle, be determined by an analysis of its X-ray diffraction pattern (e.g., Jayaweera, 1964). The set of Bragg angles is sufficient to deduce the unit cell dimensions of the lattice. The symmetry elements of a crystal structure are summarised in its space group, a knowledge of which reduces the number of parameters to be determined in the structure analysis. The presence of symmetry elements involving translation results in systematic absences of "reflections" from certain sets of lattice planes. Such absences give information on the space group of the unknown structure. To obtain the atomic positions the intensities of the reflections need to be taken into account.

2.1.2 X-ray Generators

Two X-ray generators of different design were used for the diffraction experiments, namely, (a) a Solus-Schall unit connected to a sealed tube containing the filament and target, (b) a Raymax 60 generator manufactured by Newton Victor Ltd., with interchangeable target and replaceable filament and kept continuously pumped by an oil diffusion pump coupled to a rotary pump. A sealed tube generator has a more stable X-ray output than a continuously pumped one. The radiation used was Copper $K\alpha$, wavelength 1.542Å. This was obtained by having a copper target and a nickel filter to remove the $K\beta$ component.

2.1.3 Debye - Scherrer Powder Diffraction Camera

The phase compositions of crystalline samples were examined by recording their powder diffraction patterns in two ways, (a) by a photographic method, (b) using an X-ray diffractometer with attached counter and ratemeter.

For the photographic method of recording diffraction data, a Debye - Scherrer camera, of 9 cm. diameter and manufactured by Unicam Instruments Ltd., was used. The film was mounted according to the van Arkel method. The sample for X-ray examination was prepared by loosely filling a glass capillary tube about 0.9 mm. in diameter and 1 cm. in length with the crystalline powder, and sealing both ends of the tube with an adhesive. The sample was mounted vertically along the camera axis and centred by means of two push - pull screws set at right angles to each other. The sample was rotated about the camera axis so bringing each set of lattice planes of every crystallite to a diffracting position many times during an exposure. Thus, variations in the incident X-ray intensity were taken care of. In order to eliminate the scattering of X-rays by air the camera was evacuated by having it continuously pumped during the exposure. The exposures varied up to several hours. The powder camera was used in conjunction with the Raynax [illegible] generating unit.

Kodirex X-ray film were used in the powder camera. After exposure the film was developed for 5 min. at 20° in Kodak D-19[illegible] developer, rinsed with water, fixed in Kodak [illegible]-40 fixer, washed in running water for [illegible]h and hung up to dry. The fixing time was

twice the time required for the milkiness on the film to disappear. This was usually 5 min. The films were examined and measured on an illuminated screen fitted with a scale. The intensities of the powder diffraction lines were visually compared.

2.1.4 The Counter Diffractometer

The second method of recording powder diffraction patterns was to use a Seifert-Schall X-ray diffractometer fitted with a Geiger counter and connected to a Lanax ratemeter and a chart recorder. The diffractometer works on the focussing principle described by Bragg and Brentano. The diameter of the diffractometer is 50 cm.

The sample for examination was prepared by pouring a suspension of the crystalline powder in acetone onto a glass slide. On evaporation of the organic liquid, the powder remained adhered to the slide. Sometimes it was necessary to mix an adhesive with the suspension. The glass slide containing the sample was mounted vertically at the centre of the diffractometer and rotated at half the speed of the detector. Thus, the sample was always tangential to the circle defined by the collimator diaphragm, the centre of the sample and the counter diaphragm. The diffracting positions were indicated on the ratemeter and also registered on the chart recorder. The intensity of the diffracted beams determined the readings on the ratemeter and the area under the peaks on the chart recorder. Since the peaks are recorded at different times by the diffractometer, it is necessary to have a stable incident

beam of X-radiation. The sealed tube type generator was used, therefore, with the diffractometer.

2.2 Electron Microscopy and Diffraction

Comprehensive accounts of the theory and practice of electron microscopy and diffraction are given by Zworykin et al. (1945), Ray (1965) and Hirsch et al. (1965).

2.2.1 Theory of Electron Microscopy and Diffraction

A beam of electrons possesses wave properties, the wavelength being given by the de Broglie relationship:

$$\lambda = \frac{h}{p} = \frac{h}{mv} \qquad \ldots\ldots\ (i)$$

where, λ = wavelength
h = Planck's constant
m = electron mass
v = electron velocity.

If the accelerating potential difference is V, the energy, E, of an electron is given by:

$$E = \tfrac{1}{2}mv^2 = Ve \qquad \ldots\ldots\ (ii)$$

where, e = electron charge.

Eliminating v from equations (i) and (ii),

$$\lambda = \frac{h}{\sqrt{(2meV)}}$$

A relativity correction has to be applied to this equation to account for the variation in electron mass with velocity, which itself depends on the voltage. In practice, however, the wavelength, if required, is determined by recording the diffraction pattern of a substance with known unit cell dimensions. This enables a single factor, the camera constant, $L\lambda$, to be calculated, where L is the effective camera length. If the instrument is used at the same accelerating voltage,

then λ remains constant. At an accelerating voltage of 100kV, the wavelength of an electron beam is 0.037Å.

Because electron beams possess wave properties, they can be used in a magnifying instrument with electromagnetic fields as lenses, just as light waves are used in the optical microscope with glass lenses. The theoretical limit of resolution of a microscope is half the wavelength of the radiation used. For an optical microscope this is about 2000Å. The shorter wavelength of electrons enables a much greater resolution to be achieved on the electron microscope, although this is still very far from the theoretical limit.

The construction of an electron microscope is, in principle, similar to that of the optical microscope, Figure 2.1. It involves a cathode, C, which provides a source of illuminating electrons. A high voltage applied between C and the anode, A, accelerates the electrons, which pass through a small hole in A. The condenser lens, Lc, converges the electron beam onto the specimen, S, situated in the magnetic field of the objective lens, Lo. An image, I1, is formed due to magnification by the objective lens. This is followed by further magnification by the projector lens, Lp, to form a final image, I2, on a screen, S. The microscope used in this work and described in the next section consists of two more lenses (not shown in the figure), namely, a diffraction lens and an intermediate lens, placed between the objector and the projector. The intermediate lens enables a high overall magnification to be reached without the magnifications of the individual lenses having to be excessively large. It also

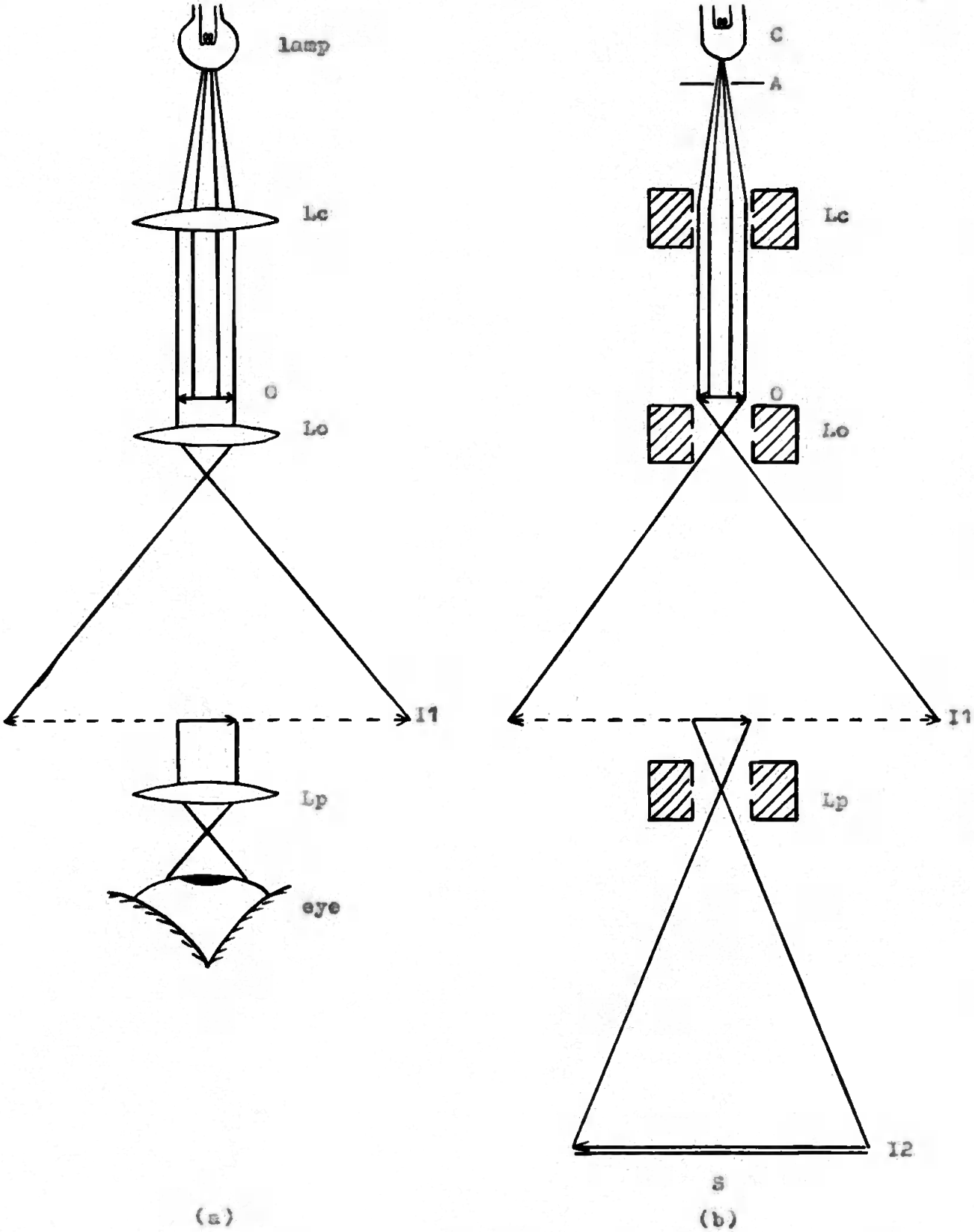

Figure 2.1 Analogy between (a) optical and (b) electron microscopes (diagrammatic).

helps to keep the length of the instrument short and to attain easily a continuously varying magnification within wide limits. The diffraction lens is energised only when diffraction patterns or low magnifications are required of the sample.

Because electrons are scattered on collision with gas molecules, it is necessary to have a high vacuum in the instrument. Focussing is achieved by the variation of the strengths of the magnetic fields by changing the currents generating them. There is provision for placing a camera within the instrument so that the image produced can be recorded.

Electron diffraction by a crystal is similar in principle to that of X-ray diffraction, but there are some important differences. First, because electrons are highly absorbed by matter, only very thin crystals can be used. Also, because of the small wavelength of electron waves, a stationary crystal will give a diffraction pattern consisting of "reflections" from a plane of reciprocal lattice points. However, for a polycrystalline specimen in random orientation, the diffraction pattern consists of the powder rings, provided the sample is sufficiently thin.

2.2.2 Apparatus

The Philips EM100B electron microscope (Van Dorsten, Nieuwdorf & Verhoeff, 1950) was used for examining microcrystalline powders. The instrument has a resolution of 25Å. The pumping system of the microscope consists of a provacuum rotary pump, a mercury diffusion pump and an oil diffusion pump. A camera preloaded with 35mm. film and placed inside the microscope enables sections of the sample to be micrographed. The magnification is varied by

adjusting the currents to the electromagnetic lenses. There are also controls for focussing and for moving the sample holder so that different areas of the grid can be observed. An image of a section of the sample is thrown on the fluorescent screen directly in front of the observer. When a micrograph of the image on the screen is required the camera is lowered into position and the shutter opened. The exposure is judged according to the brightness of the image and varies up to several seconds. The magnification is determined by reading a scale and referring to standard tables. When a diffraction micrograph is required the appropriate area of the sample is selected by means of diffraction selection diaphragms; the diffraction lens is switched on and the intermediate lens switched off. Diffraction micrographs require longer exposures because of their lower intensity. Once the instrument is ready for use, samples can be easily changed by removing the grid holder and inserting another one carrying a different sample. The evacuation time for this operation is a fraction of a minute. The microscope was usually operated at 60kV.

Films of carbon and metal were prepared in a "Speedivac" High Vacuum Coating Unit 12E6, manufactured by Edwards High Vacuum Ltd. The unit consists of a glass workchamber, evacuated by an oil diffusion pump backed by a rotary pump. Inside the chamber electrical leads are fitted for striking an arc across carbon electrodes and for the vapour deposition of metal films from a filament. The instrument panel has gauges for reading the pressure inside the chamber and controls for the electricity supply to the leads inside the chamber.

2.2.3 Preparation of Samples

Samples of the crystalline powders for microscopic examination were made by dispersing the particles on a carbon film supported on a copper grid. The thickness of the carbon film was of the order of 200Å. The copper grid was 3mm. in diameter and contained a square mesh. The length of the side of a square was 100μ. The grid was handled always by a pair of forceps with a fine grip.

The carbon film was deposited on a mica surface by striking an electric arc between spectroscopically pure carbon electrodes in the high vacuum coating unit. The arc voltage was 10 volts and the current 60 amperes. The arc was struck in about 8 bursts, each of approximately 3 seconds duration, with intervals of about 10 seconds between successive bursts to cool the electrodes. The pressure inside the chamber was kept below 10^{-4} mm. of mercury.

The carbon film was floated off on water by holding the mica plate at an angle of about 30° and with the film on its upper surface, and gradually lowering the plate below the water level until it sank. This operation of stripping the film off the mica is due to the surface tension of the water. It was facilitated by cutting off the edges of the mica sheet after deposition of the film and contaminating the mica sheet by breathing onto it before deposition.

A section of the floating film was picked up by a copper grid and the residual water absorbed by placing the grid carrying the film on filter paper. The grid and film were

transferred to a vertical cylindrical holder and locked in position with a cylindrical cap. The latter had an open end so exposing the grid. A suspension of the microcrystalline sample was made in acetone and the particles dispersed by means of an ultrasonic dispersion unit. A drop of the suspension was placed on the copper grid carrying the film and the whole assembly was placed under an infrared lamp to accelerate the evaporation of the acetone. Finally the sample was transferred into a microscope grid holder, which was inserted in the instrument.

The metal films were prepared by first depositing a carbon film on mica as above. The mica plate was then fixed inside the high vacuum unit at about 10cm. from a tungsten filament of suitable shape ("helix" for metal ribbon, "basket" for turnings and rasps). The metal to be deposited was placed in the filament and the system evacuated. The filament current was increased sufficiently slowly to avoid rapid temperature increases and permit metal stresses to be relieved, so that the turnings did not fly off the filament before evaporation. When the metal evaporated the brightness of the filament was observed to decrease temporarily due to the heat lost with the evaporating metal. The metal film together with the carbon base was stripped off the mica plate and floated on water as described for the carbon film. A section of the film was picked up on a copper grid and dried under the infrared lamp; it was then ready for use. Sometimes the metal was directly deposited onto a carbon film on a copper grid placed at the base of the

vacuum unit.

Before a series of evaporations was carried out with a filament, the latter was "flashed", i.e., its temperature raised to remove dirt etc., by passing a slightly higher current through it than was subsequently used for metal evaporation. This operation too was carried out at low pressure.

2.3 Gas Sorption

The quantity of gas adsorbed on a substance depends on, inter alia, the specific surface (i.e., the surface area per unit mass) of the adsorbent. Thus, gas sorption measurements provide information on the average particle size of a powder. A general account of the subject is given by Gregg & Sing (1967).

2.3.1 BET Method

A widely used method of surface area determination is one due to Brunauer, Emmett & Teller (1938). The BET equation given:-

$$\frac{p}{x(p_o - p)} = \frac{c - 1}{x_m c} \cdot \frac{p}{p_o} + \frac{1}{x_m c}$$

where p = pressure of adsorbate vapour in equilibrium with adsorbent,

p_o = s.v.p. of adsorbate vapour,

x = amount of vapour adsorbed,

x_m = capacity of filled monolayer,

c = a constant.

Adsorption isotherms are classified into five types, of which type II isotherms give the best agreement with the

* Refer also de Boer (1969), Joy (1965) and British Standards 4359 Part 2 (1968). See supplementary list of references.

BET equation over limited ranges of relative vapour pressure (Gregg, 1961, pp.31, 56). Thus, a plot of $\frac{p}{x(p_o - p)}$ against $\frac{p}{p_o}$ results in a straight line graph of slope $\frac{c - 1}{x_m c}$ and intercept $\frac{1}{x_m c}$. Elimination of c from these two expressions gives x_m. The adsorbate can be measured either gravimetrically or volumetrically (Gregg & Sing, 1967, p.310).

The specific surface, S, is related to x_m by the equation:-

$$S = \frac{x_m}{M} \cdot N \cdot A_m$$

where, M = molecular weight of adsorbate,

N = Avogadro number,

A_m = cross-sectional area of an adsorbate molecule in a completed monolayer.

For a substance consisting of cubo-shaped crystallites, the average particle size, l, is related to S by:-

$$S = \frac{6}{\rho l}$$

where ρ is the density of the adsorbent. The same relationship is valid for calculating the equivalent spherical diameter. Similar relationships can be derived for plate- and needle-shaped crystallite powders.

2.3.2 Apparatus

The sorption balance used is based on one designed by Gregg (1946, 1955). The balance arms are made of glass and supported on needles. One arm of the balance supports buckets for the sample and counterweights, the other arm either a solenoid or magnet enclosed in glass and surrounded

by an external solenoid. The whole assembly is enclosed in glass and connected to a system of evacuation pumps, gauges and gas reservoirs.

The current in the external solenoid is varied to obtain the balance point, which is observed by noting the position of a horizontal metal pointer attached to the balance arm against a similar fixed pointer. The instrument is calibrated by measuring the current required to observe the null point for known weights.

2.3.3 Measurement of Sorption Isotherms

The sample was placed in the specimen bucket and outgassed to remove physically adsorbed vapour. This was usually carried out at 200° by surrounding the balance limb with a furnace (Clasmon, 1964).

The adsorbate was nitrogen gas (supplied by [illegible] Ltd.) and the isotherms were measured at -195°. A Dewar flask containing boiling liquid oxygen was placed around the balance limb. The weight of the sample was determined in vacuo, and doses of nitrogen introduced into the system. Simultaneous readings of sample weight and nitrogen gas pressure were taken after equilibrium was reached.

All the nitrogen isotherms recorded in the present work were of Type II.

2.4 Volumetric Analysis

The calcium content of the solid product in the lime - urea reaction was determined by titration against

EDTA using murexide as indicator (Vogel, 1964, p.436; Blenard, 1964).*

The zinc and cadmium contents in the ammoniated solutions of the respective oxides were determined by titration against potassium ferrocyanide using 3:3'-dimethyl naphthidine sulphonic acid as indicator (Vogel, 1964, p.461).

2.5 Digital Electronic Computation

Routine mathematical computations involved in this work were carried out with the aid of two digital computers, namely, a PDP 1070 Computer and an IBM 1130 Computer. The former was programmed in a language specific to this machine, the latter in Fortran.

* See supplementary list of references

Chapter 3

CALCIUM AND MAGNESIUM NITRIDES

3.1 Preparation and Nitridation of Metal Films

3.1.1 Materials

BDH magnesium ribbon and Kahlbaum calcium turnings were used in the preparation of the metal films.

BDH magnesium turnings (for Grignard reactions) and BOC nitrogen gas were used in the nitridation.

3.1.2 Procedure

The magnesium and calcium films were deposited by evaporation from a heated filament and examined under the electron microscope. The copper grids carrying the films were transferred into a glass vessel which was evacuated and flushed with nitrogen gas at room temperature. The nitrogen pressure was then reduced to $\frac{1}{2}$ - $\frac{1}{4}$ atmosphere by pumping out the excess gas from the vessel. The whole assembly was lowered into a furnace pre-set at a given temperature. After heating for given lengths of time the vessel was taken out of the furnace and allowed to cool to room temperature. Finally the grids carrying the nitrided films were re-examined on the microscope.

The vapour deposition of magnesium film and its nitridation was followed by an attempt to nitride the metal in bulk. Magnesium turnings were heated in a nitrogen atmosphere at 900° for $3\frac{1}{4}$ h. at pressures similar to those used with films. The product was shaken with acetone to detach the nitride layers, which were examined on the

electron microscope.

3.1.3 Results

Electron micrographs and diffraction patterns of magnesium film and the changes produced therein on nitridation are presented in Plates 3.1 - 3.8. The results for calcium film are shown in Plates 3.9 - 3.12.

The attempt at nitriding magnesium turnings resulted in a small quantity of product only. The fragmentation of the non-protective nitride layers gave greater separation of individual crystallites. Their size ranges extended to those produced at higher temperatures (up to 600°), where magnesium vapourisation and nitride sintering are more extensive (e.g., cf. Plate 3.33). The quantity of nitride obtained by the nitridation of metal turnings was insufficient to give representative electron micrographs.

3.1.4 Discussion

The condensed metal films generally gave good microstructural uniformity, but tended to grow irregularly when they became too thick. The electron micrograph of a more uniform film is shown in Plate 3.1. Such a film gives a regular diffraction pattern, Plate 3.2. In contrast, Plate 3.3 shows a less uniform film and Plate 3.4 its diffraction pattern.

During the initial stages in the nitridation of magnesium films at 400° localised stresses arise due to the crystal structure and volume changes accompanying the reaction (see Table 1.3), as seen in Plates 3.5 - 3.6.

More extensive nitridation leads to rupture of the film and aggregation, Plate 3.7. This is more pronounced at higher temperatures (500°). Plate 3.8 shows a single aggregate.

Calcium films possess similar properties to those of magnesium. Thus, their uniformity decreases with increasing thickness. Plate 3.9 shows a uniform film and Plate 3.10 its diffraction pattern. Nitridation is slower with calcium than with magnesium film, e.g., there is little change in appearance (Plate 3.11) during the initial stages of nitridation at 400° (cf. Plates 3.5 -3.7), but more rapid reaction at 450° leads to film rupture and aggregation, Plate 3.12.

The observations with respect to the nitridation of magnesium turnings are consistent with those made by earlier workers and summarised in Section 1.7. The reaction of nitrogen with the metal in bulk is not sufficiently extensive under the experimental conditions used. The faster reactions with the films are interpreted on the basis of their higher activity, cf. Section 1.6. This is consistent with the observations of earlier workers, e.g., compare with the results of Roberts & Tompkins (1959, 1960) and Chandrasekaraiah & Margrave (1961) on calcium nitridation, Section 1.8.1.

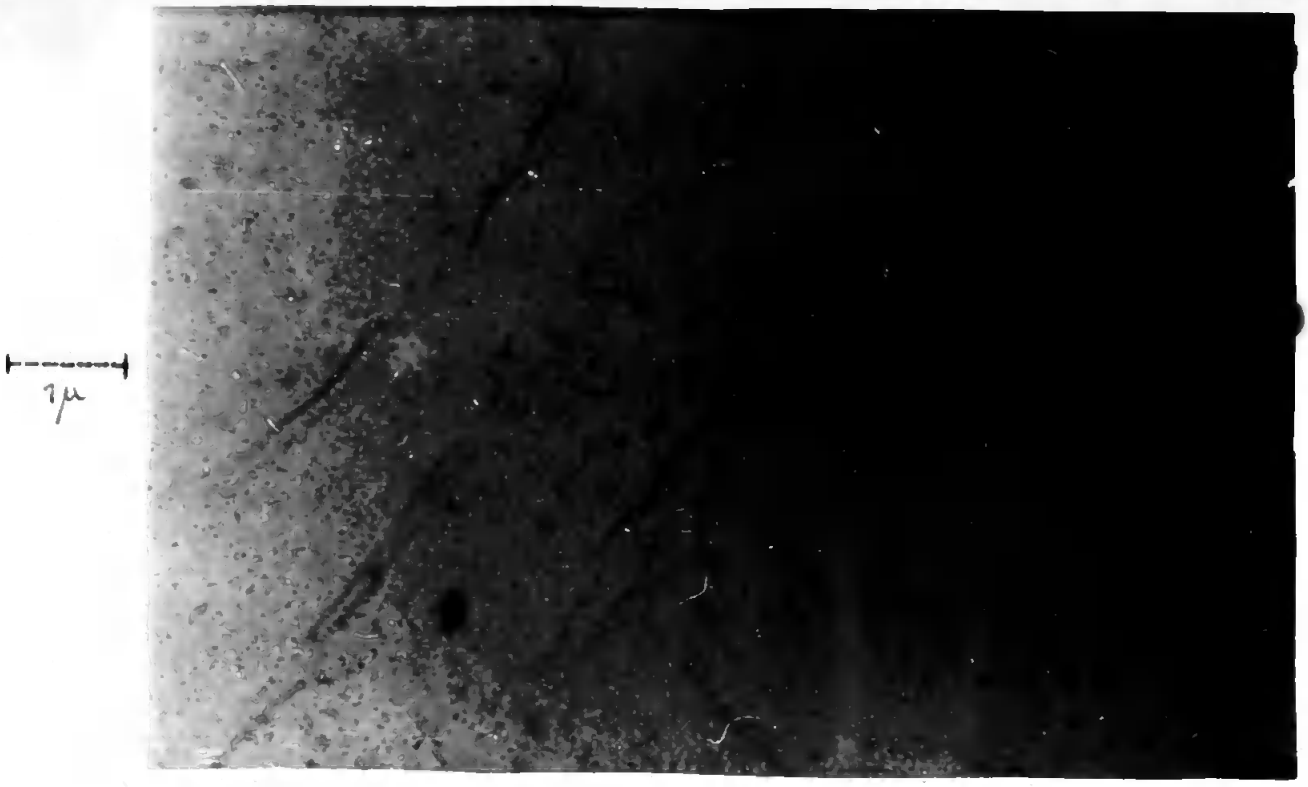

Plate 3.1 More uniform, vapour deposited magnesium film
x 15,000

Plate 3.3 Less uniform, vapour deposited magnesium film
x 15,000

T

A76
A65.

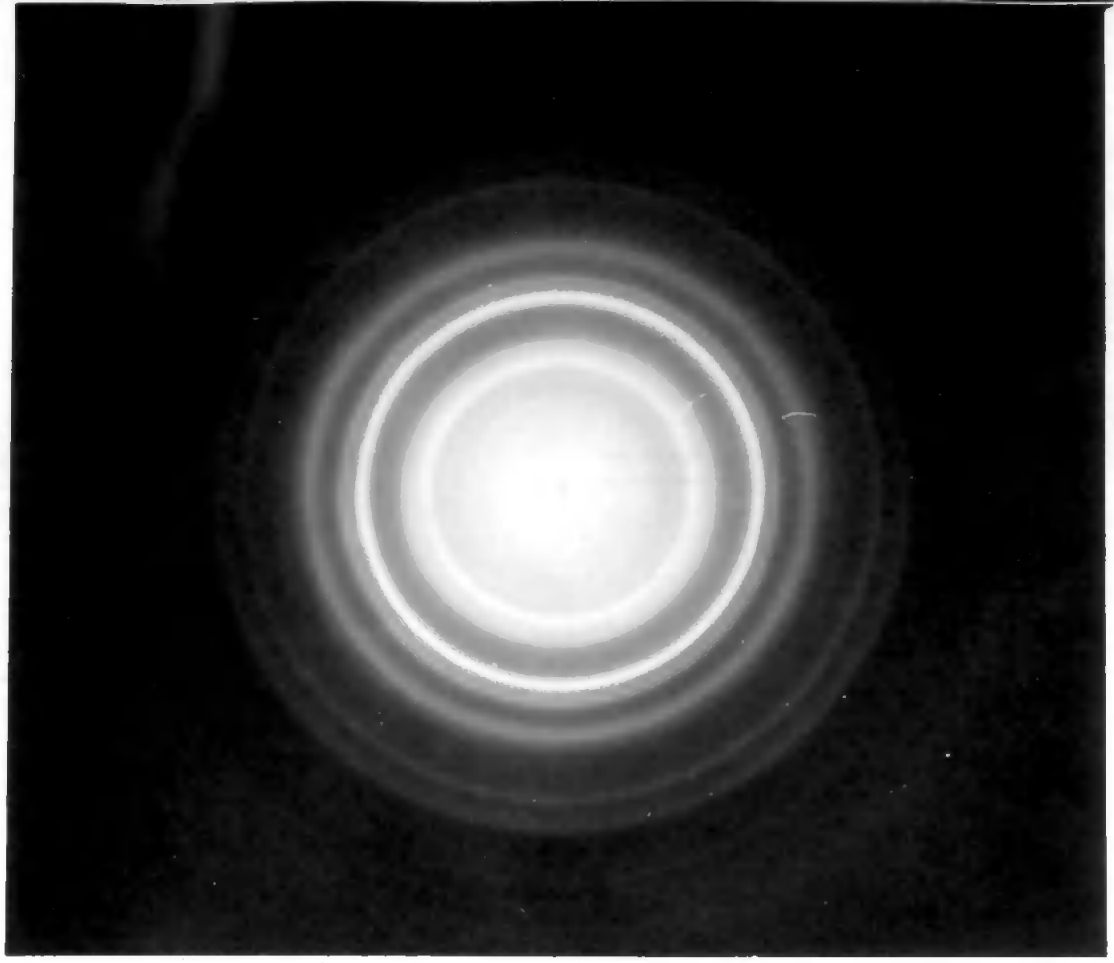

Plate 3.2 Electron diffraction pattern of more uniform magnesium film shown in Plate 3.1

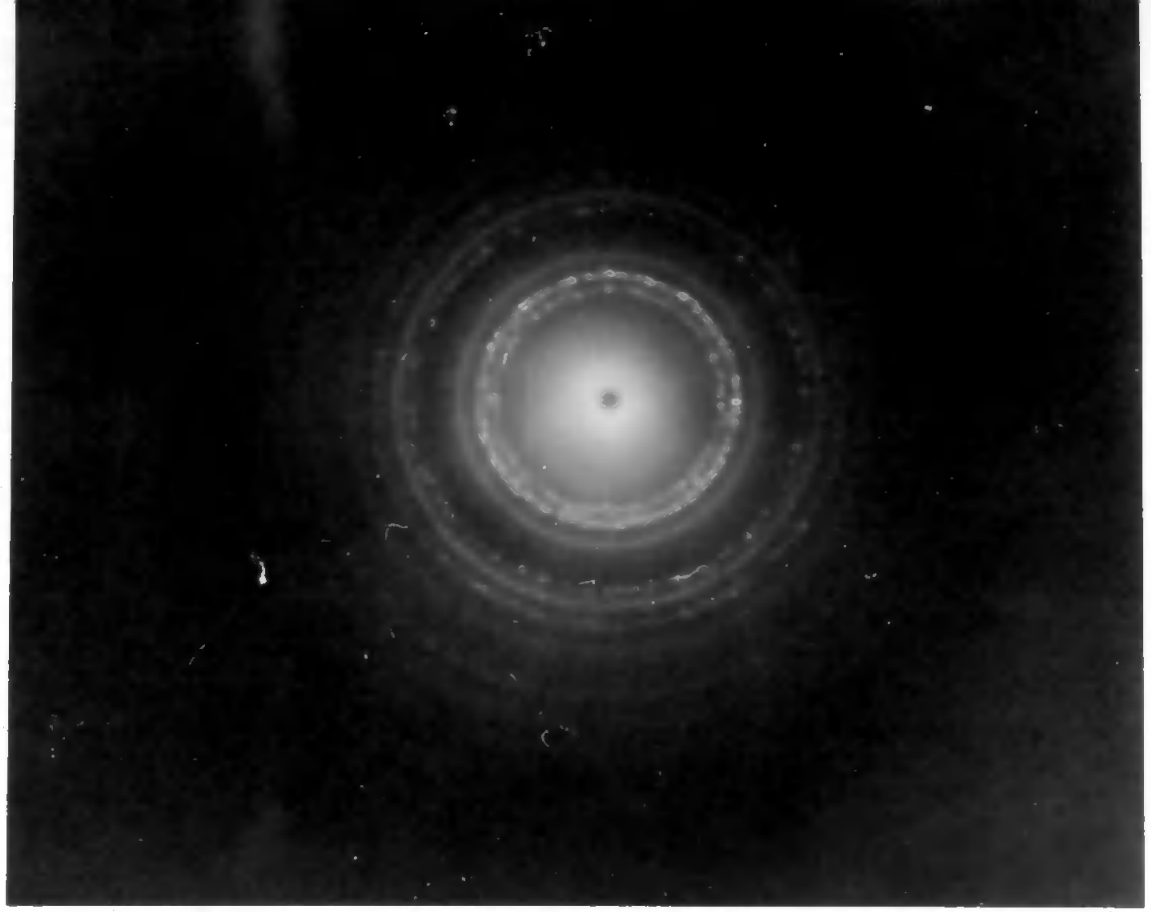

Plate 3.4 Electron diffraction pattern of less uniform magnesium film shown in Plate 3.3

A67

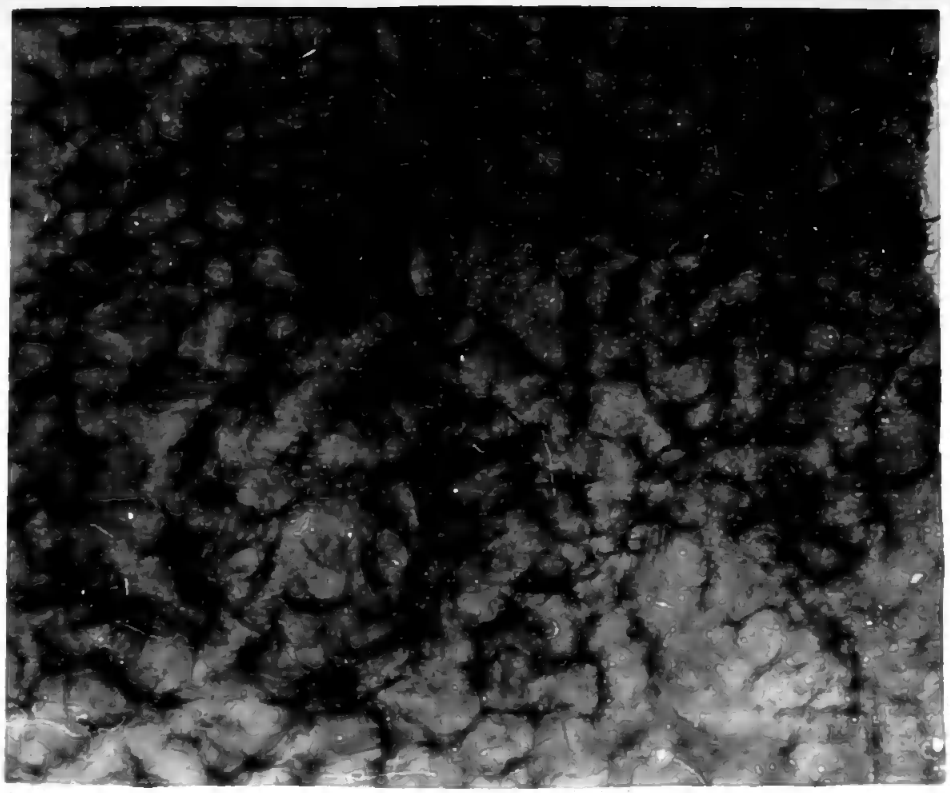

1μ

Plates 3.5 (above) and 3.6 (below) Vapour deposited magnesium film (shown in Plate 3.1) heated in nitrogen at 400° for ½ h. showing initial stages of nitridation x 15,000

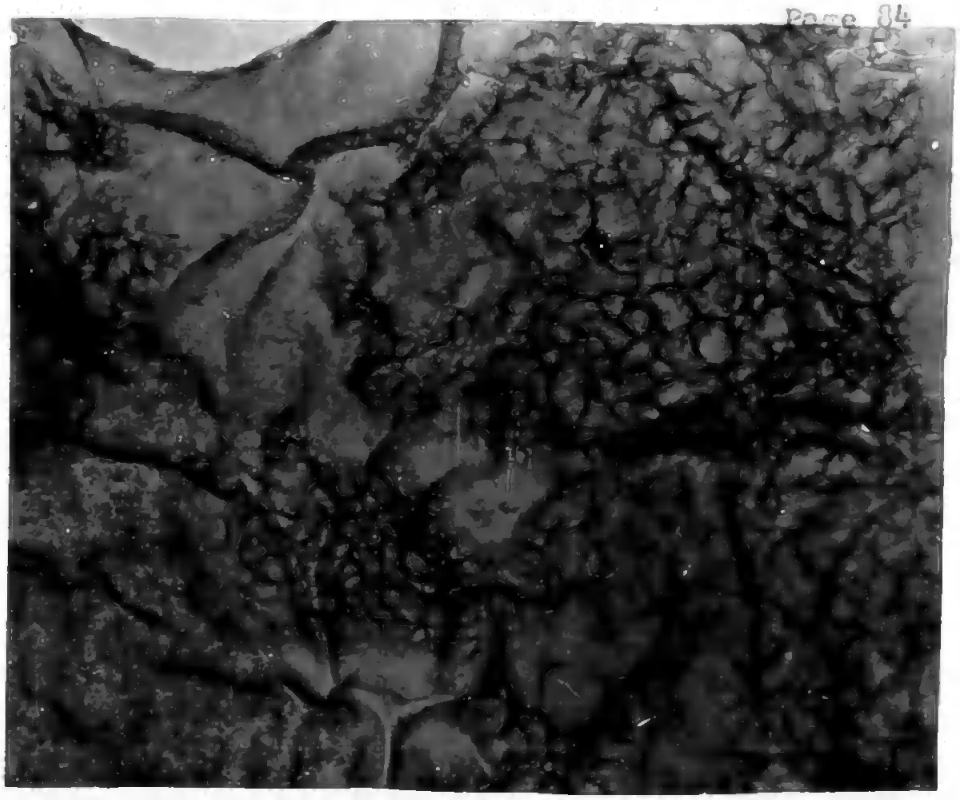

1μ

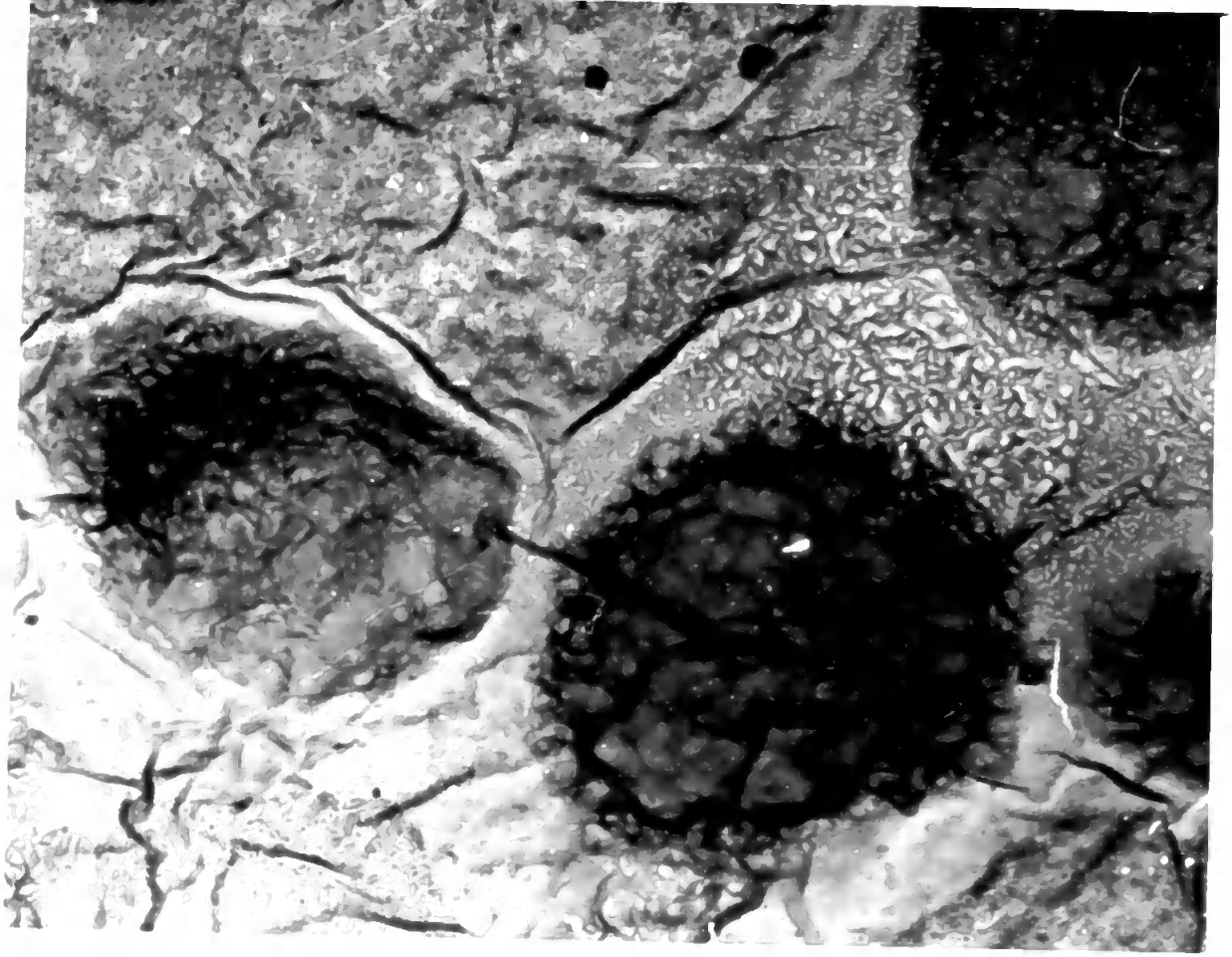

1 μ

Plate 3.7 Vapour deposited magnesium film (shown in Plate 3.1) heated in nitrogen at 400° for ¾ h. showing more extensive nitridation (cf. Plates 3.5 and 3.6) x 15,000

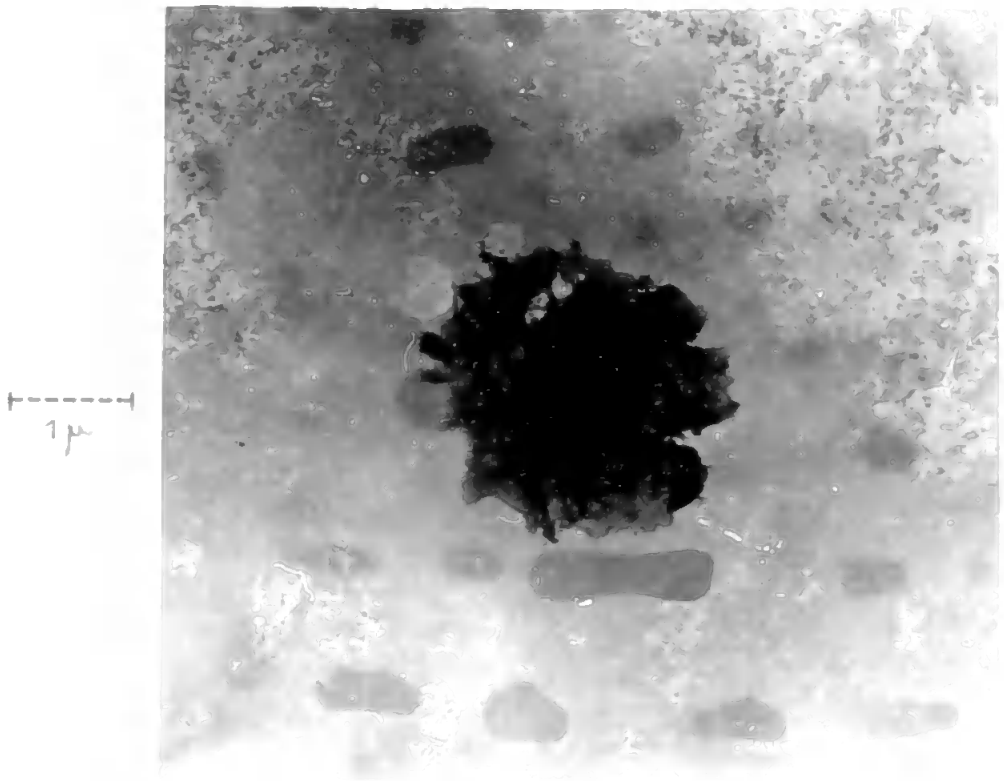

Plate 3.8 Magnesium film nitrided at 500° for 1½ h
x 15,000 (cf. Plates 3.5 - 3.7)

Plate 3.9 Vapour deposited calcium film
x 15,000

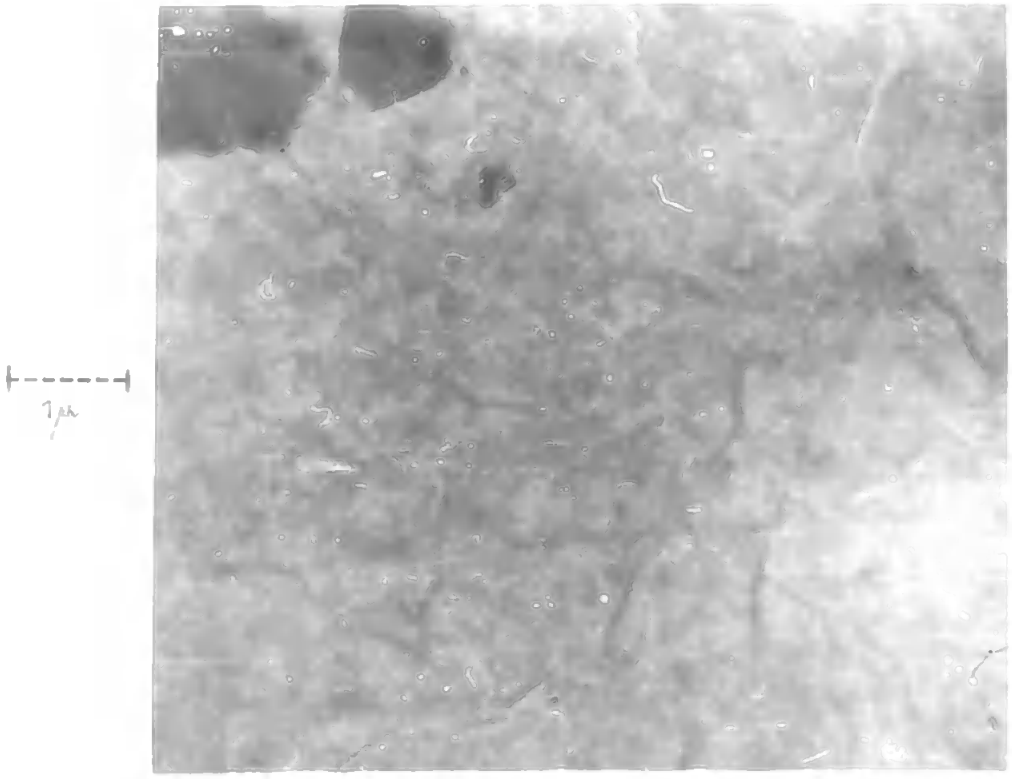

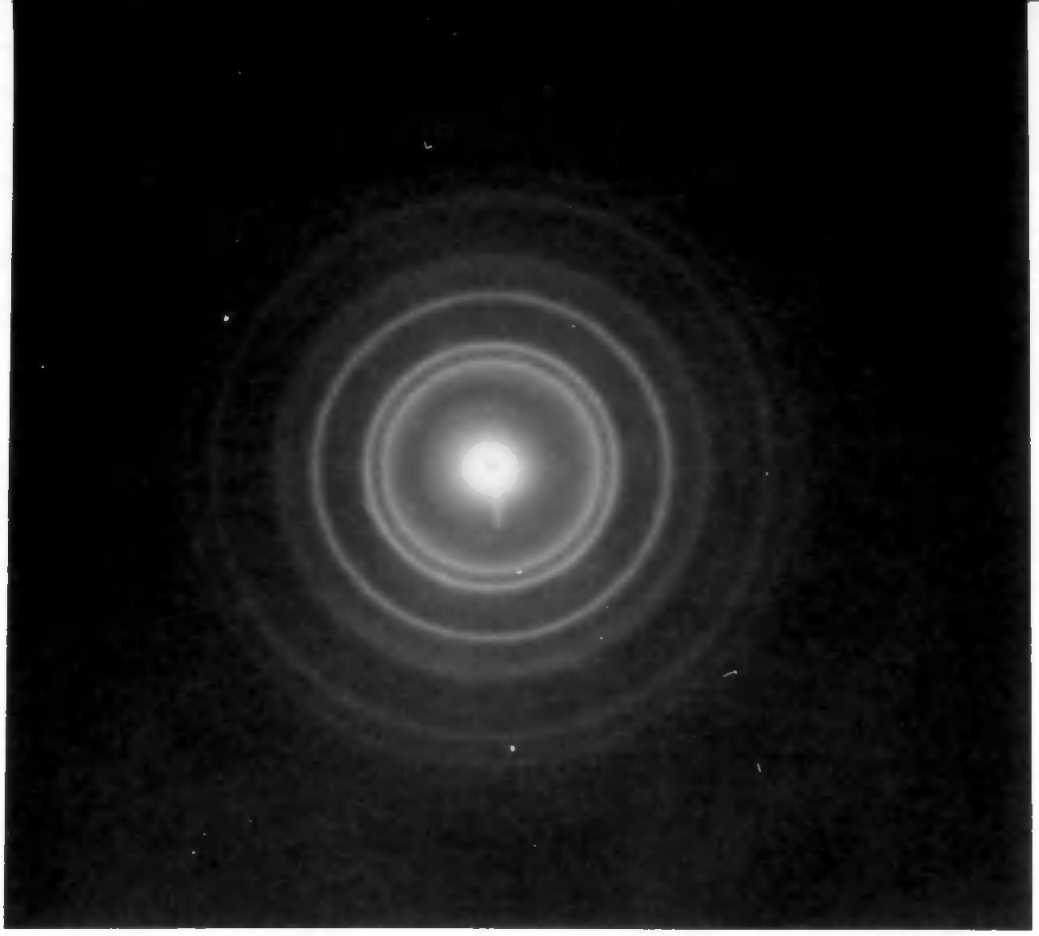

Plate 3.10 Electron diffraction pattern of calcium film shown in Plate 3.9

A 282.

1μ

Plate 3.11 Calcium film shown in Plate 3.9 heated in nitrogen at 400° for 3h. x 15,000

Plate 3.12 Calcium film shown in Plates 3.9 and 3.11 further nitrided at 450° for 1½h. x 15,000

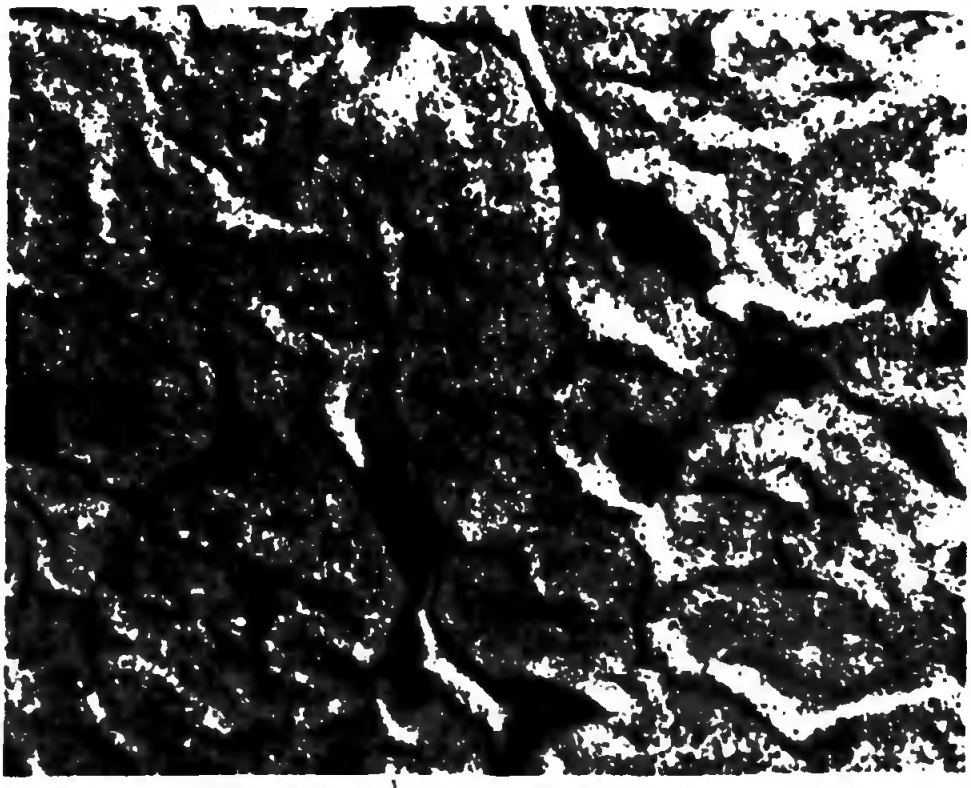

1μ

A-5221

2.2 Hydrolysis of Calcium and Magnesium Nitrides

2.2.1 Materials

The calcium and magnesium nitrides used in the following experiments were products of Alfa Inorganics, Inc. BDH precipitated magnesium and calcium hydroxides were used in the preparation of the respective oxides.

The calcium nitride was the high temperature (brown) form having a cubic (anti-Mn_2O_3, $\underline{a}$ = 11.38Å) structure. Since it was produced above 750°, it was sintered extensively, for this was much higher than its Tammann temperature (461°). The well-sintered calcium nitride, broken into lumps of about 1 mm. size, had a low specific surface ($\underline{S}$ ~~= 0.001~~ < 0.01 $m.^2g.^{-1}$).*

The magnesium nitride was a greenish-yellow powder, isomorphous with calcium nitride, ($\underline{a}$ = 9.99Å). It was not so extensively sintered and consisted of single crystals mainly of sizes varying from 20 to 100 μ ($\underline{S}$ ≃ 0.01 to 0.09 $m.^2g.^{-1}$).*

Calcium and magnesium nitrides hydrolyse rapidly, even in the presence of atmospheric water vapour. Thus, samples of the substances, including lumps several millimetres thick, crumble into finely-divided hydroxide on exposure to air.

2.2.2 Procedure

The nitride samples were 'wet' hydrolysed at 20° by adding them slowly to freshly-distilled water, which was stirred for various lengths of time. 'Wet' hydrolysis at 99° was carried out by placing the reaction vessel in a hot

* Estimated by optical microscopic examination.

water bath maintained at the required temperature.

'Dry' hydrolysis of the nitrides at 22° was carried out in a vacuum desiccator in an atmosphere of saturated water vapour. 'Dry' hydrolysis at 95° was performed by placing a boat containing the sample in a cylindrical glass chamber connected to a steam generator. In the latter procedure small quantities of moisture condensed on the sample. This was overcome by carrying out the hydrolysis at 12[illegible]° by surrounding the chamber with an outer jacket connected to a boiling xylene bath.

After hydrolysis, the products were filtered off (where necessary) and washed with acetone to arrest further reaction and ageing. They were dried at 200° in vacuo on an electrical sorption balance to remove the last traces of moisture and acetone. The surface area was determined by the B[illegible] procedure from nitrogen isotherms recorded at -19[illegible]° on the sorption balance.

The products were thermally analysed on the vacuum or thermal balances, the decomposition of calcium and magnesium hydroxides to the respective oxides being complete at 5[illegible]° in vacuo (Glasson, 1956, 1958a, 1963a, 1964; Anderson & Livery, 1961).

The phase composition and crystallinity of the samples were examined by the X-ray powder diffraction method. The crystallinity and particle shape and size were further investigated on the electron microscope.

For comparison, electron microscopic studies of the

hydration of 'active' and 'inactive' magnesia were carried out as above. These reactions have been previously studied by other techniques (Glasson, 1963a-b).

3.2.3 Results

Electron micrographs illustrating the 'wet' and 'dry' hydrolyses of calcium nitride are presented in Plates 3.13 - 3.19 and 3.21 - 3.25 respectively. For comparison, precipitated calcium hydroxide is shown in Plate 3.20. In Figures 3.1a-b are plotted the variations in specific surface and average crystallite size (equivalent spherical diameter) resulting from the 'wet' hydrolysis of calcium nitride. These are compared with the curves for the hydration of lime and the hydrolysis of metallic calcium (Glasson, 1960, 1961a).

Plates 3.26 - 3.28 and 3.33 - 3.36 illustrate the 'wet' and 'dry' hydrolyses respectively of magnesium nitride. The formation of magnesium hydroxide by other 'wet' and 'dry' methods is illustrated in Plates 3.29 - 3.32 and 3.37 - 3.39 respectively. The variations in specific surface and average crystallite size in the 'wet' hydrolysis of magnesium nitride are plotted in Figures 3.1c-d, which also compare the corresponding data for the hydration of magnesia (Glasson, 1963b).

Table 3.1 summarises the specific surface and average crystallite size for the products of hydrolysis of calcium and magnesium nitrides. X-ray analysis of these products indicates no appreciable amounts of any intermediate oxides.

Figure 3.1 Variation in specific surface, S, and average particle size, l, in the hydrolysis of calcium and magnesium nitrides with liquid water (continuous line) compared with the hydration of the respective oxides and metallic calcium (broken lines)

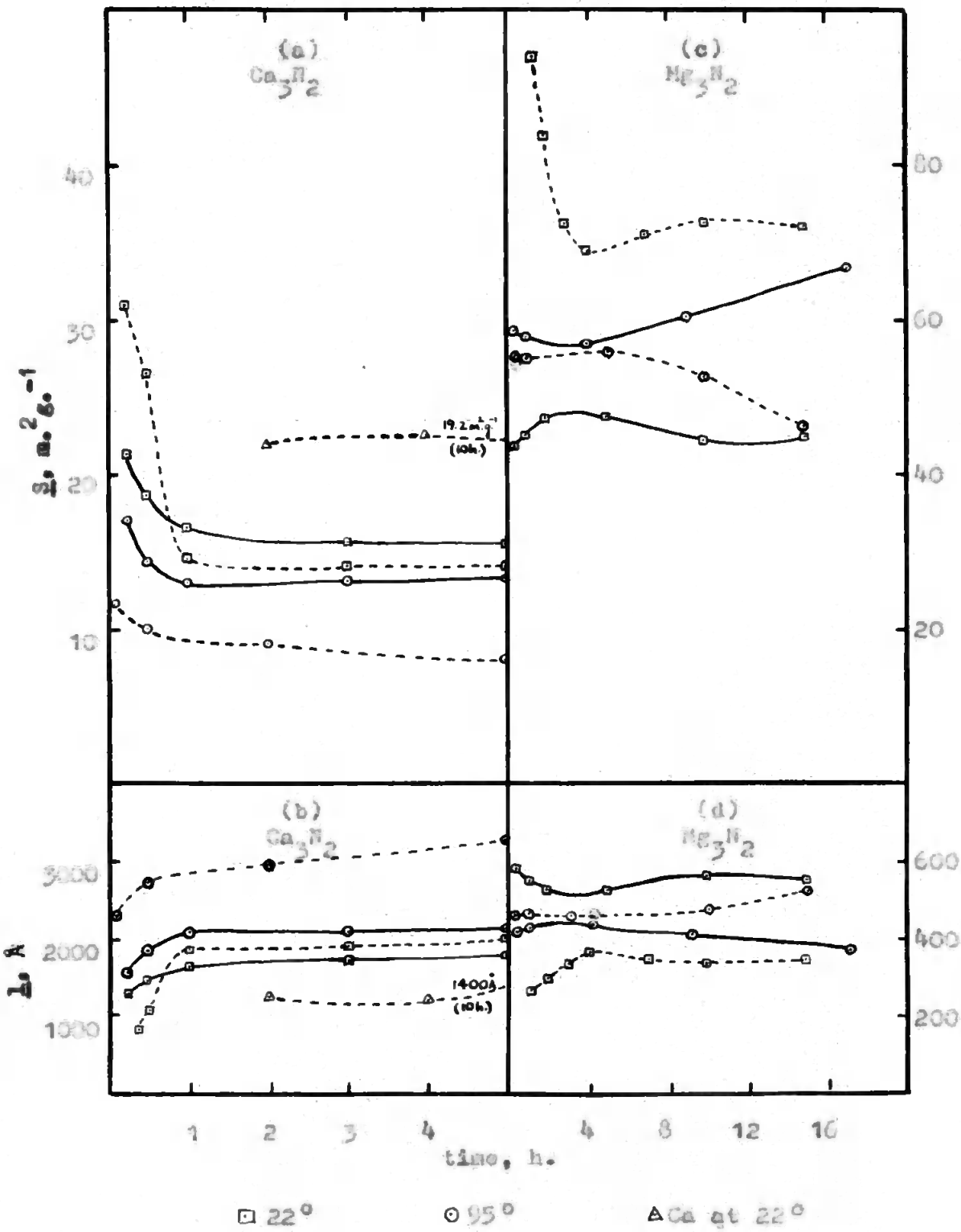

Table 3.1 Specific Surface (S in $m.^2 g.^{-1}$) and Average Crystallite Size (l in Å) of Hydrolysis Products of Calcium and Magnesium Nitrides

Hydrolysing agent	Temp.	Time	$Ca(OH)_2$		$Mg(OH)_2$	
			S	l	S	l
Liquid water	22°	5h.	15.0	1800	47.5	530
Liquid water	95°	5h.	13.0	2100	57.5	440
Air	22°	4days	3.7	7200	3.4	7400
Water vapour near s.v.p.	22°	5h.	7.2	3700	-	-
		15h.	-	-	22.7	1100

3.2.4 Discussion

The hydrolyses of both nitrides involve crystal structure and lattice changes from cubic (anti-Mn_2O_3 structure) to hexagonal (CdI_2 structure), and considerable volume expansions; fractional volume changes are 0.713 for calcium nitride and 0.970 for magnesium nitride. The absence of any oxide in the products of hydrolysis under all conditions suggests that the nitride ions are directly replaced by hydroxyl ions. The high volume changes accompanying the reactions result in the splitting off of the hydroxides, which have much higher specific surfaces and smaller crystallite sizes than the parent nitrides, cf. Pilling & Bedworth (1923) Rule for metal oxidation, Section 1.5. This effect is more pronounced for magnesium nitride, which has the larger volume change. Ageing of the hydroxides, especially in 'wet' hydrolyses, results in a subsequent increase of average crystallite size and decrease of specific surface.

In a single sample of product there are variations in particle size and external regularity of the crystallites over a wide range. Under comparable conditions calcium nitride reacts faster than the magnesium compound.

'Wet' hydrolysis of calcium nitride. The calcium nitride hydrolyses quickly in liquid water, usually within 5 min. The large volume increase accompanying the reaction leads to splitting off of the hydroxide crystallites from the original nitride particles, before the former grow or age. The ageing is more rapid at the higher temperature as shown in Figures 3.1a-b; see also Table 3.1. Thus, 1g. of calcium nitride containing about 400 crystallites yields about 6×10^{14} hydroxide crystallites in 15 min. at 22°. This figure decreases to 2×10^{14} on ageing for about 5h. Ageing results also in the formation of crystallites with a more regular external shape. These changes are illustrated in the electron micrographs presented in Plates 3.13 - 3.19, which show the 'wet' hydrolysis of calcium nitride and the subsequent progressive ageing of the hydroxide under various conditions.

Comparison with calcium hydroxide from other 'wet' methods. Under comparable conditions, the hydration of lime gives initially, smaller hydroxide crystallites at lower temperatures (22°), but larger ones at higher temperatures (95°), than in the hydrolysis of the nitride, cf. fully- and broken-lined curves in Figures 3.1a-b (Glasson, 1961a). Subsequently, however, the hydroxide formed from the nitride

ages less rapidly than that from the oxide, so that ultimately at both temperatures the product from lime is less active than that from the nitride. This is interpreted on the basis that the ammonium hydroxide formed in nitride hydrolysis suppresses the solubility of the calcium hydroxide by the common ion effect, thus inhibiting ageing.

The activity of calcium hydroxide prepared from the nitride is lower than that produced by the action of water on calcium turnings at 22°, Figures 3.1a-b (Glasson, 1961a). The latter reaction is considered to involve a two stage process, namely, (i) the initial formation of extremely small oxide crystallites, followed by, (ii) the hydration of the oxide, the latter stage being the rate-determining one.

The activities of precipitated calcium hydroxide (Plate 3.2B), prepared by double decomposition, differ from those prepared by the hydrolysis of the nitride, in that in the former, the average crystallite size is greater at the lower temperature than at the higher one (Glasson, 1960, 1961a).

'Dry' hydrolysis of calcium nitride. The hydrolysis of calcium nitride by water vapour is much slower than that by liquid water under comparable conditions of temperature. Consequently in 'dry' hydrolysis there is less splitting off of the hydroxide crystallites and smaller increases in surface areas, Table 3.1. Thus, 1g. of calcium nitride at room temperature yields 2.4×10^{13} hydroxide crystallites

with water vapour near its saturation vapour pressure, and 3.3×10^{12} crystallites with atmospheric water vapour. Nevertheless, the calcium hydroxide initially formed has a small enough particle size to exhibit X-ray line-broadening. Another significant difference is the less external regularity of the crystallites of hydroxide in 'dry' hydrolysis. These differences are due to the lower mobility of the reacting species in the 'dry' reactions.

Because of extensive sintering in the formation of calcium nitride, there are difficulties in getting a representative sample of the substance for electron microscopic examination. The crystallites observed on the copper grid are more likely to be those of the hydroxide produced by hydrolysis of the nitride. Plate 3.21 is an electron micrograph taken of a sample of calcium nitride and Plate 3.22 another sample showing the disintegration of the particles on their edges owing to hydrolysis (with atmospheric water vapour). Plate 3.23 illustrates the hydrolysis of calcium nitride by atmospheric water vapour at 22°, Plate 3.24 by saturated water vapour at 22°, and Plate 3.25 by steam at 120°.

<u>Comparison with 'dry' hydration of lime</u>. The surface areas of calcium hydroxide produced by the 'dry' hydrolysis of the nitride are less than those produced by the hydration of lime under comparable conditions (Glasson, 1958b). This is ascribed to the hydroxide crystallites in the former reaction ageing in close contact with one another, before hydrolysis is completed.

'Wet' hydrolysis of magnesium nitride. Magnesium nitride, like calcium nitride, hydrolyses quickly in liquid water, mainly within 5 min. The reaction involves similar crystal structure and lattice transformations as for calcium nitride hydrolysis. However, the larger volume change associated with magnesium nitride hydrolysis results in more extensive splitting of the hydroxide, especially in the more rapid hydrolysis at 95°, Table 3.1. Ageing is slower for the less soluble magnesium hydroxide than for calcium hydroxide. Thus, about 10^{16} hydroxide crystallites are obtained from 1g. of magnesium nitride compared with a figure of $2 - 6 \times 10^{14}$ for calcium nitride. The hydrolysis of magnesium nitride results in a larger surface area for the product at 95° than at 22°. This is in contrast with calcium nitride hydrolysis, in which the activity of the hydroxide is less at the higher temperature. Ageing of the magnesium hydroxide results also in an increase in the external regularity of the crystallites, cf. calcium nitride hydrolysis. This is evident from Plates 3.26 - 3.28, which illustrate the 'wet' hydrolysis of magnesium nitride.

Comparison with magnesium hydroxide from other 'wet' methods. The most active magnesium oxide prepared previously does not hydrate as quickly as magnesium nitride at 22°, the reaction taking several hours to complete (Glasson, 1963b). After hydration is complete the surface area and average crystallite size change comparatively little, ageing being limited because of the low solubility of

magnesium hydroxide. At comparable times, the surface area of the hydroxide from the hydration of oxide is higher than that from nitride, Figure 3.1c. Crystallite splitting in the latter case is not sufficiently extensive to give a hydroxide of the same activity as that from magnesia; Plate 3.29 is an electron micrograph of a sample of magnesia; Plate 3.30 illustrates its 'wet' hydration at 22°, showing needle-shaped hydroxide crystallites.

In the reaction at 99°, closer similarity of surface areas is observed for the hydroxides obtained from oxide and nitride, the former giving a lower value. The rates of reaction and ageing are higher at this temperature than at 22°. The hydroxide from the nitride subsequently shows an increase in specific surface before finally ageing; this may be ascribed to completion of recrystallisation of the newly-formed magnesium hydroxide to its normal lattice structure. Plate 3.31 shows a sample of magnesia 'wet' hydrated at 99°, illustrating the partial conversion of the needle-shaped hydroxide crystallites to hexagonal plates, cf. Plate 3.30.

Magnesium hydroxide precipitated at 22° is only slightly less active than hydrated magnesia under similar conditions (Glasson, 1963b). The precipitated compound consists of a larger proportion of hexagonal plates, Plate 3.32 (cf. Plates 3.30 - 3.31). This is consistent with the results of Anderson & Livery (1961).

'Dry' hydrolysis of magnesium nitride. Like calcium nitride, magnesium nitride hydrolyses more slowly with water vapour than with liquid water, resulting in less extensive splitting of the hydroxide crystallites and smaller increases in surface area, Table 3.1; e.g., 1g. of nitride at room temperature yields 1.0×10^{13} hydroxide crystallites with saturated water vapour and 3.4×10^{12} crystallites with atmospheric water vapour. Again, the hydroxide initially formed gives appreciable X-ray line broadening, but ages considerably before the reaction is complete.

Because of less extensive sintering during its formation, samples of magnesium nitride consist of sufficient numbers of crystallites small enough to be seen on the electron microscope, Plate 3.33 (cf. calcium nitride). On exposure to the atmosphere, magnesium nitride progressively hydrolyses forming needle-shaped hydroxide crystallites, which split off the nitride, Plate 3.34. The reaction is sufficiently slow to be followed by electron microscopic examination. With saturated water vapour, more active hydroxide is formed within a shorter time, Plate 3.35 and Table 3.1. Plate 3.36 illustrates steam hydrolysis at 100°; the reaction does not appear to have taken place to a great extent within the time (½h.).

Comparison with 'dry' hydration of magnesia. The 'dry' hydration of active magnesia by saturated water vapour at 22° gives eventually hydroxide of about the same activity

as that obtained under similar conditions from the nitride (Glasson, 1963b). In 15h. the extent of hydration of magnesia is about 90% and results in the initial formation of needle-shaped hydroxide crystallites, Plate 3.37 (cf. Plate 3.29), which tend to become hexagonal when aged. In 24h. further reaction is accompanied by more ageing and the hydroxide having a more hexagonal shape, Plate 3.38. At high temperatures, faster reaction and rate of ageing results in hexagonal crystallites in a shorter time, Plate 3.39.

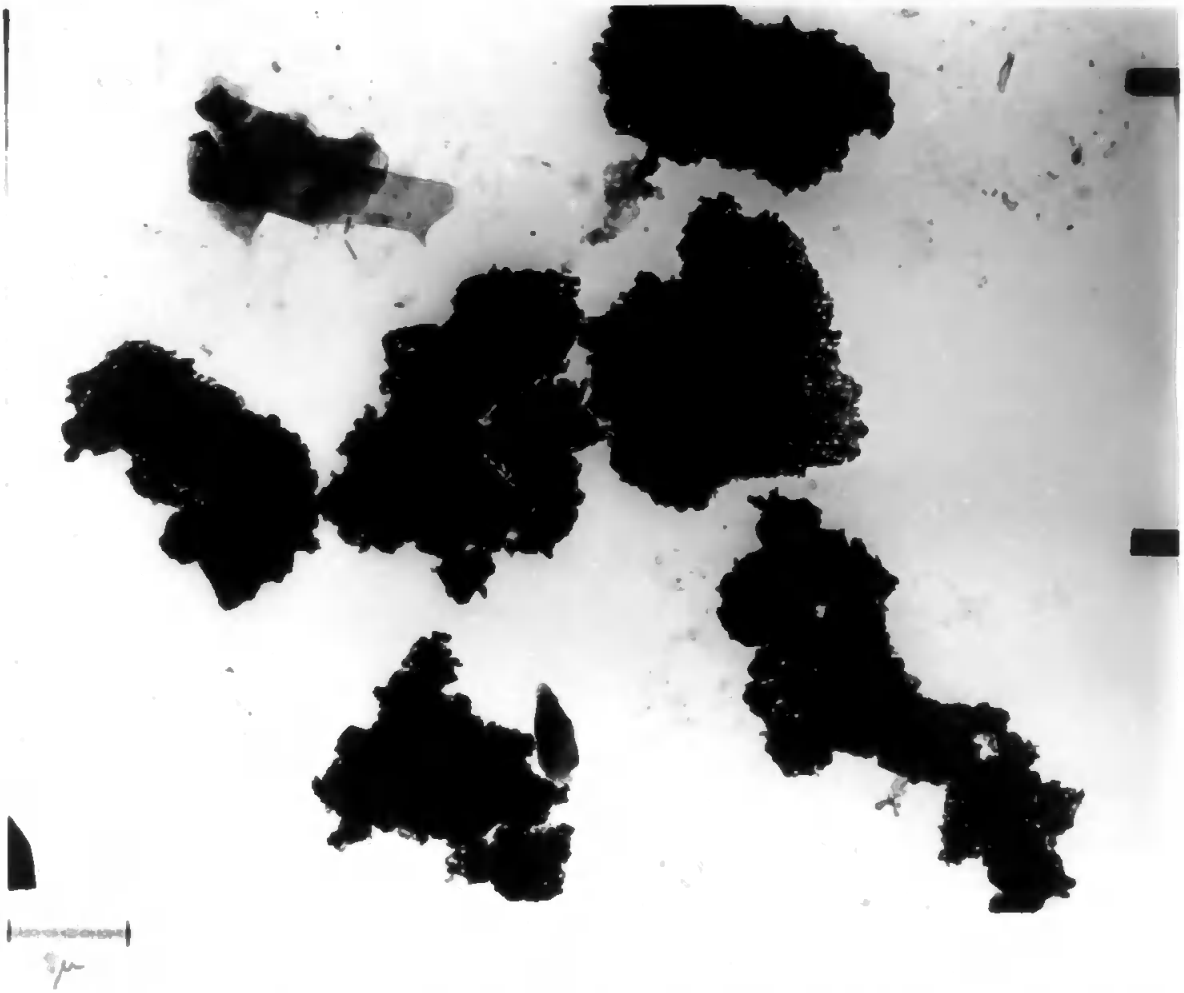

Plate 3.13 Calcium nitride 'wet' hydrolysed at 22° for 19 min. x 19,000

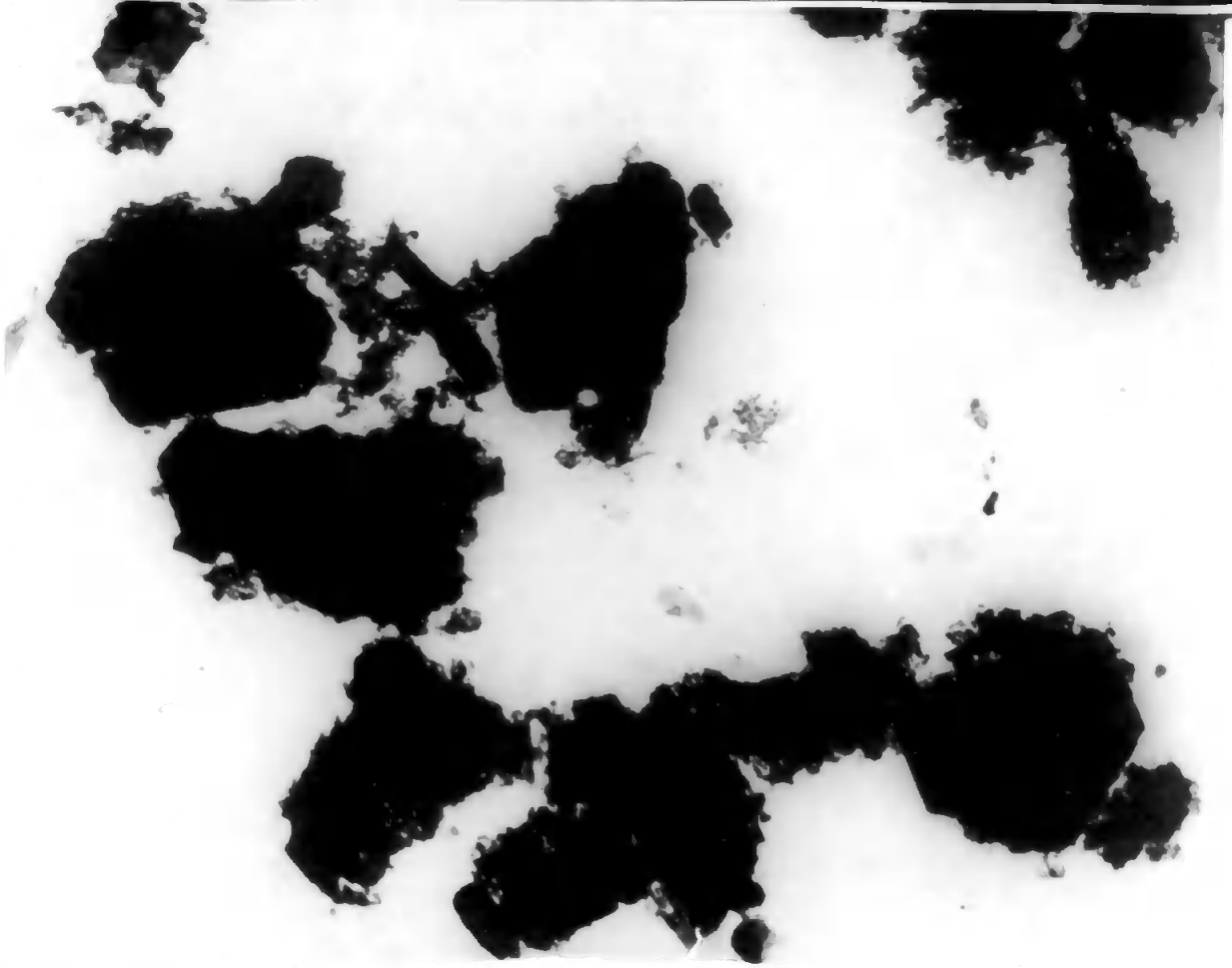

8μ

Plate 3.14 Calcium nitride 'wet' hydrolysed at 25° for 19 min. x 19,000

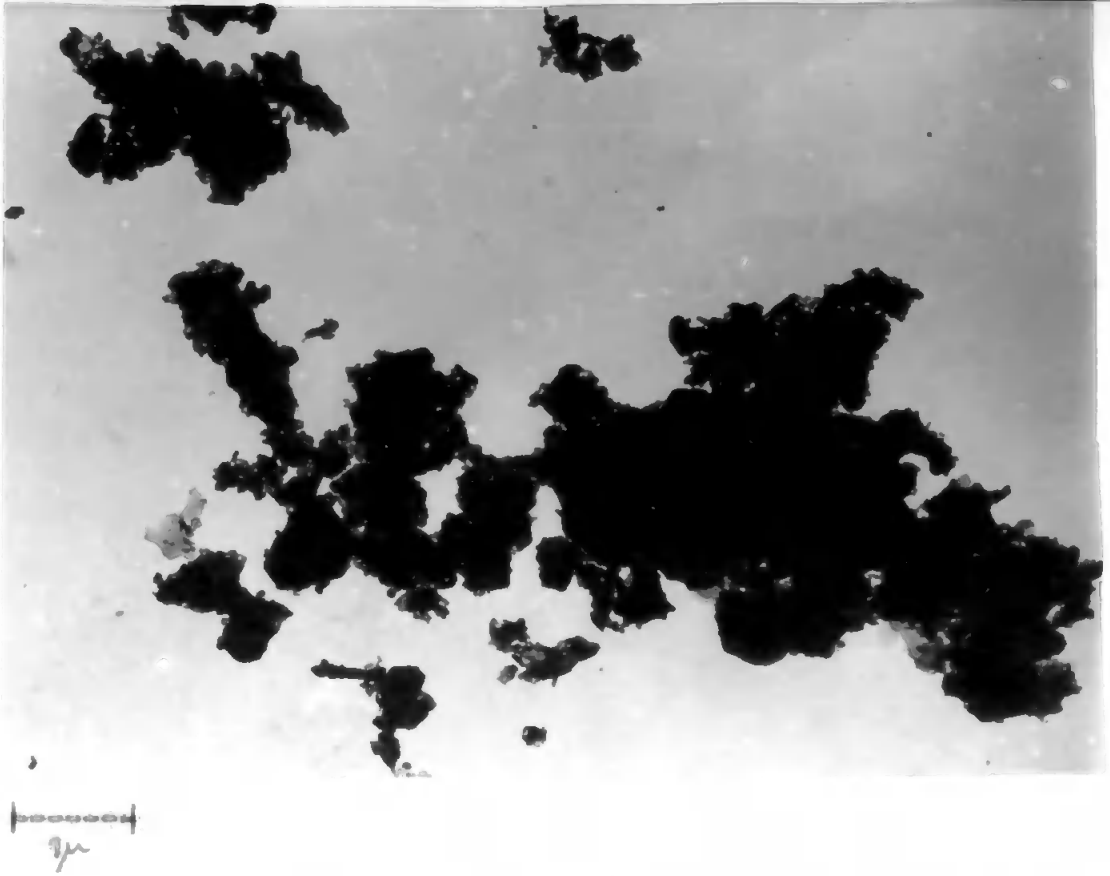

Plate 3.15 Calcium nitride 'wet' hydrolysed at 22° for 1h.
x 15,000

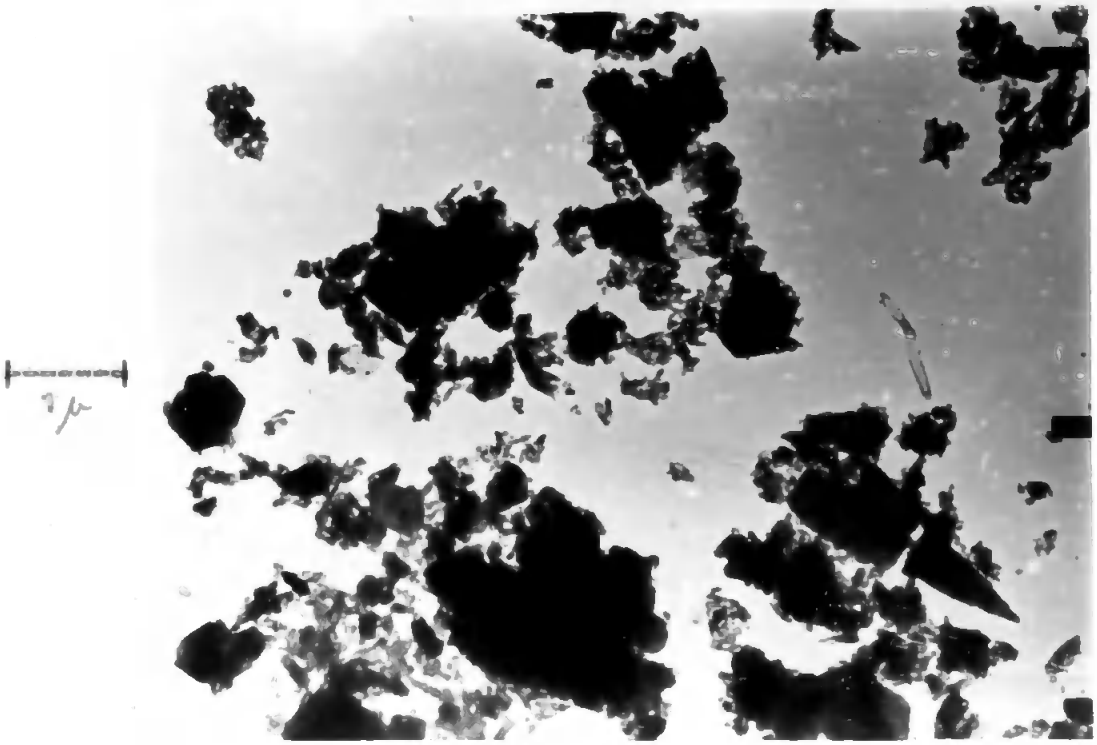

Plate 3.16 Calcium nitride 'wet' hydrolysed at 20°
for 3h. x 15,000

A242

3 3 -2

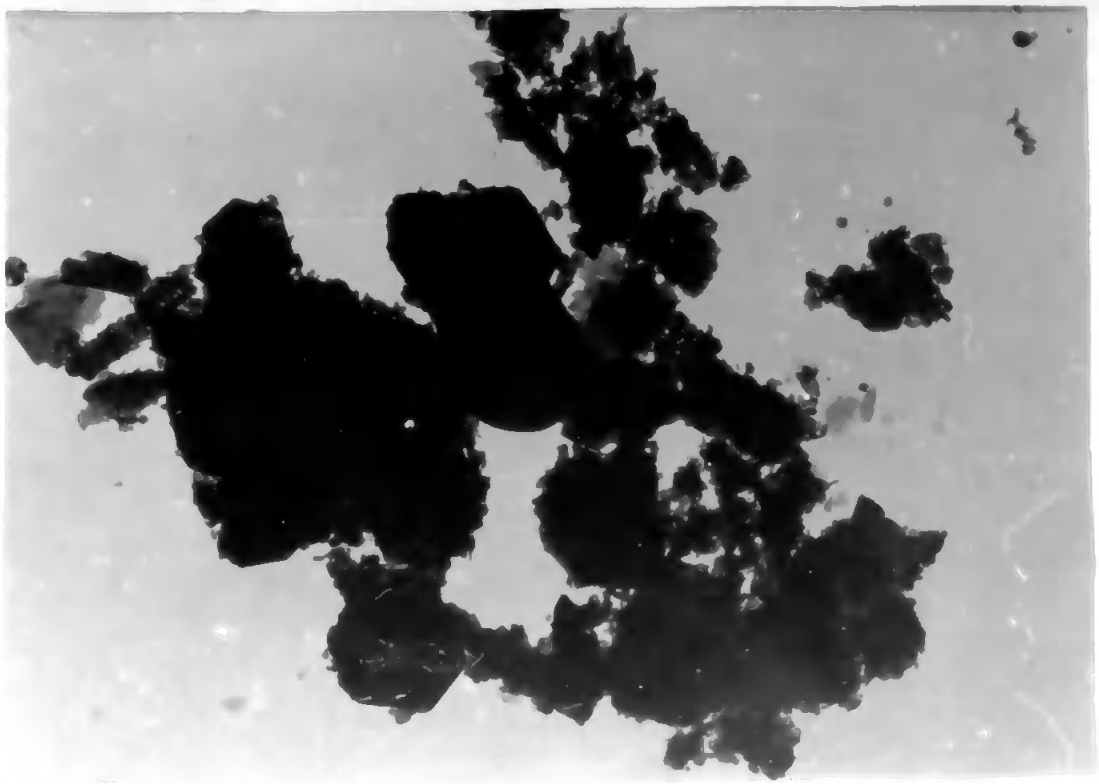

1μ

Plate 3.17 Calcium nitride 'wet' hydrolysed at 95° for 15 min. x 15,000

A-114 1/2 1.

9μ

Plate 3.18 Calcium nitride 'wet' hydrolysed at 95° for 1h.
x 15,000

1μ

Plate 3.19 Calcium nitride 'wet' hydrolysed at 95° for 5h. x 15,000

Plate 3.20 Precipitated calcium hydroxide x 15,000

Plate 3.21 Electron micrograph of a sample of calcium nitride x 15,000

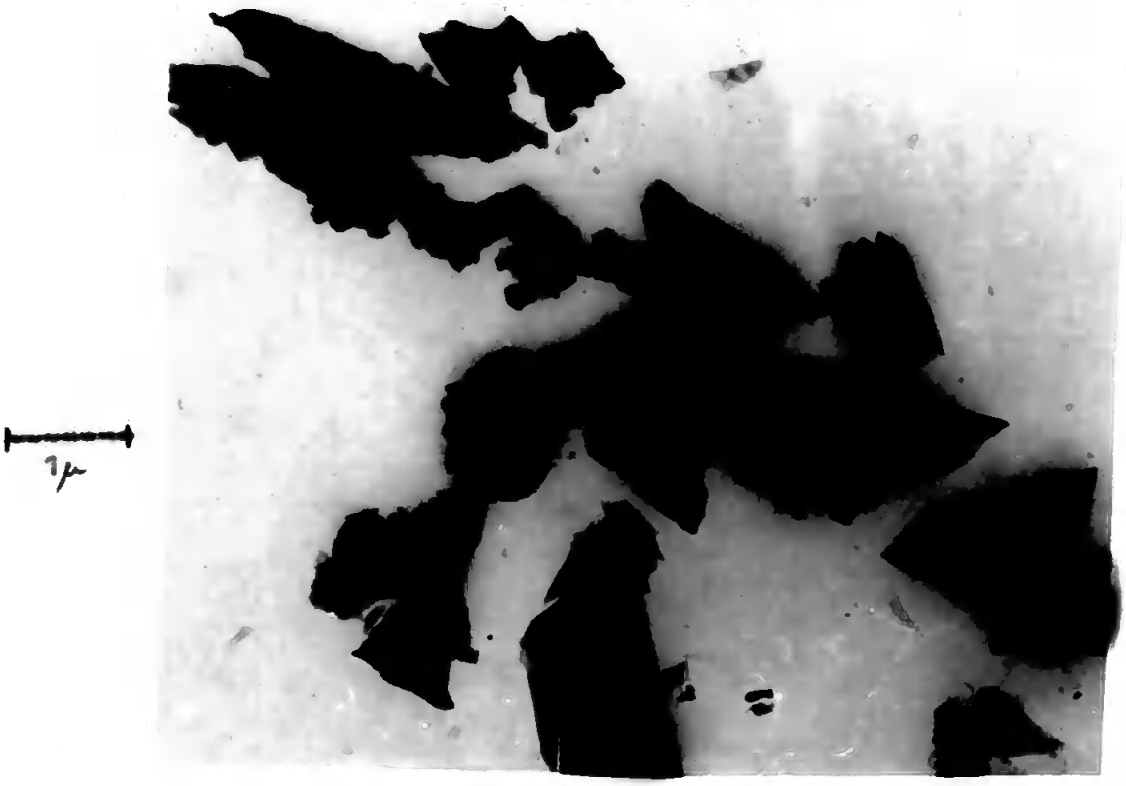

1μ

Plate 3.22 Sample of calcium nitride x 15,000

Plate 3.23 Calcium nitride hydrolysed with atmospheric water vapour at 22° for 5 days x 15,000

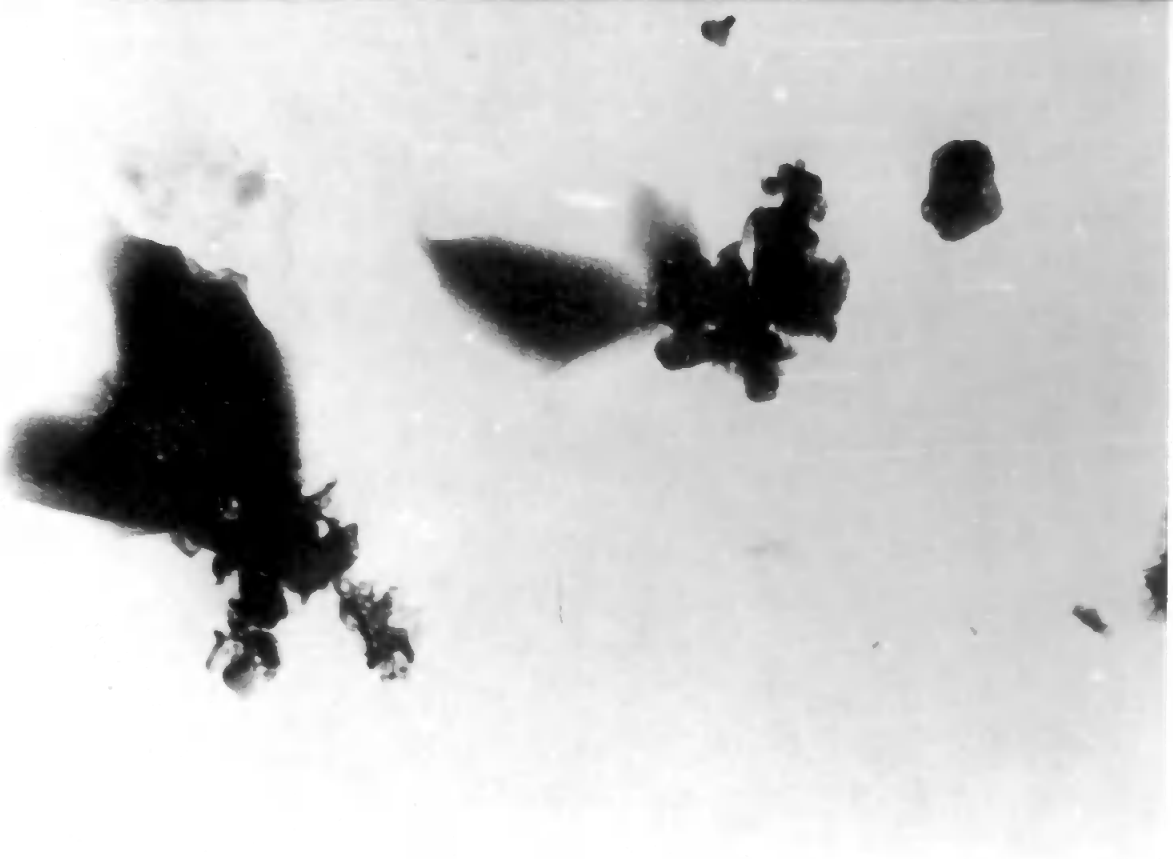

1μ

Plate 3.24 Calcium nitride hydrolysed with saturated water vapour at 22° for 4Th. x 15,000

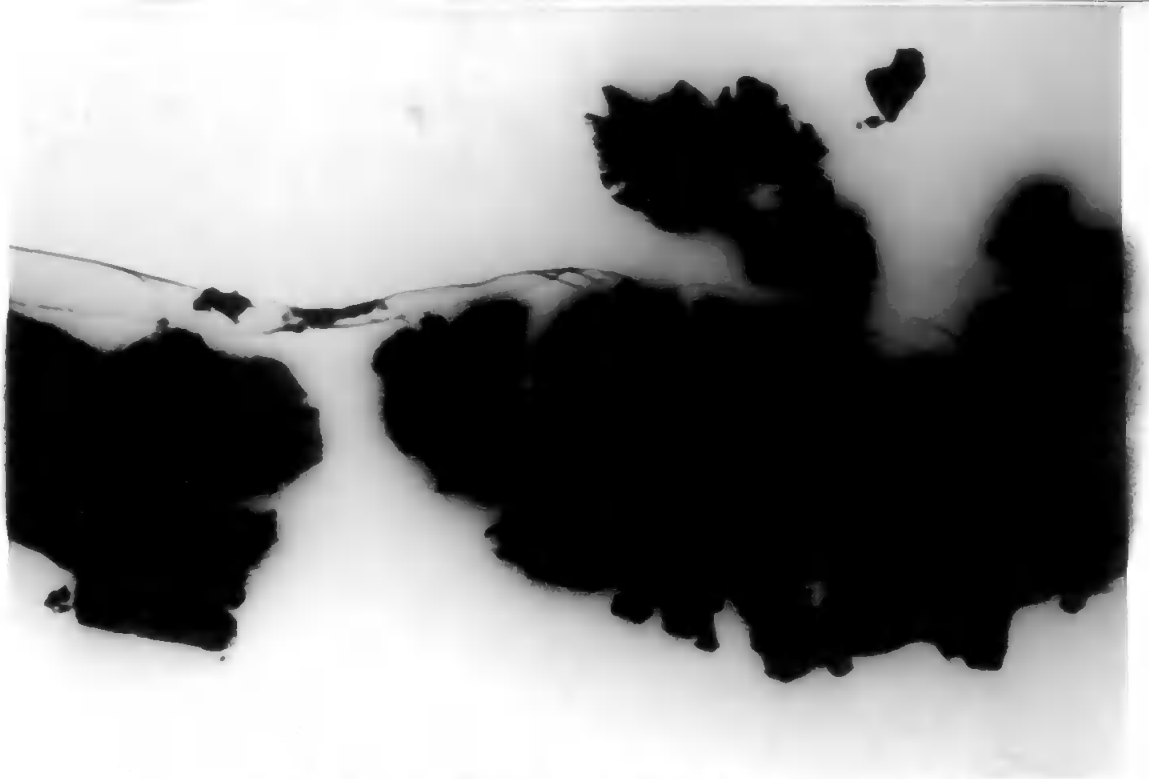

1μ

Plate 3.25 Calcium nitride hydrolysed with steam at 120° for 90 min. x 19,000

1μ

Plate 3.26 Magnesium nitride 'wet' hydrolysed at 22° for 1h. x 19,000

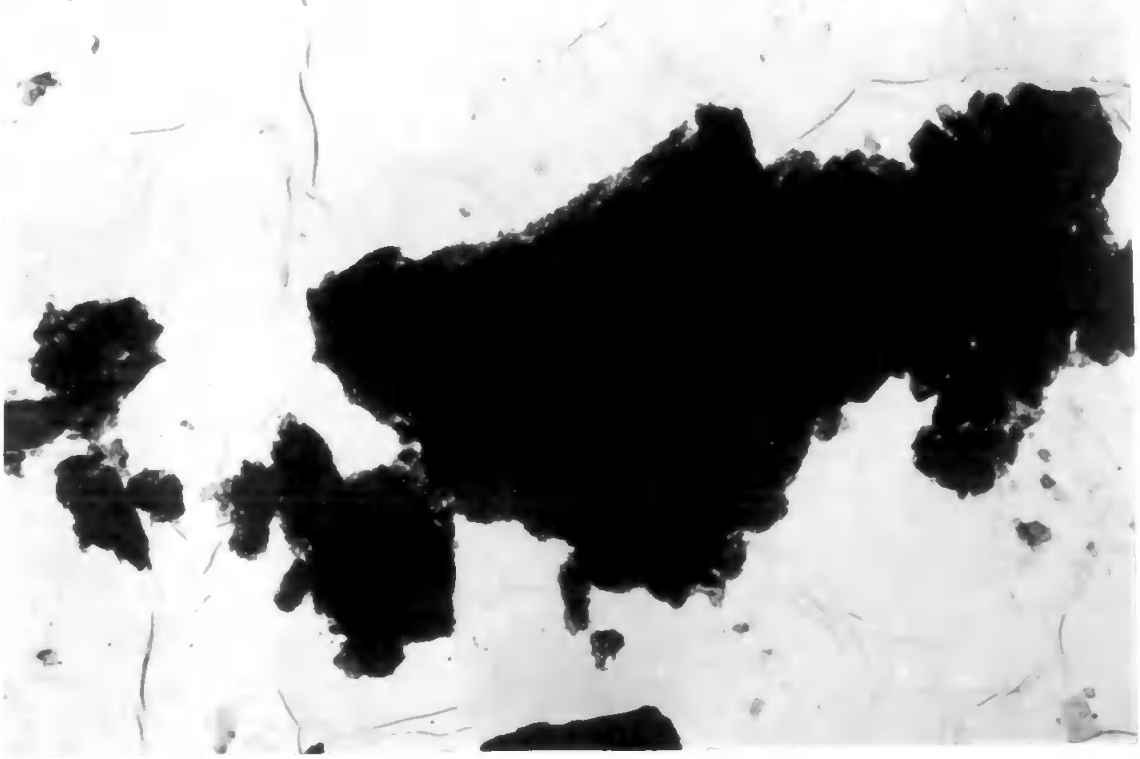

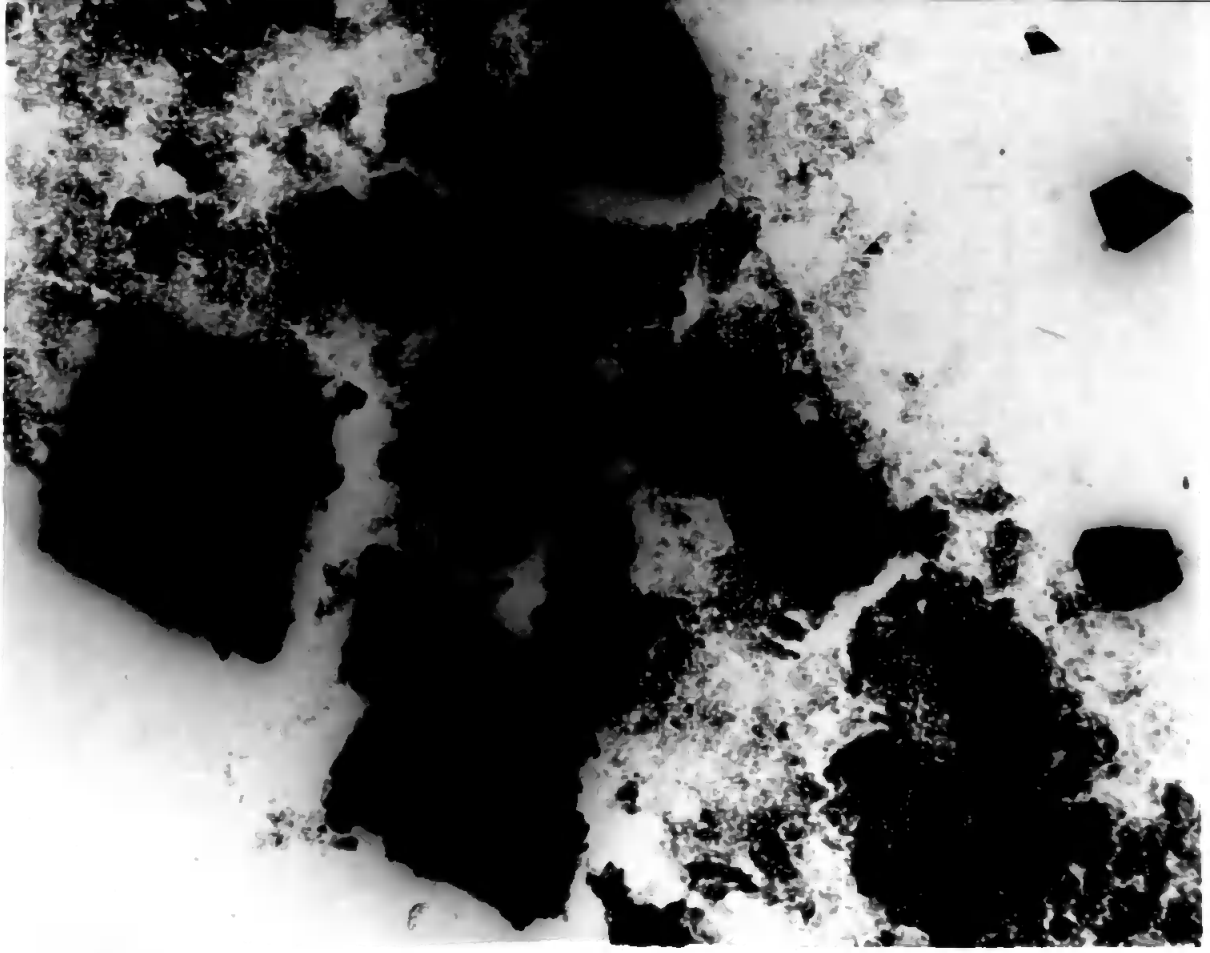

1μ

Plate 3.27 Magnesium nitride 'wet' hydrolysed at 22° for 24h.
x 15,000

A-178

1 20recs.

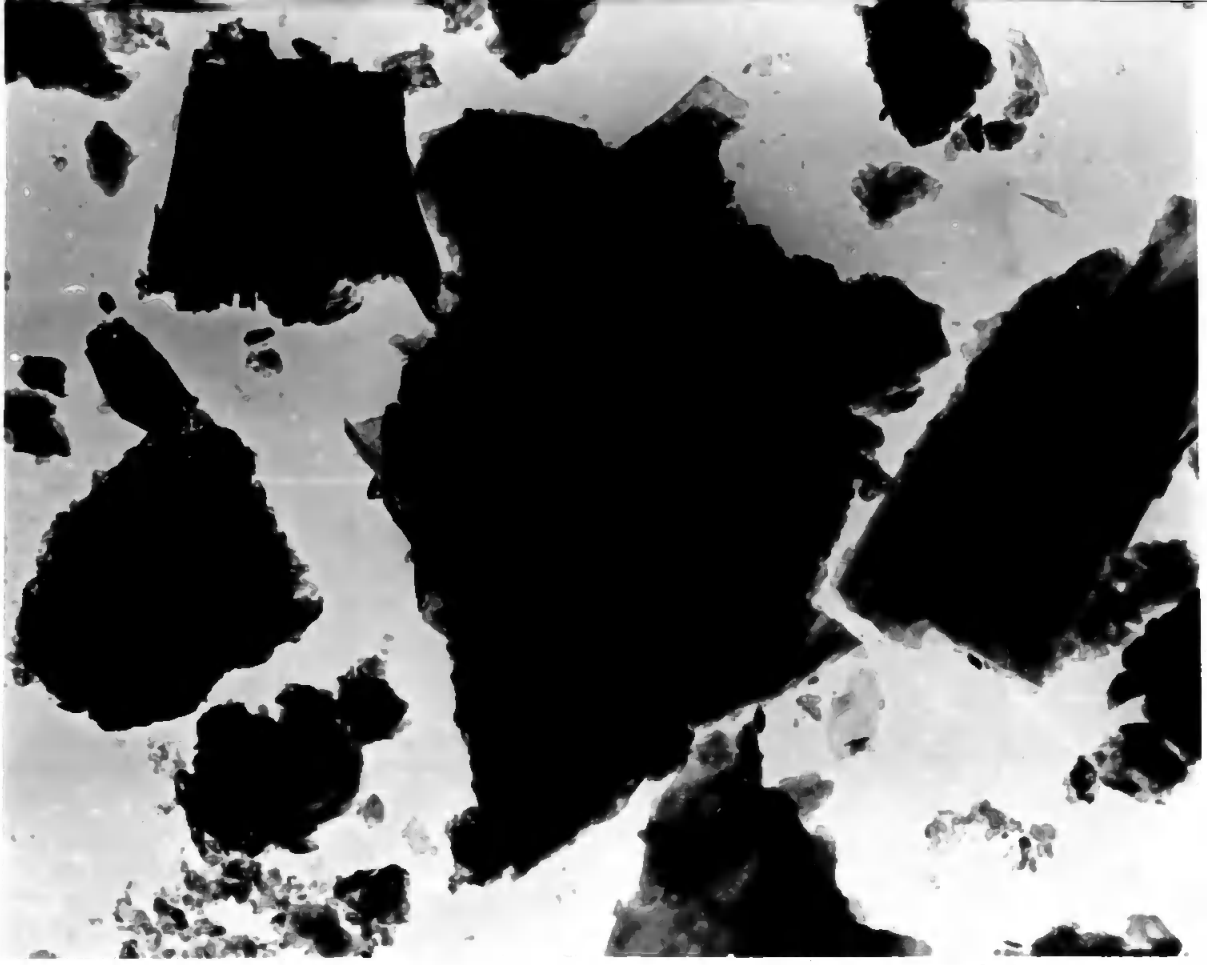

1μ

Plate 3.28 Magnesium nitride 'wet' hydrolysed at 95° for 15 min. x 15,000

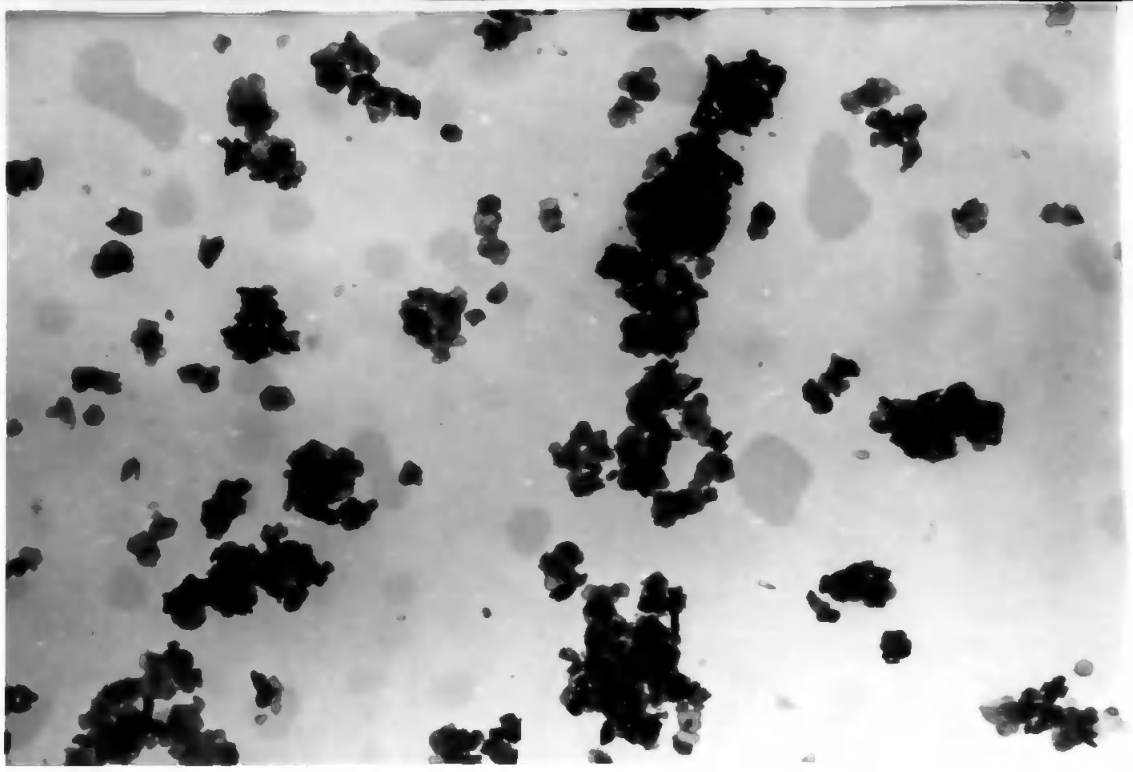

1μ

Plate 3.29 Magnesium oxide x 19,000

1μ

Plate 3.30 Magnesium oxide 'wet' hydrated at 22° for 3h.
x 15,000

A153.

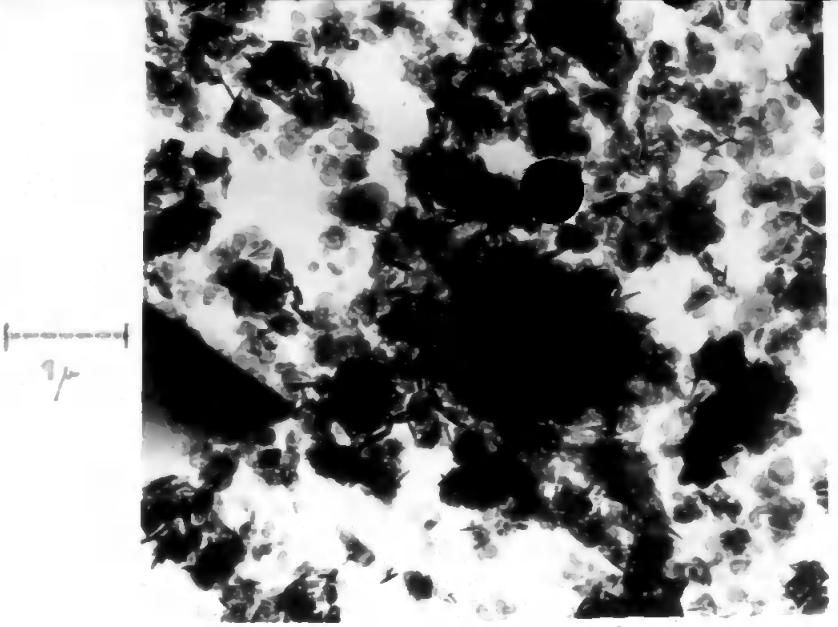

Plate 3.31 Magnesium oxide 'wet' hydrated at 99° for 1h. x 15,000

1μ

Plate 3.32 Precipitated magnesium hydroxide
x 15,000

1μ

Plate 3.33 Magnesium nitride x 15,000

A329

202.

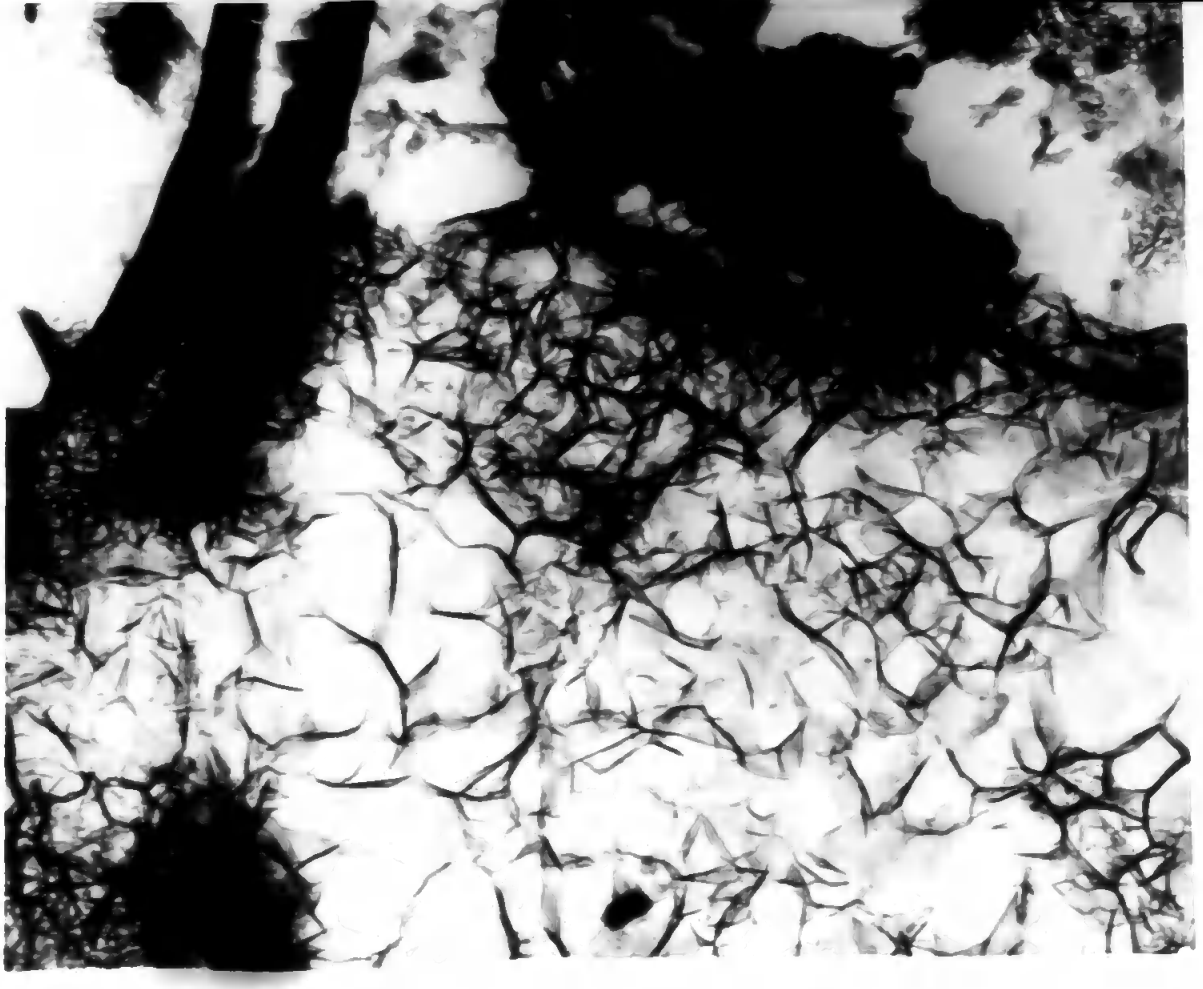

1μ

Plate 5.34 Magnesium nitride hydrolysed with atmospheric water vapour at 22° for 18 h. x 15,000

1μ

Plate 3.33 Magnesium nitride hydrolysed with saturated water vapour at 22° for 12h. x 15,000

A 358.

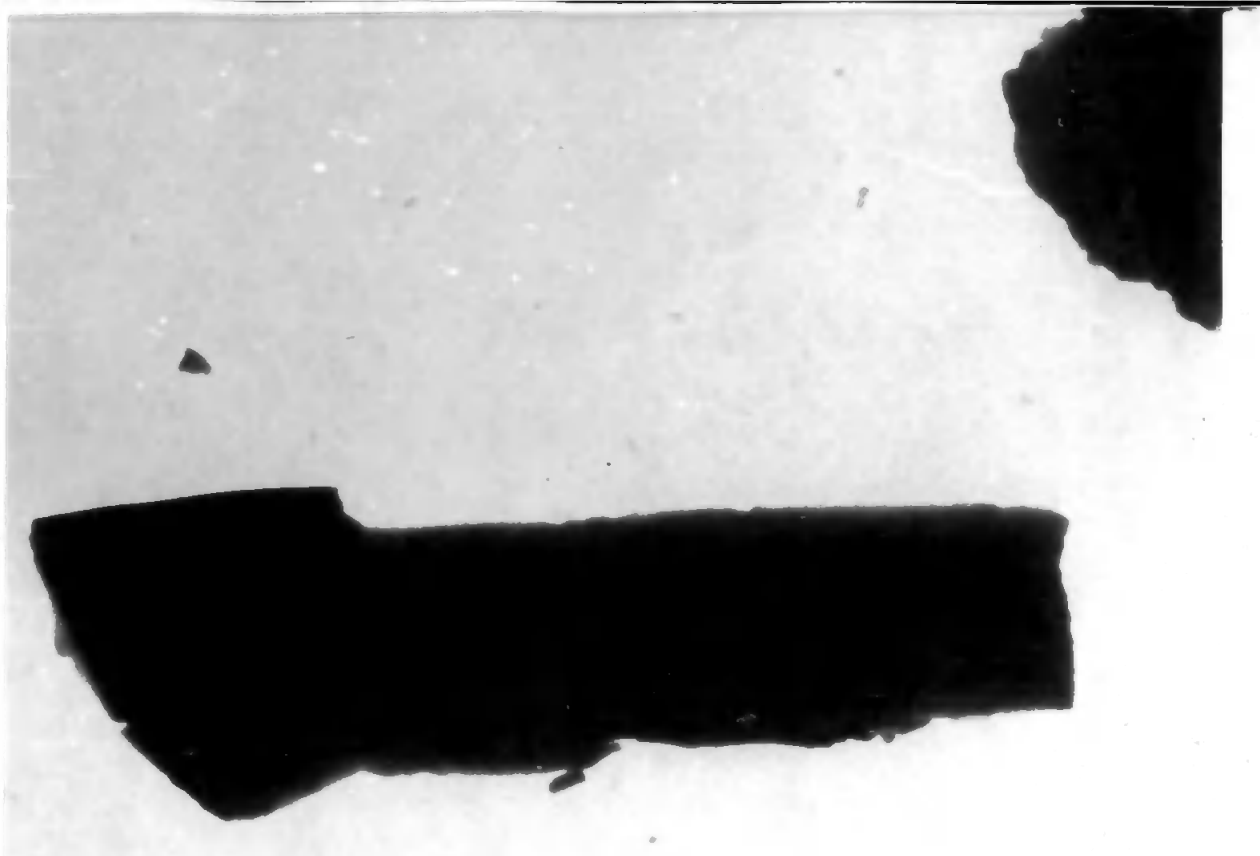

1μ

Plate 5.36 Magnesium nitride hydrolysed with steam at 120° for 30 min. x 15,000

A-9

1 5

Plate 5.37 Magnesium oxide hydrated with saturated water vapour at 22° for 10h. x 15,000

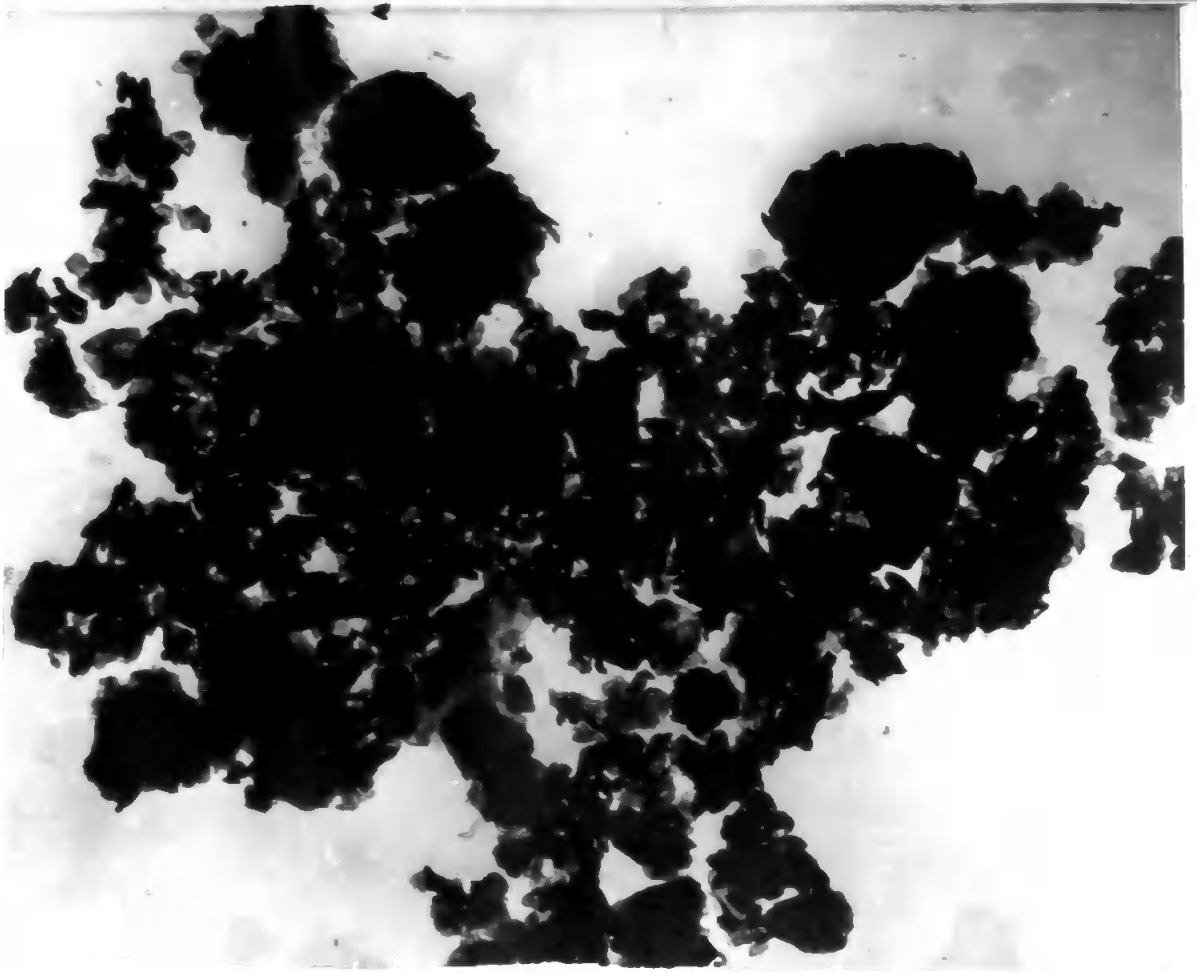

1μ

Plate 3.38 Magnesium oxide hydrated with saturated water vapour at 22° for 24h. x 15,000

A236

3 6 -1

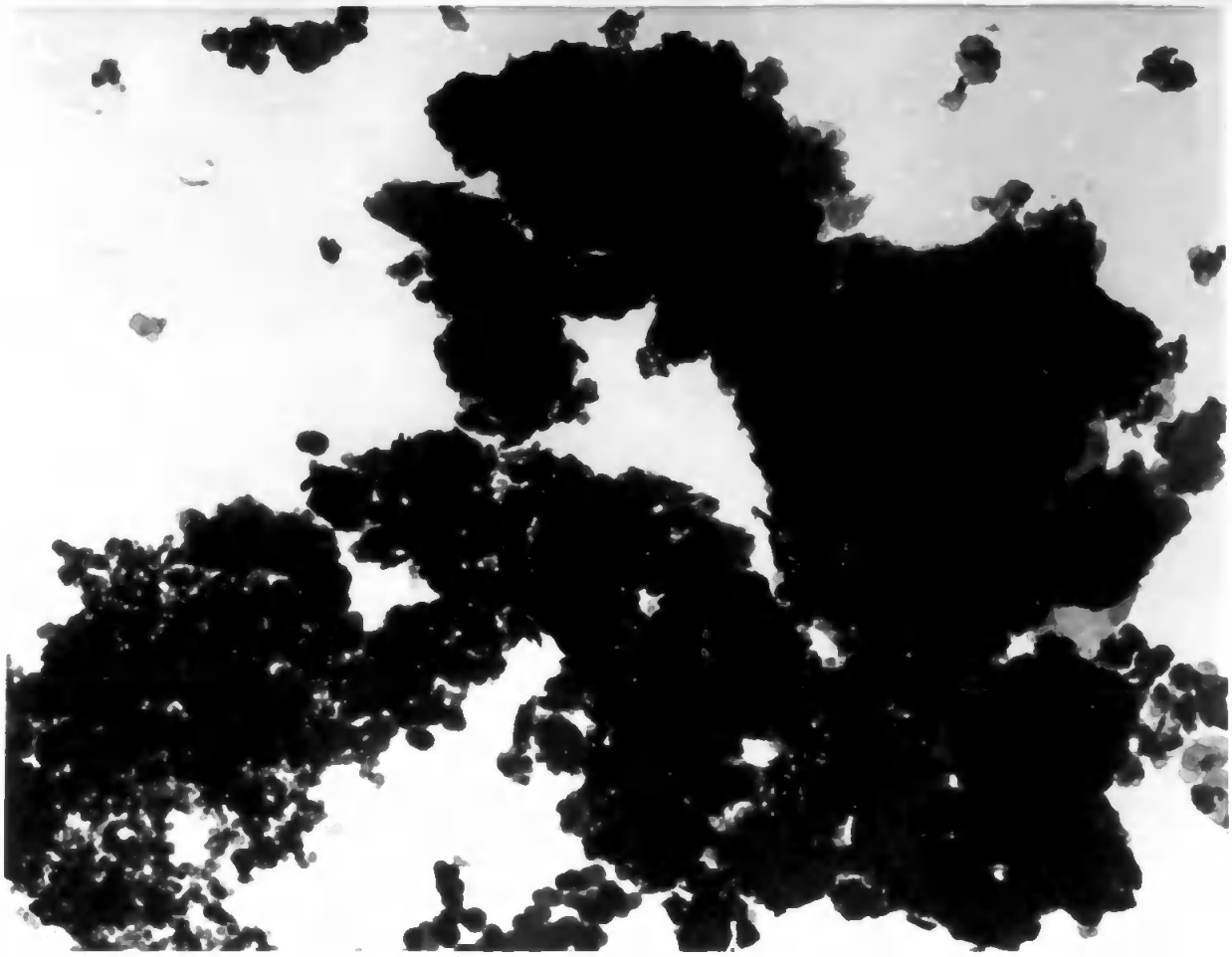

|-------| 1μ

Plate 3.39 Magnesium oxide hydrated with steam at 95° for 1h. x 15,000

62

S 2

3.3 Calcination of Calcium and Magnesium Nitrides

3.3.1 Materials

The nitrides, which were used in the calcination experiments, are the same as those used in the hydrolyses, Section 3.2.

3.3.2 Procedure

Samples of the nitrides were heated in air for various lengths of time in a furnace pre-set at the required temperature. The products were examined by methods similar to those used in the hydrolyses of the nitrides, Section 3.2.2.

3.3.3 Results

Electron micrographs illustrating the calcination of calcium and magnesium nitrides are presented in Plates 3.40 - 3.42.

3.3.4 Discussion

Fragmentation occurs when each of the two nitrides is heated in air above the decomposition temperature of the respective hydroxide. The volume contraction of about 10% accompanying the crystal lattice change of each reaction results in an increase in specific surface and a decrease in average crystallite size. Thus, the oxidation of calcium nitride at 600° is complete in 9h. and the oxide formed has a specific surface of 6.8 $m.^2g.^{-1}$ (average crystallite size, 2650Å). No appreciable sintering of the oxide occurs at 600°; e.g., after 20h. the specific surface is 7.4 $m.^2g.^{-1}$ and the average crystallite size, 2430Å, Plates 3.40 and 3.41. The small increase in specific surface signifies probably

the complete crystallisation of the newly-formed oxide. The absence of sintering in the oxide at 600° is in keeping with its high melting point (2600°) giving a Tammann temperature of 1160° and $0.3T_m$ equivalent to 685°, Section 1.6.

Calcination of magnesium nitride at 600° yields a more finely-divided oxide, Plate 3.42 (cf. Plate 3.33). The product has a specific surface of 18.9 $m.^2g.^{-1}$ (average crystallite size, 890Å) and gives appreciable X-ray line-broadening. Its formation is complete in 20h., longer than that required for calcium nitride oxidation, cf. hydrolyses of the two nitrides, Section 3.2.

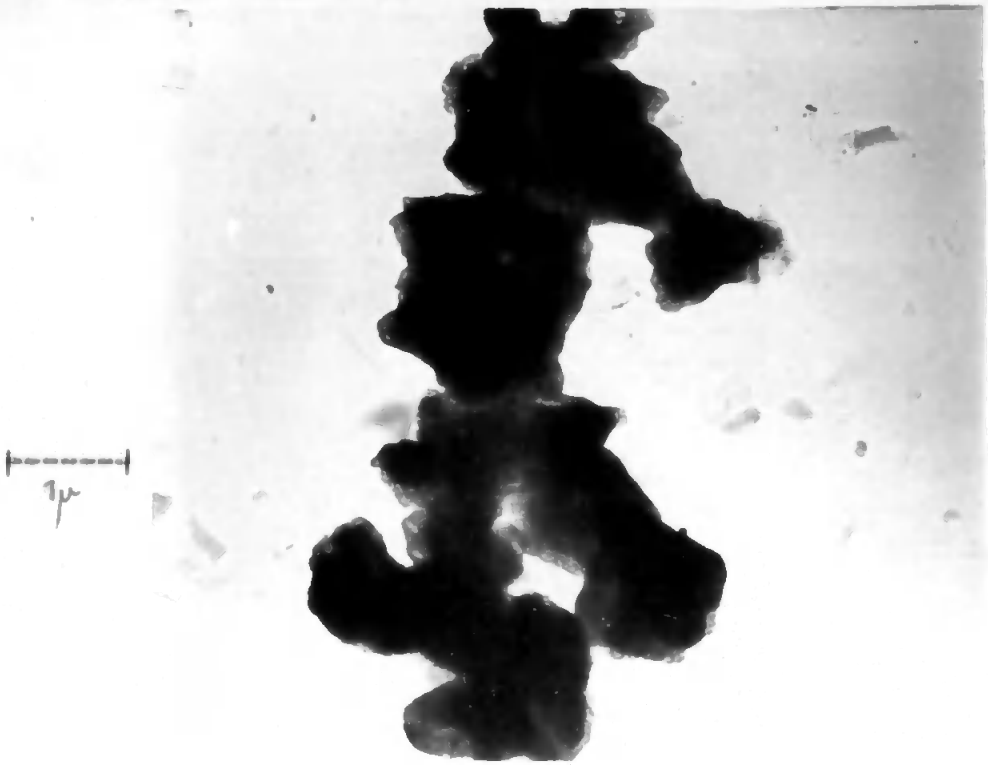

Plate 3.40 Calcium nitride calcined in air at 600° for 17h. x 15,000

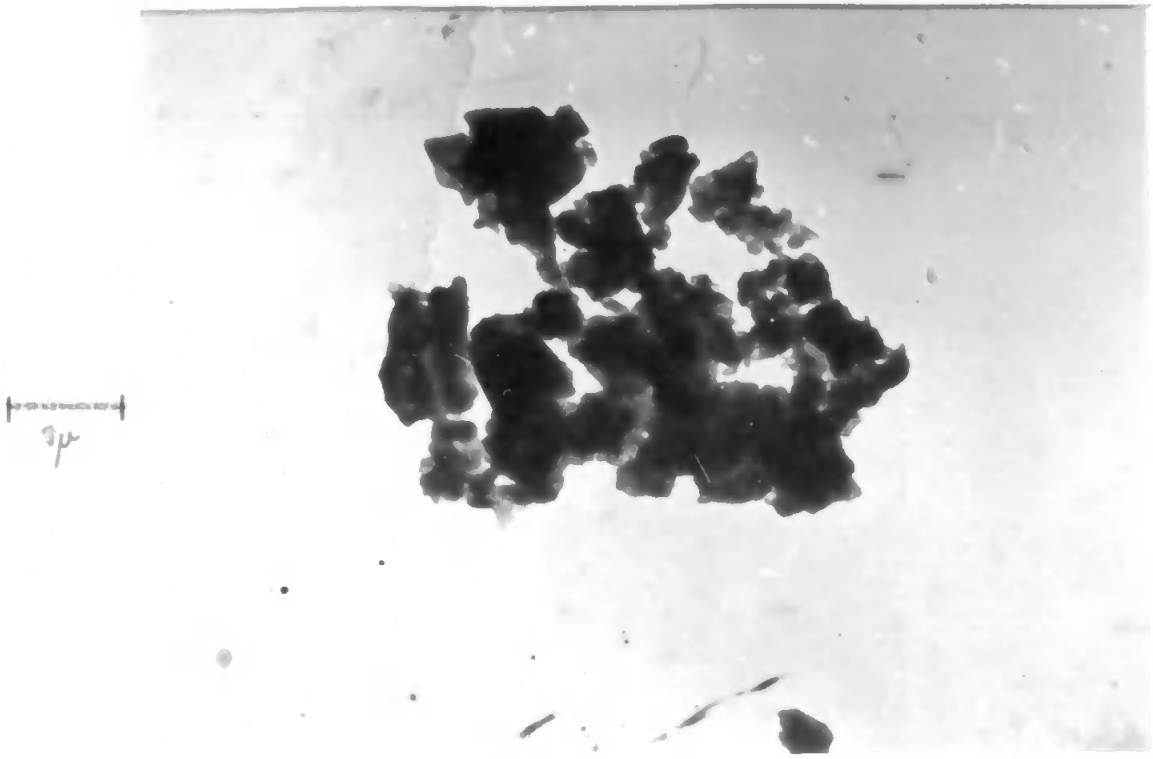

Plate 3.41 Calcium nitride calcined in air at 600°
for 72h. x 15,000

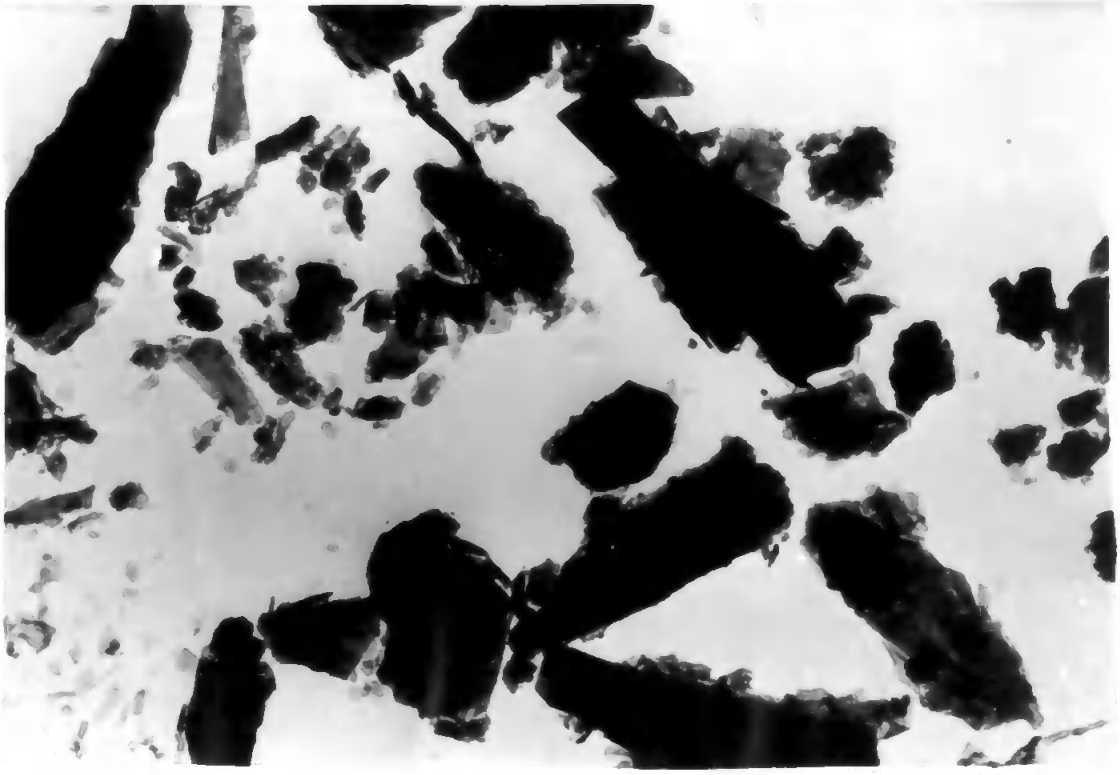

1μ

Plate 3.42 Magnesium nitride calcined in air at 600° for 20h. x 15,000

3.4 Hydrolysis of Calcium Cyanamide

3.4.1 Materials

The calcium cyanamide, urea and calcium hydroxide (precipitated) were BDH products.

3.4.2 Procedure

The hydrolysis of calcium cyanamide was carried out by procedures similar to those used with calcium and magnesium nitrides, Section 3.2.2.

Mixtures of calcium hydroxide and urea solution were boiled for various lengths of time. The calcium contents of the products were determined by titration against EDTA. The products were also investigated by methods similar to those used in the hydrolyses of the nitrides.

3.4.3 Results

Figures 3.2a-b show the variation in specific surface and average crystallite size in the carbonation of hydrated lime (7.4g.) with M-urea (250 ml.) at 95°. Plates 3.43 - 3.49 illustrate the progress of the reaction.

3.4.4 Discussion

Calcium hydroxide is formed without any carbonate when calcium cyanamide is 'dry' hydrolysed at 22° or 95° with water vapour, or 'wet' hydrolysed at 22° with water or 1% or 50% acetone - water mixtures. Hot water gives some calcitic carbonate.

Addition of urea to give a molar concentration enables lime water (up to 0.02M) to be completely converted to calcitic calcium carbonate on boiling for ½h. However, the reaction

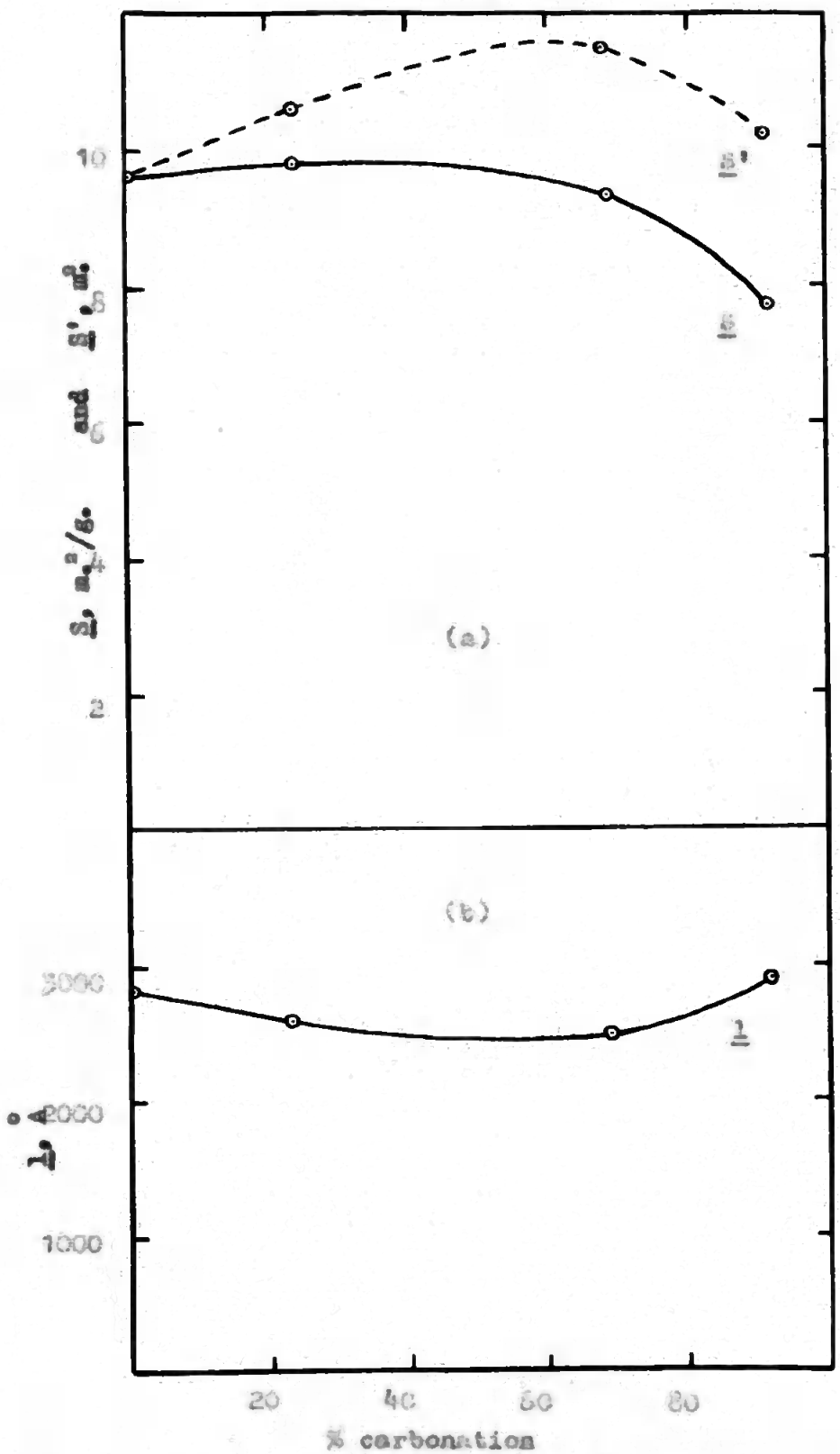

Figure 3.2 Variation in average crystallite size, L, specific surface, S, and actual surface area of products from 1g. of calcium hydroxide, S', in the carbonation of lime (7.4g.) with N-urea (200ml.) at 95°

is much slower when solid calcium hydroxide (7.4g., 0.1 mole) is added to hot M-urea solution (200 ml.). The extent of carbonation is 23.2% in 5h., 68.5% in 13h. and 91.5% in 20h. There is no great change in specific surface accompanying the reaction, Figure 3.2. Even during the early stages of the reaction, there are a few well-formed rhombic crystals of calcite, Plate 3.43, and some hexagonal ones, Plate 3.44, tending to rhombs in the size range, 3 - 7μ. Most crystals are not euhedral and are smaller than 2μ. The unreacted calcium hydroxide is in the form of small crystallites mainly less than 1μ in size. They tend to aggregate, Plate 3.45, and give slight X-ray line-broadening, which is absent in the newly-formed calcite. There is still a wide crystallite size range in the later stages of the carbonation, Plates 3.46 - 3.49, with the larger crystals acquiring sharper edges, e.g., compare Plates 3.43, 3.46 and 3.48 with one another.

Much of the carbonation would seem to occur by a "through solution" mechanism, probably via calcium cyanate, with the unchanged hydroxide causing wide variations in the growth rates of the calcitic rhombs.

The reaction permits a reduction of lime alkalinity in calcareous materials and afterwards a partial separation of the carbonate.

1μ

Plates 3.43 (above), 3.44 (below) and 3.45 (following page)
Mixture of lime (7.4g.) and N-urea (200 ml.) heated at 95°
for 5h. x 15,000

1μ

AUSTRIA.

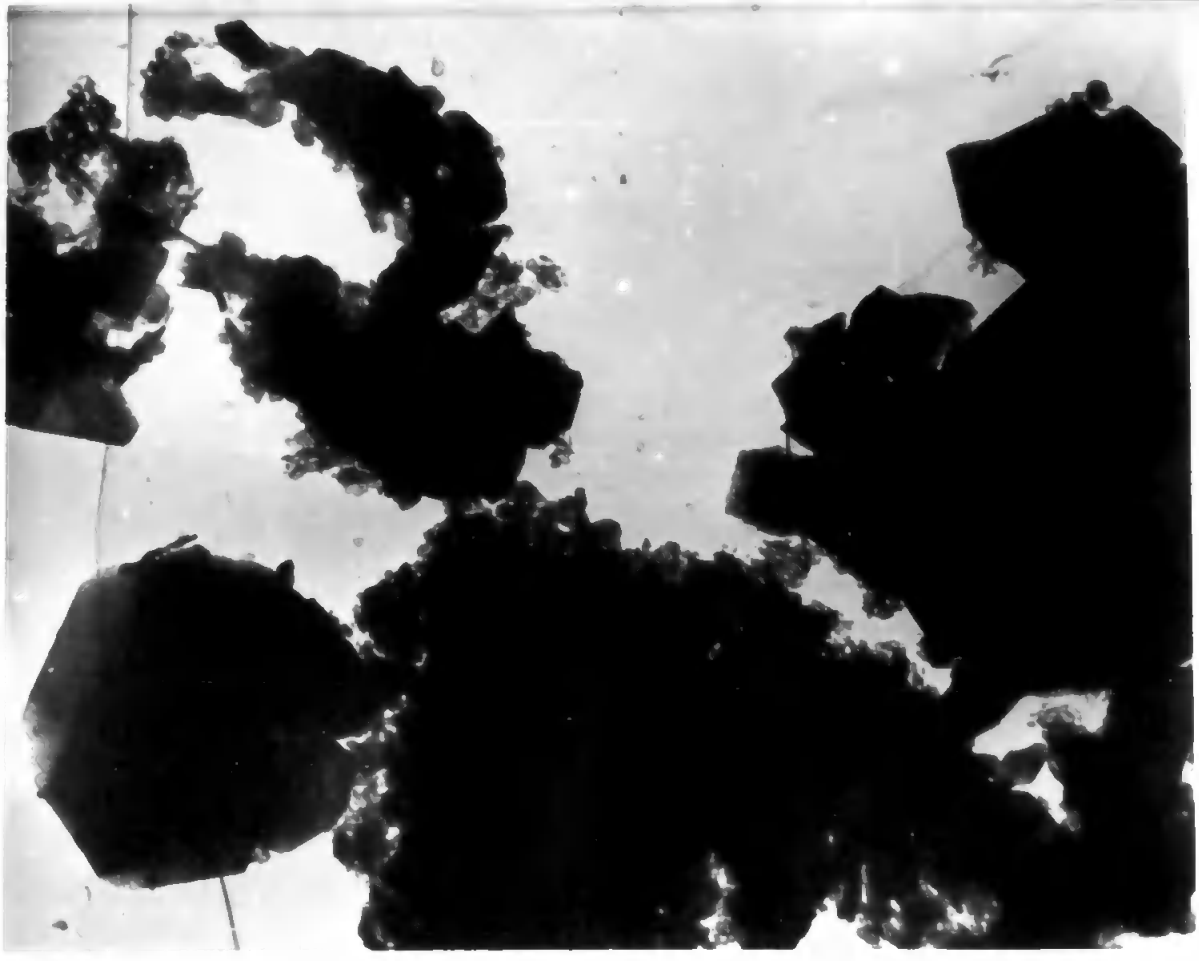

1μ

Plate 3.45 x 15,000 (See previous page)

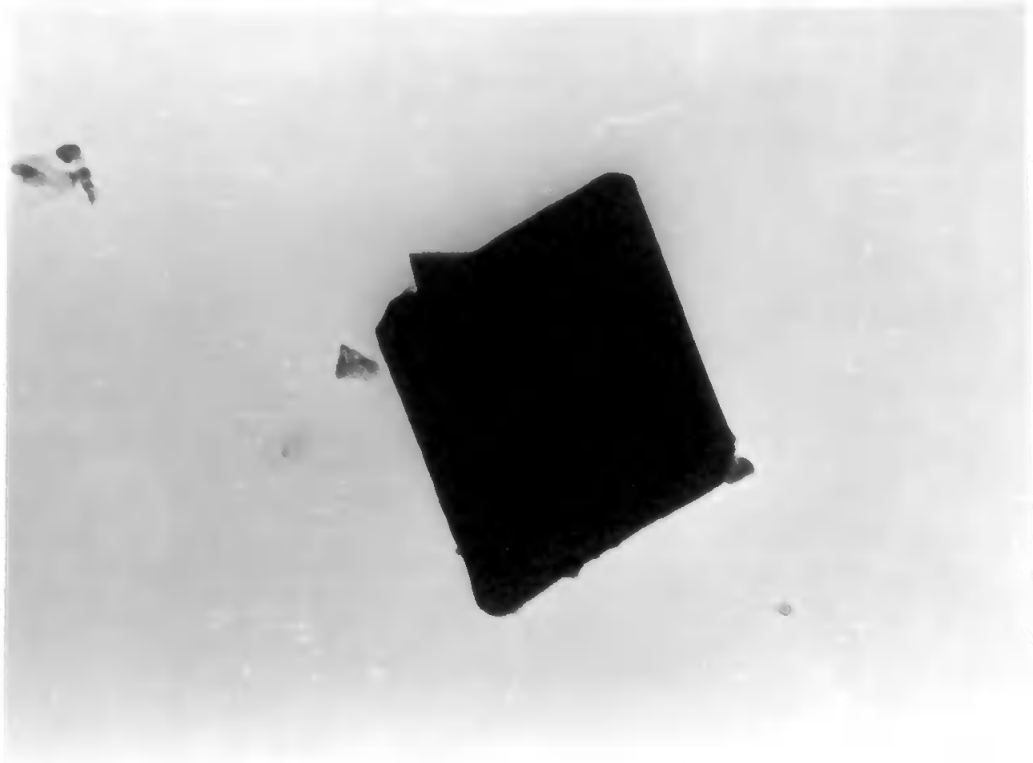

1μ

Plates 3.46 (above) and 3.47 (following page)
Mixture of lime (7.4g.) and N-urea (200 ml.) heated at 95°
for 13h. x 19,000

A 260
2 75.

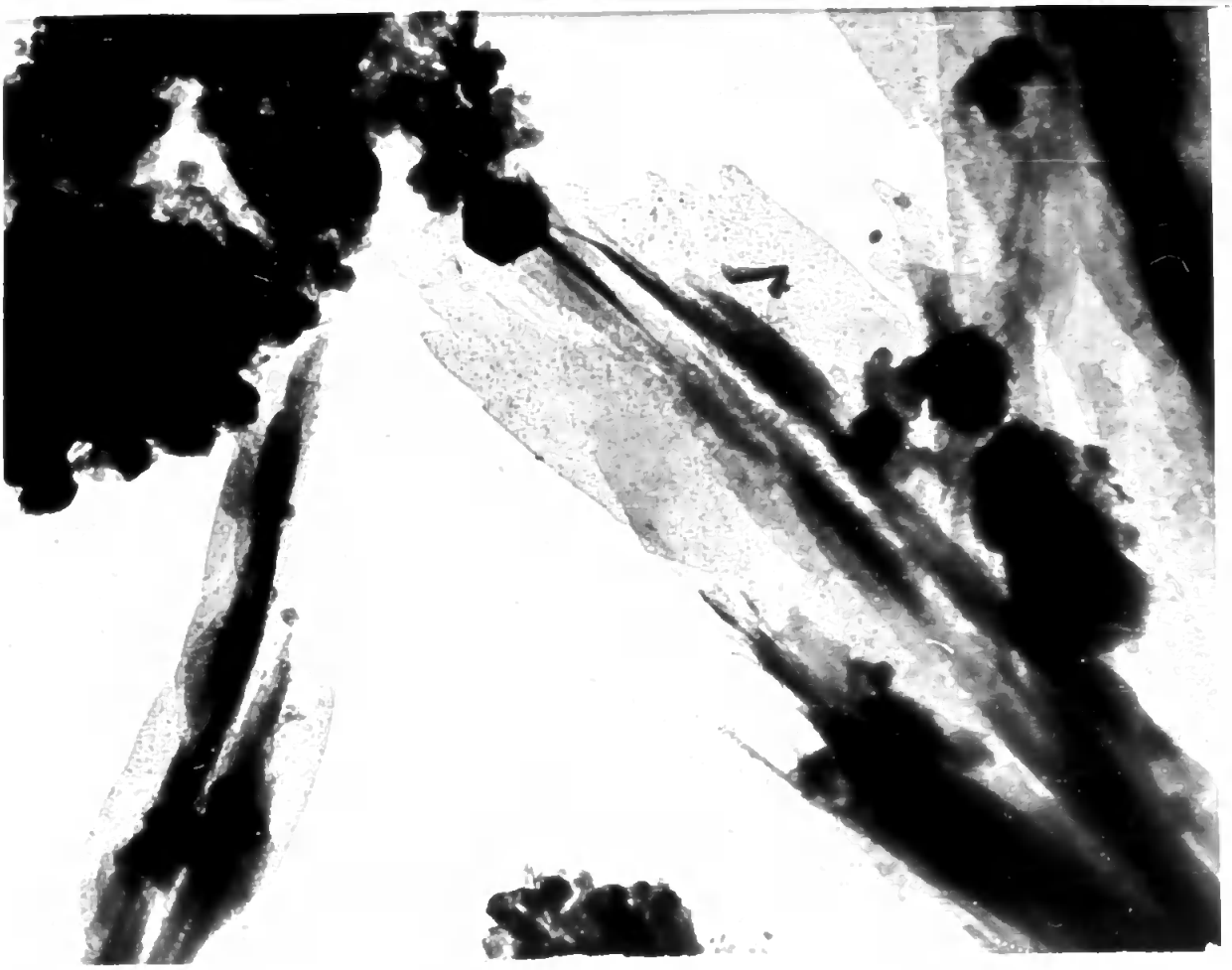

1

Plate 3.47 x 15,000 (See previous page)

A 258

4 Irion

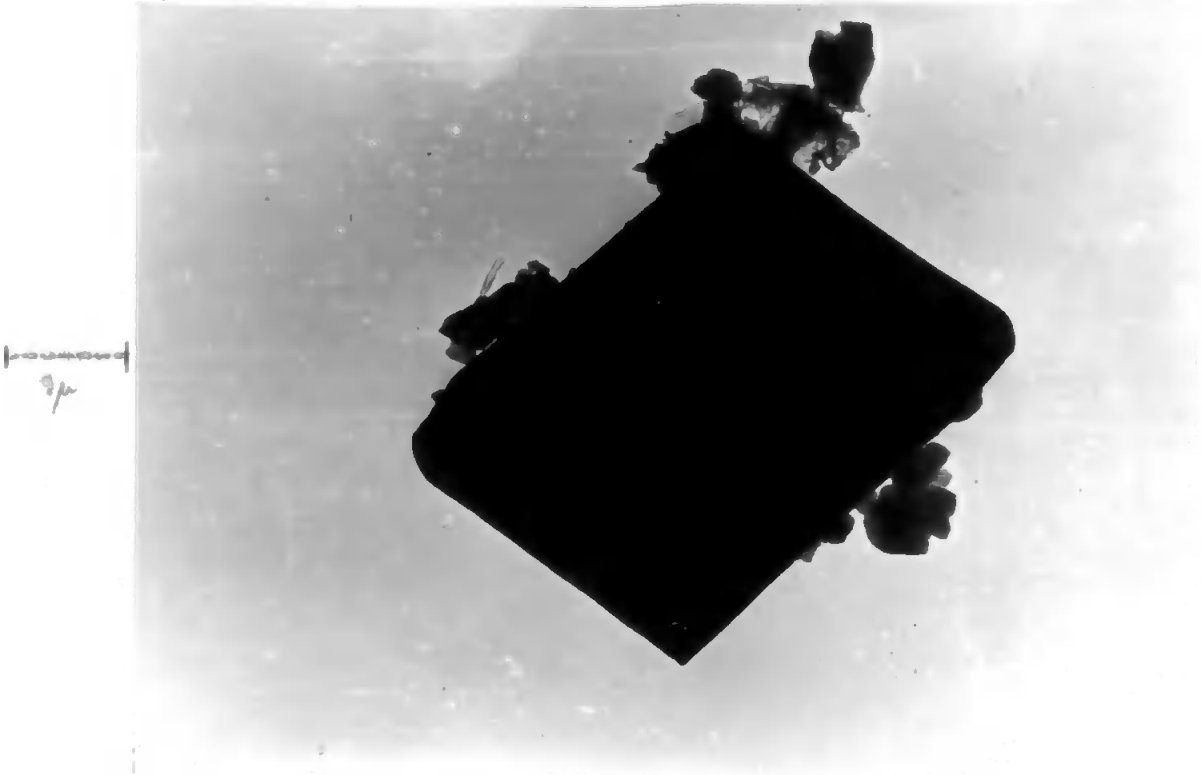

Plates 3.48 (above) and 3.49 (below)
Mixture of lime (74g.) and N-urea (200 ml.)
heated at 95° for 20h. x 19,000

Chapter 4

ZINC AND CADMIUM NITRIDES

4.1 Nitridation of Metal Films

4.1.1 Materials

Kahlbaum cadmium sticks and zinc rasps were used in the preparation of the metal films. The nitridation of the films was attempted using ICI ammonia.

4.1.2 Procedure

The metal films were prepared by vapour deposition using the same technique as that used in the preparation of magnesium and calcium films, Section 3.1.2. Nitridation of the films with ammonia was attempted by methods also analogous to those used with calcium and magnesium.

4.1.3 Results

Electron micrographs and diffraction patterns illustrating the metal films and the effect of ammonia on them are presented in Plates 4.1 - 4.6.

4.1.4 Discussion

Compared with films of calcium and magnesium (Section 3.1), those of zinc and cadmium show less microstructural uniformity, this being more pronounced for cadmium, e.g., compare Plates 3.1, 3.3, 3.9, 4.1 and 4.5 with one another.

Plate 4.1 shows a vapour deposited zinc film and Plate 4.2 its electron diffraction pattern. On heating for 1½h. at 300° in ammonia gas at a pressure of 7 cm. of mercury, no chemical reaction appears to occur, but the

metal sinters. Sintering is enhanced also when the sample is placed in the path of the beam in the electron microscope. Plates 4.3 and 4.4 illustrate the film after heating in ammonia. The growth of the crystallites of zinc, Plate 4.3, results in increased "spottiness" in the diffraction pattern, Plate 4.4 (cf. Plates 4.1 and 4.2). The results are in agreement with those of earlier workers, who also report the absence of chemical reaction between zinc and ammonia at the temperature used above, Section 1.8.1.

The results for cadmium are similar to those for zinc. No nitridation appears to occur with ammonia at 300°. Compared with films of zinc, those of cadmium possess less microstructural uniformity, the cadmium crystallites being larger and more regular in shape, Plate 4.5 (cf. Plate 4.1). The effect of sintering is shown in Plate 4.6. The films give electron diffraction patterns similar to those of zinc.

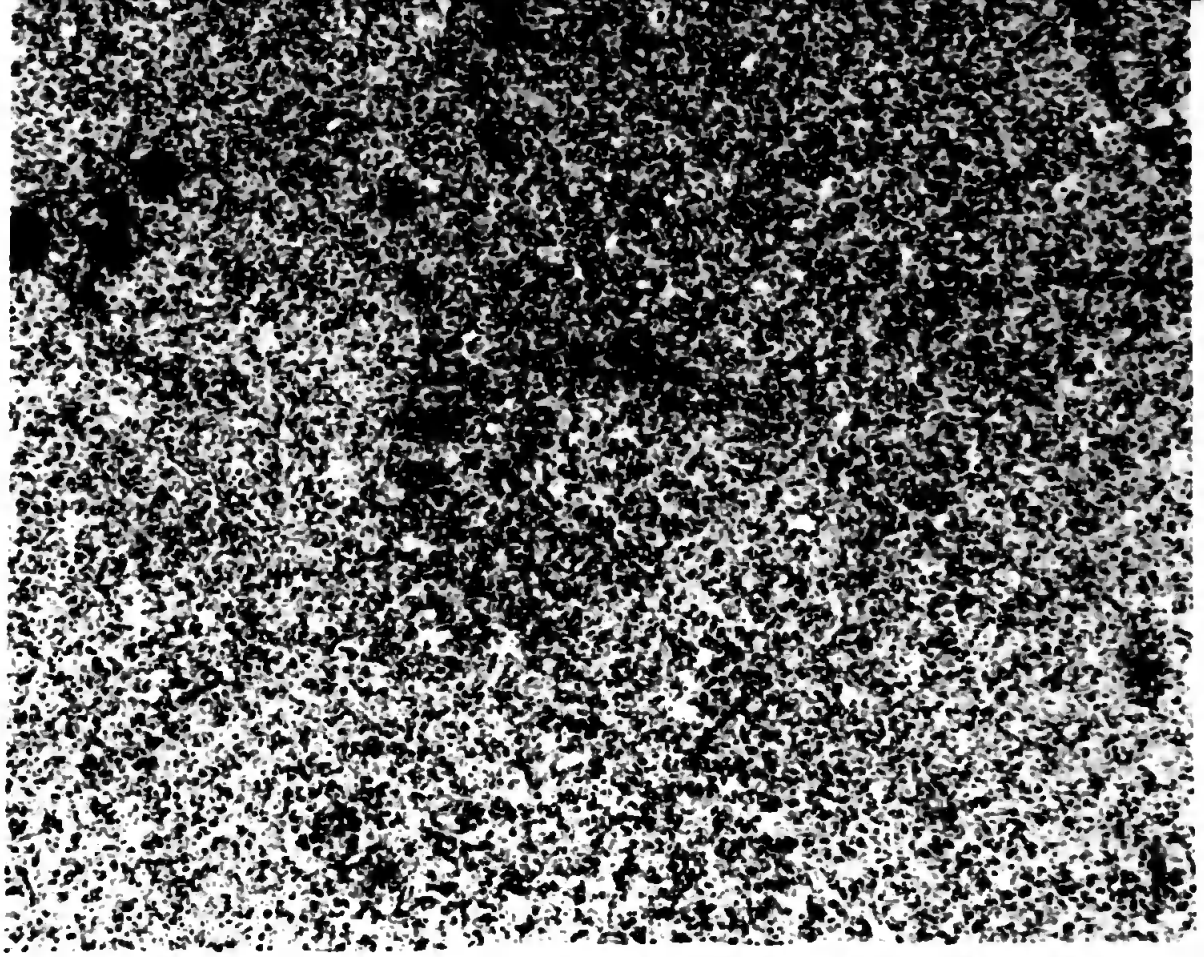

Plate 4.1 Vapour deposited zinc film x 15,000

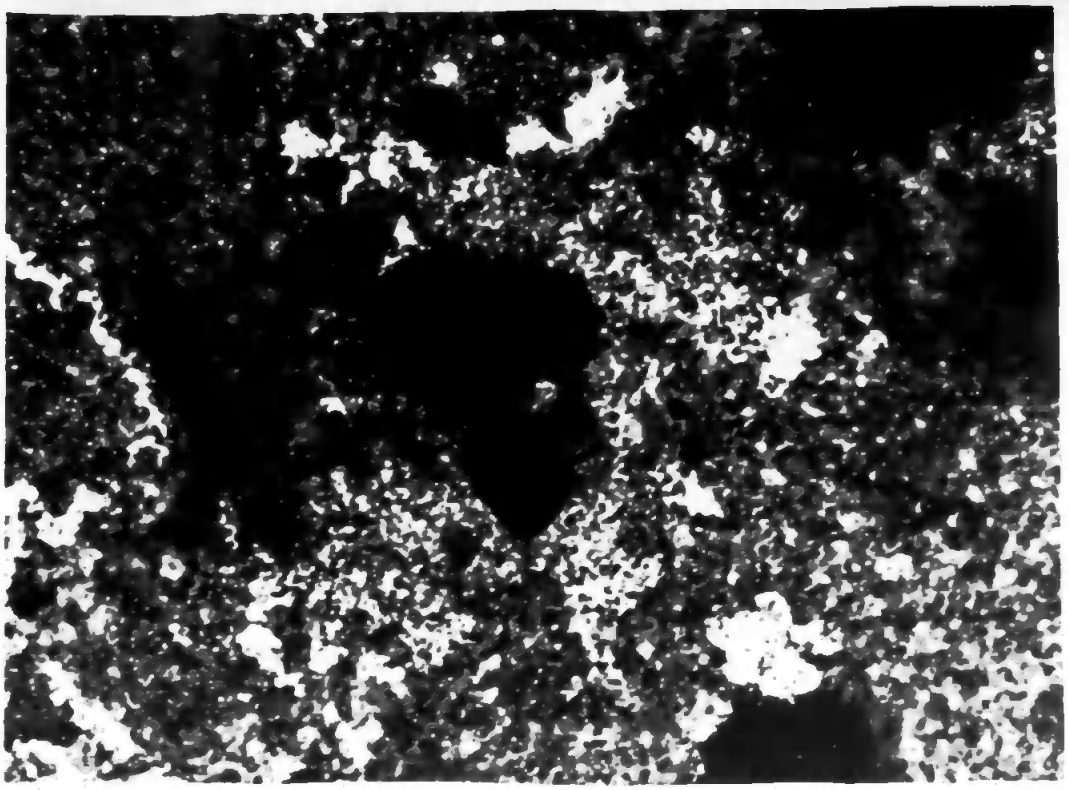

1μ

Plate 4.3 Vapour deposited zinc film heated in ammonia at 300° for 1½h. x 15,000

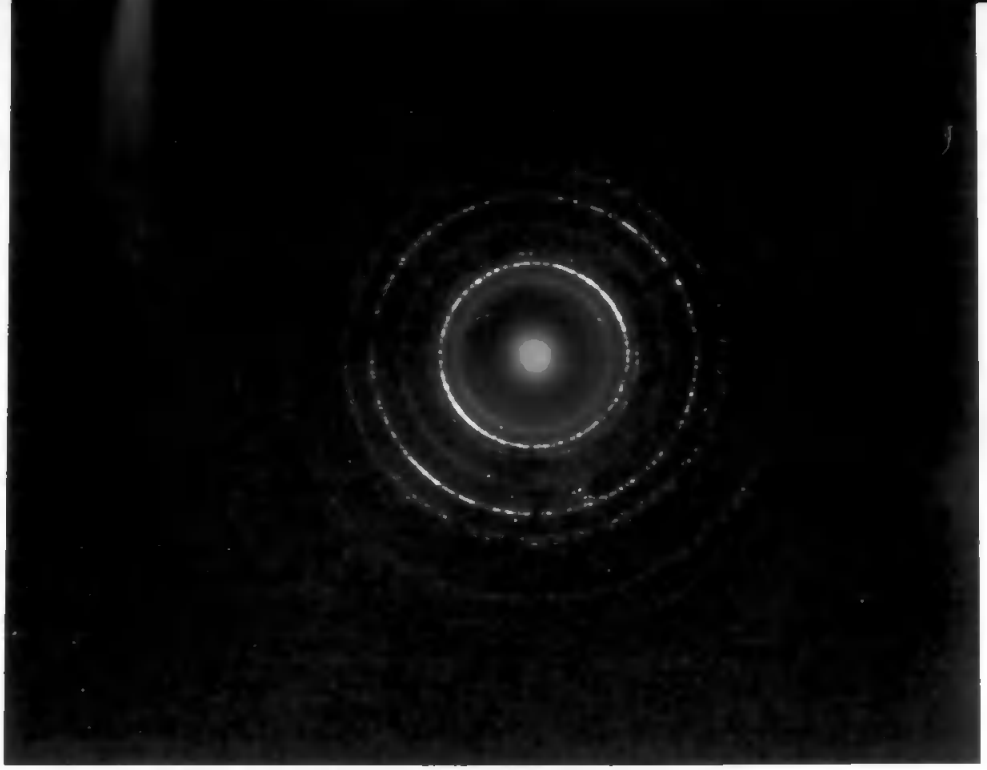

Plates 4.2 (above) and 4.4 (below)
Electron diffraction patterns of zinc film before and after heating in ammonia (cf. Plates 4.1 and 4.3)

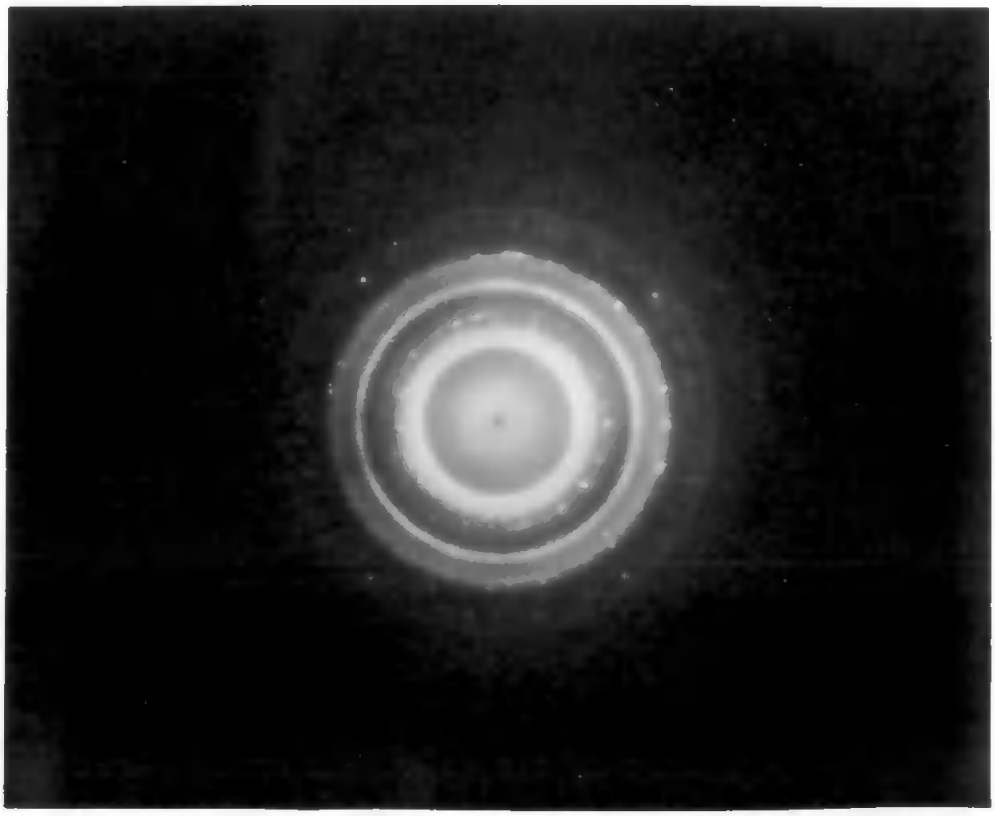

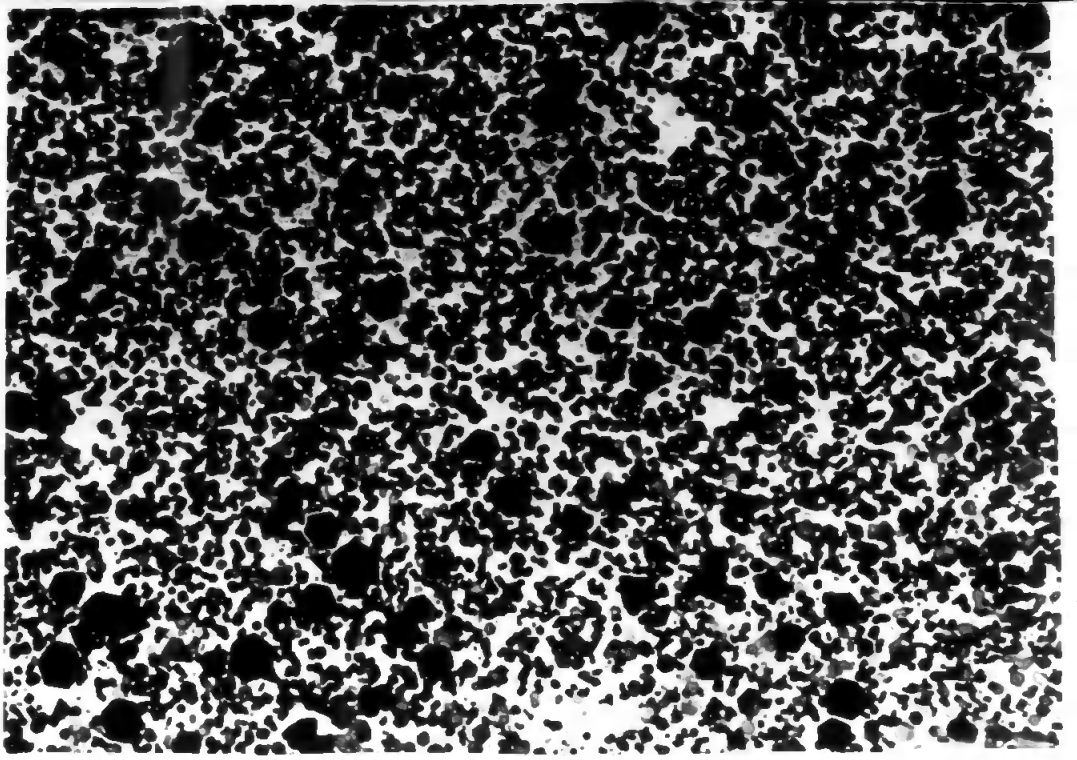

1μ

Plates 4.5 (above) and 4.6 (below)
Vapour deposited cadmium film before and after heating in ammonia at 500° for 24h. x 15,000

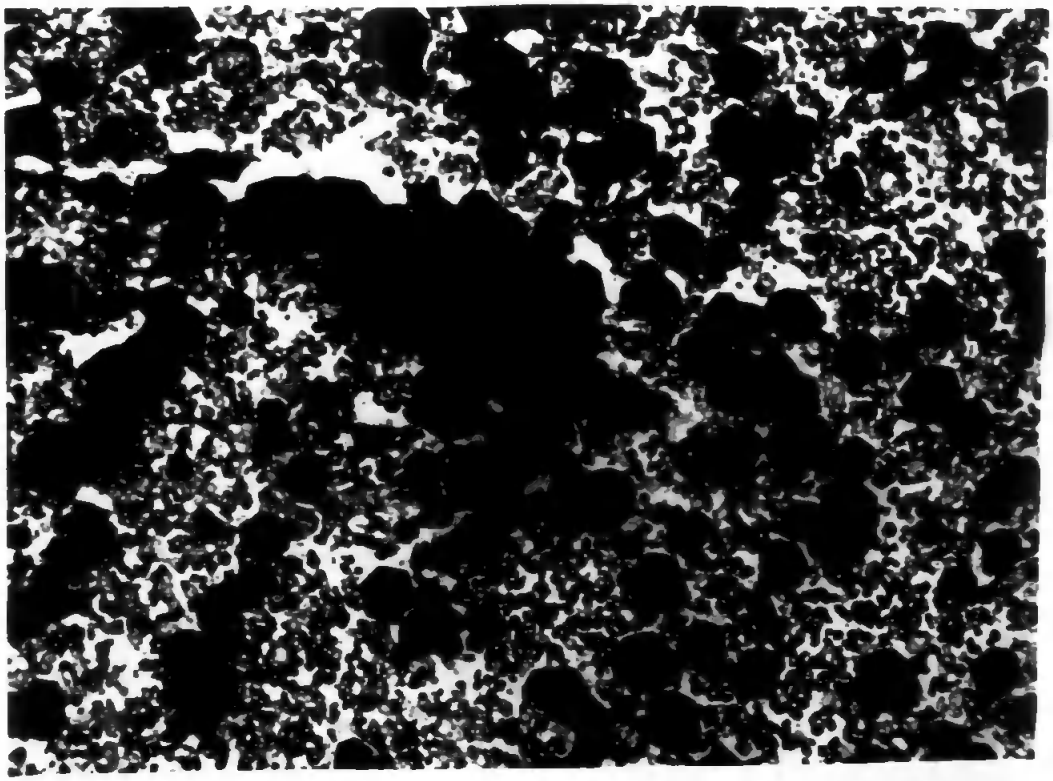

1μ

4.2 Solubility of Oxides in Ammonia

4.2.1 Materials

BDH zinc and cadmium oxides were used.

4.2.2 Procedure

Ammonia solutions of different concentrations were mixed separately with sample portions of zinc oxide, and the mixtures were shaken for several hours. The suspensions were allowed to settle and the clear saturated solutions analysed for their zinc content by titration against potassium ferrocyanide.

The procedure was repeated with cadmium oxide.

4.2.3 Results

The solubilities of the two oxides in aqueous ammonia are presented graphically in Figure 4.1. For comparison, the corresponding curve for mercuric oxide is drawn on the same scale (Slasson, 1949).

4.2.4 Discussion

At a given ammonia concentration the solubility of zinc oxide is somewhat greater than that of cadmium oxide, and much greater than that of mercuric oxide. The solubilities of zinc and cadmium oxides increase more rapidly than that of mercuric oxide with increasing ammonia concentration. The increasing solubility implies that the hydrolysis of the metal nitrides with water is enhanced by the formation of the complexes, Section 1.9.

Figure 4.1 Solubilities of zinc, cadmium and mercuric oxides in aqueous ammonia

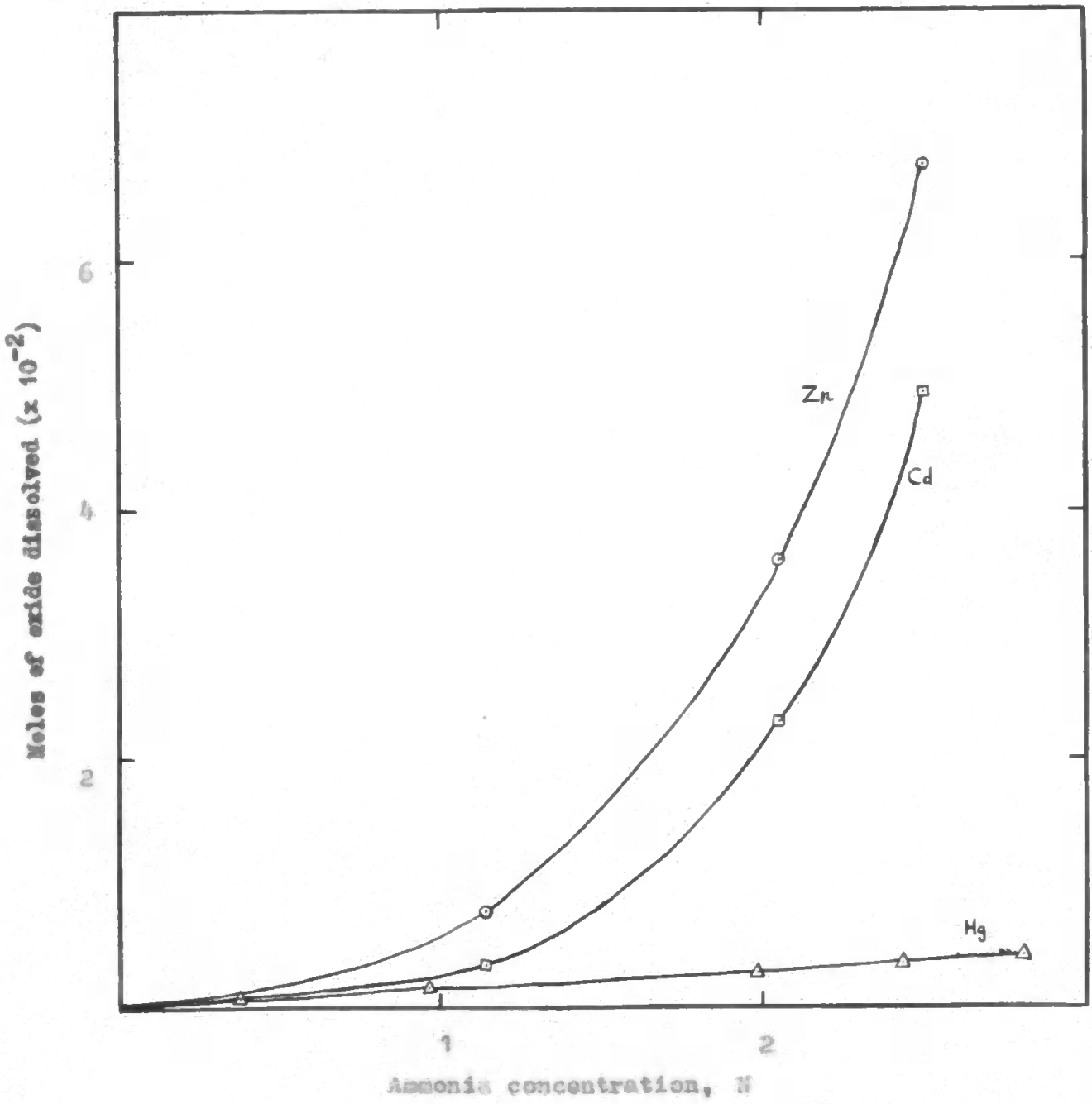

Chapter 5

BORON NITRIDE

5.1 Calcination of Boron Nitride

5.1.1 Materials

The boron nitride used in this study is a product of Alfa Inorganics Inc. It is a white powder having a flaky texture.

5.1.2 Procedure

Samples of boron nitride were calcined in air at 800° for various lengths of time. The rate of oxidation was determined by weighing the samples before and after calcination. The products were examined by X-ray diffraction, electron microscopy and surface area measurements.

5.1.3 Results

The rate of oxidation of boron nitride is shown in Figure 5.1. Electron micrographs illustrating the reaction are presented in Plates 5.1 - 5.8. The micrographs are of sample portions, which are of sufficiently fine division to be examined on the instrument.

5.1.4 Discussion

Boron nitride oxidises at 800° forming boric oxide, B_2O_3, even in the early stages of the calcination, as observed by Sagyanosky & Samsonov (1952), Section 1.12. The process is accompanied by a rapid decrease in specific surface from 11.5 $m.^2g.^{-1}$ for boron nitride to below the measurable limit of about 0.3 $m.^2g.^{-1}$ for the product (average crystallite size from 0.23μ to >2.0μ). This is

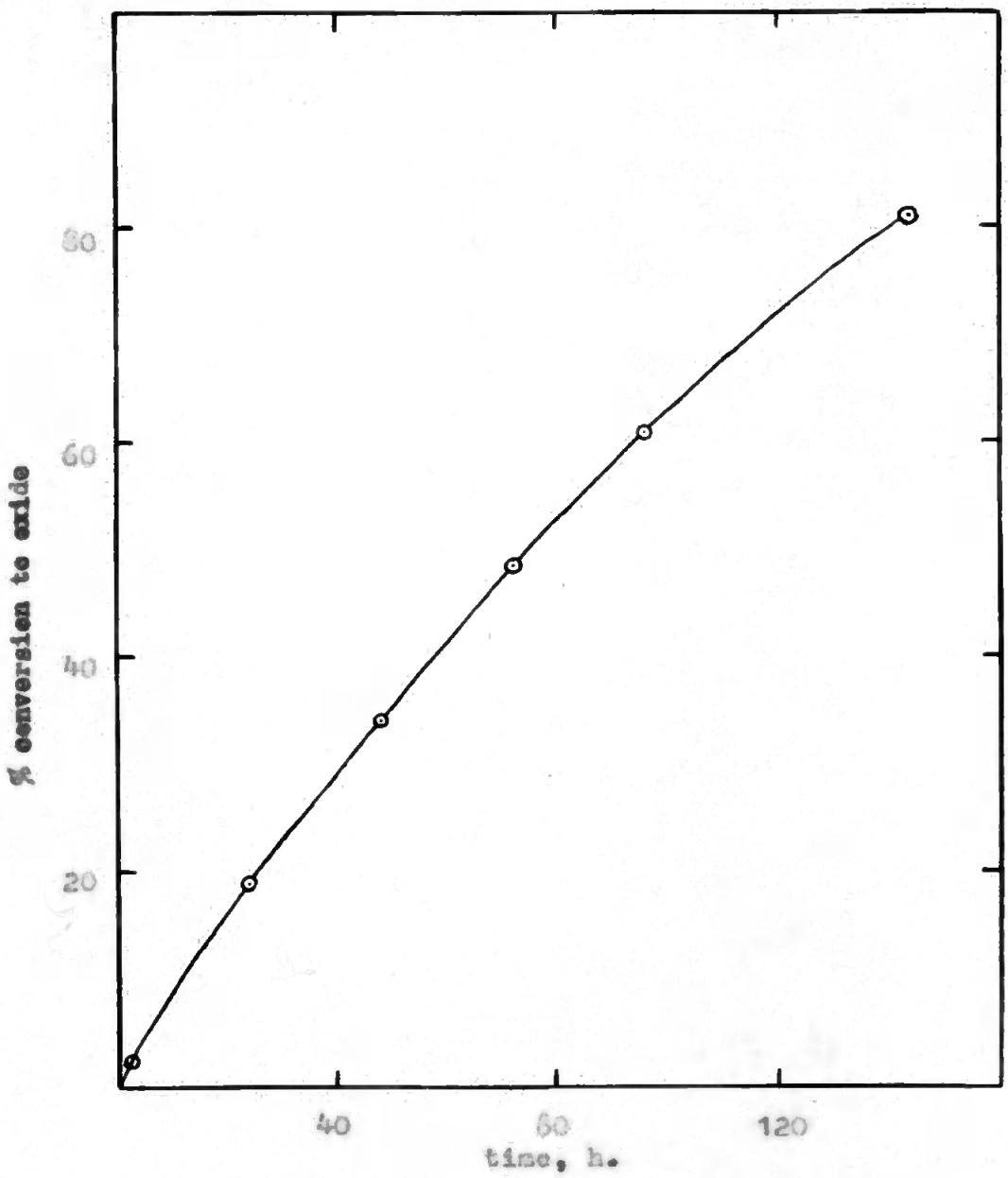

Figure 9.1 Calcination of boron nitride at 800°

attributed to the low melting point (~450°) of boric oxide, which therefore acts as a mineraliser. Thus, the products tend to bond together and shrink, cf. bonding and hot pressing of boron nitride with silica (Carborundum Co., 1965). Consequently, the rate of reaction tends to decrease as the oxidation becomes increasingly controlled by liquid or solid state diffusion, especially the latter. The effect is more pronounced for silicon nitride oxidation, which is similar to that of boron nitride, but different from aluminium nitride oxidation (Coles, Glasson & Jayaweera, 1969; see Appendix I).

Plate 5.1 is an electron micrograph showing rod-shaped and hexagonal plate-like particles in a sample of boron nitride. Calcination results initially in the rounding of the hexagonal plates, followed by their aggregation, Plates 5.2 and 5.3. Further calcination continues this aggregation (Plate 5.4) and also causes distortion of the rod-shaped particles, Plates 5.5 and 5.6. When about 80% of the nitride has been oxidised there is sufficient oxide in the divided state to change the appearance of the aggregates, Plates 5.7 and 5.8.

Plate 5.1 Boron nitride x 15,000

75

2 20

Plate 4.2 Boron nitride calcined at 800° for 5h.
x 15,000

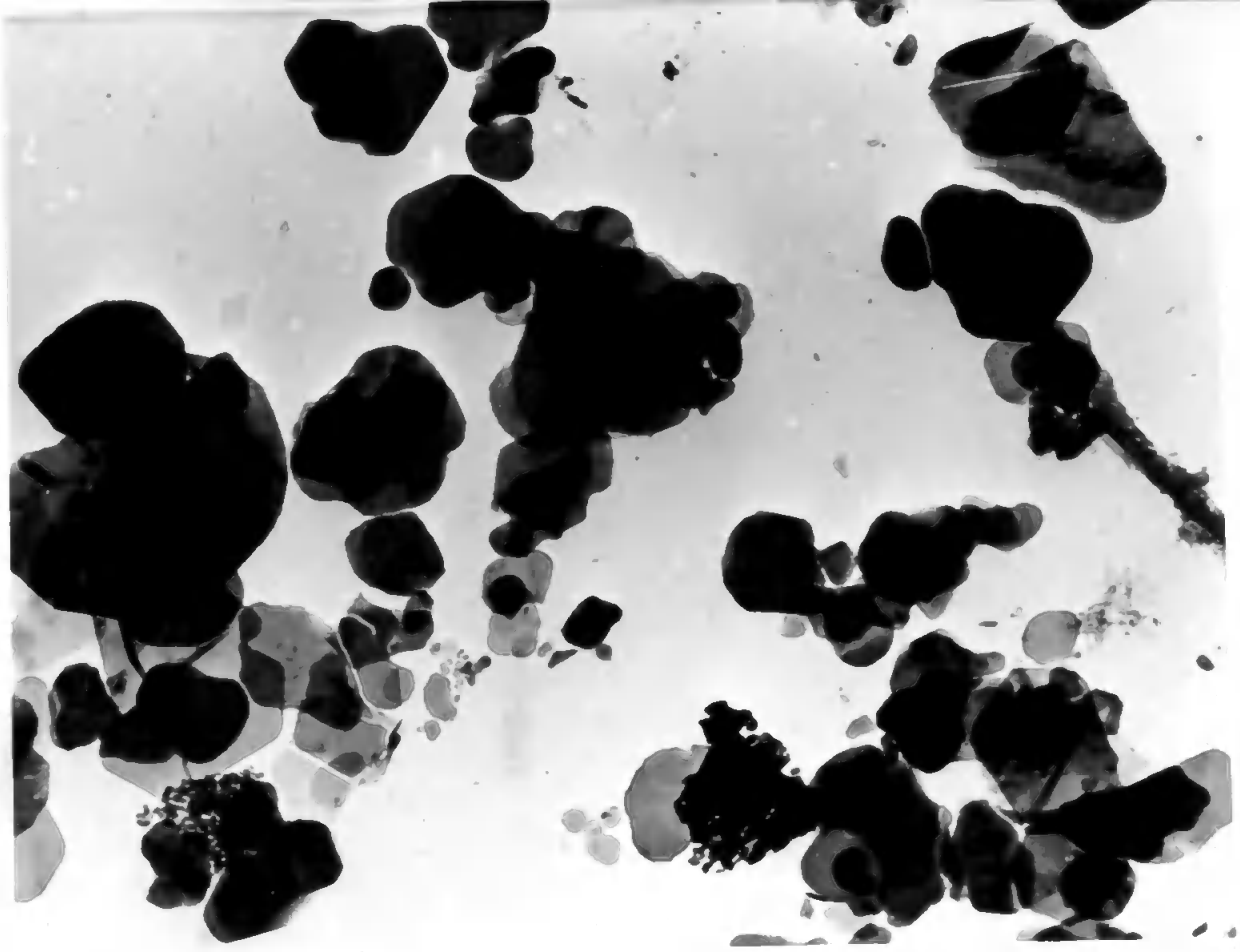

1μ

Plate 9.3 Boron nitride calcined at [illegible]° for [illegible] hr.
x 15,000

82

2 10

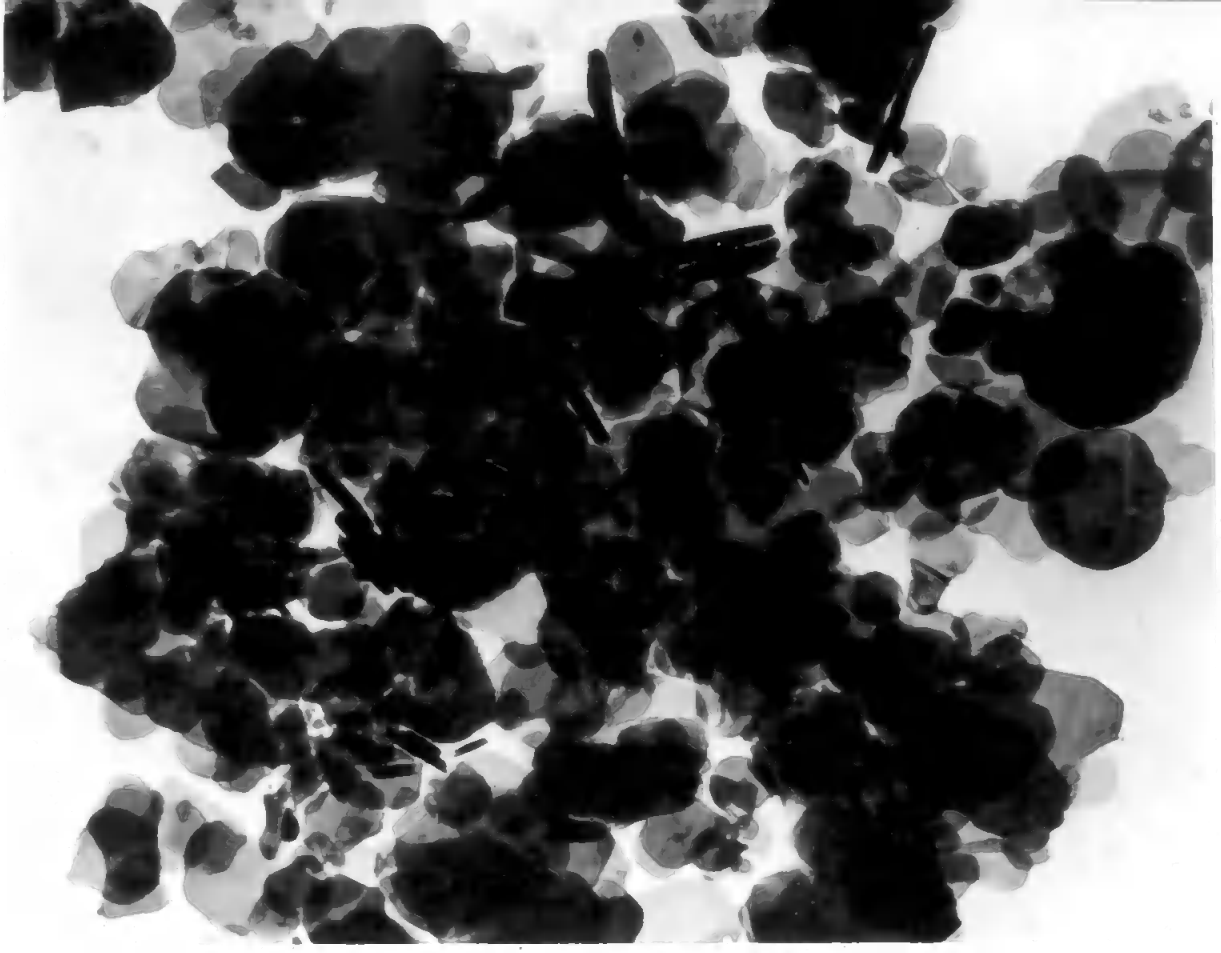

Plate 5.4 Boron nitride calcined at 600° for 2 days
x 15,000

86

1 30

1μ

Plate 5.9 Boron nitride calcined at 300° for 2 days
x 15,000

82

2 15

1μ

Plate 5.5 Boron nitride calcined at 800° for 4 days
x 15,000

1μ

Plate 5.7 Boron nitride calcined for 6 days at 600°
x 15,000

1μ

Plate 9.8 Boron nitride calcined at 800° for 6 days
x 19,000

TITANIUM AND ZIRCONIUM NITRIDES

6.1 Calcination of the Nitrides

6.1.1 Materials

The titanium and zirconium nitrides are products of Alfa Inorganics Inc. Titanium nitride is a dark greenish-brown powder. Zirconium nitride is a grey powder and contains some free metal, which shows up clearly on the X-ray powder patterns.

6.1.2 Procedure

The nitride samples were calcined in air for various lengths of time and at different temperatures, and their weight changes determined. The products were examined by methods similar to those used with the hydrolysis products of calcium and magnesium nitrides, Section 3.2.2.

6.1.3 Results

The variations in the specific surface and average crystallite size of titanium nitride with the extent of oxidation at 600° are shown in Figures 6.1a-d. The rate of oxidation at 1000° is shown in Figure 6.2. Electron micrographs illustrating the changes are presented in Plates 6.1 - 6.3.

The rate of oxidation of zirconium nitride at various temperatures is shown in Figure 6.3. The change accompanying the reaction is illustrated in Plates 6.4 - 6.5.

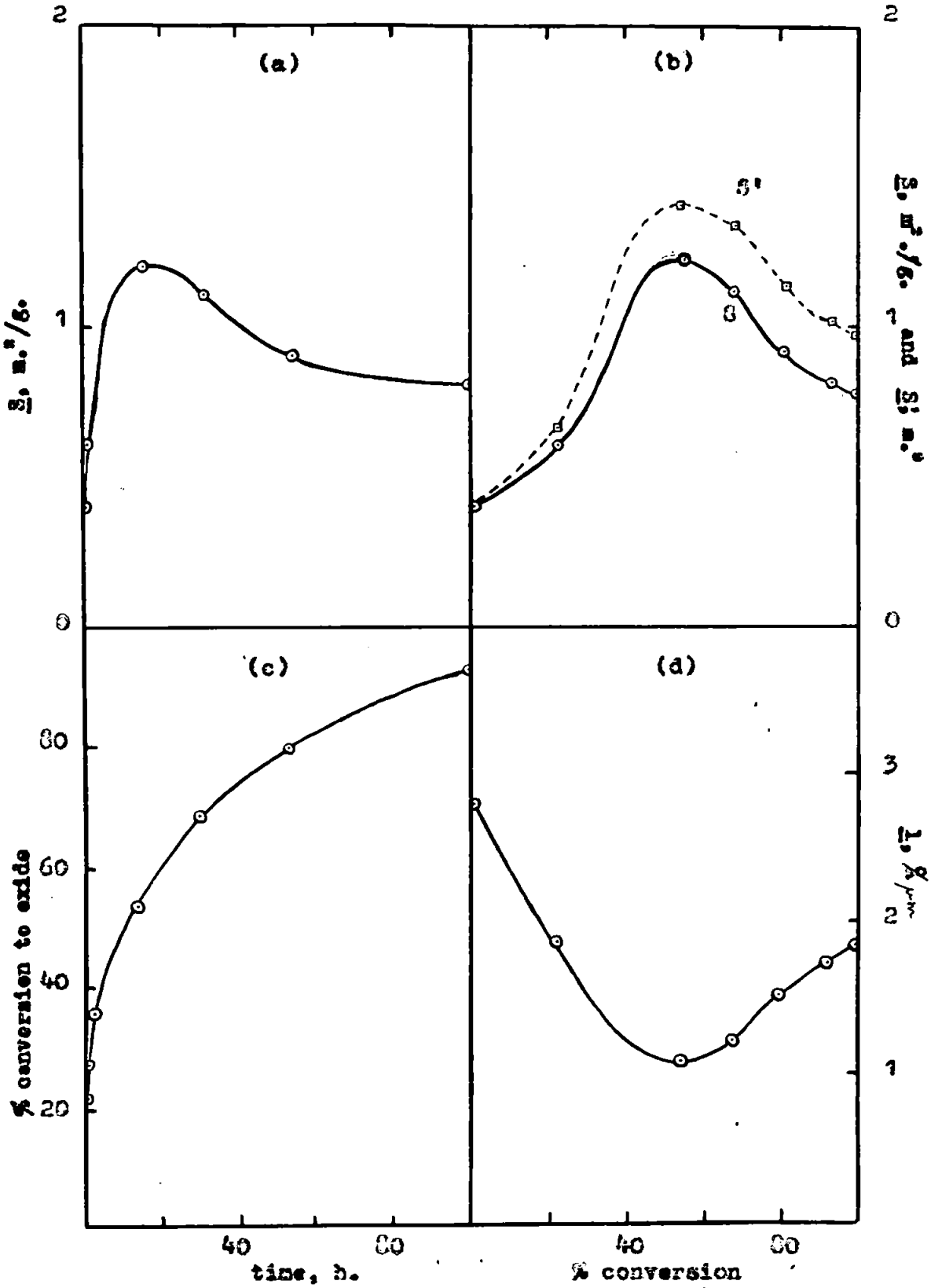

Figure 6.1 Variations in the average crystallite size, l, specific surface, S, and actual surface area, S', with the rate of oxidation in the calcination of titanium nitride in air at 600°.

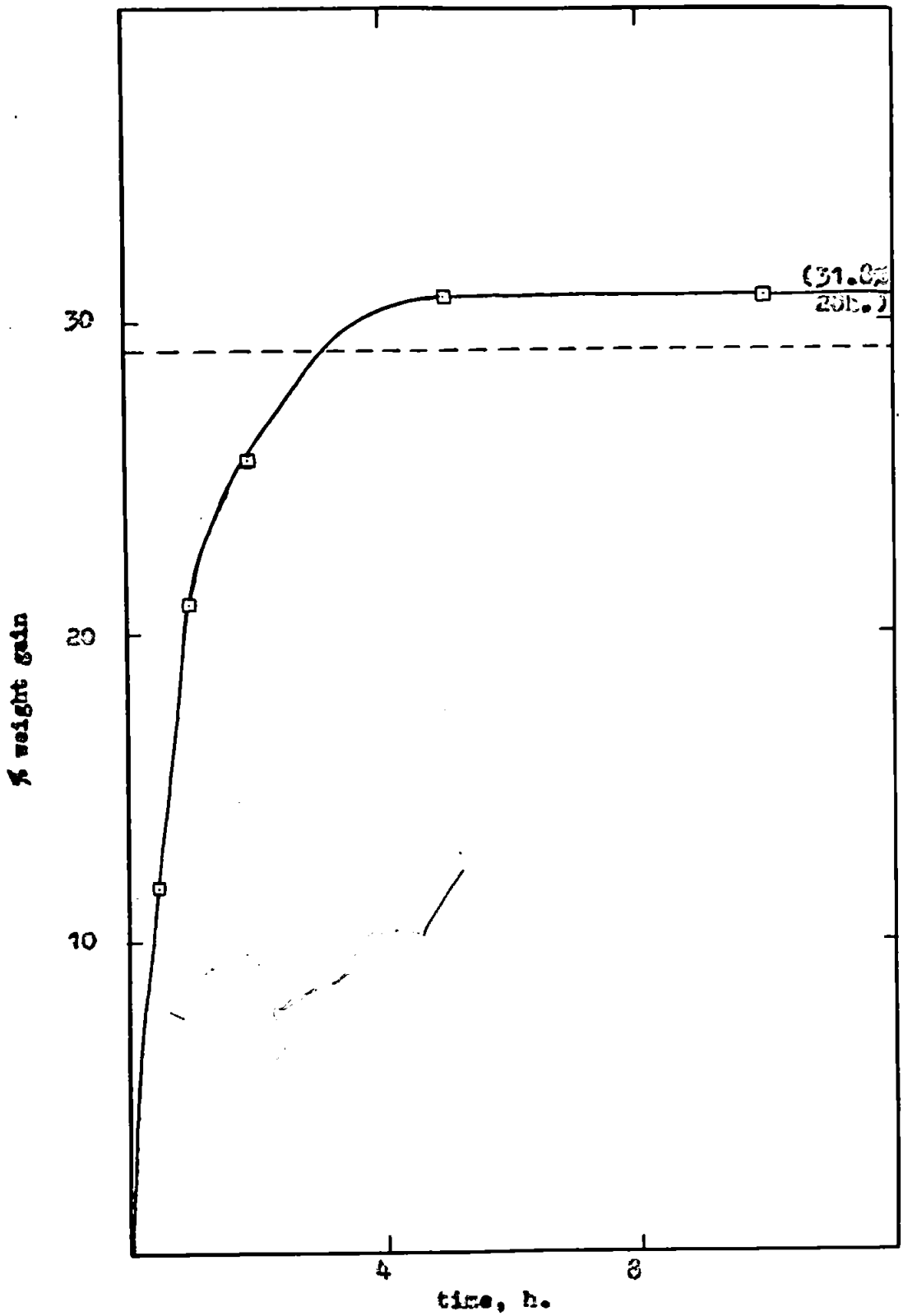

Figure 6.2 Rate of oxidation of titanium nitride at 1600°

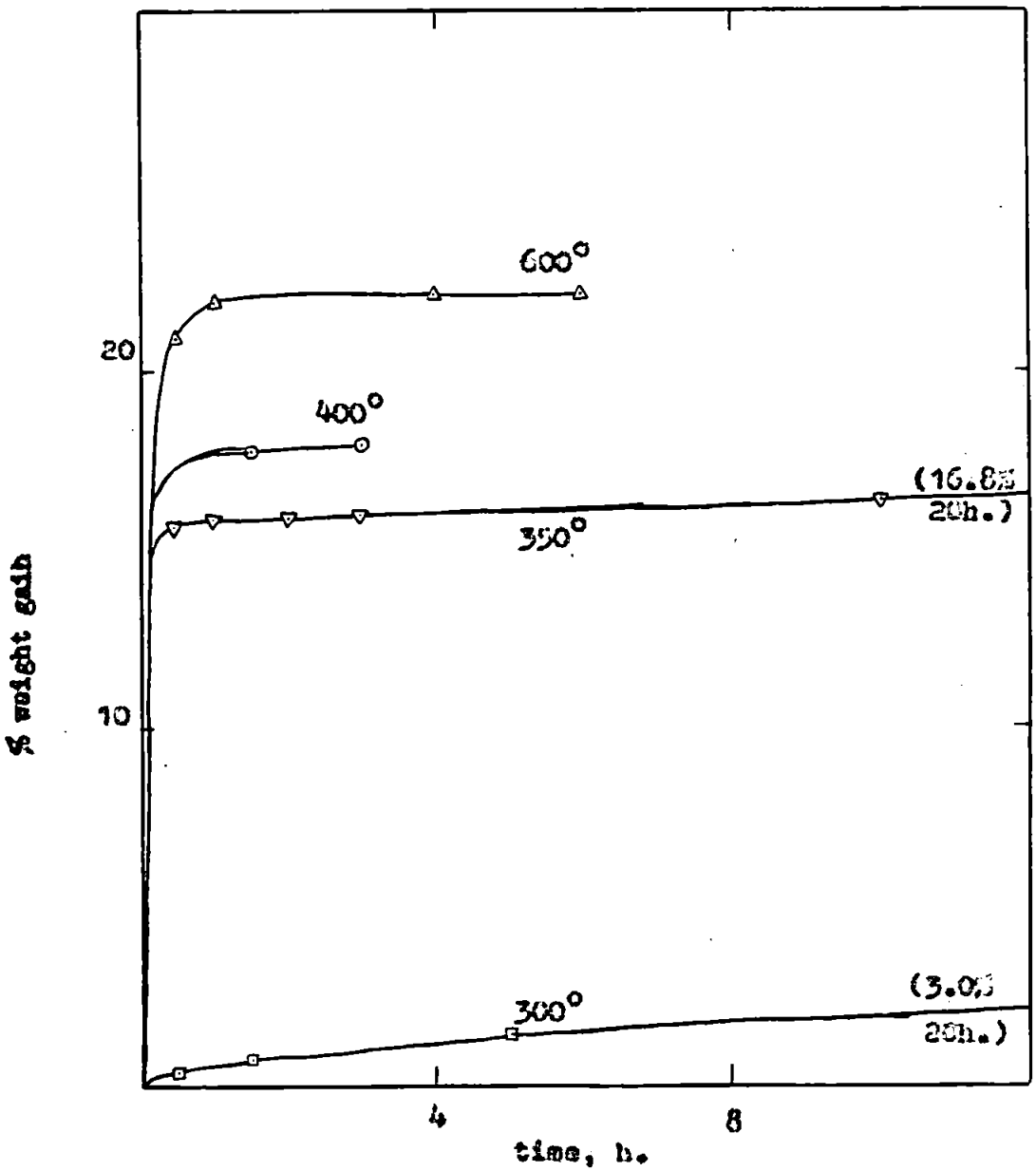

Figure 6.3 Oxidation of zirconium nitride at different temperatures

6.1.4 Discussion

Calcination of titanium nitride in air at 600° results in the tetragonal oxide (rutile, TiO_2) being formed. Figure 6.1c confirms that the weight increase is initially rapid, accelerating during the first half hour, before becoming approximately linear and then parabolic (Samsonov & Golubeva, 1956; Münster & Schlamp, 1957a-b, 1959), as is observed for aluminium nitride (Coles, Glasson & Jayaweera, 1969).

The X-ray diffraction patterns of products formed between 400 - 1000° show nitride and oxide "reflections" only, indicating no intermediate compounds with different lattice dimensions, e.g., oxynitrides. At 600° the reflections due to rutile are observed only after about 25% of nitride is oxidised. However, at 500° broadened oxide peaks appear after only 7% oxidation in 5h. The longer calcination time at the lower temperature permits crystallisation of rutile. At higher temperatures crystallisation may be retarded by the ability of oxygen to replace nitrogen up to $TiN_{0.6}O_{0.4}$ in the TiN lattice without altering its dimensions. This occurs when the binary compounds are sintered at 1700°, and is followed by a decrease in the lattice constant indicating a limited solubility of TiN in TiO (Schmitz-Dumont & Steinberg, 1954).

During the first 25% weight gain at 600°, there is comparatively little increase in specific surface, S, and the actual surface area from an initial 1g. sample of nitride, S'. This is followed by a more rapid increase

and then a decrease in these quantities as the reaction proceeds, Figures 6.1a-b, i.e., an initial increase and then a decrease in the average crystallite size, Figure 6.1d. Thus, the titania splits off to give smaller crystallites when it crystallises out from the nitride matrix during the accelerator and approximately linear stages of oxidation, cf. Plates 6.1 and 6.2. No discontinuities in the oxidation rates are observed when the samples are cooled for surface area measurements and subsequently reheated. Thus, any additional spalling at the nitride - oxide interface is negligible in the cooling process. This indicates that crystallite splitting is mainly due to the changes in crystal structure (cubic face-centred to tetragonal) and molecular volume (fractional increase of 0.630), as the nitride changes to the less dense oxide, cf. Pilling & Bedworth (1923) Rule for metal oxidation. The maximum increase in the number of crystallites calculated from surface area data according to Glasson's (1950b) method (Section 1.6) is about 20-fold, cf. oxidation of aluminium nitride at 1000° (Coles, Glasson & Jayaweera, 1969). Crystallite splitting apparently facilitates release of nitrogen, for the ultimate weight gain (after 200h.) at 600° is the theoretical value corresponding to complete conversion of TiN to TiO_2.

The factors, which contribute to the detailed shape of the initial oxidation rate curves and which are summarised in Section 1.6, apply similarly to the oxidations of titanium and aluminium nitrides (Coles, Glasson & Jayaweera, 1969).

Until a specific amount of oxide is formed, a coherent layer of titania is not produced. The nitride surface remains exposed to the reacting gas, so that the kinetics of the reaction approaches linearity, cf. Section 1.9. When there is sufficient oxide of rational crystallite size composition, it sinters to form surface films through which normal gaseous diffusion cannot easily occur. Solid state diffusion is now the rate-controlling factor, the kinetics becomes parabolic, and the surface area decreases after about 90% conversion, as is observed in Figure 6.1b.

At 600° (873°K) limited sintering by surface diffusion is likely for titanium oxide, for its melting point (1920°) gives $0.5T_m$ = 1097°K and $0.3T_m$ = 658°K; see Section 1.6. However, the much higher melting point of titanium nitride (2930°) gives $0.5T_m$ = 901°K, so that its sintering is negligible at 600°. This explains the decrease in surface area during the later stages of the oxidation when there is more oxide and less nitride, Figures 6.1a-b.

At 1000°, the oxidation is very rapid, Figure 6.2, with about 80% of the conversion occuring during the first 2h. by an advancing yellow - brown interface through the sample. Since this temperature is well above the Tammann temperature of the oxide, sintering is extensive, Plate 6.3. Weight changes indicate that the final mass of titania retains some residual nitrogen corresponding to an overall composition of SiO_2N_z, where z = 0.075. A similar behaviour has been observed by Dell, Wheeler & McIver (1966) in the oxidation

of uranium nitride, which forms products of composition, UO_3N_x, where $x = 0.2 - 0.4$.

The activity of rutile prepared by the calcination of anatase (the other tetragonal form of TiO_2) above 1000° is much higher than that of the above samples prepared from the nitride (Glasson, Johnson & Sheppard, 1969). Presumably the titania formed by the oxidation of nitride is produced in a more compact form, and also possibly gives a grain size composition more suitable for sintering.

Oxidation studies on zirconium nitride are complicated by the presence of several forms of oxide (McCullough & Trueblood, 1959; Mazdiyasni & Lynch, 1964), and also because there is some free metal in the nitride. On calcining the nitride at 300°, the zirconium metal peaks are broadened, but there is little weight gain (30% in 20h.), Figure 6.3. At 350°, the oxidation of the free metal and of the nitride is much faster, the monoclinic oxide being formed. At 400°, however, cubic zirconia is the main product. At higher temperatures, e.g., 600°, the monoclinic oxide again appears and develops more rapidly with increasing temperature. Thus, on calcining zirconium nitride at 1000° for 20h., monoclinic zirconia is the only product, Plate 6.5 (cf. Plate 6.4). At this temperature no tetragonal oxide is detected, in keeping with the observations of Lynch, Wahldiek & Robinson (1961).

Conversion of ZrN (cubic face-centred) to cubic ZrO_2 (also face-centred) involves a fractional volume increase of 0.367, which further increases to 0.521 of the initial volume

of nitride when the formation of monoclinic zirconia is complete. Crystallite splitting is expected therefore during the calcination of the nitride as observed by Hayes & Roberson (1949). The high melting point of the nitride and the oxide (2985° and 2700° respectively) imply that even at 1000° both compounds are below their Tammann temperature, but above $0.3T_m$ (equivalent to about 700° for ZrN and 620° for ZrO_2), cf. ZnN and ZnO_2. Therefore it is expected that the compounds will sinter by surface diffusion predominantly; this counteracts the effect of crystallite splitting and leads to aggregation, Plate 6.5 (cf. Plate 6.4).

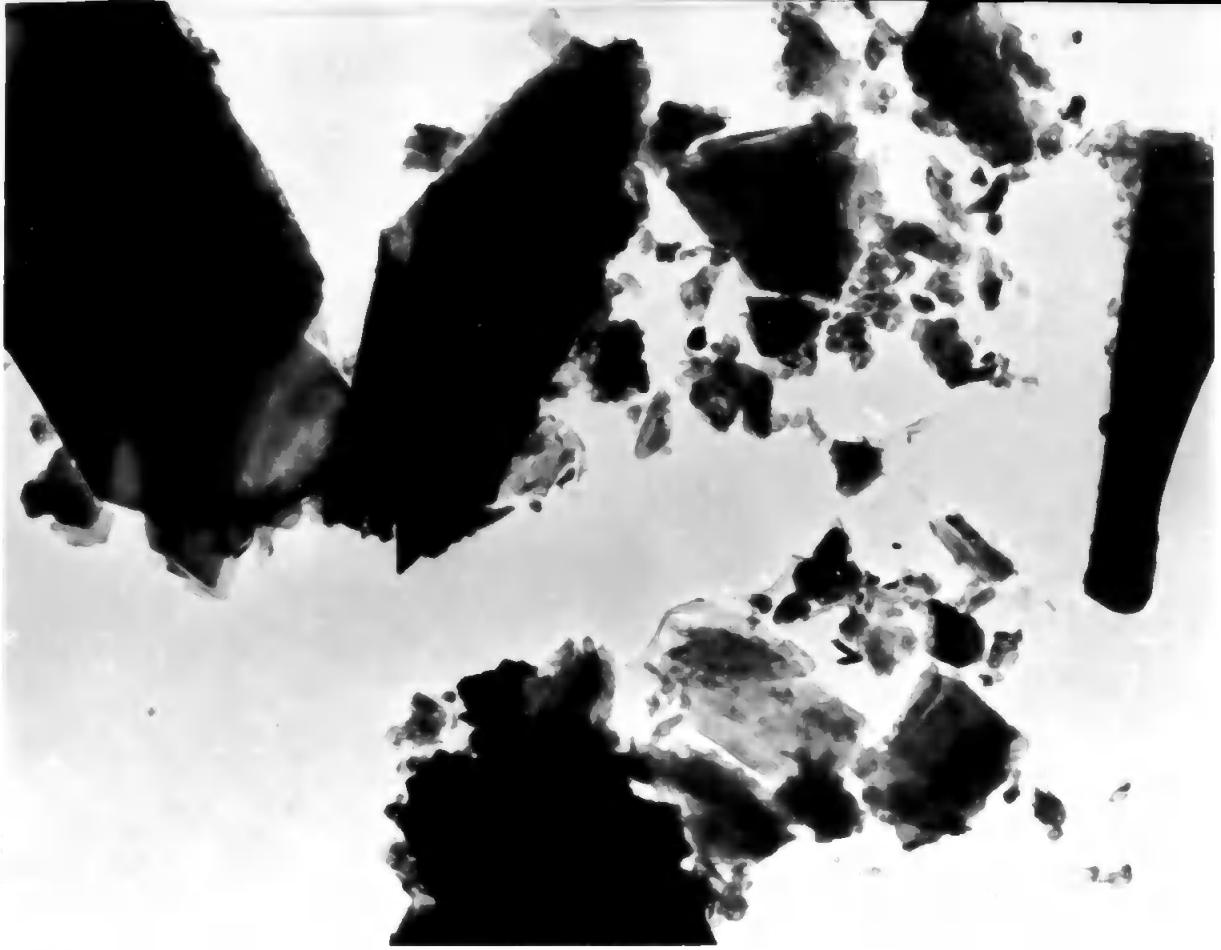

1μ

Plate [illegible].1 Titanium nitride x 19,000

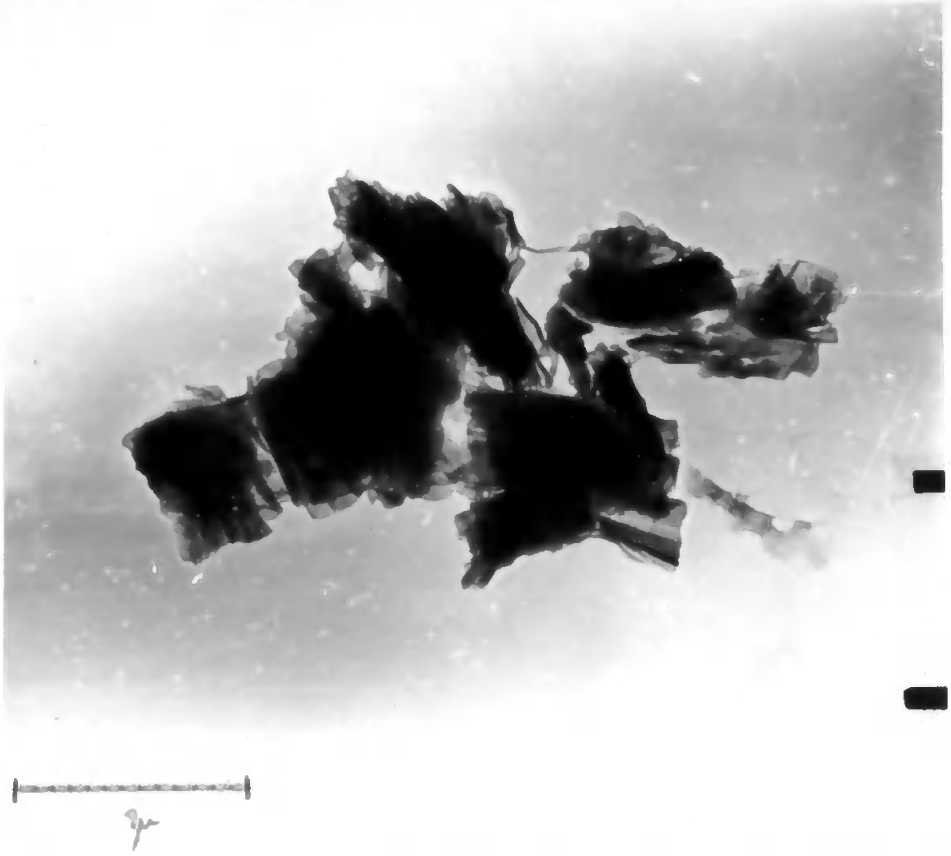

Plate 6.2 Titanium nitride calcined at 600° for 15h.
x 30,000

Plate 6.3 Titanium nitride calcined at 1000° for 20h. x 15,000

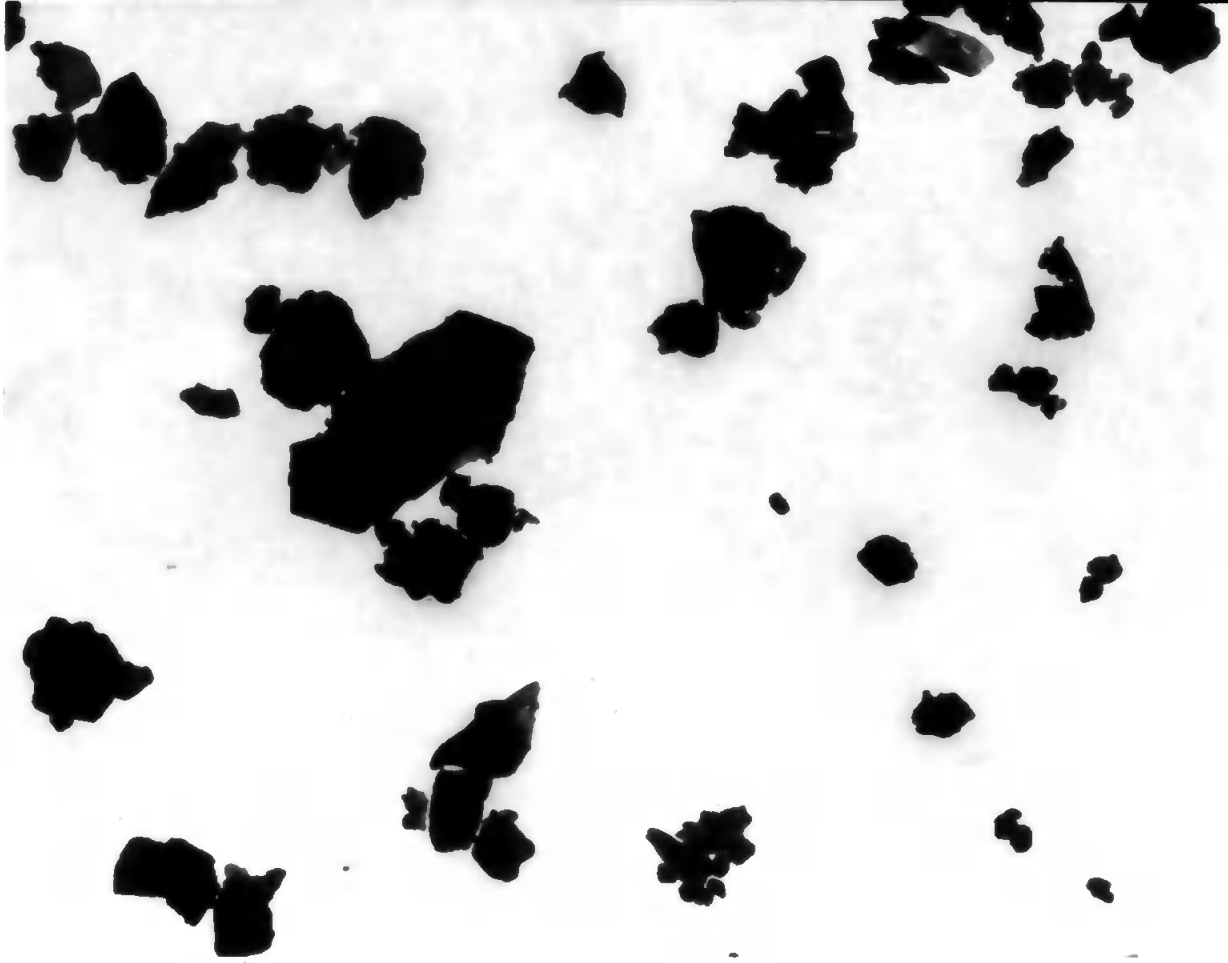

2μ

Plate 6.6 Zirconium nitride x 19,000

|------| 1μ

Plate C.5 Zirconium nitride calcined at 1000° for 2 hr.
x 15,000

1.24

2 60

Chapter 7

CONCLUDING SUMMARY

The results of the investigations reported in the previous four chapters illustrate the general principles outlined in Chapter 1. The nitrides, which have been studied in this work, namely, those of Ca, Mg, Zn, Cd, B, Ti and Zr, cover all three types in the classification (Section 1.1). Thus, the first four of the above nitrides are considered to be ionic, boron nitride is classified as covalent, whilst titanium and zirconium nitrides typify the interstitial class.

The microcrystalline uniformity of the metal films conforms to the notes on sintering stated in Section 1.6. Thus, the melting points of metallic calcium, magnesium, zinc and cadmium (1124, 923, 693 and 594°K respectively) indicate that at room temperature calcium and magnesium are well below their Tammann temperatures; whereas, zinc is about 100° below and cadmium just above their respective values. Under laboratory conditions, therefore, the extent of sintering in metallic Ca, Mg, Zn and Cd would be in decreasing order. This is in agreement with their microcrystalline uniformity, which also decreases from Ca to Cd.

The behaviour of the metal films towards attempted nitridation agrees with the thermodynamic data of the nitrides. The standard free energies of formation of the compounds increase in the order, Mg, Ca, Zn, Cd; i.e., ΔG_f^o is least negative for cadmium nitride.

The results of the hydrolyses of calcium and magnesium

nitrides under various conditions are discussed in Section 3.2.4. The properties of the products depend on the conditions of hydrolysis and the properties of the reactants. Again, the results illustrate the general principles outlined in Chapter 1.

The calcinations carried out in this work show that the three classes of nitrides behave differently. All the nitrides form the oxides on heating in air to a sufficiently high temperature, but the rates of oxidation and the properties of the oxides are different for ionic, covalent and interstitial nitrides.

Calcium and magnesium nitrides require comparatively low temperatures and short times for complete oxidation. The reactions are accompanied by fairly large changes in specific surface. Titanium and zirconium nitrides require longer times and higher temperatures for their oxidation. The increase in surface area for the oxidation of titanium nitride is less than that for the oxidations of the calcium and magnesium compounds, in spite of the larger volume changes for the reactions of the former compounds. Oxidation of the covalent boron nitride also requires high temperatures and long times. The reaction is accompanied by a decrease in specific surface. This is related to the low melting point of boron oxide, which therefore readily sinters.

Further investigations are being carried out in this Department on the formation and reactivity of titanium and zirconium nitrides. These studies are being extended to other transition metal nitrides, and also to borides, carbides and

silicides (Glasson & Jones, 1969a-b).*

* See supplementary list of references.

REFERENCES

Abe, Y. : Rev. Phy. Chem. Japan, 1959, 29, 65; ibid., 1960a, 30, 49; ibid., 1960b, 30, 53; ibid., 1960c, 30, 62; ibid., 1960d, 30, 66.

Addamiano, A. : J. Electrochem. Soc., 1961, 108, 1072.

Agte, C. & Moers, K. : Z. Anorg. Chem., 1931, 198, 233.

Akishin, P.A. & Rhodeev, Yu.G. : Zh. Neorg. Khim., 1962, 7, 941; Russ. J. Inorg. Chem., 1962, 7, 486.

Albrecht, G. & Mueller, J. : German Patent 1,149,039, 22/5/1963.

Alexander, P.P. : US Patent 2,461,018, 8/2/1949a.

" " : US Patent 2,461,019, 8/2/1949b.

" " : US Patent 2,467,047, 19/4/1949c.

Anderson, P.J. & Livery, D.S. : Powder Met., 1961, No.7, 109.

Anselin, F. & Pascard, R. : French Patent 1,335,556, 23/8/1963.

Arai, H., Hayashi, H., Nakamura, S. & Azuma, U.N. : Rep. Govt. Ind. Res. Inst. Nagoya, 1962, 11, 119.

Ariya, S.N. & Prokof'eva, E.A. : Sbornik Statei Obshchei Khim., Akad. Nauk USSR, 1953, 1, 9.

Aubry, J. & Streiff, R. : Comp. Rend., 1966, 263, 931.

Barrer, R.M. : "Diffusion In and Through Solids", 1941 (Cambridge : University Press).

Baughan, E.C. : Trans. Farad. Soc., 1959, 55, 2025.

Beisswenger, H. : Härterei-Tech. Wärmebehandl., 1958, 4, 40.

Belin, F. : Comp. Rend. Congr. Natl. Soc. Savantes Sect. Sci., 1962a, 87, 417.

" " : Bull. Soc. Chim. France, 1962b, 2229.

" " : Comp. Rend., 1962c, 254, 5938.

" " : Comp. Rend., 1962d, 255, 3164.

" " : Comp. Rend., 1964, 258, 4715.

(Elektrophysikalische Anstalt) Bernhard Berghaus : British Patent 877,675, 20/9/1961.

Blum, A. : Planseeber. Pulvermet., 1962, 10, 72.

Bradley, R.S., Munro, D.C. & Whitfield, H. : J. Inorg. Nucl. Chem., 1966, 28(9), 1803.

Drager, A. : Acta Physicochim. URSS, 1939a, 10, 593.

" " : Acta Physicochem. URSS, 1939b, 10, 887.

Brewer, L. & Krikorian, O.H. : Univ. Calif. Rad. Lab. Rep., 1956, UCRL-3352.

Brown, B.R. : see Heller, J.W.

(Aktiengesselschaft) Brown, Boveri & Cie. : British Patent 877,951, 14/1/1960.

Brunauer, S., Emmett, P.H. & Teller, E. : J. Am. Chem. Soc., 1938, 60, 309.

Byrne, A.C. : US Patent 2,497,583, 14/2/1950.

Cabrera, N. & Mott, N.F. : Rept. Prog. Phy., 1948, 12, 163.

Campbell, I.E., Powell, C.F., Nowicki, D.H. & Gonser, B.W. : J. Electrochem. Soc., 1949, 96, 318.

Campbell, I.E. & Powell, C.F. : Iron Age, 1952, 169, No. 15, 113.

Carborundum Co. : Netherlands Patent 6,410,158, 22/5/1965.

Carpenter, L.G. & Heavell, F.H. : Metallurgia, 1948, 39, 63.

Chandrasekaraiah, M.S. & Margrave, J.L. : J. Electrochem. Soc., 1961, 108, 1008.

Chilton, J.P. : "Principles of Metallic Corrosion", 2nd edn., 1968, Monographs for Teachers, No. 4,(London : RIC).

Chiotti, P. : J. Am. Ceram. Soc., 1952, 35, 123.

CIBA Ltd. : Netherlands Patent 6,516,039, 13/6/1966; British Patent 1,133,777, 20/11/1968.

Clair, J. : French Patent 1,215,862, 21/4/1960.

Clarke, J. & Jack, K.H. : Chemy. Ind., 1951, 1004.

Clausing, P. : Z. Anorg. Allgem. Chem., 1932, 208, 401.

Coates, G.E., Harris, J. & Sutcliffe, T. : J. Chem. Soc., 1951, 2762.

Cochet, A. : Z. Angew. Chem., 1931, 44, 367.

Coles, N.G., Gleeson, D.R. & Jayaweera, S.A.A. : J. Appl. Chem., 1969, 19, 178; see Appendix.

Cooper, G.F. : Proc. Brit. Ceram. Soc., 1969, No. 12, 1.

Crosato, D., Genta, V. & Maltese, P. : Gazz. Chim. Ital., 1951, 81, 827.

Cuthill, J.R., Hayes, W.D. & Soebold, F.E. : J. Res. Natl. Bur. Standards, 1960, 64A, No. 1, 119.

David, J. & Lang, J. : Comp. Rend., 1965, 261, 1005.

Davis, L.W. : US Patent 2,488,054, 15/11/1959.

de Boer, J.H. & Vast, J.D. : Rec. Trav. Chim., 1936, 55, 459.

Deeley, O.G. : British Patent 970,639, 23/9/1964.

Dell, R.M., Wheeler, V.J. & McIver, E.J. : Chem. Soc. Symposium, Aberdeen, 1966, Paper 3-3; Trans. Farad. Soc., 1966, 62, 3591.

Deutsche Gold-und-Silber-Scheideanstalt (vormals Roessler) : Belgian Patent 629,738, 1/4/1963.

Domagala, R.F., McPherson, D.J. & Hansen, M. : J. Metals, 1956, 8, AIME Trans., 206, 90.

Douglass, D.L., St. Pierre, G.R. & Speiser, R. : Met. Soc. Conf., 1961, 8, 705.

Dravnieks, A. : J. Am. Chem. Soc., 1950, 72, 3568.

Dubovik, G.V., Polishchuk, V.S. & Samsonov, G.V. : Zh. Prikl. Khim., 1964, 37, 1828; J. Appl. Chem. USSR, 1964, 37, 1812.

Duwez, P. & O'Dell, F. : J. Electrochem. Soc., 1950, 97, 299.

Ehrlich, P. : Z. Anorg. Chem., 1949, 259, 1.

Ellingham, H.J.T. : J. Soc. Chem. Ind., 1944, 63, 125.

Espenschied, H. : US Patent 2,898,193, 4/8/1959.

Evans, R.D. : J. Less-common Metals, 1965, 9, 465.

Fadeeev, I.V. & Remkova, O.G. : Zh. Neorg. Khim., 1962, 7, 980; Russ. J. Inorg. Chem., 1962, 7, 505.

Foster, L.S. : Met. Prog., 1952, 62(2), 160.

Franck, E.U. & Bodea, C. : Z. Angew. Chem., 1931, 44, 379.

Franck, H.U. & Heimann, H. : Z. Angew. Chem., 1931, 44, 372.

Fujiwara, S. : J. Chem. Soc. Japan, Ind Chem. Sect., 1950, 71, 580.

Funk, H. & Boehland, H. : Z. Anorg. Allgem. Chem., 1964, 1964, 334(3-4), 155.

Glasson, D.R. : Ph.D. Thesis, London Univ., 1949.

" " : J. Chem. Soc., 1956, 1506.

" " : J. Appl. Chem., 1958a, 8, 793.

" " : J. Appl. Chem., 1958b, 8, 798.

" " : J. Appl. Chem., 1960, 10, 38.

" " : J. Appl. Chem., 1961a, 11, 24.

" " : J. Appl. Chem., 1961b, 11, 201.

" " : J. Appl. Chem., 1963a, 13, 111.

" " : J. Appl. Chem., 1963b, 13, 119.

" " : SCI Monographs, 1964, No. 18, 401.

" " : J. Appl. Chem., 1965a, 15, 378; ibid., 1965b, 15, 384.

" " : J. Appl. Chem., 1967, 17, 91.

Glasson, D.R., Johnson, J.S. & Sheppard, N.A. : J. Appl. Chem., 1969, 19, 46.

Glasson, D.R. & O'Neill, P. : J. Appl. Chem., 1967, 17, 96.

Glasson, D.R. & Sheppard, N.A. : J. Appl. Chem., 1968, 18, 327.

Gol'dberg, N.A. & Znamenskii, Yu. D. : Dokl. Akad. Nauk SSSR, 1956, 110, 1048; Proc. Acad. Sci. USSR, Chem. Tech. Sect., 1956, 110, 119.

" " " " : Dokl. Akad. Nauk SSSR, 1958, 120, 148; Proc. Acad. Sci. USSR, Chem. Tech. Sect., 1958, 120, 93.

" " " " : Zh. Fiz. Khim., 1962, 36, 2740; Russ. J. Phy. Chem., 1962, 36, 1439.

Goodenough, J.B. : Phy. Rev., 1960, 120, 67.

" " : "Magnetism and the Chemical Bond", 1963 (New York : Wiley - Interscience).

Grdina, Yu.V., Gordeeva, L.T. & Timonina, L.G. : Izv. Vysshikh Uchebn. Zavedenii, Chernaya Met., 1962, 5, No. 6, 128.

Gregg, S.J. : J. Chem. Soc., 1946, 561.

" " : "Surface Chemistry of Solids", 1st edn., 1951, Ch. 4, pp.63-79; ibid., 2nd edn.,1961, Ch. 7, pp.300-328 (London : Chapman & Hall).

" " : J. Chem. Soc., 1953, 3940.

" " : J. Chem. Soc., 1955, 1438.

" " : "Surface Phenomena in Chemistry and Biology" (Ed. J.F. Danielli, K.G.A.Pankhurst & A.C.Riddiford), 1958, Ch. 15, pp.195-213 (London : Pergamon Press).

Gregg, S.J. & Bickley, R.I. : J. Chem. Soc.(A), 1966, 1849; Bickley, R.I. : Ph.D. Thesis, Exeter Univ., 1965.

Gregg, S.J. & Sing, K.S.W. : "Adsorption, Surface Area and Porosity", 1967 (London : Academic Press).

Gulbransen, E.A. & Andrew, K.F. : J. Metals, Trans., 1949a, 1, 515.

" " " " : J. Metals, Trans., 1949b, 1, 741.

" " " " : J. Electrochem. Soc., 1949c, 96, 364.

" " " " : J. Electrochem. Soc., 1951, 98, 241.

Guldner, W.G. & Wooten, L.A. : J. Electrochem. Soc., 1948, 93, 223.

Hägg, G. : Z. Phy. Chem.(B), 1930, 6, 221; ibid., 1931a, 12, 33.

" " : Metallwirt., 1931b, 10, 387.

" " : Ivs, 1953, 24, 345.

Hägg, G. & Mieseling, R. : J. Inst. Metals, 1952-1953, 81, 57.

Hahn, H. & Konrad, A. : Z. Anorg. Allgem. Chem., 1951, 264, 174.

Hansen, M. & Anderko, K. : "Constitution of Binary Alloys", 2nd edn., 1958, p.402 (New York : McGraw-Hill).

Hartmann, H. & Fröhlich, H.J. : Z. Anorg. Chem., 1934, 218, 190.

Hayashi, Y. et al. : J. Ceram. Assn. Japan, 1968, 76(9), 307.

Hayes, E.T. & Roberson, A.H. : J. Electrochem. Soc., 1949, 96, 142.

Hirsch, P.B., Howie, A., Nicholson, R.B., Pashley, D.W. & Whelan, M.J. : "Electron Microscopy of Thin Crystals", 1965 (London : Butterworth).

Hoch, M., Dingledy, D.P. & Johnston, H.L. : J. Am. Chem. Soc., 1955, 77, 304.

Holmberg, B. : Acta Chem. Scand., 1962, 16, 1255.

Hough, R.L. : "Refractory Reinforcements for Ablative Plastics, Part I, Synthesis and Reaction Mechanisms of Fibrous Zirconium Nitride", 1962, ASD-TDR-62-200, AD 291903 (Ohio : Wright-Patterson AFB).

Hughes, W. & Harris, B : British Patent 787,516, 11/12/1957.

Hume-Rothery, W. : Ann. Rep. Prog. Chem., 1949, 46, 42.

" " " : Phil. Mag., 1953, 44, 1154.

Ishii, R. : Papers Inst. Phy. Chem. Res. Tokyo, 1943, 41, 1.

Ishii, R. & Wada, I. : Bull. Inst. Phy. Chem. Res. Tokyo, 1943, 22, 112.

Jack, K.H. : Proc. Roy. Soc.(A), 1948, 195, 41.

Jacob, K.D., Krase, N.J. & Braham, J.M. : Ind. Eng. Chem., 1924, 16, 684.

Jacobsen, A.E. : US Patent 2,672,400, 16/3/1954.

Jacobson, C.A. (Ed.) : "Encyclopedia of Chemical Reactions", Vol. II, 1948 (New York : Rheinhold).

Jayaweera, S.A.A. : M.Sc. Thesis, London Univ., 1964.

Jeffe, R.I. & Campbell, I.E. : USAEC, 1948, No. NP-266,205,300.

Jenkins, A.E. : J. Inst Metals, 1954, 82, 213.

Joncich, M.J., Vaughn, J.W. & Knutsen, D.P. : Canad. J. Chem., 1966, 44, 137.

Juza, R. : Adv. Inorg. Chem. Radiochem., 1966, 9, 81.

Juza, R., Neuber, A. & Hahn, H. : Z. Anorg. Allgem. Chem., 1938, 232, 273.

Kay, D.H. (Ed.) : "Techniques for Electron Microscopy", 1965 (Oxford : Blackwell).

Kazaryan, P.E. : Khim. Prom., 1964, 681.

Kemlet, J. : US Patent 2,839,366, 17/6/1958.

Kempter, C.P., Krikorian, N.H. & McGuire, J.C. : J. Phy. Chem., 1957, 61, 1237.

Kieffer, R. & Benesovsky, F. : Metall, 1952, 6, 171; ibid., 243.

Kiessling, R. : Acta Chem. Scand., 1950, 4, 209.

" " : Fortschr. Chem. Forsch., 1954, 3, 41.

" " : Met. Rev., 1957, 2, No. 5, 77.

" " : Powder Met., 1959, No. 3, 177.

Kiessling, R. & Liu, Y.H. : J. Metals, 1951, 3, 639.

Kirchevskii, I.R. & Khazanova, N.Z. : Zh. Fiz. Khim., 1950, 24, 1188.

Kruse, H.J. & Yee, J.Y. : J. Am. Chem. Soc., 1924, 46, 1358.

Krikorian, O.H. : Univ. Calif. Rad. Lab. Rep., 1955, UCRL-2888.

Kubaschewski, O. & Hopkins, B.E. : "Oxidation of Metals and Alloys", 1962, (London : Butterworth).

Laffite, P., Elchardus, E. & Grandadam, P. : Rev. Ind. Min., 1936, No. 375, 861.

Laffite, P & Grandadam, P. : Comp. Rend., 1935, 200, 1039.

Lang, J. & Laurent, Y. : Bull. Soc. Chim. France, 1963, 1546.

Lanzau, W.R. : US Patent 2,922,699, 21/1/1960.

Laplanche, R. : Met. Constr. Rec., 1963, 95(10), 849; ibid., (11), 937.

Livery, D.T., O'Neill, J.S. & Hey, A.W. : Proc. 3rd Int. Materials Symposium, Berkeley, California, 1966, 800.

Lohberg, K., Gagel, H. & Ruppert, W. : German Patent 1,028,542, 24/4/1958.

Lorentz, H.R. & Binskowski, B.B. : J. Electrochem. Soc., 1962, 109, 24.

Luberoff, B.J., Rickles, R.N. & Stuchell, R.W. : US Patent 3,261,666, 19/7/1966.

Lynch, C.T., Vahldiek, F.W. & Robinson, L.D. : J. Am. Ceram. Soc., 1961, 44, 147.

Lyntaya, H.D., & Samsonov, G.V. : Redkie Redkozem. Elementy. Tekhn., Akad. Nauk Ukr. SSR, Inst. Probl. Materialoved., 1964, 116.

MacFarlane, R.J. & Tomphins, F.C. : Trans. Farad. Soc., 1962, 58, 997.

Mallett, M.W., Baroody, E.M., Nelson, H.E. & Papp, C.A. : J. Electrochem. Soc., 1955, 100, 103.

Mallett, M.W., Nelle, J. & Cleland, B.D. : J. Electrochem. Soc., 1954, 101, 1.

May, F.M. & Cook, C.C. : US Patent 2,959,469, 8/11/1960.

May, F.M. & Levasheff, V.V. : US Patent 2,824,787, 25/2/1958.

Mandiyasni, R.S. & Lynch, C.T. : Special Ceramics, 1964, 115.

McCullough, J.D. & Trueblood, K.N. : Acta Cryst., 1959, 12, 507.

Mellor, J.W. : "Comprehensive Treatise on Inorganic and Theoretical Chemistry", Vol. VIII, 1927*, pp.97-144 (London : Longmans); Brown, D.R. : Supplement to Vol. VIII, Part I, 1969, pp.150-239 (London : Longmans).

Minemura, Y., Nakajima, T. & Sannomiya, Y. : Denki Kagaku, 1961a, 29, 317; ibid., 1961c, 29, 486.

Minemura, Y., Suto, I., Nakajima, T. & Sannomiya, Y. : Denki Kagaku, 1961b, 29, 400.

Minenko, M.M. & Nazarchuk, T.N. : Poroosh. Met., Akad. Nauk Ukr. RSR, 1965, 5(6), 53.

Minkevich, A.N. : Metallov. Term. Obrabotka Met.; 1964, No. 3, 4.

Minkevich, A.N., Taimar, A.D. & Kot'ev, Yu.A. : Metalloved. Obrabotka Metallov, 1956, No. 7, 39.

Mitchell, D.W. : Ind. Eng. Chem., 1949, 41, 2027.

Mitchell, D.W. & Dawes, C. : Metal Treat., 1964, 31(220), 3; ibid., (221), 49; ibid., (222), 88; ibid., (224), 195.

Moeller, T. : "Inorganic Chemistry", 1952 (New York : Wiley).

Moers, K. : Z. Anorg. Allgem. Chem., 1931, 198, 243.

---

* Approximate year of publication

** Metal Sci. Heat Treat., 1964, No. 3, 127.

Moody, G.J. & Thomas, J.D.R. : J. Chem. Educ., 1966, 43, 205.

Moore, C.H. : Ceram. Age, 1948, 52, 281.

Moreau, C. & Philippot, J. : Bull. Soc. Chim. France, 1963, 283.

Mueller, J. : German Patent 1,108,246, 9/7/1959.

Münster, A. : Angew. Chem., 1957, 69, 201.

" " : Z. Elektrochem., 1959, 63, 827.

Münster, A., Rinck, G. & Ruppert, W. : Z. Phy. Chem., Frankf. Ausg., 1956, 9, 228.

Münster, A. & Ruppert, W. : Naturwissenschaften, 1952, 39, 349.

" " " " : Z. Elektrochem., 1953a, 57, 558.

" " " " : Z. Elektrochem., 1953b, 57, 564.

" " " " : German Patent 919,859, 4/11/1954.

Münster, A. & Gagel, K. : Z. Elektrochem., 1953, 57, 571.

Münster, A. & Schlamp, G. : Z. Phy. Chem., Frankf. Ausg., 1957a, 13, 59; Ibid., 1957b, 13, 76.

" " " " : Proc. 16th Int. Congr. Pure Appl. Chem., Paris, Min. Chem. Sect., 1957c, 691. (London : Butterworth).

Münster, A. & Weber, R. : US Patent 2,836,514, 27/5/1958.

Muroi, S. & Somono, M. : Nippon Kinzoku Gakkaishi, 1966, 30(1), 26.

Muruguleccscu, I. & Ciomaru, D. : Rev. Chim. Acad. Rep. Pop. Roumaine, 1960, 5, 251; ibid., 289.

National Lead Co. : British Patent 745,468, 29/2/1956.

Naylor, B.F. : J. Am. Chem. Soc., 1946, 68, 370.

Neshpor, V.S. : "Refractory Transition Metal Compounds" (Ed. G.V.Samsonov), 1964, Ch. 7, pp.62-106 (New York : Academic Press).

Neugebauer, J. Hegedus, A.J. & Willner, T. : Z. Anorg. Allgem. Chem., 1959, 302, 90.

Niederhause, D.O. : US Patent 3,032,397, 1/5/1962.

Olette, M. & Ancey-Moret, M.F. : Rev. Métall., 1963, 60, 569.

Olson, C.M. : US Patent 2,413,778, 7/1/1947.

Opfermann, W. : Monatsber. Deut. Akad. Wiss. Berlin, 1964, 6(2), 92.

Palty, A., Margolin, H. & Nilsen, J. : Trans. Am. Soc. Metals, 1954, 46, 312.

Patterson, R.J. : US Patent 3,321,337, 23/5/1967.

Pauling, L. : Phy. Rev., 1938, 54, 899.

" " : "Nature of the Chemical Bond", 2nd edn., 1940, pp.401-422; ibid., 3rd edn., 1960, pp.393-448 (Ithaca, NY : Cornell Univ. Press).

" " : J. Am. Chem. Soc., 1947, 69, 542.

" " : J. Chem. Soc., 1948, 1461.

" " : Proc. Roy. Soc.(A), 1949, 196, 343.

Pauling, L. & Swing, R.J. : Rev. Mod. Phy., 1948, 20, 112.

Pearson, J. & Linde, U.J.C. : J. Iron & Steel Inst., 1953, 175, 52.

Pease, R.S. : Nature, 1950, 165, 722.

Peiser, H.S., Rooksby, H.P. & Wilson, A.J.C. (Ed.) : "X-ray Diffraction by Polycrystalline Materials", Part I, 1960 (London : Chapman & Hall).

Pilling, N.B. & Bedworth, R.E. : J. Inst. Metals, 1923, 29, 529.

Pokorny, E.A. : British Patent 942,853, 27/11/1963.

Pollard, F.H. & Fowles, G.W.A. : J. Chem. Soc., 1952, 2444.

Pollard, F.H. & Woodward, P. : J. Chem. Soc., 1948, 1709.

" " " " : Trans. Farad. Soc., 1950, 46, 190.

Polzeniuss, F.E. : Chem. Ztg., 1907, 31, 958.

Porter, J.L. : GB Patent 2,487,474, 8/11/1949.

Portnoi, K.I. & Levinskii, Yu.V. : Issled. Splavov. Tsvetn. Metal, Akad. Nauk SSSR, Inst. Met., 1963, No. 4, 279.

Powell, C.F., Oxley, J.H. & Blocher, J.M. : "Vapour Deposition", 1966 (New York : Wiley).

Pranke, R.J. : J. Ind. Eng. Chem., 1913, 5, 180.

Prosvirin, B.I. : Vest. Metallopromm., 1937, 17(12), 102.

Renner, Von Th. : Z. Anorg. Allgem. Chem., 1959, 298, 22.

Revzin, I.G. & Ma'yanov, L.G. : USSR Patent 141,094, 15/11/1961.

Rice, D.W. : Proc. 3rd Int. Materials Symposium, Berkeley, California, 1966, 579.

" " : Proc. Brit. Ceram. Soc., 1969, No. 12, 99.

Richardson, F.D. & Grant, N.J. : J. Metals, 1954, 6, AIME Trans., 200, 69.

Roberts, M.W. & Tompkins, F.C. : Proc. Roy. Soc.(A), 1959, 251, 369.

" " " " : J. Chim. Phy., 1960, 57, 562.

Roeck, H. : Chem. Ztg., 1964a, 88, 191; ibid., 1964b, 88, 271.

Rundle, R.E. : Acta Cryst., 1948, 1, 180.

Ruppert, U. : German Patent 970,456, 18/9/1958a.

" " : German Patent 1,041,320, 16/10/1958b.

Ruppert, U. & Schwedler, O. : US Patent 2,869,791, 23/12/1958.

" " " " : German Patent 1,056,458, 30/4/1959.

Saito, H. & Ushio, M. : J. Ceram. Assn. Japan, 1969, 77, 1.

Saliberov, S.N., Levinskii, Yu.V., Khvostikov, V.D. & Levinkaya, M.Sh.: Fiz. Metal. Metalloved., 1964, 18(6), 836.

Samsonov, G.V. : Dokl. Akad. Nauk SSSR, 1953a, 93, 689.

" " : Dokl. Akad. Nauk SSSR, 1953b, 93, 859.

" " : Izv. Sekt. Fiz. Khim. Anal., 1956a, 27, 97.

" " : Zh. Fiz. Khim., 1956b, 30, 2058.

" " : Zh. Tekh. Fiz., 1956c, 26, 715; Soviet Phy., Tech. Phy., 1957, 1, 695.

" " : "Handbook of High Temperature Materials, No. 2, Properties Index", 1964a (New York : Plenum Press).

" " : "Refractory Transition Metal Compounds" (Ed. G.V. Samsonov), 1964b, Ch. 1, pp.1-12 (New York : Academic Press).

" " : Ukr. Khim. Zh., 1965, 31(10), 1005; NLL Translation RTS-4233, December 1967.

Samsonov, G.V. & Golubeva, N.K. : Zh. Prikl. Khim., 1956, 30, 1258.

Samsonov, G.V. & Grodshteyn, A.L. : Zh. Fiz. Khim., 1956, 30, 379.

Samsonov, G.V., Markovskiy, L. Ya., Shigach, A.N. & Velyashko, M.G. : "Bor, ego Soedineniya i Splavy", 1960 (Kiev : Akad. Nauk Ukr. SSR); "Boron, its Compounds and Alloys", 1962a, USAEC Translation No. 5032.

Samsonov, G.V. & Neshpor, V.S. : Sbornik Nauchn. Trudov Nauch.-Tekh. Chshchestva Tsvetnoi Met., Moskov. Inst. Tsvetn. Metal. Zolota, 1958, No. 29, 361.

Samsonov, G.V., Neshpor, V.S. & Kunditsova, G.A. : Radiotekh. Elektron., 1957, 2, 631; Radio Eng. Electr., 1957, 2, No.5, 155.

Samsonov, G.V., Neshpor, V.S. & Paderno, Yu.B. : Ukr. Fiz. Zh., 1959a, 4, 509.

Samsonov, G.V. & Petrash, N.V. : Metalloved. Obrabotka Met., 1955, No. 4, 19.

Samsonov, G.V. & Sleptsov, V.M. : Dopovidi Akad. Nauk Ukr. RSR, 1959, 1116.

" " " " : Kinetika i Katalis, Akad. Nauk SSSR, Sb. Statei, 1960, 129.

Samsonov, G.V. & Verkhoglyadova, T.S. : Zh. Strukt. Khim., 1961b, 2, 617.

Samsonov, G.V., Verkhoglyadova, T.S., Antonova, M.M. & Dubovik, T.V. : Metallokeram. Mater. Metody. Issled., Akad. Nauk Ukr. SSR, Inform. Mater., 1959b, 53.

Samsonov, G.V., Verkhoglyadova, T.S. & Dubovik, T.V. : Porosh. Met., Akad. Nauk Ukr. SSR, 1961a, 1, No. 4, 9.

Sarkisov, E.S. : Zh. Fiz. Khim., 1954, 28, 627.

Sato, S. & Yamano, K. : Rep. Sci. Res. Inst. Japan, 31, 418; J. Sci. Res. Inst. Tokyo, 1955, 49, 325.

Schmitz-Dumont, O. & Steinberg, K. : Naturwissenschaften, 1954, 41, 117.

Schneider, A. Heymer, G. & Klotz, H. : German Patent 1,160,189, 12/12/1963.

Schomate, C.H. : J. Am. Chem. Soc., 1946, 68, 310.

Schumb, W.C. & O'Malley, R.F. : Inorg. Chem., 1964, 3(6), 922.

Schwarzkopf, P. : Powder Met. Bull., 1950, 5, 68.

Schwarzkopf, P. & Glaser, F.W. : Proc.3rd Int. Congr. Electrothermics, 1953, 1213; Z. Metallkunde, 1955, 46, 393.

Schwarzkopf, P. & Kieffer, R. : "Refractory Hard Metals: Borides, Carbides, Nitrides and Silicides", 1953 (New York : MacMillan).

Seith, W. & Kubaschewski, O. : Z. Elektrochem., 1935, 41, 551.

Septier, A., Gaunit, M. & Baruch, P. : Comp. Rend., 1952, 234, 105.

Shaffer, P.T.B. : "Handbook of High Temperature Materials, No. 1, Materials Index", 1964 (New York : Plenum Press).

Shamir, J. & Binenboym, J. : Inorg. Nucl. Chem. Letters, 1966, 2(4), 117.

Shushunov, V.A. & Baryshnikov, Yu.N. : Zh. Fiz. Khim., 1953, 27, 783.

Sifferlen, R. : Comp. Rend., 1964, 259(8), 1520.

Sillén, L.G. & Martell, A.E. (Compilers) : "Stability Constants of Metal - Ion Complexes", 1964, Special Publication No. 17 (London : Chemical Society).

Smirnov, A.V. & Machinkov, A.D. : Metalloved. Term. Obrabotka Metallov, 1960, (7), 42; Metal Sci. Heat Treat., 1960, 599.

Société Belge du Titane, S.A. : Belgian Patent 522,487, 16/12/1963.

Solman, A. : J. Appl. Chem., 1951, 1, 98.

Sowa, V.J. : US Patent 2,686,815, 12/8/1952.

Spriggs, R.M. & Atterson, L. : Proc. 3rd Int. Materials Symposium, Berkeley, California, 1966, 701.

Sterling, H.F., Alexander, J.H. & Joyce, R.J. : Le Vide, 1966, No. Spécial AVIScm., 88.

Sterling, H.F. & Swann, R.C.G. : Solid State Electronics, 1965, 8, 653.

Sthapitanonda, P. & Margrave, J.L. : J. Phy. Chem., 1956, 60, 1628.

Stokes, C.S. & Knipe, W.L. : Ind. Eng. Chem., 1960, 52, 287.

Suchet, J. : US Patent 2,952,559, 13/9/1960.

Takamura, A. : Nippon Kinzoku Gakkaishi, 1960, 24, 509.

Taylor, A. & Kagle, B.J. : "Crystallographic Data on Metal and Alloy Structures", 1963 (New York : Dover).

Taylor, K.M. : Ind. Eng. Chem., 1955, 47, 2506.

" " : Materials and Methods, 1956, 43, No. 1, 88.

Toren, E.H. : Comp. Rend., 1948a, 226, 905.

" " : Rev. Fac. Sci. Univ. Istanbul, 1948b, 13A, 147.

Ubbelohde, A.R. : Trans. Farad. Soc., 1932, 28, 279.

" " : Proc. Roy. Soc.(A), 1937, 122, 295.

Umanskii, Ya.S. : Izv. Sek. Fiz. Khim. Anal., 1943, 16, 127.

Umezu, S. : Proc. Imp. Acad. Tokyo, 1931, 7, 353.

van Arkel, A.E. : Metallwirtschaft, 1934, 13, 511.

" " : "Molecules and Crystals", 1956 (London : Butterworth).

van Arkel, A.E. & de Boer, J.H. : Z. Anorg. Chem., 1929, 148, 345.

van Doreten, A.C., Niewdorp, H. & Verhoeff, A. : Philips Tech. Rev., 1950, 12, No. 2, 33.

Vereshchagin, L.F., Gubova, Z.V., Zurenkova, E.N. & Novin, N.I. : Dokl. Akad. Nauk SSSR, 1968, 178, 72; Soviet Phy. - Dokl., 1968, 13, 25.

Vernilyea, D.A. : Acta Metallurgia, 1957, 5, 492.

Vogel, A.I. : "Text-Book of Quantitative Inorganic Chemistry", 3rd edn., 1964 (London : Longmans).

von Antropoff, A. & Germann, E. : Z. Phy. Chem., 1928, 137, 209.

von Stackelberg, M. & Paulus, R. : Z. Phy. Chem.(B), 1933, 22, 305.

von Stackelberg, M., Schnorrenberg, E., Paulus, R. & Speiss, K.F. : Z. Phy. Chem.(A), 1935, 175, 127.

Wagner, C. : Z. Phy. Chem.(B), 1933, 21, 25.

Wasilewski, R.J. & Kehl, G.L. : J. Inst. Metals, 1954, 83, 94.

Wentorf, R.F. : J. Chem. Phy., 1957, 26, 956.

" " : US Patent 2,947,617, 2/8/1960.

Wheat, T.A. & Carruthers, W.G. : Science of Ceramics, 1968, 4, 33.

Wicks, C.E. & Block, F.E. : "Thermodynamic Properties of 65 Elements - their Oxides, Halides, Carbides and Nitrides", 1963, Bulletin 605 of the US Bureau of Mines (Washington : US Department of the Interior).

Wiener, G.W. & Berger, J.A. : J. Metals, 1955, 7, AIME Trans., 203, 360.

Wyatt, J.L. & Grant, N.J. : Trans. Am. Soc. Metals, 1954, 46, 540.

" " " " : US Patent 2,804,410, 27/8/1957.

Zagyanskii, I.L. & Samsonov, G.V. : Zh. Prikl. Khim., 1952, 25, 557; Chem. Coll. No. 2, Soviet Res. Glass Ceram. - Refractories, 1949-1955, 15.

Zelikman, A.N. & Govorits, N.N. : Zh. Prikl. Khim., 1950, 23, 689; Chem. Coll. No. 2, Soviet Res. Glass Ceram. - Refractories, 1949-1955, 23.

Zworykin, V.K., Morton, G.A., Ramberg, E.G., Hillier, J. & Vance, A.W. "Electron Optics and the Electron Microscope", 1945 (New York : Wiley).

Supplementary List of References

British Standards 4359 Part I, 1969.

de Boer, J.H. : Proceedings of the International Symposium on Surface Area Determination, Bristol, July 1969, SCI Monograph (in press).

Glasson, D.R. & Jones, J.A. : J. Appl. Chem., 1969a, 19, 125.

" " " " : J. Appl. Chem., 1969b, 19, 137.

Joy, A.S. : Proceedings of the International Symposium on Surface Area Determination, Bristol, July 1969, SCI Monograph (in press).

Blezard, R.G : SCI Monographs, 1964, No. 18, 222

APPENDIX

Reprints of Published Papers

1. "Surface Nitridation and Hydrolysis of Metals". Paper read at the International Symposium on the Surface Phenomena of Metals, held at Brunel University, London, September 1967, SCI Monograph No. 28, pp.353-364.

2. "Formation and Reactivity of Nitrides, Part I : Review and Introduction". Journal of Applied Chemistry, 1968, Volume 18, pp.65-77.

3. "Formation and Reactivity of Nitrides, Part II : Calcium and Magnesium Nitrides and Calcium Cyanamide". Journal of Applied Chemistry, 1968, Volume 18, pp.77-83.

4. "Formation and Reactivity of Nitrides, Part III : Boron, Aluminium and Silicon Nitrides". Journal of Applied Chemistry, 1969, Volume 19, pp.178-181.

5. "Formation and Reactivity of Nitrides, Part IV : Titanium and Zirconium Nitrides". Journal of Applied Chemistry, 1969, Volume 19, pp.182-184.

Note:- In paper 4 above (i.e., Part III of series on Nitrides), the studies on boron nitride only are the work of the author of this thesis, carried out under the supervision of Dr. D.R. Glasson. The work on aluminium and silicon nitrides is that of the other co-author.

SURFACE NITRIDATION AND HYDROLYSIS OF METALS

By D. R. GLASSON and S. A. A. JAYAWEERA

(John Graymore Chemistry Laboratories, College of Technology, Plymouth)

Conditions for nitridation of metals are discussed kinetically, and compared with direct oxidation. Examples are given of the nitridation of more active metals such as calcium and magnesium and less active ones such as titanium and zirconium. Mechanical stability of nitride films and their reactivity towards water (vapour and liquid) are correlated with changes in crystal structure and particle size.

X-ray and electron-micrograph studies are related to rates of nitridation and changes in surface areas (and average crystallite sizes determined by gas sorption. Hydrolysis of the nitrides and ageing of the hydrous products are similarly studied.

Introduction

Production of nitride coatings

Nitridation of metals has become increasingly important with their more extensive use at higher temperatures. Surface nitridation was first systematically studied by Newman,[1] who deposited pure metals on the cathode in an electric-discharge tube by distillation *in vacuo*. The relative uptakes of nitrogen on metals such as Ca, Mg, Zn, Cd, Hg, Sn, Sb and Bi, under the influence of the electric discharge, were measured by comparison of the absorption with the amount of hydrogen liberated by the current passing through an electrolytic cell, no uptakes on Pb, Tl and As were detected.

Nitride coatings have been produced subsequently by heating the base metal (or material with the particular metal coating) in a nitrogen, ammonia, or nitrogen + hydrogen atmosphere. Often, the nitrogen uptake rate decreases considerably after formation of a thin surface skin of nitride. Several hours are necessary for coatings of more than 1 or 2 mm thickness, unless much higher temperatures are used to ensure adequate diffusion across the nitride layer. Thus, direct deposition methods[2-7] are often preferred industrially; in these the nitride is deposited on the heated specimen from a gaseous mixture of a suitable volatile halide and nitrogen + hydrogen.

Mechanism of nitridation

The same principles as those for oxide film growth are expected to apply to nitridation of metals. Formation of calcium nitride[8,9] is consistent with the thin film theory of Mott & Cabrera,[10] the rate being controlled by the diffusion of cations through the product layer. The rate also depends on the first power of the nitrogen pressure, and this suggests reversible adsorption to form a surface complex MN_{2-x}. In lithium nitridation,[11] the rate initially increases in accord with hemispherical growth of nitride into the metal. Above a critical thickness, the rate becomes constant, at which time the energy of activation is negligibly small, the pressure dependence of the rate suggests that the controlling process is the movement of gaseous nitrogen through the porous nitride layer by streamline and Knudsen flow.

Metal evaporation occasionally accompanies nitridation, as shown by electropolished magnesium in very pure nitrogen[12] at 10 cm Hg pressure at about 500°. Higher nitrogen pressures produce 'breakaways', i.e. sudden increases in weight gain, explained in terms of the formation and growth of cavities at the nitride/metal interface, with rupture of the film covering the cavity. Thin films permit the magnesium vapour to escape without reacting with nitrogen within the cracks. Hence, very pure magnesium nitride is manufactured by heating magnesium above the sublimation temperature but below its m.p.[13,14] A limited amount of nitrogen (or ammonia) is admitted to initiate surface nitriding. Conversion of all the metal to nitride is then completed by heating it to a temperature sufficient to cause the sublimed magnesium to break through the surface coating of nitride, and by gradual admittance of additional amounts of nitrogen. The ionic nitrides of Group II, M_3N_2, mostly have CaF_2 or Mn_2O_3-type crystal structures. In Mg_3N_2, the N^{3-} ions occupy lattice positions corresponding to Ca^{2+} in CaF_2, with the Mg^{2+} filling $\frac{3}{4}$ of the F^- positions. The vacancies facilitate diffusion of Mg^{2+} through the nitride layer.

Effect of oxygen and water on nitridation

In nitride production, usually oxygen must be excluded, since it prevents nitrogen reacting with the clean metal surfaces. Sometimes formation of an initial nitride surface layer protects the surface against any subsequent oxygen attack and allows nitridation to proceed, e.g. with Ca. The nitride layer is destroyed by hydrolysis (water vapour or liquid). However, by which the nitride ions are replaced by hydroxyl ions, since each N^{3-} is replaced by $3OH^-$, the film becomes very weak and ruptures whilst very thin.[12] At higher temperatures decomposition of the hydroxide to oxide causes further fragmentation.[15] Thus, in magnesium nitridation at temperatures between 400° and 650°, evaporation of metal is pro-

moted by traces of water vapour but inhibited by oxygen. Changes in phase composition, surface area and sizes of crystallite and aggregate during nitride hydrolysis have been studied by the authors.[15]

Hydrolysis of zinc, cadmium and mercuric nitrides, e.g. $Zn_3N_2 + 6H_2O \rightarrow 3Zn(OH)_2 + 2NH_3$, is enhanced, particularly at lower temperatures, by the solubility of their oxides and hydroxides being increased in ammonia. Complexes of the type $M(NH_3)_x(OH)_2$ are formed, where $x \leqslant 4$ for Zn and Cd and $\leqslant 2$ for Hg.[16] Soluble caustic alkalis also promote nitride dissolution for nitrides of Zn and also B, Al and Si. Pressed, extruded or slip-cast silicon powder can be directly nitrided,[17,18] but the presence of oxygen reduces the nitriding rate. Hydrolysis of aluminium nitride forms part of the Serpek process; possible uses of other metals for nitrogen fixation have been discussed by Soliman.[19]

Most interstitial metal nitrides are not hydrolysed so readily, but some of them, e.g. Ti, Zr, Th and U, are converted to oxides on being heated in air. Thorium mononitride (ThN) oxidises rapidly and quantitatively in moist air at room temperature even in ingot form, but powdered mononitrides of uranium,[20] titanium and zirconium are quite stable at 100° in boiling water. UN powder ignites in dry oxygen[20] at about 300°. Nitrides of titanium and zirconium produce TiO_2 (rutile) and ZrO_2 (tetragonal form) when calcined at temperatures between 400° and 1000° and 300° and 1000°, respectively, and cause indirect corrosion after the metals have nitrided at higher temperatures.

Experimental

Materials

Calcium and magnesium turnings were evaporated *in vacuo* from a heated filament in an electron microscope shadowing unit. The metal vapours were condensed as films on pieces of mica that had been coated previously with carbon films. The filament current was increased sufficiently slowly to avoid rapid temperature increases and permit metal stresses to be released, so that the turnings did not fly off the filament before evaporation. These films were nitrided at different temperatures for various times, and larger amounts of nitride were produced by direct nitridation of the metal turnings.

Nitridation of calcium below 600° gives mainly the black form of Ca_3N_2 (pseudo-hexagonal, $a = 3{\cdot}53$Å, $c = 4{\cdot}11$Å) which irreversibly changes to the brown form at 600–750°. The higher-temperature form (cubic Mn_2O_3 $D5_3$-type, $a = 11{\cdot}38$Å) was hydrolysed.

This form readily sintered above 750°, which is much higher than the Tammann temperature of 731 K or 461°C, and gave specific surfaces S of less than 0·01 m^2g^{-1}. The magnesium nitride (cubic Mn_2O_3 $D5_3$-type, $a = 9{\cdot}95$Å) did not sinter so extensively, and bulk samples mainly consisted of single crystals of sizes 20 to 100μ ($S = 0{\cdot}01$ to $0{\cdot}05$ m^2g^{-1}), but the surface areas of layers initially formed on sheet magnesium indicated average crystallite sizes of only about 1μ.

Nitrides of zinc and cadmium were best obtained by heating the finely divided metals in ammonia. Surface nitridation of mercury by streaming nitrogen activated by electric discharge at 2 mm pressure gives small amounts of a compound considered to be Hg_3N.[21] Mercurous nitride is stable up to 100° and readily hydrolysed by water and alkalis. Mercuric nitride, Hg_3N_2, was only obtained by reaction of ammonia gas with finely divided yellow mercuric oxide at room temperature.[16] Weight losses occurred in accordance with the equation, $3HgO + 2NH_3$ (gas) $= Hg_3N_2 + 3H_2O$(vap.), give to a hard brown mass of nitride, sensitive to detonation on being powdered. Oxidised mercury (as in cut-off valves, etc.) forms nitride with liquid ammonia in which it is appreciably soluble, e.g. Hg_3N_2 in liq. NH_3 converts hydrazobenzene to azobenzene.[22]

Samples of titanium nitride (cubic F-type, $a = 4{\cdot}24$Å) and zirconium nitride (cubic F-type, $a = 4{\cdot}56$Å) were obtained from the tetrachloride vapour and nitrogen–hydrogen,[3] and by heating the metals in nitrogen. The titanium nitride was stable up to 1000°, but the zirconium nitride showed a range of homogeneity from nearly stoicheiometric ZrN (13·3 wt.-%, 50 atom-% N) at 600° to lower nitrogen contents at temperatures up to 1800°. Thus, a typical sample of nitrided zirconium contained only 10·32 wt.-%, 42·8 atom-% N.

Procedure

Metal nitridation, hydrolysis and oxidation of the nitrides were followed by weight changes on vacuum[23–25] and thermal balances.[26] The nitrides were 'dry' and 'wet' hydrated with water vapour and liquid water at lower temperatures by procedures similar to those previously used in the hydration of lime and magnesia[27–30] at 22° and 95°. Since hydrolysis was rapid for calcium and magnesium nitrides, even in the presence of atmospheric water vapour, some samples (including lumps of nitride several mm thick) were exposed to the air for certain times.

On hydrolysis, all the samples disintegrated into more finely

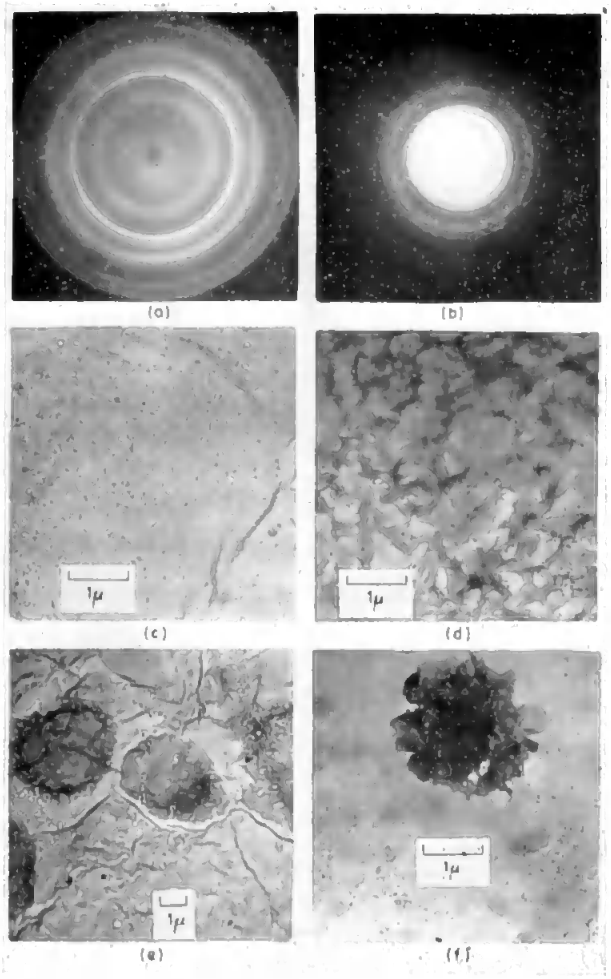

FIG. 1. *Electron micrographs of the surface nitridation of magnesium*

(a) Electron diffraction pattern of condensed metal film of magnesium
(b) Electron diffraction pattern of a non-uniform magnesium film
(c) Condensed metal film of magnesium (Magnification 7500)
(d) Initial stages of magnesium nitridation at 400°c (Magnification 7500)
(e) More extensive magnesium nitridation (Magnification 3500)
(f) Magnesium nitridation at 500°c (Magnification 7500)

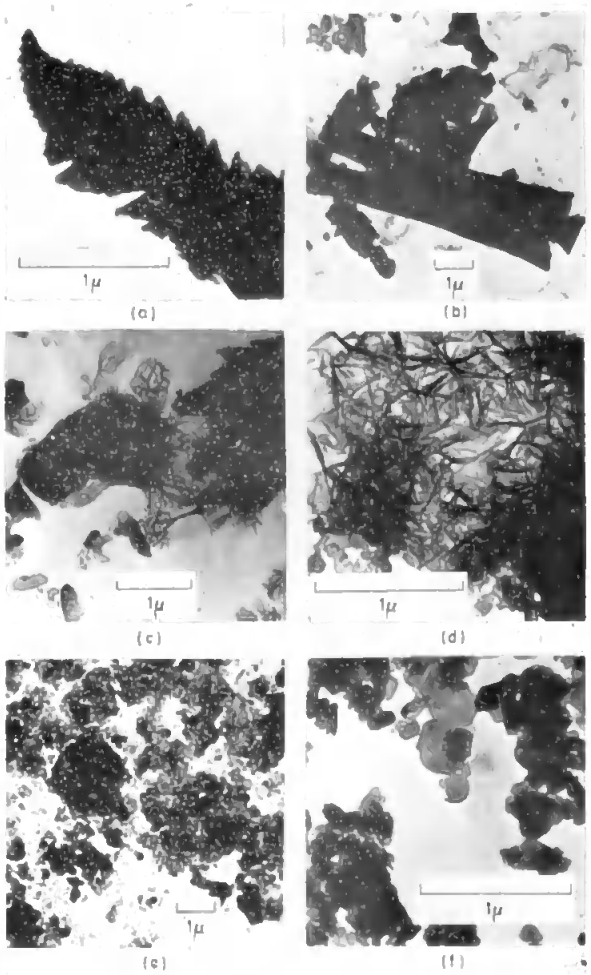

FIG. 2. *Electron micrographs of 'dry' and 'wet' hydrolysis of nitrides of calcium and magnesium*

(a) Ca_3N_2 steam hydrated at 130° for ½ h (Magnification 20,000)
(b) Mg_3N_2 before hydration (Magnification 5000)
(c) Mg_3N_2 hydrolysed by H_2O vapour near s.v.p. at 22° for 15 h (Magnification 10,000)
(d) Another part of sample (c) (Magnification 20,000)
(e) Mg_3N_2 hydrolysed with liquid water at 22° for 15 h (Magnification 5000)
(f) Precipitated $Mg(OH)_2$ (Magnification 20,000)

Table I

Hydrolysis of nitrides of calcium and magnesium

Hydrolysis conditions	S for $Ca(OH)_2$ m^2g^{-1}	Av. cryst. size, Å	S for $Mg(OH)_2$ m^2g^{-1}	Av. cryst. size, Å
Liquid H_2O, 22°, 5 h	15·0	1800	47·5	530
Liquid H_2O, 95°, 5 h	13·0	2100	57·5	440
Air, 22°, 4 days	3·7	7200	3·4	7400
H_2O vap. near s.v.p., 22°, 5 h for Ca_3N_2, 15 h for Mg_3N_2	7·2	3700	22·7	1100

is shown in Fig. 1 (c). This gives a regular diffraction pattern (a), in contrast with that for a non-uniform film in (b). Changes during the initial stages of magnesium nitridation at 400°, caused by localised stresses arising from crystal structure and volume variations, are shown in (d). More extensive nitridation produces rupture of the film and aggregation (e). This is more pronounced at higher temperatures (above 500°); a typical single aggregate is shown under higher magnification in (f). Nitridation of metal turnings at 500° and detachment of the nitride layers by shaking them with acetone gave greater separation of individual crystallites. Their size ranges extended to those obtained at higher temperatures (up to 600°, Fig. 2 (b)) where vaporisation of magnesium and nitride sintering were more extensive.

Hydrolysis of calcium and magnesium nitrides involves changes in the type of crystal structure (cubic Mn_2O_3 $D5_3$-type to hexagonal) and volume increases (0·713 and 0·970 of the original volumes) as the nitrides are converted to the less dense hydroxides. This leads to splitting of crystallites and increases in surface areas.[15] Samples of Ca_3N_2 and Mg_3N_2 of about 1 mm and 20–100μ crystallite size respectively (S below 0·05 m^2g^{-1}) 'wet' hydrolyse to hydroxide of only about 0·2μ and 0·05μ average crystallite size (Table I). The larger volume changes evidently produce more extensive splitting of the crystallites in the Mg_3N_2 hydrolysis, especially in the very rapid hydrolysis at 95°. Ageing (Ostwald ripening) is also slower for the less soluble magnesium hydroxide compared with the calcium hydroxide. 1 g Ca_3N_2 containing about 400 crystallites produces about 6×10^{14} $Ca(OH)_2$-crystallites (in ½ h at 22°) decreasing to 2×10^{14} on ageing for about 5 h, while about 10^{16} crystallites of $Mg(OH)_2$ per g Mg_3N_2 are obtained. The slower 'dry' hydrolyses with water vapour near s.v.p. and atmospheric water

vapour give less extensive splitting, viz. $2{\cdot}4 \times 10^{13}$ and $3{\cdot}3 \times 10^{13}$ $Ca(OH)_2$-crystallites or $1{\cdot}0 \times 10^{15}$ and $3{\cdot}4 \times 10^{12}$ $Mg(OH)_2$-crystallites per g nitride.

Development of hydroxide from nitride hydrolysis is shown by the electron micrographs in Fig. 2, in which (a) shows the splitting at the surface of a Ca_3N_2 crystal attacked by steam at 130°, (c) and (d) illustrate the growth of $Mg(OH)_2$ crystallites in the 'dry' hydrolysis of Mg_3N_2 at 22° (1–20μ fraction)(b), and (e) shows the disperse nature of the hydroxide obtained on 'wet' hydrolysing the Mg_3N_2 at 22°. These hydroxide samples lack any hexagonal features shown by precipitated and aged hydroxide (f) and give broadened X-ray patterns.

Nitrides of zinc and cadmium, and mercuric nitride

Zn_3N_2, Cd_3N_2 and Hg_3N_2 are rapidly hydrolysed, since their oxides and hydroxides dissolve in aqueous ammonia, as illustrated by the solubility curves in Fig. 3. Measurements of pH and electrical conductivity show that complex bases of the type $M(NH_3)_x(OH)_2$ are formed in solution, where $x \leqslant 4$ for M = Zn or Cd[15] and $x \leqslant 2$ for Hg.[16] These bases are stronger than ammonia and comparable with $Ag(NH_3)_2OH$ formed when silver oxide dissolves in ammonia.[33,34]

Nitrides of titanium and zirconium

Conversions of TiN and ZrN to TiO_2 and ZrO_2 are shown by the weight-gain rate curves in Fig. 1. Only rutile(tetragonal)-type TiO_2 and tetragonal ZrO_2 are formed. Initial weight increases are generally comparatively rapid, and the oxide X-ray patterns are only given after about a quarter of the total weight increases are recorded. At the lower temperatures, there are increases in specific surface. Splitting of crystallites must result from the changes in type of crystal structure (cubic F-type to tetragonal) and volume increases (0·630 and 0·411 of the original volumes) as the nitrides are converted to the less dense oxides.

In the conversion of TiN to TiO_2 at 600°, there is little increase in surface during the first quarter of the total weight gain, with the TiN lattice being essentially retained. However, it increased from 0·4 m^2g^{-1} (average crystallite size, 2·8μ) to 1·2 m^2g^{-1} (1·1μ) at half total weight gain, when the TiO_2 is no longer amorphous to X-radiation. This crystallite splitting (about 20-fold in the above example) evidently facilitates release of nitrogen, since the material ultimately (after 200 h) reaches constant weight corresponding to the calculated weight loss or complete conversion (cf.

FORMATION AND REACTIVITY OF NITRIDES

I. REVIEW AND INTRODUCTION

By D. R. GLASSON and S. A. A. JAYAWEERA

Methods of nitride production are summarised and their thermodynamics surveyed. Crystal structures and types of bonding in binary and ternary nitride compounds are classified and discussed. Kinetics of nitride formation are related to structural changes in the materials, which control diffusion of metals and nitrogen and cause nitride scaling. Metal nitridation with ammonia and nitride formation during ammonia synthesis are discussed.

Information so far available on the sintering of nitrides and its effect on their chemical reactivity is reviewed. This effect is influenced by additives or impurities such as oxides formed by partial nitride hydrolysis and oxidation. Sintering and hot pressing increase the resistance of nitrides to hydrolysis and oxidation, so that they become more suitable for use as refractories. Often, corrosion resistance of nitride layers on metal surfaces is impaired by poor scaling resistance in air or oxygen at comparatively low temperatures. The kinetics and products of oxidation of nitrides so far studied, notably AlN, TiN and UN, depend mainly on the intrinsic reactivity of the material and the available surface at which oxidation can occur.

Subsequent work will be concerned with changes in phase composition, surface area and crystallite and aggregate sizes and their correlation with production, sintering, hydrolysis and oxidation conditions for single and mixed nitrides. Suitable experimental techniques are summarised in this paper.

Introduction

The more extensive use of metals and refractories at higher temperatures has increased the industrial importance of nitrides. Those of special interest as refractories, e.g., Ti, Zr, Hf, Nb and Ta nitrides, have high melting points (ca. 3000°) and thermal stability. Although B, Al, Si and V also form high melting point nitrides, these decompose at temperatures below the m.p., but still above the medium temperature range (> 1500°). The lower melting point, less stable nitrides, e.g., of alkaline- and rare-earth metals, Li, Cr, Mo, W, Mn and Fe are of some interest as coatings. Nitrided metal surfaces are often subject to hydrolysis and oxidation, these processes constituting indirect metallic corrosion.

Nitrides (and some carbides) of metals of the fourth and fifth odd (A) subgroups of the Periodic Table have been important in high melting point cermets.[1] When combined with metals such as cobalt, they form hard-cast alloys.[2,3] Fabrication involves powder metallurgical methods such as sintering and hot pressing.[3] High m.p. combined with good non-scaling properties make these materials suitable for jet propulsion and rocket technology, and for refractory vessels used in melting alloys of the even (B) subgroup metals. Low reactivity towards normally corrosive chemicals and high electrical conductivity permit their application as electrode materials in fused salt electrolysis. Nitrides of metals in groups VI to VIII, especially double nitrides and carbonitrides, are important in nitrided steels, but can be formed independently of the process of hardening by nitriding. The nitrides of Cr, Mn and Fe are also of theoretical interest in connection with ferro-, antiferro- and ferri-magnetism.[2]

Methods of nitride production

Nitrides can be produced by heating the elements in a nitrogen, ammonia, or nitrogen + hydrogen atmosphere.[4] Variations on these methods,[5] governed thermodynamically by heats of formation, include heating the metal amalgams, e.g., Ca, Ba, Mn and Fe, or the metal oxides + aluminium or magnesium, e.g. Ce, La, Nd, Pr and U, or the metal oxides + carbon, e.g., Mg and Si. Sometimes, however, heating metal carbides in nitrogen produces carbonitrides such as cyanides and cyanamides of Ca, Sr and Ba.[6,7] Nitrides may be obtained also by decomposing suitable metal amides, e.g., Zn, Cd and Ba;[5,8] also Co[9] and Ni.[10] Occasionally, metal oxides react with ammonia at certain temperatures to give nitrides, e.g., Hg[11] and Ga,[12] which is the reversal of nitride hydrolysis.

The more stable nitrides, e.g., Ti, Zr, Hf, V and Ta, may be deposited directly on heated surfaces from gaseous mixtures of suitable volatile metal halides and nitrogen + hydrogen.[13-20] This method is preferred, particularly when metal surface nitridation slows down considerably after formation of a thin skin of nitride. Several hours are required for coatings of more than 1 or 2 mm thickness, unless much higher temperatures are used to ensure adequate diffusion across the nitride layer. Small TiN crystallites have been obtained in the cooled anode cavities, when $TiCl_4$ is introduced into the N_2-A stream of a plasma burner.[21,22] Hydrogen is not required, since the elements are ionised in the plasma beam.

Thermodynamics of nitride formation

Nitridation of metals by nitrogen or ammonia gas has become more important with the increased availability of high purity metals. The nitrides produced are those in equilibrium at the temperature and nitrogen pressure conditions. Thus, TiN,[14,23] VN[24] and CrN[25] are formed at temperatures between 1100° and 1600° at 1 atm. nitrogen. In the Mn–N system, nitrogen pressure changes from 1 to 200 atm. at about 750° increase the N-content of the product from 22 to 32 atom-%.[26,27] Nitridation by streaming ammonia is advantageous where equilibrium between ammonia and metal (giving nitride + hydrogen) is established rapidly, as compared with dissociation equilibrium in the gas phase. This produces nitrides of iron,[28] cobalt[29] and nickel[30] which have low enthalpies of formation and very high nitrogen equilibrium pressures at their preparation temperatures. Sometimes, lower nitrides, e.g., Fe_4N, are formed, using ammonia + hydrogen mixtures of NH_3/H_2 volume ratios corresponding to lower nitrogen pressures.[28,31,32] Reduction of metallic oxides with carbon in nitrogen applies only to nitrides of high thermal stability[33] and gives impure products. Hence, titanium dioxide (in 1 atm. nitrogen) forms

TiN below 1600° and TiC above this temperature; the reaction is complicated by TiN readily forming mixed crystals with TiC, and by TiO having a limited solubility in TiN.[20]

The stability of nitrides and their production at various temperatures are related to their standard free energies of formation, ΔG_T°;[34,35] more negative values of ΔG_T° indicate stabler compounds. These are compared for some of the more important nitrides on an Ellingham diagram[36] (Fig. 1), showing the temperature variation of ΔG_T° per g atom of metal (a) or nitrogen (b). Metal nitrides of the fourth and fifth odd (A) subgroups, e.g., TiN and ZrN, have the greatest stability. This progressively decreases for nitrides in the lower groups, and for transition metal nitrides in groups VI to VIII. The iron nitrides, Fe_2N and Fe_4N, are relatively unstable, having positive ΔG_T° values for a fairly wide temperature range. Similarly, ΔG_T° values for NH_3 (per g atom H or N) indicate that ammonia is less stable than most nitrides.

From Fig. 1 (b), the standard free energy changes for the reaction of a metal with ammonia (forming nitride and hydrogen) can be compared for different metals. Thus for Ca_3N_2 formation, ΔG_T° for $3/2Ca + NH_3 \rightarrow \frac{1}{2}Ca_3N_2 + 3/2H_2$, is the difference between the values for the reactions:— $3/2Ca + \frac{1}{2}N_2 \rightarrow \frac{1}{2}Ca_3N_2$ and $3/2H_2 + \frac{1}{2}N_2 \rightarrow NH_3$. Hence, the difference between the graphs for $\frac{1}{2}Ca_3N_2$ and NH_3 in Fig. 1 (b) indicates the relative ease of nitride formation, when the materials are in their standard states. All of the nitrides in Fig. 1, except Fe_2N and Fe_4N at lower temperatures, can be formed from the metal and ammonia. However, although energetically feasible, these reactions may be kinetically unfavourable. This applies especially to solid state reactions, when binary and ternary nitride compounds are formed by heating metals with nitrogen-rich nitrides. Fine grain sizes and pressing of the well-homogenised material facilitate the reactions, e.g., for Ti–, V–, Cr– and Mn–N systems; decomposition of ε-Fe_2N mixed with Mo powder produces ternary compounds in the Fe–Mo–N system.[37] Iron impurities often appear to accelerate nitriding of elements.

The thermodynamics of nitride formation from metal halides and ammonia or nitrogen–hydrogen gas mixtures, has been developed by Münster & Ruppert.[19,38,39] Free energy equations for the reactions:—

$TiCl_4\,(g) + 2H_2\,(g) + \frac{1}{2}N_2\,(g) \rightarrow TiN\,(s) + 4HCl\,(g)$ and $TiCl_4\,(g) + 2Fe\,(s) + \frac{1}{2}N_2\,(g) \rightarrow TiN\,(s) + 2FeCl_2\,(g)$, show that on an iron substrate, nitride forms primarily by displacement at temperatures below 1100°—1200°. Experimentally, TiN is deposited by hydrogen reduction above 650°; between 500° and 650° a dark blue incomplete reduction product, probably impure TiNCl, is co-deposited. The suspended particles of TiN formed in the gas phase settle on the substrate and give somewhat porous deposits. Thin coherent non-porous coatings are formed by displacement, in the absence of hydrogen. The very low solubility of iron in TiN stops the reaction, but the coatings can be thickened subsequently by hydrogen reduction. Chloride

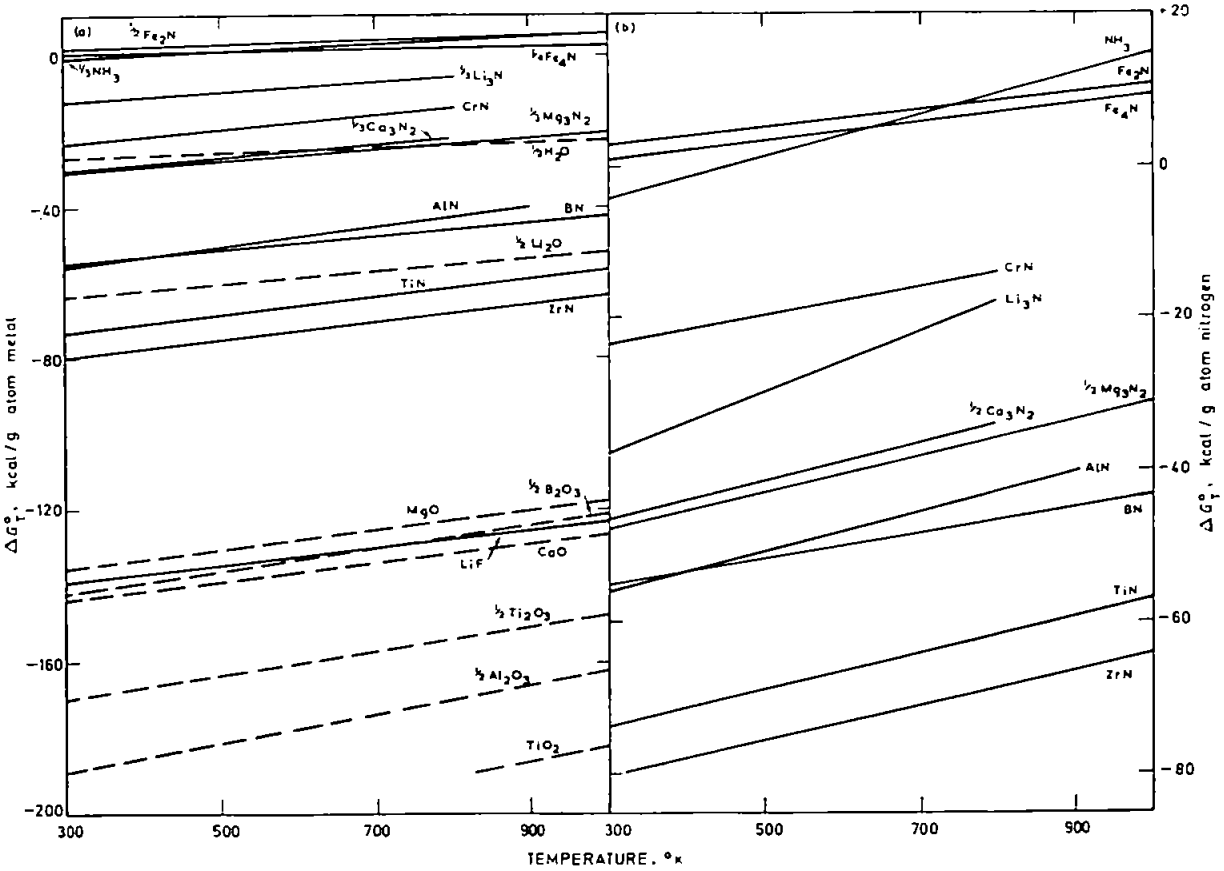

Fig. 1. *Ellingham diagrams for some nitrides, oxides and fluorides*

reduction and direct deposition methods have been compared for group IV A and V A nitrides,[14] and summarised for boron nitride.[40]

Structure of nitrides

Nitrides are classified generally as ionic, covalent and interstitial.[5]

Ionic nitrides are typified by lithium in group I (Li_3N) and the alkaline-earth metals in group II (M_3N_2). Nitride formation by the other alkali metals in group I is restricted by crystal structure conditions. The ability of the elements to form stable nitrides is indicated by comparing heats of formation (kcal per equiv.) of corresponding oxides and fluorides[41] which are more stable than the nitrides, their standard free energies varying similarly with temperatures, cf. Fig. 1 (a) and Fig. 2. Since the radii of F^-, O^{2-} and N^{3-} are similar, variations in heats of formation will depend mainly on the negative ion charge; electron affinities, E, and crystal energies, U, will be affected. E is expected to predominate in compounds with large positive ions of low charge, so that the heat of formation decreases with increasing negative ion charge, e.g., LiF, Li_2O and Li_3N have heats of formation of 146, 71 and 15 kcal per equiv. respectively. The sharper decrease from NaF (136) to Na_2O (50) suggests a very low value for Na_3N, which is evidently unstable at room temperature and has so far not been prepared in the pure condition. The Madelung constant is significant in that it is unfavourable for Li_3N and high for the fluoride. Thus, the decrease in heat of formation from fluoride to nitride is much greater than in the group III series AlF_3 (110), Al_2O_3 (63) and AlN (27), where the nitride has the higher Madelung constant.

Comparison of the molecular susceptibilities of Mg, Zn and Cd nitrides shows that the polarising action of the metal ion decreases from Mg to Zn to Cd.[42] Nitrides in group III (B, Al, Ga) and group IV (Si, Sn) show covalent character.

Interstitial nitrides are formed mainly by transition metals. The small N atoms occupy some or all of the interstices in the metallic lattices, which are generally close-packed. This gives simple nitride structures, such as the rock-salt lattice, the form of which depends on the number of N-occupied interstices and their type (tetra- or octa-hedral), e.g., ScN, LaN, CeN, PrN, TiN, ZrN and Fe_2N. Ranges of homogeneity vary; UN is an extreme example, having the stoicheiometric composition of the compound. Uranium also forms higher nitrides, viz., U_2N_3 and products with N-contents up to that of UN_2, cf. Table I. The composition of interstitial nitrides with a narrow range of homogeneity is not determined by the metal valency, in contrast to some transition metal oxides, also having narrow homogeneity ranges.

Refractory nitrides

The interstitial nitrides are usually extremely hard materials with high m.p. They have thermal and electrical conductivities comparable with those of metals; some of them become superconductors at very low temperatures. Thus, they are one group of a class of materials termed 'hard metals'[1,43–47] or 'metal-like' refractory compounds.[48–50] These materials form one of three fundamental classes of refractory compounds; (1) compounds of metals with non-metals, such as borides, carbides, nitrides, oxides, silicides, phosphides and sulphides; (2) compounds of non-metals with each other, such as carbides, nitrides, sulphides and phosphides of boron and silicon, and also alloys of B and Si;

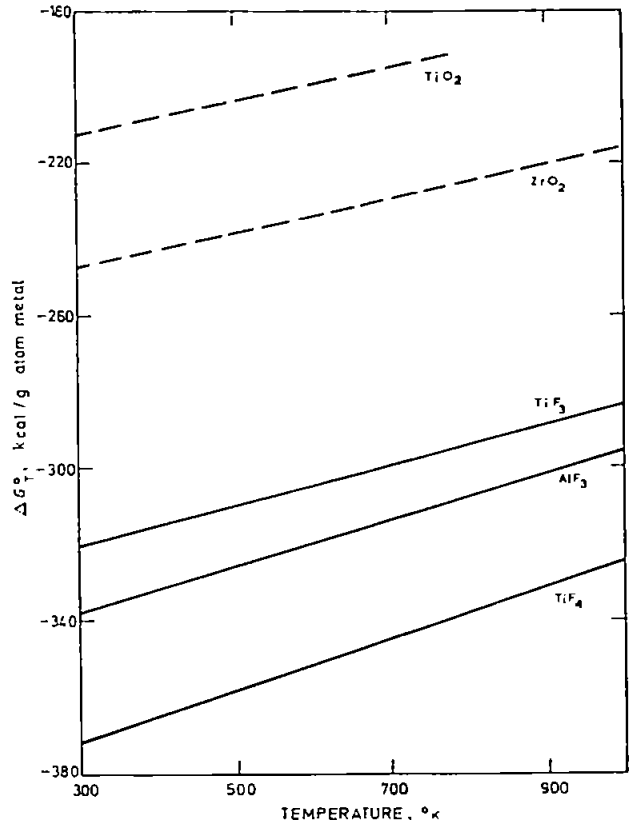

Fig. 2. *Ellingham diagrams for some oxides and fluorides*

(3) compounds of metals with each other, known as intermetallic compounds.

The character of the chemical bond between the components of these compounds is mainly metallic or covalent with a small proportion of ionic bond. These types of bond are established mainly by transition metals with non-metals having ionisation potentials sufficiently low to avoid exclusive ionic bond formation; they are also formed between two non-metals and certain metals with each other. The metallic components of refractory compounds include elements of the odd subgroups of groups III to VII, group VIII, lanthanides, actinides and aluminium. The non-metallic components include light non-metals of the short periods (B, C, N, O, Si, P, S). The chemical bond in the lattices of these compounds (in addition to the *s*- and *p*-electrons of the metallic and non-metallic components respectively) is formed also by the electrons of the deeper incomplete *d*- and *f*-levels of the transition metals. Isolated atoms of metals of the odd subgroup of group II, the alkaline-earth metals, do not have any electrons in the *d*- and *f*-shells, but in compounds with non-metals, energy states corresponding to these shells may occur.[48–50] The 'metal-like' refractory compounds are heterodesmic in the character of their chemical bonding, with the proportion of each type of bond being determined by the criteria and features of the crystal structure.

Nitrides have correspondingly greater proportions of ionic bond, because of the higher ionisation potential of nitrogen compared with the other non-metal refractory components. This is more evident in nitrides of metals having a low acceptor capacity (Mo, W, Re), while the nitrides of Nb, Ta and Cr show a combination of metallic and ionic bond, with the

TABLE I

Fractional volume and crystal lattice changes on nitridations

Nitride	Fractional volume change	Crystal lattice change to: Element	Crystal lattice change to: Nitride
Li_3N	−0·30	Cubic b.c., a = 3·51 Å.	hexagonal, a = 3·66 Å., c = 3·89 Å.
Be_3N_2	+0·39	Hexagonal c.p. Mg (A3), a = 2·28 Å., c = 3·58 Å.	cubic Mn_2O_3 ($D5_3$), a = 8·15 Å.
Mg_3N_2	−0·11	Hexagonal Mg (A3), a = 3·21 Å., c = 5·21 Å.	cubic Mn_2O_3 ($D5_3$), a = 9·95 Å.
Ca_3N_2 (High temp.)	−0·31	(γ) Cubic b.c. W (A2), a = 4·38 Å.	cubic Mn_2O_3 ($D5_3$), a = 11·38 Å.
Sr_3N_2	−0·25	Hexagonal Mg (A3), a = 4·31 Å., c = 7·05 Å. or cubic b.c., a = 4·84 Å.	pseudo-hexagonal[146]
Ba_3N_2	−0·19	Cubic b.c., W (A2), a = 5·02 Å.	pseudo-hexagonal[146]
Zn_3N_2	+0·27	Hexagonal Mg (A3), a = 2·66 Å., c = 4·94 Å.	cubic Mn_2O_3 ($D5_3$), a = 9·74 Å.
Cd_3N_2	+0·22	Hexagonal Mg (A3), a = 2·98 Å., c = 5·62 Å.	cubic Mn_2O_3 ($D5_3$), a = 10·80 Å.
BN	+0·17	Tetragonal, a = 8·73 Å., c = 5·03 Å.	hexagonal, a = 2·50 Å., c = 6·66 Å.
AlN	+0·25	Cubic, Cu (Al), a = 4·05 Å.	hexagonal, wurtzite (B4), a = 3·11 Å., c = 4·97 Å.
GaN	+0·19	Orthorhombic, a = 4·524 Å., b = 4·523 Å., c = 7·661 Å.	hexagonal, wurztite (B4), a = 3·18 Å., c = 5·17 Å.
InN	+0·19	Tetragonal, a = 3·25 Å., c = 4·94 Å.	hexagonal, wurtzite (B4), a = 3·54 Å., c = 5·70 Å.
Si_3N_4 (α)	+0·22	Cubic, diamond (A4),	hexagonal, a = 7·75 Å., c = 5·62 Å.
Si_3N_4 (β)	+0·22	a = 5·43 Å.	hexagonal (phenacite), a = 7·60 Å., c = 2·91 Å.
LaN	−0·01 to −0·02	(α) Hexagonal Mg (A3), a = 3·76 Å., c = 6·06 Å., (β) Cubic Cu (Al), a = 5·30 Å.	cubic NaCl (Bl), a = 5·28 Å.
CeN (Low temp.)	−0·08 to −0·07	(α) Cubic Cu (Al), a = 5·16 Å., (β) hexagonal Mg (A3), a = 3·65 Å., c = 5·96 Å.	cubic NaCl (Bl), a = 5·02 Å.
TiN (Low temp.)	+0·05 to +0·08	(β) Cubic b.c. W (A2), a = 3·30 Å., (α) hexagonal Mg (A3), a = 2·95 Å., c = 4·68 Å.	cubic NaCl (Bl), a = 4·24 Å.
ZrN (Low temp.)	no change to +0·03	(β) Cubic b.c., W (A2), a = 3·60 Å., (α) hexagonal Mg (A3), a = 3·23 Å., c = 5·15 Å.,	cubic NaCl (Bl), a = 4·56 Å.
ThN (Low temp.)	+0·01 to +0·07	(β) Cubic b.c., W (A2), a = 4·11 Å., (α) cubic Cu (Al), a = 5·08 Å.	cubic NaCl (Bl), a = 5·20 Å.
VN	+0·27	Cubic b.c., W (A2), a = 3·03 Å.	cubic NaCl (Bl), a = 4·13 Å.
NbN (ε)	+0·18	Cubic b.c., W (A2), a = 3·30 Å.	hexagonal, Y-MoC (B_i), a = 2·97 Å., c = 5·53 Å.
TaN (ε)	+0·26	Cubic b.c., W (A2), a = 3·31 Å.	hexagonal, CoSn (B_{35}), a = 5·19 Å., c = 2·91 Å.
CrN	+0·49	(α) Cubic b.c., W (A2), a = 2·88 Å.	cubic NaCl (Bl), a = 4·15 Å.
Cr_2N	+0·21	,, (at N-poor boundary)	hexagonal superlattice (L'3), a = 4·76 Å., c = 4·44 Å.
MoN (δ)	+0·21	Cubic b.c., W (A2), a = 3·15 Å.	hexagonal superlattice, a = 5·72 Å., c = 5·61 Å.
Mo_2N (γ-) (Low temp.)	+0·09	,,	cubic NaCl (Bl), a = 4·16 Å.
WN (δ)	+1·16	Cubic b.c., W (A2), a = 3·17 Å. (at N-rich boundary)	hexagonal (WC, B_h), a = 2·89 Å., c = 2·83 Å.
W_2N (β-)	+0·39	,,	cubic NaCl (Bl), a = 4·13 Å.
UN	+0·41	(α) orthorhombic, a = 2·86 Å., b = 5·88 Å., c = 4·94 Å.	cubic NaCl (Bl), a = 4·89 Å.
U_2N_3	+0·84	,,	cubic Mn_2O_3 ($D5_3$), a = 10·70 Å. or trigonal, La_2O_3 ($D5_2$), a = 3·69 Å., c = 5·83 Å.
UN_2	+0·91	,,	cubic, CaF_2 (Cl), a = 5·32 Å.

b.c. = body-centred c.p. = close packed

latter preponderating. Decreasing the nitrogen content of the nitride phases, within their homogeneity ranges, strengthens the metal to metal bonds and weakens the bonds of the metal atom cores with the nitrogen. Fairly wide breaks in the lattice energy states become possible, and determine the semi-conductor properties of nitrides having N-deficient lattices.

The proportion of ionic bond in metal oxides having high acceptor characteristics (Ti, Zr, Hf, V) is rather less than in the corresponding nitrides, since oxygen has a lower ionisation potential than nitrogen. These differences will be more pronounced for the lower oxides.

The second class of refractory compounds includes B and Si nitrides[51-54] (so-called non-metallic refractory compounds). Their bond character is also heterodesmic, but with covalent bonding predominating. They have semi-conductor properties as well as high electrical resistance at room temperature. Generally, their structure consists of layer chain or skeletal structural groups or patterns, and they either melt with decomposition or decompose before reaching the m.p.

Three elements, Be, Mg and Al (typical elements of groups II and III) are intermediate in their ability to form refractory metal-like and non-metallic compounds. Fairly refractory semi-conductors are given with non-metals,[48] e.g., Be, Mg and Al borides and AlN, and these three metals also can form intermetallic compounds.

Relationship between bonding and crystal structure of binary compounds

Hägg[43,44] suggested that binary interstitial compounds of the transition elements had simple 'normal' structures when the radius ratio, $r_x:r_m$ of the non-metal and metal atoms was less than 0·59:1. Many of the compounds giving radius ratios greater than 0·59:1 are still metallic in character, but their structures become more complex with decreasing size of the metal atom. Higher non-metal concentrations increase the unit cell dimensions of the interstitial phases, effectively making the radius ratio less favourable for normal structures. Later research indicates that this limiting radius ratio rule is valid only for carbides, the nitrides generally having lower radius ratios.[1]

Usually, the metal atoms in the interstitial compounds are arranged differently from the original metal lattices. The non-metal atoms occupy those interstices where they can remain in contact with the metal atoms. The face-centred cubic, close-packed hexagonal and body-centred cubic lattices have two types of interstices—tetrahedral and octahedral with co-ordination numbers of 4 and 6 respectively. The octahedral hole is perfectly regular in the two close-packed structures (face-centred cubic and close-packed hexagonal), but has tetragonal symmetry in the body-centred cubic structure. The only interstices of the simple hexagonal unit cell are the large 6-fold co-ordinated sites at the centres of trigonal prisms of metal atoms.

In the interstitial structures, not all of the holes of one type are necessarily occupied, so that many homogeneous phases show wide composition ranges. Nevertheless, homogeneity ranges of phases often include, or approximate to, some simple stoicheiometric composition corresponding to the occupation of a definite fraction of the number of available interstices. In the cubic close-packed lattice, the large octahedral interstices are occupied only if the radius ratio exceeds 0·41:1. Many monocarbides and mononitrides (MX-type) have radius ratios within the range 0·41—0·59:1, and have rock-salt structures irrespective of whether the original metal has a cubic close-packed structure or not.

Pauling-Rundle theory

Rundle[45] considered that the metal to non-metal bonding is octahedral, with 6 equal bonds being directed from the non-metal towards the corners of an octahedron. Pauling's basic concept[55-57] of the resonance of the 4 covalent C- or N-bonds amongst the 6 positions is developed by Rundle and Schwarzkopf.[1] Physical properties such as hardness, high m.p. and electrical conductivity are interpreted partly on the basis of resonating bond structures and on ionic structures, involving essentially homopolar and heteropolar forces. Krebs[58] suggested a resonance system of π-bonds between the 3 *p*-orbitals of N and the t_{2g}-orbitals of the metal.

Electronic states for refractories

Bilz[59] regarded isolated XM_6 co-ordination polyhedra within the lattice as 'XM_6 molecules', and presented a molecular orbital scheme of their bonding. He appended a calculation of the electronic states for refractories, MX, based on the band theory of metals. Thus, metallic character is expected to develop with increased electron occupation of the *d*-band in the series ScN, TiN, VN. This is supported by nuclear magnetic resonance measurements[60] on ScN and VN, where ScN resembles a half-metal. However, the expected increase in metallic character is not shown in the trend of electrical conductivities.[61]

Goodenough[62] describes nitrides with a rock-salt structure as 'ionic compounds with metallic conductivity', and in particular related to the oxides. The bond is partly ionic because of the electronegativity difference between the metal and nitrogen, and also partly covalent. In the metallic bond in transition metals, electron distribution between localised and more delocalised bonding states is determined by a critical distance, R_c.[63] Above about 2·9 Å the electrons are localised, but below this value 'collective' electrons are present.[64] Electrical conductivity is associated with partial filling of the t_{2g}-bands by collective electrons, and is limited to compounds where the metal–metal distances are less than R_c, as in nitrides. Rock-salt structured nitrides are formed only if 3 or less *d*-electrons are available in the formally trivalent cation, when the e_g-orbitals are empty and the t_{2g}-orbitals are either half or less than half filled. Great electronegativity differences produce a large forbidden zone, with the bonding electrons belonging mainly to the nitrogen sublattice; the bonding *s*- and *p*-e_g-electrons are predominantly on the nitrogen (ScN). Decreasing electronegativity differences confer a stronger e_g character on the bonding electrons. Increasing covalent bond character may lead to cation-anion-cation exchange interaction, e.g., CrN.

Special bonding relationships intermediate between the two extremes exist for γ-CrN (rock-salt lattice). Transition from cubic to orthorhombic symmetry is associated with localisation of the covalent bond and accords with changes in magnetic properties.[65] Nitrides of the Perovskite type, M_4N (M = Fe or Mn) are classified by Goodenough[62] as interstitial alloys, where the M–N bond is predominantly in character, i.e., N is probably present as a neutral atom. This agrees with Kuriyama's determination of the N atomic scattering factor in Mn_4N,[66] showing nitrogen to be present as either N^0 or N^{1-}. These results conflict with Elliott's de-

terminations for Fe_4N, which show N^{3-} as the probable species.[67] Mekata's qualitative band scheme for ε-Mn_4N is based on a neutron diffraction study,[68] and is a modification of Goodenough's scheme for cubic-F Mn, differing in the energetic arrangement of the e_g- and t_{2g}-bands relative to one another.

Ubbelohde-Samsonov theory

Ubbelohde's interpretation of the interstitial dissolution of hydrogen in palladium, tantalum and titanium[69,70] has been extended by Umanskiy to carbides and nitrides.[71,72] Seith & Kubaschewski[73] and Prosvirin[74] have demonstrated the ionic character of dissolved carbon and nitrogen in iron. Further development by Samsonov & Neshpor[49,75–78] implies transfer of non-metal valence electrons into the electron cloud of the compound, at least partially filling the electron-defect of the metal atoms. The additional forces of the donor–acceptor interaction greatly strengthen the interatomic bond. Thus, Jack interprets the structure of iron,[79] cobalt[80] and nickel[81] nitrides, carbides and carbonitrides on the basis of electron transfer from the interstitial C and N atoms to the metal lattice. The degree of participation in the bond (of incomplete *d*- and *f*-electron levels) and the distribution of electron concentration in the crystal lattice is expressed by the quantity, $1/Nn$, 'acceptor ability', where n is the number of electrons in the incomplete level and N is the principal quantum number of this level.[75] Decreasing 'acceptor ability' causes corresponding decreases[48] in electrical conductivity, heat of formation, lattice energy[82–86] and hardness. The electron density also depends on the ionisation potentials of the non-metal atoms, their electron-donor ability increasing in the direction of O, N, C, B, Si.[87–90]

The essentially metallic character of the interatomic bond is comparable with the Hume-Rothery electron phases,[88–90] the nature of the crystal structure depending on the electron concentration. Increasing concentration produces a sequence of crystal lattices, viz., body-centred cubic, base-centred hexagonal, face-centred cubic, simple hexagonal, for similar atomic radii ratios, $r_x:r_m$, where X = B, Si, C, N. The face-centred cubic lattice, most characteristic of group IV and V metal carbides and nitrides corresponds to an electron concentration of 5·5 to 6 electrons per atom. Nevertheless, formation of crystal structures characteristic for metal compounds does not necessarily arise from the transitional nature of their atomic components. Thus, nitrides of rare earth metals are mainly ionic,[91,92] yet crystallise in face-centred cubic (NaCl-type) lattices, similar to monoborides and monocarbides of group IV and V transition metals having metallic properties.

Wiener & Berger demonstrated that the occupation of incomplete *d*-shells of the metal atoms by electrons donated from the non-metal atoms reduced the magnetic moment.[93] Results for Fe, Co and Ni nitrides suggested donation of about 3 electrons by each N atom. The nitrogen was regarded as a positive ion or as forming a covalent bond by interaction of the *p*-electrons of N with the unpaired *d*-electrons of the nearest neighbour atoms. Likewise, Kiessling found that the ferro-magnetic properties of Mn, Fe, Co and Ni borides showed effective increases of 0·5 to 1 in the number of *d*-electrons compared with the pure metals.[94]

There have been only limited studies of the energy spectrum of electrons in metallic compounds. These include an approximate quantum mechanical analysis of the electron structure of the interstitial phase TiC and TiN,[59] and investigations of the *X*-ray spectra of Ti, V, Nb and Cr nitrides.[95–99] The latter are interpreted by the splitting of the 3*d*-level into t_{2g}- and e_g- levels by the crystal field in the octahedral environment.

Relationship between bonding and crystal structure of ternary compounds

Binary nitrides may change their character considerably on combination with a third element, either metallic or non-metallic. Partial exchange of a transition metal for a neighbouring transition metal produces only a small difference between the properties of the binary and ternary compounds. Introduction of one of the even (B) subgroup metals or partial replacement of nitrogen by carbon or oxygen, each have a much greater effect on the nature of the bonding. The products become polar in character when the third component is a very base metal or a strongly electronegative non-metal. The ternary compounds so far examined have been classified by Juza,[2] and their properties are summarised here in relation to what is known of their crystal structures.

Ternary metallic phases—double nitrides

Mixed crystals of the NaCl-type

There are mixed nitrides of odd subgroups IV, V and Cr.[100–103]

Hexagonal phases

These are formed when Mn, Fe, Co and Ni partially replace Ta in ε-TaN or δ-TaN (for Mn only)[101] or Co and Ni replacing Ti and Mo in TiN and MoN, giving products having a tungsten carbide-type lattice,[104] cf. also Ni arsenide structure. Numerous ternary nitrides in Cr, Cr/Ni and Cr/Mn steels both with and without substantial carbon contents have been reported.[105]

Mixed crystals of the Perovskite type

Mixed crystals of composition $Mn_{(4-x)}M_xN_{(1-x)/4}\ \square_{x/4}$, (where M = Cr, Mn, Ni, Cu, Zn and □ denotes holes in the nitrogen sublattice) derived from Mn_4N have been investigated. The magnetic moments per unit cell of the ferrimagnetic mixed crystals depend systematically on the foreign metal content.[106,107] Neutron diffraction studies indicate two sublattices in Mn_4N in which Mn_f is replaceable by Cr and Mn_c by Ni, Cu or Zn.[108] Mixed crystals $Mn_{(4-x)}In_xN$ and $Mn_{(4-x)}Sn_xN$, with no vacancies in the N sublattice, give discrepancies.[68] Ternary ferromagnetic compounds are derived from Fe_4N when Fe is replaced by Ni or Pt.[93]

T/M phases

These are double nitrides where a transition metal, T, coexists with an even subgroup element, M. Nitrogen is again surrounded by 6 T atoms in an essentially octahedral arrangement, and the M atoms are not bonded to N.[109] Crystal structures identified include:—Some 'Perovskite phases', T_3MN (T = Cr, Mn, Fe, Co, Ni and M = Cu, Ag, Mg, Zn, Al, Ga, In, Ge, Sn;[110–112] also Ti_3InN and Ti_3TlN[113]). Hexagonal 'H phases', T_2MN (T = Ti, or V, M = Al, Ga, In or Ge).[114] β-Mn phases, T_3M_2N, i.e., $Mo_{13}Fe_7N_4$ which approximates to $Mo_{12}Fe_8N_4$ or Mo_3Fe_2N;[115] the analogues V_3Zn_2N and V_3Ga_2N contain an even subgroup metal at the 8-fold position in the β-Mn cubic system.[114] 'η-carbide phases', T_4M_2N (T = Ti, Zr, Hf, Nb and M = Zn or Zr). Nitrides such as Ti_4Zn_2N have been discovered by Benesovsky,[114] where the non-metal is at the centre of a deformed

octahedron. These structures are analogous to η-carbides such as W_3Fe_3C and Mo_4Fe_2C[116] and η-oxides such as Ti_4Cu_2O.[117] Subsequently, η-nitrides, T_3M_3N (T = Mn, Fe, Co, Ni and M = Mo or W) have been reported,[118] and the structure of η-Fe_3Mo_3N recently established.[119]

Ternary metallic phases—carbonitrides

Isotypic nitrides and carbides form continuous series of mixed crystals, e.g., TiN and TiC.[59,61] The metal atom radii must differ by less than 15%, and the metal and non-metal can be varied simultaneously, e.g., TiN with HfC, VC, NbC; VN with TiC, NbC. Lattice constants of the mixed crystals closely follow Vegard's rule.[100] Chromium carbonitrides (NaCl-type lattice) are obtained from nitrided steels or electrolytically.[120] Only part of the nitrogen is replaced by carbon, since there is no isotypic Cr carbide. There is more extensive replacement of N by C in ε-Mn_4N, giving compositions up to $Mn_4N_{0.2}C_{0.8}$.[106,121]

Carbonitrides of iron and other transition metals are formed in steel hardening processes by fused alkali cyaniding or gas cementation.[122] The rapidly acting nitrogen probably accelerates subsequent carbiding. Jack has illustrated their relation to the binary iron nitrides.[79] The orthorhombic ζ-carbonitride extends from Fe_2N to $FeC_{0.75}N_{0.25}$, becoming ferromagnetic.[123] The hexagonal carbonitride, cf. ε-phase in Fe–N system, ranging from Fe_3 (C,N) to Fe_2 (C,N) has a maximum C content of 16 atom-% and is also ferromagnetic. There is very little replacement of N by C in the γ′-phase, Fe_4N; the ferromagnetic product when heated disproportionates to hexagonal Fe_3 (C,N) and α-Fe.[79,123]

Cobalt carbonitrides resemble those of iron. Both Co_2N and Co_2C are orthorhombic with closely similar lattice constants. Thus, when Co_2N is heated with CO at 340°, all of the N is replaced by C. The lattice constants of the intermediate mixed crystals of Co_2(N,C) change uniformly with the N/C ratio. There is only partial replacement of N by C in Co_3N, since no isotypic carbide, Co_3C, exists.[80] Nickel nitride, Ni_3N, can be carbided; both Ni_3N and Ni_3C are hexagonal with almost identical lattice dimensions.[81]

Nitride oxides

Although TiN and TiO have almost the same lattice constants, they do not form a series of mixed crystals. The lattice constant of TiN remains unchanged from TiN to $TiN_{0.6}O_{0.4}$ when the binary compounds are sintered at 1700°. Subsequent lattice constant decreases indicate a limited solubility of TiN in TiO but not of TiO in TiN.[124] The semi-conductivity of thin TiN films with a small oxygen content[20] conflicts with other electrical data on the effect of oxygen on TiN in bulk.[125]

Nitridation and oxidation of V[126], Cr[127] and Co[29] compounds gives products believed to contain some nitride oxides. Aluminium oxynitrides are possibly formed at high temperatures (above 1650°) in reducing atmospheres.[128–130] Recently, the so-called α-Si_3N_4 has been shown to contain oxygen, giving a defect structure of approximate composition $Si_{11.5}N_{15}O_{0.5}$.[131] The same chemical and structural relationships are observed for α- and β-germanium nitrides.[131]

Polar ternary compounds—double nitrides

Lithium nitride, Li_3N, forms mixed crystals up to a composition $Li_{2.5}M_{0.5}N$, where M = Co, Ni and Cu. The heavy metal atom occupies 00½ sites in hexagonal Li_3N, and the mixed crystals retain the predominantly salt-like character of Li_3N.[132] Reactions of Li_3N with Ti, V, Cr, Mn and Fe produce Li_5TiN_3,[133] Li_7VN_4,[134] Li_9CrN_5,[135] Li_7MnN_4[136] and Li_3FeN_2,[137] which are also mainly polar. Except for Li_3FeN_2, they have a superstructure of the antifluorite lattice all having N ions cubically close-packed and the metal ions in the tetrahedral holes. There are always 2 cations per anion. In contrast to the interstitial compounds, the nitrogen ions are surrounded by 8 cations.

Polar ternary compounds—nitride halides

These are MNX, where M = Ti, Zr, Th and X = Cl, Br, I. Ammonolysis of the halides at higher temperatures gives Ti compounds with a pronounced layer lattice like FeOCl. The sequence XTiNNTiX occurs in the *c*-axis direction. The halogens are assumed to be ionic, but the polar component of the bond within the cationic layer $(TiNNTi)_n^{2n+}$ is expected to be small.[138]

Kinetics of nitride formation

Metal nitridation is expected to conform to the same principles applying to oxide film growth.[139] Thus, the thin film theory of Mott & Cabrera[140] is consistent with the kinetics for the formation of calcium nitride,[141,142] where the rate is controlled by diffusion of cations through the product layer. Rates depending on the first power of the nitrogen pressure suggest reversible adsorption to form surface complexes of type $M(N_2^-)$. The mechanical stability of the nitride layer is important in determining rate and extent of nitridation. Its strength depends on the differences in molecular volume and type of crystal lattice of the nitride compared with the original metal (cf. Pilling-Bedworth rule for oxidised metals[143]), and also on the rate of nitride sintering.

Higher temperatures enhance sintering, i.e., they promote recrystallisation of the newly-formed nitride, but also increase evaporation of the metal below the nitride layer. This is exemplified by electropolished magnesium in very pure nitrogen[144] at 10 cm Hg pressure above 500°, and is illustrated further by electron-micrographs of nitrided magnesium[145] and calcium discussed in Part II. In subsequent papers, changes in phase composition, surface area, average crystallite and aggregate sizes will correlate with nitridation conditions.

Table 1 summarises molecular volume and crystal lattice changes accompanying nitridation of several of the more important elements. Calculations are based on *X*-ray examination, densities being deduced from metal and nitride crystal structures existent at temperatures normally used for nitridation. Volume changes are expressed as fractions of the original metal volume, allowing for weight increases during nitridation; expansions and contractions are indicated by + and − signs respectively. For reference in subsequent researches, the crystal structure dimensions have been checked experimentally by the authors against those given in the literature.[146,147] Where small decreases in unit cell size are caused by sintering of the newly-formed nitride, the lowest limiting value is recorded, e.g., for Ca_3N_2, *a* falls from 11·42 Å to 11·38 Å on sintering.

Nitridation rates often obey linear and parabolic laws, analogous to those found for metal oxidations.[139] Thus, nitridation of aluminium[4,148] closely conforms to a linear rate law at temperatures between 530° and 580°, whereas a

parabolic rate law is more suitable for the interpretation at higher temperatures, viz., 580°—625°. Nitridations of metals of the odd subgroups IV A and V A (Ti, Zr, Hf, Th, U, V, Nb, Ta) generally progress parabolically.[139] Results suggest direct diffusion of nitrogen into the metal. Factors causing slight deviations from the parabolic rate law in the earlier reaction stages are probably similar to those encountered in metal oxidations,[149] viz., decreases in surface heterogeneity and specific surface as the reaction proceeds, changes in local surface temperatures caused by the heat of reaction, solubility effects, impurity concentrations and possible changes in nitride composition.

Nitride scaling on metals

Formation of non-uniform, i.e., porous or cracked, scales depends partly on the Pilling-Bedworth rule,[143] which is probably less significant for scales that grow by outward migration of matter.[150] It is more important for scales where the diffusion is from the surface towards the metal-scale interface. Fractional volume changes are comparatively small for the formation of the group IV A metal nitrides, TiN, ZrN and ThN (Table I). Hence, titanium nitride films flake much less than those of the oxidised metal[151-154] (fractional volume change for rutile, TiO_2, formation = 0·73). Both nitrogen and oxygen are involved in the scaling of zirconium in air. The two-layered scale ultimately formed consists of an outer white or buff scale (ZrO_2) and an inner black scale (ZrO_2, ZrN and possibly N). The white scale predominates below ·1050° and the black above that temperature.[155] Similarly, V, Nb and Ta in group V A form oxides of exceptionally large volume ratios (fractional volume changes of 2·19, 1·68 and 1·50 for their pentoxides) compared with the nitrides (Table I). The resultant extensive rupturing of the oxide films changes the kinetics from parabolic to approximately linear at lower temperatures, 500—700°, for Nb[156-159] and Ta;[160-162] sintering of the oxide film at higher temperatures complicates the relationship between the gas pressure and oxidation rate.[157-158] If the scale becomes coherent and protective, the reaction may practically be stopped, even when the scale is completely detached from the metal surface, e.g., 'asymptotic' oxidation of Nb at 1250°.[163] Nitridation of Th becomes paralinear at higher temperatures (above 1370°), following the appearance of dark grey scale on top of the golden film adjacent to the metal.[164]

The group IV A and V A metals nitride much more slowly than they oxidise at corresponding temperatures.[165] Rates of nitrogen diffusion through α- and β-Ti and TiN indicate that the nitridations are controlled ultimately by diffusion through titanium and the surface nitride layer.[154] The initial controlling reaction is more likely diffusion through α-Ti. Likewise, the low activation energies for nitrogen diffusion in β-Zr compared with those for the nitridation,[166] indicate that the rate of solution in the β-phase is not the rate-determining process.[167] Nitridations of the other group IV A and V A metals are similar. The nitride films make the reaction rates practically insensitive to nitrogen gas pressure variations, and the film thickness is governed by the rate of nitride formation and the rate of solution in the metal.[100,165,168-170]

The M-N systems with M = V, Nb and Ta are very similar for low N-contents, but differ for high N-contents. The nitrogen solubilities in the metal lattices are only about 2 atom-%.[171] The 'interstitial' structure type, M_2N, is common for the three M-N systems;[24,172-176] the metal atoms are hexagonally close-packed and the N atoms are in one of the two metal atom octahedra of the unit cell. This phase has a comparatively broad homogeneity range with the upper phase limit closely corresponding to the composition, M_2N. A continuous solid solution series V_2N–Nb_2N–Ta_2N most probably exists.[172] The $NbN_{0\cdot8-0\cdot9}$ and $TaN_{0\cdot8-0\cdot9}$ phases are isomorphous, but there is no analogous V-N phase reported. The ε-phase in the Nb-N system (Table I) represents the transitional state between the atomic arrangements in the γ- and δ-phases.[172]

Nitridation of uranium is more complicated. Reaction rates with nitrogen (1 atm pressure) measured volumetrically indicate parabolic nitridation with some deviations initially and after the period of parabolic kinetics.[177] The surface nitride formed at temperatures between 550° and 750° is mainly UN_2 (probably deficient in nitrogen): at higher temperatures, viz., 775—900°, the three nitrides, UN, U_2N_3 and UN_2 form a rather roughened scale surface. The region between UN and U_2N_3 consists of 2 phases, but that between U_2N_3 and UN_2 is a homogeneous solid solution: the crystal structure changes from a distorted (U_2N_3) to a true CaF_2-type[178] (UN_2), Table I. However, Vaughan, regards U_2N_3 as being isomorphous with Th_2N_3 and suggests it is polymorphic (2 forms).[179] Reaction between nitrogen and uranium or thorium films has been followed by surface potential studies.[180] At higher nitrogen pressures, rapid variations in the rates of change in potential with time are associated with the formation of higher nitrides at the surfaces.

Metal nitridation with ammonia

The comparatively few kinetic studies of nitride formation with ammonia mainly relate to metal catalysts for nitrogen fixation. Metallic chromium, molybdenum and tungsten do not react appreciably with nitrogen at 900° under ordinary pressures.[181,182] They readily react with ammonia, even at lower temperatures (700—900°) giving single or mixed nitrides, MN and M_2N (Table I), where M = Cr,[25,183,184] Mo[185,186] or W.[187-191] This also applies to chromium borides[189] and ferrochrome metal.[25,192] The latter reaction is controlled by the comparative solubilities of nitrogen in chromium and iron at different temperatures and pressures.[192] Heats of decomposition of Cr_2N and Fe_4N to saturated solid solutions compared with enthalpies of formation, indicate heat absorptions of about 5000 cal. per g. atom N dissolving in either of the two body-centred cubic solvents. This accords with the similar electronic distributions of Cr and Fe about the N atoms. The much lower stability of Fe_4N compared with Cr_2N derives from the smaller radii of the octahedral interstices available for N atoms (1·89 Å compared with 2·13 Å).

Iron is generally nitrided by NH_3–H_2 mixtures of atmospheric pressure flowing over iron powder at rates sufficient to ensure only slight ammonia dissociation. At 450°, the product contains γ'-Fe_4N, its N-content depending on the NH_3/H_2 ratio. When pure ammonia is used, the ε- and ζ-nitrides are formed above and below 450° respectively.[193-195] At higher temperatures, viz., 700—750°, nitrogen-austenite (γ-phase) and nitrogen-martensite can be obtained.[196] The transformation of Fe_2N to Fe_4N at 400—600° is retarded considerably by small amounts of iron sulphide.[197]

Iron nitridation kinetics between 375° and 500° with NH_3–H_2 mixtures of atmospheric pressure are ascribed to opposing reactions: (1) $2NH_3 + 2xFe \rightarrow 2Fe_xN + 3H_2$; (2) $2Fe_xN \rightarrow 2xFe + N_2$. Reaction (1) depends on the rate of

nitrogen diffusion through the iron and iron nitrides, and becomes slower as more nitride forms, until equilibrium is reached between the two reactions.[198] The final N content increases at higher temperatures or ammonia concentrations. Gaseous nitrogen molecules do not react with iron vapour (1200—1500°K, 0·1 mm Hg),[198] and the kinetics of the decomposition of ε-iron nitride are of second order with respect to the interstitial N concentration.[199] The rate-determining process is believed to be the combination of pairs of N atoms at the solid surface.

Nitride formation during ammonia synthesis

Soliman[4] has studied the kinetics of ammonia synthesis using the following operational cycle for a series of metals, M, such as Ca:—(1) $3X+N_2 \rightarrow X_3N_2$; (2) $X_3N_2+6H_2 \rightarrow 3XH_2+2NH_3$; (3) $3XH_2+2N_2 \rightarrow X_3N_2+2NH_3$. Rates of reaction (1) are particularly sensitive to gas pressure where the nitride layer is fragmented and does not cover the metal surface completely, cf. negative volume changes in Table I. Reactions (2) and (3) must have relatively high rates at temperatures and pressures at which appreciable amounts of ammonia can exist in equilibrium with its decomposition products. Reaction (3) is exemplified by the production of pure UN from the metal hydride using nitrogen or the calculated amount of ammonia.[200] The iron catalysts used in the ammonia synthesis form neither nitrides nor hydrides by direct combination of the elements. However, there appears to be some (irreversible) activated nitrogen adsorption and some (reversible) solution of hydrogen. The rate of ammonia synthesis is of the same order as that of nitrogen adsorption over a wide temperature range.[201]

Reactivity of nitrides

Sintering of nitrides

The chemical reactivity of nitrides is controlled considerably by the extent to which they have been sintered during their formation and any subsequent calcination. At present, there is much more information available on the sintering of oxides which is expected to resemble that of nitrides. Theories of sintering have been developed by Hüttig,[109] Kingery,[202] Coble,[203,204] Kuczynski,[205] White[206] and Fedorchenko & Skorokhod.[207] Sintering is enchanced by compacting the powdered nitride, e.g., Be, La, Ti, Th, U, Ta, before calcining *in vacuo* to prevent possible hydrolysis and oxidation.[208]

Hot pressing often extensively densifies materials,[1] giving almost theoretical densities for oxides such as MgO, CaO and Al_2O_3.[209] A prerequisite is the production of finely-divided material with suitable particle size range. Development is limited by impurities, particularly gas-producing contaminants such as hydroxides and carbonates. Hence, often vacuum hot pressing is preferred.[210] Sintering is accelerated generally by low-melting additives,[211] but these may cause serious reductions in optical and mechanical properties. However, TiN is extremely brittle and may be sintered with a metal such as Co to give a satisfactory cermet, or may be used as a surface coating.[20] The thermodynamics of the sintering of TiN in the presence of carbon[212] and the defect structure and bonding of ZrN containing excess nitrogen have been described.[213]

The microhardness of V and Cr nitrides varies with bonding changes during progressive metal nitriding and subsequent sintering;[214] the lower nitrides, V_3N and Cr_2N are harder than VN and CrN. Apart from nitride formation, introduction of nitrogen into metallic chromium increases brittleness by locally distorting the metal lattice and lowering the cold-brittleness boundary.[215,216] Hardness and other mechanical properties of surface nitrided iron arise from nitride deposits which cause iron lattice deformation[217] blocking the glide planes.[218]

Nitride sintering is influenced by partial nitride hydrolysis and oxidation forming oxide impurities. When BN is purified at higher temperatures to reduce oxide content, the increased particle size makes subsequent hot pressing more difficult.[219] This nitride may be bonded and hot pressed successfully with silica glass.[220]

Hydrolysis and oxidation of nitrides

The resistance of powdered refractory nitrides to the action of water and aqueous acids and alkalis has been summarised by Samsonov.[48] In nitride production, usually oxygen must be excluded, for it prevents nitrogen from reacting with the clean metal surfaces. Occasionally, formation of an initial nitride surface layer protects against any subsequent oxygen attack, and permits nitridation to proceed. When the nitride layer is destabilised by hydrolysis (water vapour or liquid), the nitride ions are replaced by hydroxyl ions: since each N^{3-} is replaced by 3 OH^-, the film becomes very weak and ruptures whilst very thin.[145] At higher temperatures, decomposition of the hydroxides to oxides causes further fragmentation.[221] Thus, in magnesium nitridation between 400° and 650°, metal evaporation is promoted by traces of water vapour but inhibited by oxygen.

Hydrolysis of zinc, cadmium and mercuric nitrides, e.g. $Zn_3N_2+6H_2O \rightarrow 3Zn(OH)_2+2NH_3$, is enhanced, particularly at low temperatures, by the solubility of their oxides and hydroxides being increased in ammonia.[145] Complexes of the type $M(NH_3)_x(OH)_2$ are formed when $x \leqslant 4$ for M = Zn and Cd and $x \leqslant 2$ for Hg.[11] Soluble caustic alkalis also promote dissolution for Zn and for B, Al and Si nitrides.

Aluminium nitride hydrolysis forms part of the Serpek process, which has been revived by Pechiney[222] for the continuous production of 98% AlN. This nitride has become more important as a refractory since its resistance to attack by water vapour was found to increase considerably when it was sintered at 2000°.[223] The present authors (work to be published) find that aluminium nitride is oxidised appreciably to alumina by air or oxygen at temperatures above 600°. The oxidation rate depends mainly on (i) the intrinsic reactivity of the material and (ii) the available surface at which oxidation can occur. It generally obeys a parabolic law,[224] but the activation energies vary considerably even for samples of similar specific surfaces. The differences may be caused by initial films of oxide impurities accelerating crystallisation of oxide subsequently formed, and they are being further investigated and compared with nitride hydrolysis.

Boron and silicon nitrides are oxidised appreciably at temperatures above 800°, and this may involve formation of intermediate nitride–oxide defect structures such as $Si_{11.5}N_{15}O_{0.5}$ (α-Si_3N_4)[131] reviewed above. The presence of oxygen reduces the rate of nitridation of pressed extruded or slip-cast silicon powder.[52,54] Sintering and hot pressing of these nitrides[225–227] is expected to progressively increase their resistance to hydrolysis and oxidation. This should permit silicon nitride to be used successfully for lime kiln tuyères, without its mechanical properties being seriously impaired by the kiln atmosphere. Similarly, nitrides of Sc and rare earth metals are intermediate in chemical behaviour between the

polar nitrides of the alkaline earth metals (group II A) and nitrides of typical transition metals such as Ti and Zr (group IV A).[2,48]

Most interstitial nitrides are less readily hydrolysed, but some of them, e.g., Ti, Zr, Hf, Th, V, Cr, Mo, W and U, are converted to oxides on calcining in air. Thorium mononitride (ThN) oxidises rapidly and quantitatively in moist air at room temperature even in ingot form, but powdered uranium,[228] titanium and zirconium mononitrides are quite stable at 100° in boiling water, UN powder ignites in dry oxygen[228] at about 300°, but W_2N, Mo_2N and CrN have an increasing oxidation stability. The mononitrides of V, Nb and Ta are somewhat more stable, oxidising between 500° and 850°, while losing nitrogen. Titanium and zirconium nitrides produce TiO_2 (rutile) and ZrO_2 (tetragonal form) when calcined at temperatures between 400—1000° and 300—1000° respectively, causing indirect corrosion after the metals have nitrided at higher temperatures.

The only interstitial nitride oxidations that have been studied in any detail are those of TiN[229,230] and UN.[228] They illustrate factors to consider and problems to be encountered in further investigations of other transition metal nitride oxidations. Although the corrosion resistance of surface layers of TiN is excellent, the scaling resistance in air (or oxygen) is not very good. Oxidations with paralinear kinetics[230,231] between 625° and 1075° give scales consisting of rutile and possibly thin films of TiO-TiN solid solutions[231] adjacent to the metal. Platinum marker experiments[229,230] show that the oxide–nitride interface moves away from the oxide–gas interface. This indicates that oxygen rather than Ti diffusion is rate-determining at least in the parabolic stage of the oxidation, cf. diffusion of anion vacancies in the TiO_2 (*n*-type conductor),[232,233] which controls oxidation of Ti between 600° and 700° and gives a similar energy of activation.[234] The linear portion of the rate curve suggests that a phase boundary reaction may finally become rate-controlling. Probably, the atomic nitrogen diffuses from the metal to the outer scale surface where it then forms gaseous molecules, as in the decomposition of ε-iron nitride described above.[199] Small amounts of nitrogen are retained in the oxide layer, and some may have dissolved in the nitride phase (deficient in N) when freed by the oxidation reaction. The present authors have found that the amount of nitrogen retained depends on the reaction rate, sintering temperature and changes in crystallite sizes of the materials (to be reported in detail later). Final products of compositions such as $TiO_2.N_{0.075}$ resemble $UO_3.N_{0.2-0.4}$ given when UN oxidises;[228] the latter is sensitive also to crystallite size variations and both the intermediate U_2N_3 and UO_2 are epitaxially orientated with respect to the UN.

Subsequent work will be concerned with changes in phase composition, surface area and crystallite and aggregate sizes and their correlation with production, sintering, hydrolysis and oxidation conditions for single and mixed nitrides. Experimental techniques are summarised in the following section.

Experimental techniques

Materials

Thin metal films for nitridation are obtained by evaporating metal turnings *in vacuo* from a heated filament in an electron microscope shadowing unit. The metal vapours are condensed on pieces of mica or copper grids that have been coated previously with carbon films. The filament currents are increased sufficiently slowly to avoid rapid temperature increases and permit metal stresses to be released, so that the turnings do not fly off the filament before evaporation. These films are nitrided at different temperatures for various times.

Larger amounts of nitride are produced by direct nitridation of the metal turnings or powder. Other methods of nitride production have been summarised at the beginning of this paper. The nitrides are hot pressed using apparatus designed by Scholtz,[235] Roeder & Scholtz[236] and Oudemans.[237]

Procedure

Metal nitridation, hydrolysis and oxidation of the nitrides are followed by weight changes on vacuum[238-240] and thermal[241] balances. Samples are outgassed usually at 200° *in vacuo* before determination of their surface areas by the B.E.T. procedure[242] from nitrogen (or occasionally oxygen) isotherms recorded at −183° on an electrical sorption balance. The deduced average crystallite sizes (equivalent spherical diameters) are compared with particle size ranges determined by optical or electron microscope or sedimentation balance. Where necessary, particle size fractions of the materials are sintered or hot pressed for further lengths of time at fixed temperatures.

Phase composition identification

Samples are examined for phase composition and crystallinity using an *X*-ray powder camera and a Solus-Schall *X*-ray diffractometer with Geiger counter and Panax ratemeter. The average crystallite size of some of the phases can be determined from *X*-ray line- or peak-broadening.[243] Certain samples are further examined by optical and electron-microscopes (Philips EM-100).

Acknowledgments

The authors thank Dr. S. J. Gregg for his interest and encouragement in this work; Mrs. M. Sheppard for her assistance in the verification of *X*-ray data; the University of London Research Fund, the Imperial Chemical Industries Research Fund and the Science Research Council for grants for apparatus and a S.R.C. Research Technicianship (for M.S.).

John Graymore Chemistry Laboratories,
College of Technology,
Plymouth

Received 28 June, 1967;
amended manuscript 3 January, 1968

References

1 Schwarzkopf, P., & Kieffer, R., 'Refractory hard metals', 1953 (New York: Wiley)
2 Juza, R., 'Advances in inorganic chemistry and radiochemistry', (Eds. Emeléus & Sharp) 1966, Vol. 9, p. 81
3 Schwarzkopf, P., & Kieffer, R., 'Cemented carbides', 1960 (New York: Wiley)
4 Soliman, A., *J. appl. Chem., Lond.*, 1951, **1**, 98
5 Mellor, J. W., 'Comprehensive treatise on inorganic and theoretical chemistry', Vol. 8, p. 97 (London: Longmans); *ibid.*, Vol. 8 (Suppl.), p. 150
6 Cochet, A., *Z. angew. Chem.*, 1931, **44**, 367
7 Franck, H. H., & Heimann, H., *Z. angew. Chem.*, 1931, **44**, 372
8 Juza, R., Neuber, A., & Hahn, H., *Z. anorg. Chem.*, 1938, **239**, 273

[9] Schmitz-Dumont, O., *Z. Elektrochem.*, 1956, **60**, 866
[10] Watt, G. W., & Davies, D. D., *J. Am. chem. Soc.*, 1948, **70**, 3753
[11] Glasson, D. R., Thesis, Univ. London, 1949
[12] Lorenz, M. R., & Binkowski, B. B., *J. electrochem. Soc.*, 1962, **109**, 24
[13] van Arkel, A. E., & de Boer, J. H., *Z. anorg. Chem.*, 1925, **148**, 345
[14] Agte, C., & Moers, K., *Z. anorg. Chem.*, 1931, **198**, 243
[15] Becker, K., *Phys. Z.*, 1933, **34**, 185
[16] van Arkel, A. E., *Metallwirt., Metallwiss, Metalltech.*, 1934, **13**, 511
[17] Pollard, F. H., & Woodward, P., *J. chem. Soc.*, 1948, p. 1709; *Trans. Faraday Soc.*, 1950, **46**, 190
[18] Campbell, I. E., Powell, C. F., Nowicki, D. H., & Gonser, B. W., *J. electrochem. Soc.*, 1949, **96**, 318
[19] Münster, A., & Ruppert, W., *Z. Elektrochem.*, 1953, **57**, 564
[20] Münster, A., *Angew. Chem.*, 1957, **69**, 281
[21] Stokes, C. S., & Knipe, W. W., *Ind. Engng Chem.*, 1960, **52**, 287
[22] Opfermann, W., *Mber. dt. Akad. Wiss., Berl.*, 1964, **6**, 92
[23] Ehrlich, P., *Z. anorg. Chem.*, 1949, **259**, 1
[24] Hahn, H., *Z. anorg. Chem.*, 1949, **258**, 58
[25] Blix, R., *Z. phys. Chem.*, 1929, (B), **3**, 229
[26] Schenk, R., & Kortengraber, A., *Z. anorg. Chem.*, 1933, **210**, 273
[27] Guilland, C., & Wyart, J., *J. Rech. Cent. natn. Rech. scient.*, 1947, **3**, 123
[28] Lehrer, E., *Z. Elektrochem.*, 1930, **36**, 383
[29] Juza, R., & Sachsze, W., *Z. anorg. Chem.*, 1947, **253**, 95
[30] Juza, R., & Sachsze, W., *Z. anorg. Chem.*, 1943, **251**, 201
[31] Paranjpe, V. G., Cohen, M., Bever, B. M., & Floe, C. F., *J. Metals, N.Y.*, 1950, **188**, 261
[32] Fast, J. D., *Philips tech. Rev.*, 1948, **10**, 27
[33] Friederich, E., & Sittig, L., *Z. anorg. Chem.*, 1925, **143**, 293
[34] Margrave, J. L., & Sthapitanonda, P., *J. phys. Chem., Ithaca*, 1955, **59**, 1231
[35] Wicks, C. E., & Block, F. E., *Bull.* 605, *U.S. Bur. Mines*, 1963
[36] Ellingham, H. J. T., *J. Soc. chem. Ind., Lond.*, 1944, **63**, 125
[37] Evans, D. A., Thesis, Univ. Durham, 1957
[38] Münster, A., & Ruppert, W., *Z. Elektrochem.*, 1953, **57**, 558
[39] Münster, A., Rinck, G., & Ruppert, W., *Z. phys. Chem., Frankf. Ausg.*, 1956, **9**, 228
[40] Powell, C. F., Oxley, J. H., & Blocher, J. M., 'Vapour deposition', 1966, p. 381 (New York: Wiley)
[41] van Arkel, A. E., 'Molecules and crystals', 1956, p. 63 (London: Butterworths)
[42] Croato, U., Genta, V., & Maltese, P., *Gazz. chim. ital.*, 1951, **81**, 827
[43] Hägg, G., *Metallwirt., Metallwiss, Metalltech.*, 1931, **10**, 387
[44] Hägg, G., *Z. phys. Chem.*, 1931, (B), **12**, 33
[45] Rundle, R. E., *Acta. crystallogr.*, 1948, **1**, 180
[46] Hägg, G., *I.V.A.*, 1953, **24**, 345
[47] Rowden, W. F., *Metallurgy Bull.*, 1950, **5**, No. 5/6
[48] Shaffer, P. T. B., & Samsonov, G. V., 'High temperature materials', 1964, Handbooks 1 and 2 (New York: Plenum)
[49] Samsonov, G. V., 'Refractory transition metal compounds', 1964 (London: Academic Press)
[50] Samsonov, G. V., *Ukr. khim. Zh.*, 1965, **31**, (10), 1005 (N.L.L. translation, RTS 4233: Dec. 1967); summarised in *Izv. Akad. Nauk SSSR*, 1967, **58**, (10), 76
[51] Thompson, R., & Wood, A. A. R., *Chem. Engr*, 1963, p. CE 51
[52] Popper, P., & Ruddlesden, S. N., *Nature, Lond.*, 1957, **179**, 1129
[53] Hardie, D., & Jack, K. H., *Nature, Lond.*, 1957, **180**, 332
[54] Gill, R. M., & Spence, G., *Refract. J.*, 1962, p. 92
[55] Pauling, L., 'The nature of the chemical bond', 1940, p. 420 (Ithaca, N.Y.: Cornell University Press)
[56] Pauling, L., *J. Am. chem. Soc.*, 1947, **69**, 542
[57] Pauling, L., *Proc. R., Soc.*, 1949, (A), **196**, 343
[58] Krebs, H., *Acta. crystallogr.*, 1956, **9**, 95
[59] Bilz, H., *Z. phys. Chem.*, 1958, **153**, 338
[60] Kume, K., & Yamagishi, H., *J. phys. Soc. Japan*, 1964, **19**, 414
[61] L'vov, S. M., Nemchenko, V. F., & Samsonov, G. V., *Ukr. fiz. Zh.*, 1962, **7**, 331
[62] Goodenough, J. B., 'Magnetism and the chemical bond', 1963 (New York: Wiley, Interscience)
[63] Mott, N. F., *Nuovo Cim*, 1958, (10), **7**, suppl. 312
[64] Goodenough, J. B., *Phys. Rev.*, 1960, **120**, 67
[65] Goodenough, J. B., *Phys. Rev.*, 1960, **117**, 1442
[66] Kuriyama, M., Hosoya, S., & Suzuki, T., *Phys. Rev.*, 1963, **130** 898
[67] Elliott, N., *Phys. Rev.*, 1963, **129**, 1120
[68] Mekata, M., *J. phys. Soc. Japan*, 1962, **17**, 796
[69] Ubbelohde, A. R., *Trans. Faraday Soc.*, 1931, **28**, 284
[70] Ubbelohde, A. R., *Proc. R. Soc.*, 1937, (A), **159**, 295
[71] Umanskiy, Y. S., *Dokl. (Proc.) Acad. Sci. U.S.S.R., phys. Chem. Sect.*, 1943, **26**, 127
[72] Samsonov, G. V., & Umanskiy, Y. S., 'Solid compounds of refractory metals', 1957 (Moscow: Metallurgizdat)
[73] Seith, W., & Kubaschewski, O., *Z. Elektrochem.*, 1935, **41**, 551
[74] Prosvirin, B. I., *Vest. Metalloprom.*, 1937, **17**, (12), 102
[75] Samsonov, G. V., *Zh. fiz. Khim.*, 1956, **30**, 2058
[76] Samsonov, G. V., & Neshpor, V. S., *Dokl. Akad. Nauk SSSR*, 1958, **122**, 1021
[77] Samsonov, G. V., Neshpor, V. S., & Paderno, Y. B., *Ukr. fiz. Zh.*, 1959, **4**, 509
[78] Samsonov, G. V., & Neshpor, V. S., 'Powder metallurgy and strength of materials', 1959, No. 7, pp. 7 and 99 (Kiev: Izdvo Akad. Nauk SSSR)
[79] Jack, K. H., *Proc. R. Soc.*, 1948, (A), **195**, 41
[80] Clarke, J., & Jack, K. H., *Chemy Ind.*, 1951, p. 1004
[81] Jack, K. H., *Acta crystallogr.*, 1950, **3**, 392
[82] Sarkisov, E. S., *Dokl. Akad. Nauk SSSR*, 1947, **58**, 1337
[83] Sarkisov, E. S., *Zh. fiz. Khim.*, 1954, **28**, 627
[84] Samsonov, G. V., & Neshpor, V. S., *Zh. fiz. Khim.*, 1958, **32**, 2424
[85] Baughan, E. C., *Trans. Faraday Soc.*, 1959, **55**, 2025
[86] Shulishova, O. I., 'High temperature cermet materials', 1962 (Kiev: Izd. Akad. Nauk SSSR)
[87] Samsonov, G. V., *Dokl. Akad. Nauk SSSR*, 1953, **93**, 359
[88] Kiessling, R., *Fortschr. chem. Forsch.*, 1954, **3**, 41
[89] Kiessling, R., *Powder Metall.*, 1958, No. **3**, 177
[90] Robins, D. A., *Powder Metall.*, 1958, No. **1-2**, 172
[91] Jandell, A., *Z. anorg. Chem.*, 1956, **288**, 81
[92] Klemm, W., & Winkelmann, G., *Z. anorg. Chem.*, 1956, **288**, 87
[93] Wiener, G. W., & Berger, A. J., *J. Metals, N.Y.*, 1955, **7**, 360
[94] Kiessling, R., *Metall. Rev.*, 1957, **2**, 5
[95] Vanyshteyn, E. Y., & Vasili'yev, Y. N., *Dokl. Akad. Nauk SSSR*, 1957, **114**, 53
[96] Vanyshteyn, E. Y., & Zhurakovskiy, Y. A., *Dokl. Akad. Nauk SSSR*, 1958, **122**, 365; *ibid.*, 1959, **127**, 534; *ibid.*, 1959, **128**, 595; *ibid.*, 1959, **129**, 6
[97] Nemnonov, S. N., & Men'shikov, A. Z., *Izv. Akad. Nauk SSSR (Ser. Fiz.)*, 1959, **23**, 587
[98] Korsunskiy, M. I., & Genkin, Y. Y., 'Heat resisting materials seminar', 1958, Bull. No. 5 (Kiev: Izdvo Akad. Nauk SSSR)
[99] Karal'nik, S. M., Nikolayeva, L. G., & Korolenko, Y. I., *Ukr. fiz. Zh.*, 1959, **4**, 404
[100] Duwez, P., & Odell, F., *J. electrochem. Soc.*, 1950, **97**, 299
[101] Schonberg, N., *Acta chem. scand.*, 1954, **8**, 213
[102] Nowotny, H., Benesovsky, F., & Rudy, E., *Mh. Chem.*, 1960, **91**, 348
[103] Ito, F., Tsuchida, T., & Takaki, H., *J. phys. Soc. Japan*, 1964, **19**, (1), 136
[104] Schönberg, N., *Acta metall.*, 1954, **2**, 427
[105] Maratray, F., *Publs Inst. Rech. Sidér.*, 1954 (B), **75**, 47
[106] Juza, R., & Puff, H., *Z. Elektrochem.*, 1957, **61**, 810
[107] Juza, R., Deneke, K., & Puff, H., *Z. Elektrochem.*, 1959, **63**, 551
[108] Takei, W. J., Shirane, G., & Fraser, B. C., *Phys. Rev.*, 1960, **119**, 122
[109] Hüttig, G. F., *Kolloidzeitschrift*, 1941, **97**, 281
[110] Stadelmaier, H. H., & Tong, S. Y., *Z. Metallk.*, 1961, **52**, 477
[111] Stadelmaier, H. H., *Z. Metallk.*, 1961, **52**, 758
[112] Stadelmaier, H. H., & Fraker, A. C., *Z. Metallk.*, 1962, **53**, 48
[113] Jeitschko, W., Nowotny, H., & Benesovsky, F., *Mh. Chem.*, 1964, **95**, 436
[114] Jeitschko, W., Nowotny, H., & Benesovsky, F., *Mh. Chem.*, 1963, **94**, 1198; *ibid.*, 1964, **95**, 156, 178
[115] Evans, D. A., & Jack, K. H., *Acta crystallogr.*, 1957, **10**, 769
[116] Kiessling, R., Proc. Int. Symp. on Reactivity of Solids, Gothenberg, 1952, p. 1065
[117] Schönberg, N., *Nature, Lond.*, 1951, **168**, 558
[118] Schönberg, N., *Acta chem. scand.*, 1954, **8**, 932
[119] Coles, N. G., Thesis, Univ. Newcastle, 1967
[120] Hume-Rothery, W., Raynor, G. V., & Little, A. T., *J. Iron Steel Inst.*, 1942, **145**, 129
[121] Bouchaud, J. P., & Fruchart, R., *Bull. Soc. chim. Fr.*, 1964, **2**, 1579

[122] Schrader, H., *Trans. Indian Inst. Metals*, 1949, **3**, 185
[123] Bridelle, R., *Ann. Chim.*, 1955, (12), **10**, 24
[124] Schmitz-Dumont, O., & Steinberg, K., *Naturwissenschaften*, 1954, **41**, 117
[125] Samsonov, G. V., Verkhoglyadova, T. S., L'vov, S. M., & Nemschenko, V. F., *Dokl. Akad. Nauk. SSSR*, 1962, **142**, 862
[126] Roubin, M. P., & Paris, J. M., *C. r.hebd. Séanc. Acad. Sci., Paris*, 1965, **260**, 3088
[127] Roubin, M. P., & Paris, J. M., *ibid.*, 1965, **260**, 3981
[128] Yamaguchi, G., & Yamagida, H., *Bull. chem. Soc. Japan*, 1959, **32**, 1264
[129] Lejus, A. M., *Bull. Soc. chim. Fr.*, 1962, **11/12**, 2123
[130] Lejus, A. M., *Rev. hte. Temp. Refract.*, 1964, **1**, 53
[131] Grieveson, P., Jack, K. H., & Wild, S., Special Ceramics Symposium, 1967, in press (Stoke-on-Trent: Br. ceram. Res. Assocn.)
[132] Sachsze, W., & Juza, R., *Z. anorg. Chem.*, 1949, **259**, 278
[133] Juza, R., Weber, H. H., & Meyer-Simon, E., *Z. anorg. Chem.*, 1953, **273**, 48
[134] Juza, R., Gieren, W., & Haug, J., *Z. anorg. Chem.*, 1959, **300**, 61
[135] Juza, R., & Haug, J., *Z. anorg. Chem.*, 1961, **309**, 276
[136] Juza, R., Anschutz, E., & Puff, H., *Angew. Chem.*, 1959, **71**, 161
[137] Frankenburger, W., Andrussov, L., & Durr, F., *Z. Elektrochem.*, 1928, **34**, 632
[138] Juza, R., & Heners, J., *Z. anorg. Chem.*, 1964, **332**, 159
[139] Kubaschewski, O., & Hopkins, B. E., 'Oxidation of metals and alloys', 1962 (London: Butterworths)
[140] Cabrera, N., & Mott, N. F., *Rep. Prog. Phys.*, 1948, **12**, 163
[141] von Antropoff, A., & Germann, E., *Z. phys. Chem.*, 1928, **137**, 209
[142] Roberts, M. W., & Tompkins, F. C., *Proc. R. Soc.*, 1959, **251**, (A), 369
[143] Pilling, N. B., & Bedworth, R. E., *J. Inst. Metals*, 1923, **29**, 529
[144] Bickley, R. I., & Gregg, S. J., *J. chem. Soc.*, 1966, (A), p. 1849
[145] Glasson, D. R., & Jayaweera, S. A. A., 'Surface phenomena of metals', *Soc. chem. Ind. Monogr. No.* 28, 1967, in press (London: The Society)
[146] von Stackelberg, M., & Paulus, R., *Z. phys. Chem.*, 1933, **22**, 305
[147] Taylor, A., & Kagle, B. J., 'Crystallographic data on metal and alloy structures', 1962 (London: Constable)
[148] Sthapitanonda, P., & Margrave, J. L., *J. phys. Chem., Ithaca*, 1956, **60**, 1628
[149] Gulbransen, E. A., & Andrew, K. F., *J. electrochem. Soc.*, 1951, **98**, 241
[150] Vermilyea, D. A., *Acta metall.*, 1957, **5**, 492
[151] Carpenter, L. G., & Reavell, F. R., *Metallurgia*, 1948, **39**, 63
[152] Gulbransen, E. A., & Andrew, K. F., *J. Metals., N. Y.*, 1949, **1**, No. 10, 741
[153] Richardson, L. S., & Grant, N. J., *Trans. metall. Soc. A.I.M.E.*, 1954, **200**, 69
[154] Wasilewski, R. J., & Kehl, G. L., *J. Inst. Metals*, 1954, **83**, 94
[155] Phalnikar, C. A., & Baldwin, W. M., jun., *Proc. Soc. Am. Test. Mater.*, 1952, **51**, 1038
[156] Argent, B. B., & Phelps, B., *J. less-common Metals*, 1960, **2**, 181
[157] Hurlen, T., Kjollesdal, H., Markali, J., & Norman, N., *Publ. Cent. Inst. Ind. Res., Oslo-Blindern*, Apr., 1959
[158] Kofstad, P., & Kjollesdal, H., *Trans. metall. Soc. A.I.M.E.*, 1961, **221**, 285
[159] Cathcart, J. V., Campbell, J. J., & Smith, G. P., *J. electrochem. Soc.*, 1958, **105**, 442
[160] Gebhart, E., & Seghezzi, H. D., *Z. Metallk.*, 1959, **50**, 248
[161] Peterson, R. C., Fassell, W. M., & Wadsworth, M. E., *Trans. Am. Inst. Min. metall. Engrs.*, 1954, **200**, 1038
[162] Cathcart, J. V., Bakish, R., & Norton, D. R., *J. electrochem. Soc.*, 1960, **107**, 668
[163] Kubaschewski, O., & Schneider, A., *J. Inst. Metals*, 1949, **75**, 403
[164] Gerds, A. F., & Mallett, M. W., *J. electrochem. Soc.*, 1954, **101**, 171 and 175
[165] Gulbransen, E. A., & Andrew, K. F., *J. electrochem. Soc.*, 1950, **97**, 383 and 396
[166] Gulbransen, E. A., & Andrew, K. F., *J. Metals, N. Y.*, 1949, **1**, No. 8, 515
[167] Mallett, M. W., Belle, J., & Cleland, B. B., *J. electrochem. Soc.*, 1954, **101**, 1
[168] Gulbransen, E. A., & Andrew, K. F., *J. electrochem. Soc.*, 1949, **96**, 354
[169] Gulbransen, E. A., & Andrew, K. F., *J. Metals., N. Y.*, 1950, **188**, 586
[170] Ang, C. Y., *Acta metall.*, 1953, **1**, 123
[171] Brauer, G., & Jander, J. *Z. anorg. Chem.*, 1952 **270**, 160
[172] Schönberg, N., *Acta chem. scand.*, 1954, **8**, 199, 208
[173] Epelbaum, V. A., & Ormont, B. F., *J. phys. Chem., SSSR*, 1947, **21**, 3
[174] Rostoker, W., & Yamamoto, A., *Trans. Am. Soc. Metals*, 1953, Prepr. No. 29
[175] Brauer, G., & Zapp, K. H., *Naturwissenschaften*, 1953, **40**, 604
[176] Brauer, G., & Zapp, K. H., *Z. anorg. Chem.*, 1954, **277**, 129
[177] Mallett, M. W., & Gerds, A. F., *J. electrochem. Soc.*, 1955, **102**, 292
[178] Rundle, R. E., Baenziger, N. C., Wilson, A. S., & McDonald, R. A., *J. Am. chem. Soc.*, 1948, **70**, 99
[179] Vaughan, D. A., *J. Metals, N. Y.*, 1956, **8**, 78
[180] Rivière, J. C., 'Surface phenomena of metals', *Soc. chem. Ind. Monogr. No.* 28, 1968, in press (London: The Society)
[181] Duparc, L., Wenger, P., & Schusselé, W., *Helv. chim. Acta*, 1930, **13**, 917
[182] Neumann, B., Kröger, C., & Haebler, H., *Z. anorg. Chem.*, 1931, **196**, 65
[183] Korolev, M. L., *Izv. Akad. Nauk SSSR, Otdel. Tekh. Nauk*, 1953, p. 1465
[184] Eriksson, S., *Jernkont. Annlr*, 1934, **118**, 530
[185] Ghosh, S. P., *J. Indian chem. Soc.*, 1952, **29**, 484
[186] Sieverts, A., & Zapf, G., *Z. anorg. Chem.*, 1936, **229**, 161
[187] Hägg, G., *Z. phys. Chem.*, 1930, (B), **7**, 339
[188] Laffitte, P., & Grandadam, P., *C.r. hebd. Séanc. Acad. Sci., Paris*, 1935, **200**, 1039
[189] Kiessling, R., & Liu, Y. H., *J. Metals, N. Y.*, 1951, **3**, *Trans.* p. 639
[190] Kiessling, R., & Peterson, L., *Acta metall.*, 1954, **2**, 675
[191] Schönberg, N., *Acta chem. scand.*, 1954, **8**, 204
[192] Seybolt, A. U., & Oriani, R. A., *J. Metals, N. Y.*, 1956, **8**, *Trans.* p. 556
[193] Kohlschütter, H. W., & Lohnes, K., *Z. anorg. Chem.*, 1947, **255**, 73
[194] Jack, K. H., *Proc. R. Soc.*, 1948, (A), **195**, 34
[195] Jack, K. H., *Acta crystallogr.*, 1952, **5**, 404
[196] Jack, K. H., *Proc. R. Soc.*, 1951, (A), **208**, 200
[197] Kohlschütter, H. W., & Pavel, M., *Z. anorg. Chem.*, 1947, **255**, 65
[198] Krichevsky, I. R., & Khazanova, N. E., *Dokl. Akad. Nauk SSSR*, 1950, **71**, 481
[199] Goodeve, C., & Jack, K. H., *Discuss. Faraday Soc.*, 1948, No. 4, 82
[200] Katz, J. J., & Seaborg, G. T., 'Chemistry of the actinide elements', 1957, review by Hoekstra & Katz (London: Methuen)
[201] Emmett, P. H., & Harkness, R. W., *J. Am. chem. Soc.*, 1935, **57**, 1631
[202] Kingery, W. D., 'Introduction to ceramics', 1960, p. 353 (New York: Wiley)
[203] Coble, R. L., *J. appl. Phys.*, 1961, **32**, 787, 793
[204] Coble, R. L., 'Fundamental phenomena in the material sciences', 1964, Vol. 1 (New York: Plenum Press)
[205] Kuczynski, G. C., 'Theory of solid state sintering', 1961 (New York: Wiley, Interscience)
[206] White, J., 'Science of ceramics', *Proc. Br. ceram. Soc.*, 1962, **1**, 305; *ibid.*, 1965, **3**, 155 (London: Academic Press)
[207] Fedorchenko, I. M., & Skorokhod, V. V., *Izv. Akad. Nauk SSSR*, 1967, **58**, (10), 29; 'Progress in inorganic materials', 50th Anniversary Publication, Akad. Nauk SSSR, October 1967
[208] Chiotti, P., *J. Am. ceram. Soc.*, 1952, **35**, 123
[209] Rice, R., 'Science of ceramics', *Proc. Br. ceram. Soc.*, in the press
[210] Fulrath, R. M., *ibid.*
[211] Glasson, D. R., *J. appl. Chem., Lond.*, 1967, **17**, 91
[212] Blum, A., *Planseeber. PulvMetall.*, 1962, **10**, 72
[213] Straumanis, M. E., Faunce, C. A., & James, W. J., *Inorg. Chem.*, 1966, **5**, 2027
[214] Samsonov, G. V., & Verkhoglyadova, T. S., *Dokl. Akad. Nauk SSSR*, 1962, **142**, 608
[215] Kischkin, S. T., & Panassjuik, O., *Dokl. Akad. Nauk SSSR*, 1957, **113**, 1263
[216] Weaver, C. W., *Nature, Lond.*, 1957, **180**, 806
[217] Imai, Y., & Ishizaki, T., *Sci. Rep. Res. Inst. Tohoku Univ.*, 1962, (A), **14**, 203
[218] Fry, A., *J. Iron Steel Inst.*, 1932, **125**, 191

[219] Ruddlesden, S. N., 'Special ceramics', Proc. Symp. Br. ceram. Res. Assocn, 1962, p. 341 (London: Academic Press)
[220] Carborundum Co., B.P. 1,052,295
[221] Glasson, D. R., *J. appl. Chem., Lond.*, 1963, **13**, 111
[222] Clair, J., Fr.P. 1,175,373 (1957)
[223] Long, G., & Foster, L. M., *J. Am. ceram. Soc.*, 1959, **42**, 53
[224] Cooper, C. F., George, C. M., & Hopkins, S. W. J., 'Special ceramics.' Proc. Symp. Br. ceram. Res. Assocn, 1962, p. 49 (London: Academic Press)
[225] Taylor, K. M., & Lenie, C., *J. electrochem. Soc.*, 1960, **107**, 308
[226] Parr, N. L., Martin, G. E., & May, E. R. W., 'Special ceramics', Proc. Symp. Br. ceram. Res. Assocn, 1960, p. 102 (London: Heywood)
[227] Thompson, D. S., & Pratt, P. L., *Proc. Br. ceram. Soc.*, 1966, **6**, 75
[228] Dell, R. M., Wheeler, V. J., & McIver, E. J., Chem. Soc. Symposium, Aberdeen, 1966, Paper 3-3; *Trans. Faraday Soc.*, 1966, **62**, 3591
[229] Münster, A., & Schlamp, G., Proc. 16th Int. Congr. Pure and appl. Chem., Paris, 1957, Min. Chem. Section, p. 691 (London: Butterworth); *Z. phys. Chem.*, 1957, (N.F.), **13**, 59; *ibid.*, 1958, **15**, 176
[230] Münster, A., *Z. Elektrochem.*, 1959, **63**, 807
[231] Samsonov, G. V., & Golubeva, N. K., *J. phys. Chem., Moscow*, 1956, **30**, 1258
[232] Hauffe, K., *Wiss. Z. Univ. Greifswald*, 1951–2, **1**, 1
[233] Grunewald, H., *Annln Phys. Lpz.*, 1954, **14**, 121, 129
[234] Tylecote, R. F., & Mitchell, T. E., *J. Iron. Steel Inst.*, 1960, **196**, 445
[235] Scholtz, S., 'Special ceramics', Proc. Symp. Br. ceram. Res. Assocn, 1962, p. 293 (London: Academic Press)
[236] Roeder, E., & Scholtz, S., 'Special ceramics', Proc. Symp. Br. ceram. Res. Assocn, 1964, p. 269 (London: Academic Press)
[237] Oudemans, G. J., *Proc. Br. ceram. Soc.*, 1967 in press
[238] Gregg, S. J., *J. chem. Soc.*, 1946, p. 561
[239] Sartorius-Werke, 'Electrono-Vacuum Balances', 1963 (Göttingen: Sartorius-Werke, A.-G.)
[240] C. I. Electronics, 'Microforce Balances', 1966 (Wimborne, Dorset, England; C. I. Electronics, Ltd.)
[241] Gregg, S. J., & Winsor, G. W., *Analyst, Lond.*, 1945, **70**, 336
[242] Brunauer, S., Emmett, P. H., & Teller, E., *J. Am. chem. Soc.*, 1938, **60**, 309
[243] Glasson, D. R., *J. appl. Chem., Lond.*, 1964, **14**, 121

FORMATION AND REACTIVITY OF NITRIDES

II.* CALCIUM AND MAGNESIUM NITRIDES AND CALCIUM CYANAMIDE

By D. R. GLASSON and S. A. A. JAYAWEERA

Samples of calcium and magnesium nitrides have been prepared and hydrolysed 'dry' with water vapour and steam or 'wet' with liquid water. Changes in phase composition, surface area, crystallite and aggregate sizes have been correlated with hydrolysis conditions and compared with 'dry' and 'wet' hydration of lime and magnesia. The reactions involve the splitting of nitride and oxide crystallites and the subsequent ageing of the newly formed calcium and magnesium hydroxides.

Hydrolysis of calcium cyanamide has been studied similarly. The intermediate product, hydrated lime, has been separately reacted with urea solutions and gives calcitic rhombs having a wide crystallite size range.

Introduction

Calcium and magnesium nitrides are formed by direct combination of the metals with nitrogen at temperatures above 300°.

Calcium nitride

Nitridation of pure calcium at 400—450° takes place in three stages,[1] (1) a fast reaction involving only Ca atoms at the crystal surface, (2) a very slow reaction for atoms below the thin surface layer of Ca_3N_2, and (3) a second fast reaction after the nitride layer has attained a definite thickness. Soliman[2] found that there is a maximum nitridation rate at 425°, below which temperature the reaction is autocatalytic;[3] the induction period decreases rapidly with increasing temperature above 330°. The nitridation rate increases considerably at higher gas pressures, but the nitride formed below 600° is mainly the black form[4] (pseudohexagonal, a = 3·533 Å, c = 4·11 Å), which irreversibly changes to the brown form at 600—750°.

The higher temperature form of Ca_3N_2 is cubic (Mn_2O_3, $D5_3$-type, a = 11·38 Å) and is used commercially as a desulphurising agent for blast furnace metal.[5] In the nitride production, oxygen must be excluded since it prevents nitrogen reacting with the fresh calcium surface. Formation of an initial nitride surface layer protects against any subsequent oxygen attack, and permits nitriding to proceed. The nitride layer is destabilised, however, by hydrolysis (water vapour or liquid). In the present work, changes in phase composition, surface area, crystallite and aggregate sizes during nitride hydrolysis are studied. These are compared with the hydrolysis of magnesium nitride and the formation of calcium hydroxide from metallic calcium and from quicklime.

Magnesium nitride

Metal-free magnesium nitride is obtained by passing nitrogen over magnesium filings[6] (in an iron boat) heated at 650—700° (3—4 h) and later at 950° (12 h). Nitridation is accompanied by metal evaporation even at lower temperatures of 500° for electropolished magnesium in very pure nitrogen[7] at 10 cm. Hg pressure. At higher nitrogen pressures, there are 'breakaways', i.e., sudden increases in nitridation rates, explained in terms of the formation and growth of cavities at the nitride–metal interface, with rupture of the

*Part I: previous paper.

film covering the cavity. The magnesium vapour escapes through thin films without reacting with the nitrogen within the cracks. Thus, very pure magnesium nitride is manufactured by heating magnesium above the sublimation temperature, but below its m.p.[8] A limited amount of nitrogen (or ammonia) is admitted to initiate surface nitriding. Conversion of all the metal to the nitride is then completed at a temperature sufficient for the sublimed magnesium to break through the nitride surface coating, and gradually admitting additional amounts of nitrogen.

The nitride layers are destabilised by hydrolysis (water vapour or liquid) when the nitride ions are replaced by hydroxyl ions; since each N^{3-} is replaced by 3 OH^-, the films become very weak and rupture whilst very thin. At higher temperatures, decomposition of the hydroxide to oxide causes further fragmentation.[9] Hence, in magnesium nitridation between 400° and 650°, metal evaporation is promoted by traces of water vapour but inhibited by oxygen.

Calcium cyanamide

Pure calcium cyanamide is obtained by decomposing calcium cyanide at 600° in nitrogen;[10] reaction between lime and hydrocyanic acid yields a maximum of 35% $Ca(CN)_2$ at 350° which decomposes at higher temperatures. Nitridation of calcium carbide also produces calcium cyanamide. Equilibrium in the system CaC_2–N_2–C–$CaCN_2$ at temperatures between 1220° and 1390° is bivariant, and is determined by the concentration of a solution of CaC_2 in $CaCN_2$, which is the true reactant. The reaction $CaC_2 + N_2 = CaCN_2 + C$, is completely reversible up to 1325°. At 1120—1130°, $CaCN_2$ is stable under a nitrogen pressure of 1 atm.

Calcium cyanamide is hydrolysed by steam (as in the process for nitrogen fixation) or more slowly by moisture in soil (when used as a fertiliser). The overall hydrolysis has been represented by the equation $CaCN_2 + 3H_2O = CaCO_3 + 2NH_3$, but initially CN_2^- is replaced by OH^- to form $Ca(OH)_2$ as an intermediate. Urea formed from the hydrolysis of the cyanamide ions reacts with the hydrated lime to produce calcium carbonate. These changes have been followed by *X*-ray analysis and investigation of the phase composition, surface area and crystallite and aggregate size variations when hydrated lime reacts with urea solutions.

Experimental

Materials

The high-temperature (brown) form of calcium nitride was used. Since it was produced above 750°, sintering occurred readily, for this was well above the Tammann temperature (half m.p. in °K) of 734°K or 461°C. The well-sintered calcium nitride was broken into pieces of about 1 mm size (specific surface, *S*, corresponded to about 0·001 $m^2 g^{-1}$). The magnesium nitride consisted mainly of single crystals of sizes between 20 and 100 μ. (S = 0·01 to 0·05 $m^2 g^{-1}$). Smaller amounts of nitrides were formed by nitriding vapour deposited metal films supported on electron microscope grids (copper grids carrying carbon films coated with metal).[11] Calcium cyanamide, calcium hydroxide and urea (B.D.H. grade) were also used.

Procedure

The nitrides were 'dry' and 'wet' hydrolysed with water vapour and liquid water by procedures similar to those previously used in the hydration of lime and magnesia[12] at 22° and 95°. Since hydrolysis was rapid, even in the presence of atmospheric water vapour, certain samples (including lumps of nitride several mm thick) were exposed to the air for various periods. On hydrolysis, all the samples disintegrated into finely-divided material. As before,[12] the products were filtered off (where necessary) and washed with 50 ml portions of acetone to prevent further reaction and ageing. They were then dried at 200° *in vacuo* before determination of their surface areas by the B.E.T. procedure[13] from nitrogen isotherms recorded at −183° on an electrical sorption balance.[14]

Phase composition identification

The products were thermally analysed on the vacuum[14] or thermal[15] balances, decomposition of the calcium and magnesium hydroxides being completed at 500° *in vacuo*.[16] The lime and magnesia contents were determined[12(f)] also by acid dissolution and alkali back-titration methods, any unchanged nitrides being completely hydrolysed in hot solution, to check for ammonia (and thus nitrogen) content. Calcium and magnesium contents were determined by titration with EDTA.

Some of the samples were examined for phase composition and crystallinity using an *X*-ray powder camera and a Solus-Schall *X*-ray diffractometer (Cu Kα-radiation) with Geiger counter and Panax rate-meter. Certain samples were examined further by optical and electron-microscopes (Philips EM-100).

Results

Electron micrographs showing changes in crystallite and aggregate sizes during nitridation of calcium are presented in Fig. 1.

Fig. 2 shows the variations in specific surface, *S*, and average crystallite size (equivalent spherical diameter) resulting from the 'wet' hydration of calcium nitride, (a) and (c), and magnesium nitride, (b) and (d)—fully-lined curves. These are compared with corresponding changes when lime and magnesia are hydrated and calcium turnings (about 1 mm size) react with water (broken-lined curves).

In Fig. 3 and 4, electron micrographs are presented, showing the hydrolysis of calcium and magnesium nitrides and the reaction between lime and urea solution.

Fig. 5 shows the variations in specific surface during the carbonation of hydrated lime (7·4 g) with M-urea (200 ml) at 95°.

Discussion

Nitridation of calcium

Fractional volume changes (Table I, preceding paper) are generally greater for the formation of the more ionic nitrides. Surface layers of these nitrides readily fragment and are usually non-protective to further nitridation of the underlying metal. The ionic nitrides of group II, M_3N_2, mostly have CaF_2– or Mn_2O_3-type crystal structures. Thus, in Mg_3N_2, the N^{3-} ions occupy lattice positions corresponding to Ca^{2+} in CaF_2, with the Mg^{2+} filling three-quarters of the F^- positions. The vacancies facilitate diffusion of Mg^{2+} through the nitride layer during nitridation.

Nitride layer fragmentation is illustrated by electron micrographs of calcium nitrided at different temperatures for various times, as shown in Fig. 1. The condensed metal films generally give good micro-structural uniformity, but tend to grow irregularly when becoming too thick. The more uni-

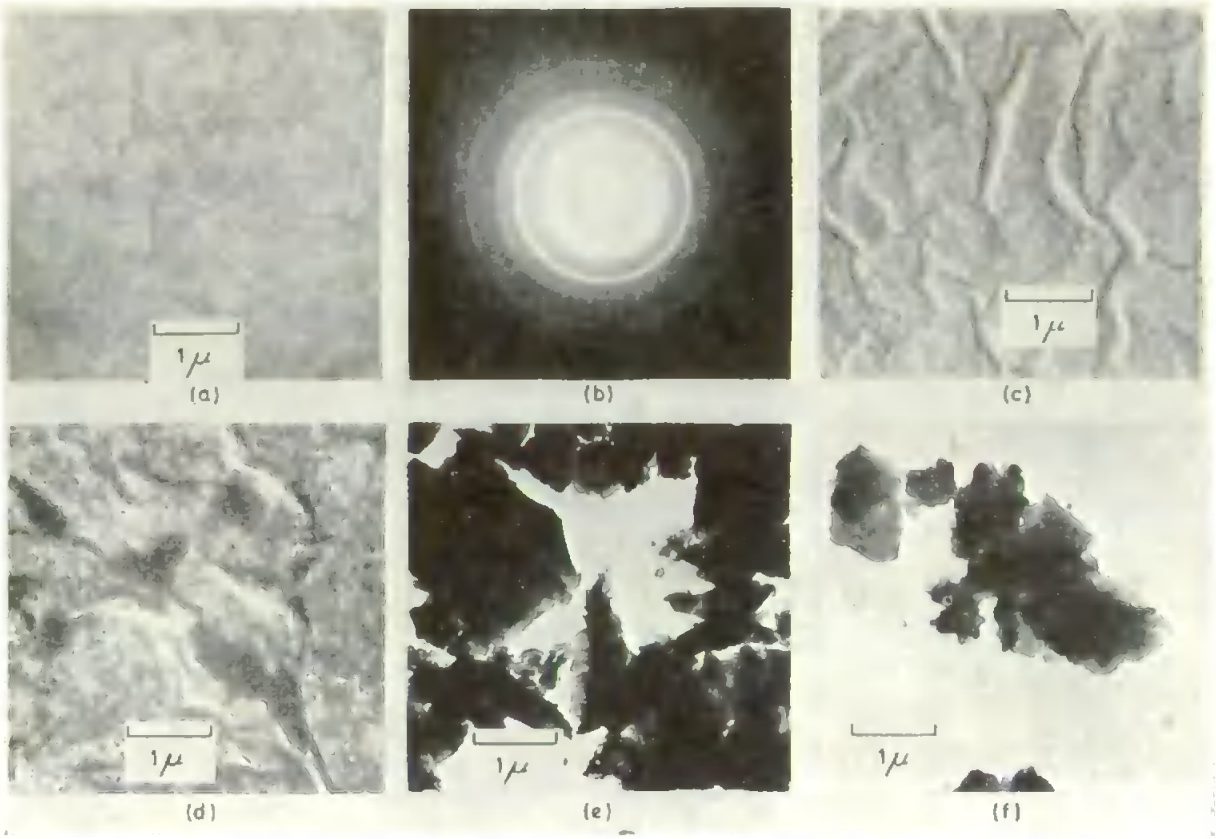

Fig. 1. *Electron-micrographs of the nitridation of calcium*

(a) Condensed metal film of calcium
(b) Electron diffraction pattern of (a)
(c) Calcium film nitrided at 400° for 3 h
(d) Calcium film nitrided at 450° for 1 h
(e) Calcium nitride (partly hydrolysed by atmospheric water vapour)
(f) Calcium nitride calcined at 600° for 20 h in air (→CaO)

form calcium film, Fig. 1 (a) gives a regular diffraction pattern, Fig. 1 (b). There is little change in appearance during the initial stages of nitration at 400°, Fig. 1 (c), but more rapid nitridation at 450° produces rupture of the film and aggregation, Fig. 1 (d).

Calcium nitride aggregates from direct nitridation of metal turnings are shown in Fig. 1 (e). They have been allowed to partly hydrolyse by exposure to atmospheric water vapour, forming more finely-divided calcium hydroxide at the outer parts. There is a crystal lattice change (cubic Mn_2O_3, $D5_3$-type to hexagonal) and a fractional volume expansion of 0·713, so that the hydroxide is split off and has a much higher specific surface and smaller average crystallite size than the original nitride (discussed more fully later).

Fragmentation also occurs when calcium and magnesium nitrides are heated in air above the decomposition temperatures for their respective hydroxides. Crystal lattice changes and volume contractions of about 10% lead to increases in specific surface and decreases in average crystallite sizes. The calcium oxide produced at 600° is shown in Fig. 1 (f). Its formation is complete within 5 h ($S = 6{\cdot}8\ m^2\ g^{-1}$, average crystallite size, 2650 Å), and the oxide does not sinter appreciably at 600°; after 20 h, $S = 7{\cdot}4\ m^2\ g^{-1}$, 2430 Å, the small increase in S probably marking the complete recrystallisation of the newly-formed oxide.[9] The more finely-divided magnesium oxide ($S = 18{\cdot}9\ m^2\ g^{-1}$) gives appreciable X-ray line-broadening, formation being practically completed in 20 h at 600°.

'Wet' hydrolysis of calcium nitride

The calcium nitride samples hydrolyse quickly in liquid water, usually within 5 min. The calcium hydroxide ages more rapidly at the higher temperature, as indicated by the fully-lined curves in Figs. 2 (a) and 2 (c). Hydroxide crystallites are evidently split off from the calcium nitride particles, as they are from calcium oxide in lime hydration,[12(c)] before they grow or age. 1 g Ca_3N_2 containing about 400 crystallites yielded about 6×10^{14} $Ca(OH)_2$-crystallites (in ¼ h at 22°) decreasing to 2×10^{14} on ageing for about 5 h. Electron micrographs in Figs. 3 (d), (e) and (f) show the progressive fragmentation of the Ca_3N_2-crystallites (and aggregates) and the ageing of the $Ca(OH)_2$ to give hexagonal-shaped crystallites; these are found similarly in hydrated limes or in hydroxide precipitated from solution by double decomposition and subsequently aged.

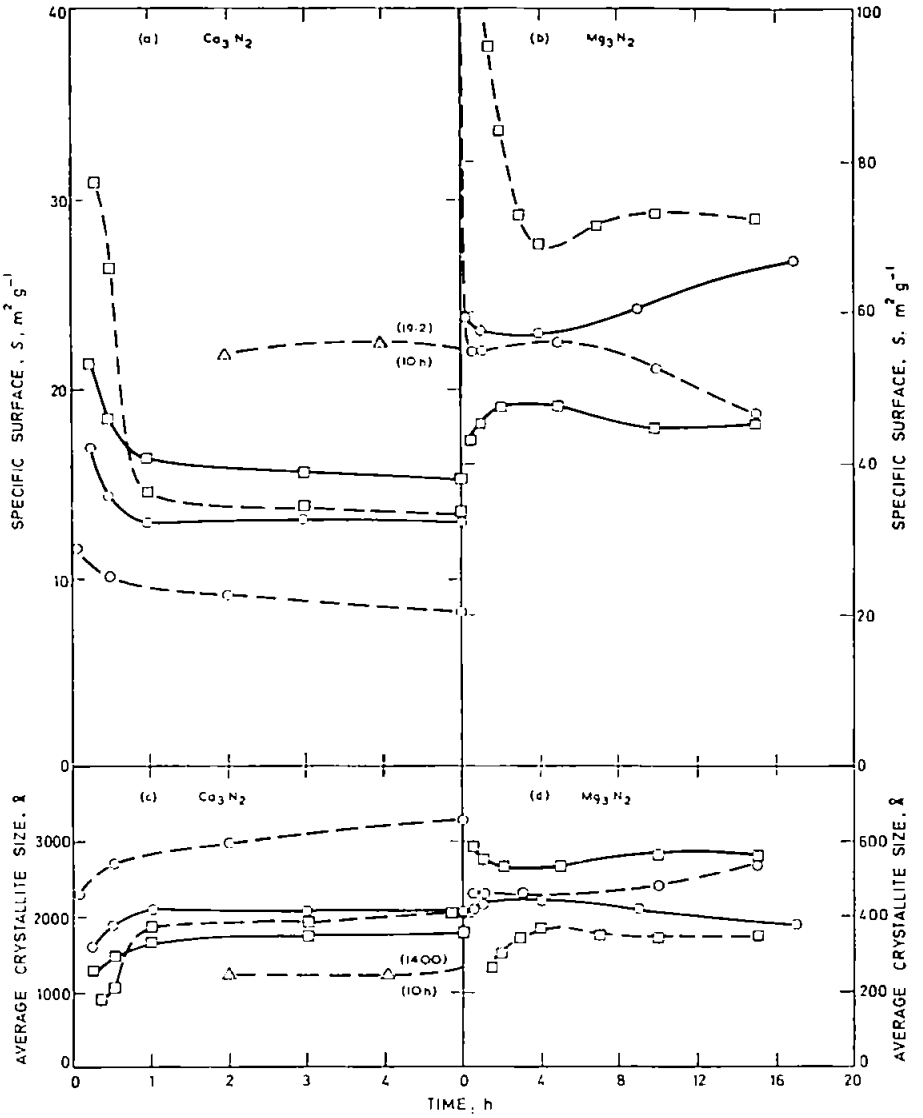

Fig. 2. *Hydrolysis of calcium and magnesium nitrides by liquid water at different temperatures*
□ 22° ○ 95° △ Ca at 22°
– – – – represent hydration and ageing of CaO and MgO

Comparison with 'wet' hydration of lime

Limes hydrating at rates comparable with the nitride hydrolysis initially give smaller $Ca(OH)_2$-crystallites at lower temperatures, but larger crystallites at higher temperatures, cf. pairs of fully- and broken-lined curves at 22° and 95° in Figs. 2 (a) and (c). Subsequently, the hydrated lime from the nitride ages less rapidly, so that ultimately the hydrated lime from the calcium oxide becomes the less active at 22°. The ammonium hydroxide formed in the nitride hydrolysis depresses the calcium hydroxide solubility by the common-ion effect, thus inhibiting ageing (by dissolution mechanisms as involved in Ostwald ripening).

Comparison with the action of water on calcium

The activity of the hydrated lime from the nitride is lower than that produced at the surface of calcium turnings at 22° (Figs. 2 (a) and (c)), which was expected to involve hydration of extremely small calcium oxide crystallites at a rate comparable with their formation;[12(c)] the hydroxide prepared from the metal had specific surfaces and average crystallite sizes similar to that separating as small primary crystallites by double decomposition from solution. No appreciable amounts of any intermediate calcium oxide were detected, even in the *X*-ray traces or photographs for the 'dry' hydrolysis of calcium nitride at 22°, so that direct replacement of nitride ions by hydroxyl ions is indicated.

'Dry' hydrolysis of calcium nitride

In the slower 'dry' hydrolysis of calcium nitride where there is less mobility than under 'wet' conditions, much smaller surface area increases are recorded. Hydrolysis in water vapour near saturation at 22° is complete within 5 h, giving hydroxide of specific surface, $S = 7{\cdot}2\ m^2\ g^{-1}$, average crystallite size, 3700 Å, while hydrolysis over 4 days by atmos-

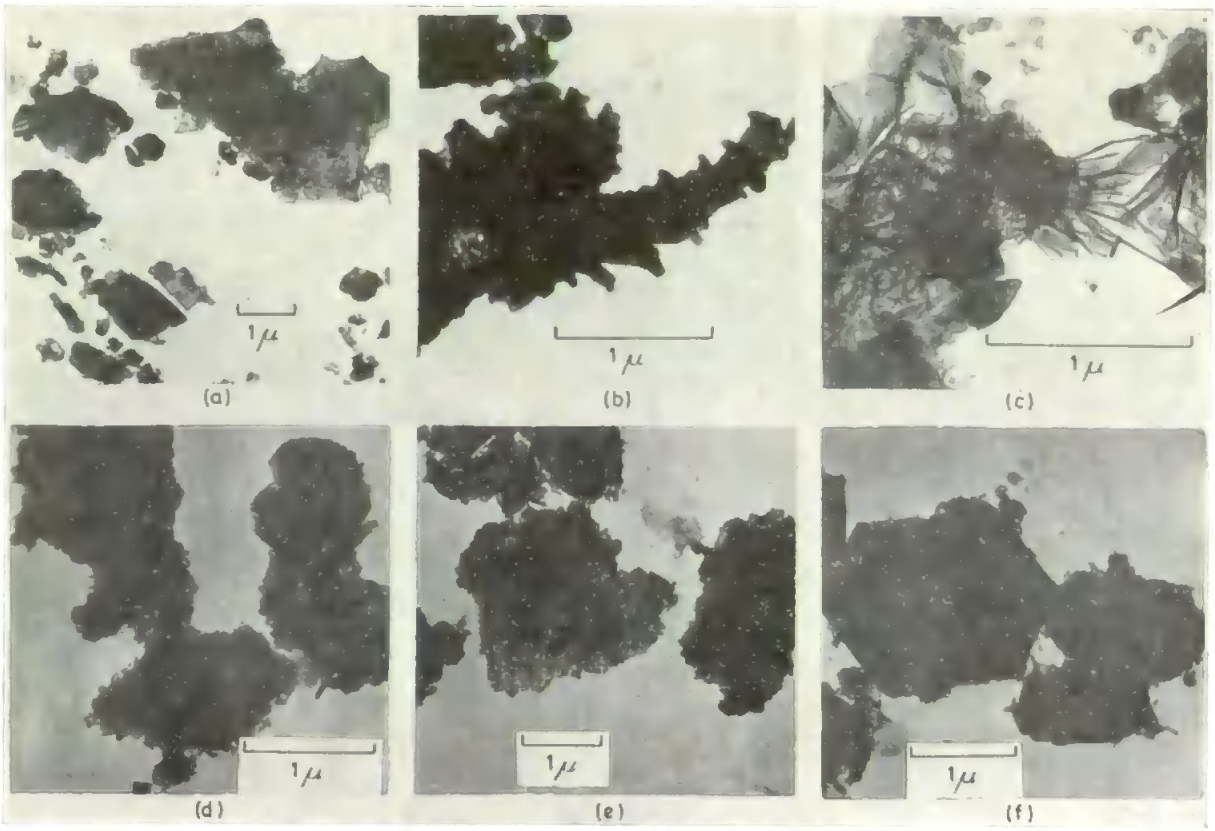

Fig. 3. *Electron-micrographs of the hydrolysis of calcium and magnesium nitrides*

(a) Ca_3N_2 partly 'dry' hydrolysed by water vapour at 22°
(b) Ca_3N_2 partly 'dry' hydrolysed by steam at 130°
(c) Mg_3N_2 partly 'dry' hydrolysed by water vapour at 22°
(d), (e) and (f) progressive 'wet' hydrolysis of Ca_3N_2 and subsequent ageing of the $Ca(OH)_2$ by liquid H_2O at 22°

pheric water vapour gives hydroxide where $S = 3{\cdot}7\ m^2\ g^{-1}$ (7200 Å). Nevertheless, the calcium hydroxide initially formed gives quite appreciable *X*-ray line-broadening, but close contact of the crystallites of the product enables it to age considerably before hydrolysis is completed. This resembles the extensive ageing of highly active calcium hydroxide from 'dry' hydrated lime.[12(a)] Splitting of the calcium nitride crystallites (and aggregates) in the earlier stages of hydrolysis by water vapour and steam is illustrated electron-micrographically in Figs. 3 (a) and (b). There is more extensive splitting in the hydrolysis of magnesium nitride crystallites by water vapour (Fig. 3 (c)).

'Wet' hydrolysis of magnesium nitride

The magnesium nitride samples hydrolyse quickly in liquid water, mainly within 5 min, as does calcium nitride. Hydrolysis involves similar changes in crystal structure (cubic Mn_2O_3, $D5_3$-type to hexagonal) and considerable volume increases (0·970 and 0·713 of the original volumes) as the magnesium and calcium nitrides convert to the less dense hydroxides of only about 0·05 μ and 0·2 μ average crystallite sizes (Fig. 2). The larger volume changes evidently cause more extensive splitting of the crystallites in the magnesium nitride hydrolyses, especially in the very rapid hydrolysis at 95°. Ageing (Ostwald ripening) is slower for the less soluble magnesium hydroxide compared with the calcium hydroxide. About 10^{16} crystallites of $Mg(OH)_2$ per g Mg_3N_2 are obtained compared with $2—6 \times 10^{14}$ $Ca(OH)_2$-crystallites per g Ca_3N_2.

Comparison with 'wet' hydration of magnesia

The most active magnesium oxide prepared previously[12(d)] does not hydrate as quickly as magnesium nitride at 22°. After hydration is complete in 4 h at 22°, the surface area and average crystallite size remain practically constant, ageing being limited by the low solubility of the hydroxide. Crystallite splitting during the nitride hydrolysis is not sufficiently extensive to give a hydroxide of the same activity. Closer similarity of surface area (and crystallite size) is given on 'wet' hydrating at 95°, where the reaction rates and ageing are faster. The hydroxide from the nitride subsequently shows some increase in surface before finally ageing, which may be ascribed to completion of recrystallisation of the newly formed magnesium hydroxide to its normal lattice structure.[12(a)]

'Dry' hydrolysis of magnesium nitride

The slower 'dry' hydrolysis of magnesium nitride produces much smaller surface area increases, as found for calcium nitride. Hydrolysis at 22° with water vapour near

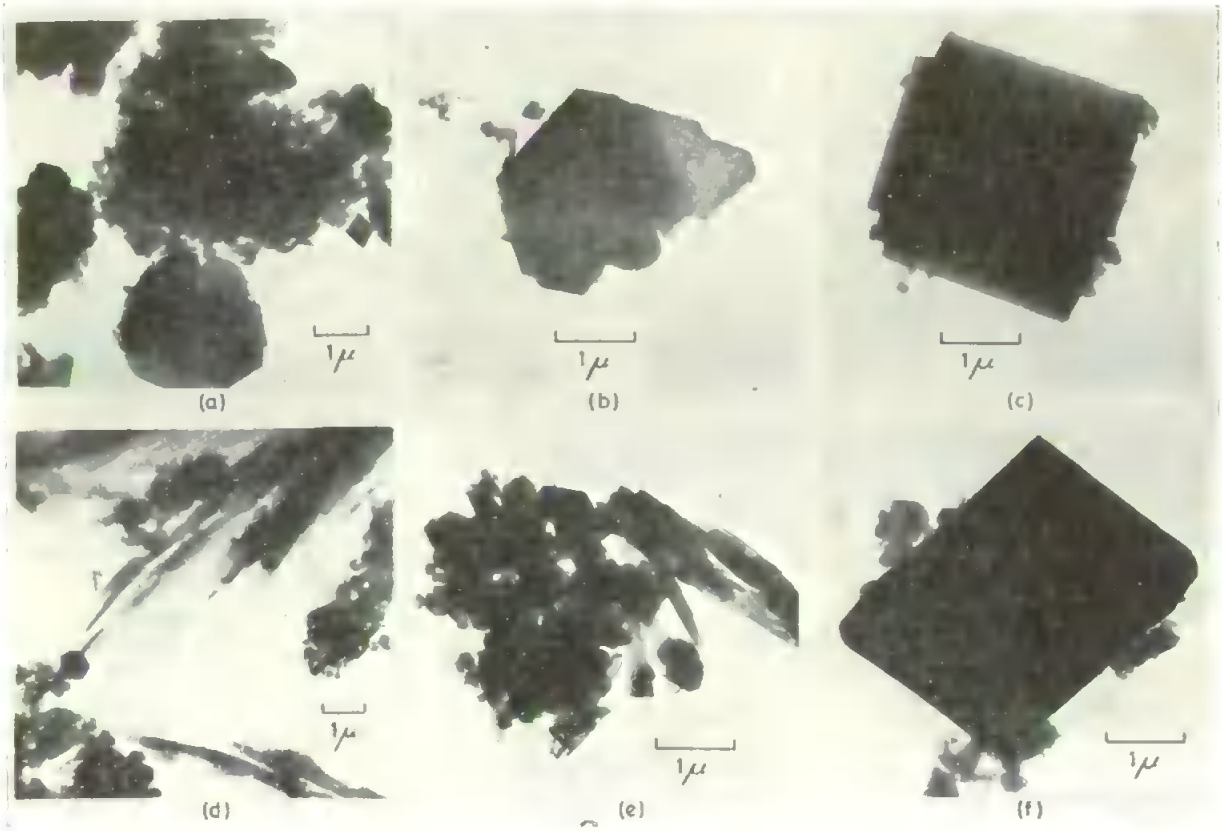

Fig. 4. *Electron-micrographs of hydrated lime carbonation in urea solution*

(7·4 g $Ca(OH)_2$ heated with 200 ml M-urea at 95°)
(a), (b) and (c) 23·4% carbonation after 5 h
(d) 68·5% carbonation after 13 h
(e) and (f) 91·5% carbonation after 20 h

s.v.p. (15 h) and atmospheric water vapour (4 days) gives surface areas of only 22·7 and 3·4 $m^2 g^{-1}$, and average crystallite sizes of 1100 and 7400 Å. Again, the hydroxide initially formed (cf. Fig. 5 (c)) gives quite appreciable *X*-ray line-broadening, but ages considerably before hydrolysis is completed.

Hydrolysis of calcium cyanamide

Calcium hydroxide is formed without any calcium carbonate when calcium cyanamide is 'dry' hydrolysed at 22° or 95° with water vapour, or 'wet' hydrolysed at 22° in liquid water or 1% or 50% water/acetone mixtures; hot water gives some calcitic calcium carbonate.

Addition of urea to give a molar concentration enables limewater (up to 0·02M) to be completely converted to calcitic calcium carbonate on boiling for ½ h. Mainly rhombic crystals of 5—30 μ size (mostly ca. 15 μ) are given after 5 h, with a few masses of small (1—2 μ) irregular crystals. Solid calcium hydroxide is slowly converted to calcitic calcium carbonate in a hot solution of M-urea. About ¼ (23·2%) was carbonated after 5 h with no remarkable overall change in surface area (Fig. 5), but the remaining hydroxide gave slight *X*-ray line-broadening which was absent from the newly formed carbonate. Electron micrographs, Fig. 4 (a), (b) and (c), show that even in the earlier stages, there are already a few well-formed rhombic crystals of calcitic calcium carbonate and some hexagonal (tending to rhombs) about 3—7 μ in size. Most crystals are not euhedral and are below 2 μ in size. The remaining calcium hydroxide is present as masses of small crystals which tend to aggregate and are mainly below 1 μ in size.

The overall surface area does not sharply diminish during the later stages of the carbonation (Figs. 4 (d), (e) and (f)), and the final product (20 h, 94% carbonate) still has a wide crystallite size range, with the larger crystals acquiring sharper edges (contrast (c) and (f)). Much of this carbonation would seem to occur by a 'through solution' mechanism, probably via calcium cyanate, with the unchanged hydroxide causing wide variations in the growth rates of the calcitic rhombs. The reaction permits a reduction of lime alkalinity in calcareous materials and afterwards partial separation of the carbonate.

Acknowledgments

The authors thank Dr. S. J. Gregg for his interest and encouragement in this work; Mrs. M. Sheppard for her assistance in the analytical work; the University of London Research Fund, the Imperial Chemical Industries Research

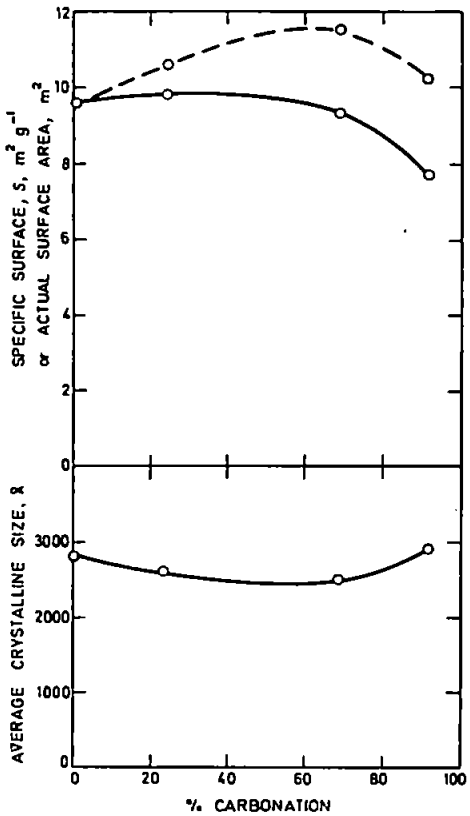

Fig. 5. *Surface area and average crystallite size of hydrated lime carbonated in* M*-urea solution at* 95°.

——— sp. surfaces, S, ($m^2\ g^{-1}$)

- - - - - - actual surface areas (m^2) of products from 1 g $Ca(OH)_2$

Fund and the Science Research Council for grants for apparatus and a S.R.C. Research Technicianship (for M.S.).

John Graymore Chemistry Laboratories,
College of Technology,
Plymouth.

Received 28 June, 1967;
amended manuscript 3 January, 1968

References

[1] von Antropoff, A., & Germann, E., *Z. phys. Chem.*, 1928, **137**, 209; Roberts, M. W., & Tompkins, F. C., *Proc. R. Soc.*, 1959, **251**, (A), 369
[2] Soliman, A., *J. appl. Chem., Lond.*, 1951, **1**, 98
[3] Shushunov, V. A., & Baryshnikov, Y. N., *Zh. fiz. Khim.*, 1953, **27**, 703
[4] Franck, H. H., Bredig, M. A., & Hoffman, Gl., *Naturwisssenschaften*, 1933, **21**, 330; Hartmann, H., & Frohlich, H. J., *Z. anorg. Chem.*, 1934, **218**, 190
[5] Langner, A. J., Br. Iron Steel Res. Assn. Conf. on Foundry Steel Making, Sept. 1949, p. 15
[6] Mitchell, D. W., *Ind. Engng Chem.*, 1949, **41**, 2027
[7] Gregg, S. J., & Bickley, R. I., *J. chem. Soc.*, 1966, (A), p. 1849
[8] Davis, L. W., U.S.P. 2,488, 054; 15/11/49
[9] Glasson, D. R., *J. appl. Chem., Lond.*, 1963, **13**, 111
[10] Franck, H. H., & Heimann, H., *Z. angew. Chem.*, 1931, **44**, 372
[11] Glasson, D. R., & Jayaweera, S. A. A., Part I (previous paper) and 'Surface phenomena of metals', *Soc. chem. Ind. Monogr. No.* 28, 1968, in press (London: The Society)
[12] Glasson, D. R., *J. appl. Chem., Lond.*, (a) 1958, **8**, 798; (b) *ibid.*, 1960, **10**, 38; (c) *ibid.*, 1961, **11**, 24; (d) *ibid.*, 1963, **13**, 119; (e) *ibid.*, 1964, **14**, 125; (f) *ibid.*, 1965, **15**, 378
[13] Brunauer, S., Emmett, P. H., & Teller, E., *J. Am. chem. Soc.*, 1938, **60**, 309
[14] Gregg, S. J., *J. chem. Soc.*, 1946, p. 561; Sartorius-Werke, 'Electrono-Vacuum Balances', 1963 (Göttingen: Sartorius-Werke, A.-G.); C. I. Electronics, 'Microforce Balances', 1966 (Wimborne, Dorset, England; C. I. Electronics, Ltd.)
[15] Gregg, S. J., & Winsor, G. W., *Analyst, Lond.*, 1945, **70**, 336
[16] Glasson, D. R., 'Analysis of calcareous materials', *Soc. chem. Ind. Monogr. No.* 18, 1964, p. 401 (London: The Society)

FORMATION AND REACTIVITY OF NITRIDES

III.* BORON, ALUMINIUM AND SILICON NITRIDES

By N. G. COLES, D. R. GLASSON and S. A. A. JAYAWEERA

The reactivities of boron, aluminium and silicon nitrides have been compared. Samples of these nitrides have been converted to oxides by being calcined in air. Changes in phase composition, surface area, crystallite and aggregate sizes have been correlated with oxidation time and temperature.

Crystallites of alumina, α-Al_2O_3, split off from the remaining aluminium nitride before they sinter and inhibit further oxidation. The diboron trioxide, B_2O_3, and silica, SiO_2 (α-cristobalite), immediately act as mineralisers for the remaining boron and silicon nitrides, and progressively retard the oxidations.

Introduction

The formation, hydrolysis and oxidation of the ionic calcium and magnesium nitrides, Ca_3N_2 and Mg_3N_2, have been described in Part II.[1] More recently, the authors have found that zinc and cadmium films do not nitride in nitrogen or ammonia at temperatures below their m.p., 420° and 320° respectively. The nitrides, Zn_3N_2 and Cd_3N_2, are formed only at appreciable rates at temperatures above 600°. They are hydrolysed rapidly to ammonia-soluble complexes, $M(NH_3)_x(OH)_2$, where $x \leqslant 4$ for M = Zn or Cd.[2] Comparison of the molecular susceptibilities of Mg, Zn and Cd nitrides shows that the polarising action of the metal ion decreases from Mg to Zn to Cd. Nitrides in Group III (B, Al, Ga) and Group IV (Si, Sn) show covalent character and are more resistant to hydrolysis and oxidation.[3] In the present paper, the reactivities of the covalent nitrides of B, Al and Si are compared with one another.

Thermodynamics of nitride formation and the relation between bonding and crystal structure have been discussed in Part I.[3] Boron nitride is more chemically reactive than nitrides of Al and Si.[4] Finely divided BN is hydrolysed slowly by hot water and dissolves completely in boiling 20% NaOH within 30 min. Dissolution is perceptible also at 20° in acids and alkalis.[5] Reactions between aluminium nitride or silicon nitride and hot water are inhibited by coatings of hydrated alumina or silica on the outside of the material. Hydrolysis is generally slow in mineral acids and alkalis,[6,7] but there is complete dissolution of aluminium nitride in 30% Na_2CO_3 at 80° and of silicon nitride in boiling HF.[8] All of these nitrides are oxidised in air at higher temperatures. Boron nitride powder oxidises appreciably above 800°,[3,9,10] the rate depending substantially on the preliminary calcination temperature.[11] Nitrides of aluminium and silicon oxidise at temperatures above 600° and 800° respectively, and again oxidation rates depend mainly on the intrinsic reactivity of the material and the available surface at which oxidation can occur.[3] Changes in phase composition, surface area and crystallite and aggregate sizes are now correlated with sintering and oxidation conditions for the above nitrides.

Experimental

Procedure

Separate portions of powdered nitrides of boron, aluminium and silicon (Alfa Inorganics Inc.) were calcined in air for various times at fixed temperatures. Oxidation rates were estimated from weight changes of the samples during calcination.[2] The cooled products were outgassed at 200° *in vacuo* before their specific surfaces were determined by B.E.T. procedure[12] from nitrogen isotherms recorded at −183° on an electrical sorption balance.[13,14] The deduced average crystallite sizes (equivalent spherical diameters) were compared with particle size ranges determined by optical or electron microscopy.

Phase composition identification

Samples were examined for phase composition and crystallinity using an *X*-ray powder camera and a Solus-Schall *X*-ray diffractometer with Geiger counter and Panax ratemeter. Certain samples were further examined by optical and electron microscopes (Philips EM-100).

Results

Fig. 1 (a), (b) and (e) shows the overall variations in specific surface, *S*, and average crystallite size during the conversion of aluminium nitride to alumina at 1000° in air. These are compared with oxidation rates Fig. 1 (d), changes in the number of crystallites Fig. 1 (c), and average crystallite sizes of the individual unchanged AlN and its oxidation product, α-Al_2O_3 Fig. 1 (f). Corresponding variations in the aggregate sizes are summarised in Table I.

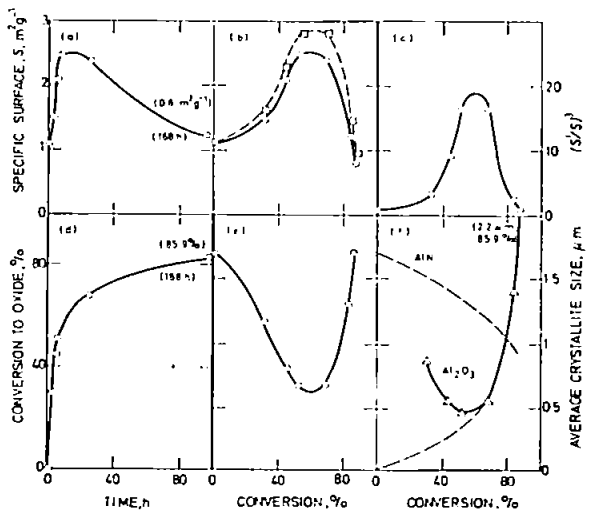

Fig. 1. *Calcination of aluminium nitride in air at* 1000°C

In (b), broken curve represents actual surface area (*S'*) for an initial one-gramme sample of aluminium nitride

*Part II: *J. appl. Chem., Lond.*, 1968, **18**, 77

TABLE I

Variations in aggregate sizes during the conversion of AlN to α-Al_2O_3 at 1000°C in air

Time, h	Conversion, %	Range of aggregate size, μm
0	0	1—2
5	51·3	3—5
24	67·7	3—6
96	82·7	3—7
168	85·9	4—8

The samples of boron nitride and silicon nitride had specific surfaces, S, = 11·5 and 1·7 $m^2 g^{-1}$; average crystallite sizes, 0·23 and 1·1 μm respectively. They oxidised in air at 800° and 1000—1200°; rates are shown in Fig. 2, where they are compared with those for aluminium nitride at 900—1100°. Electron micrographs of the nitrides and their oxidation products are presented in Figs 3 and 4.

Discussion

Oxidation of aluminium nitride

Aluminium nitride, AlN, is converted to α-Al_2O_3 at 1000° in air. *X*-ray powder photographs and diffractometer traces give no indications of any oxynitrides being formed at temperatures between 800—1100°. The oxidation at 1000°, Fig. 1 (d), accelerates somewhat during the conversion of the first 50% of the nitride, and then becomes progressively

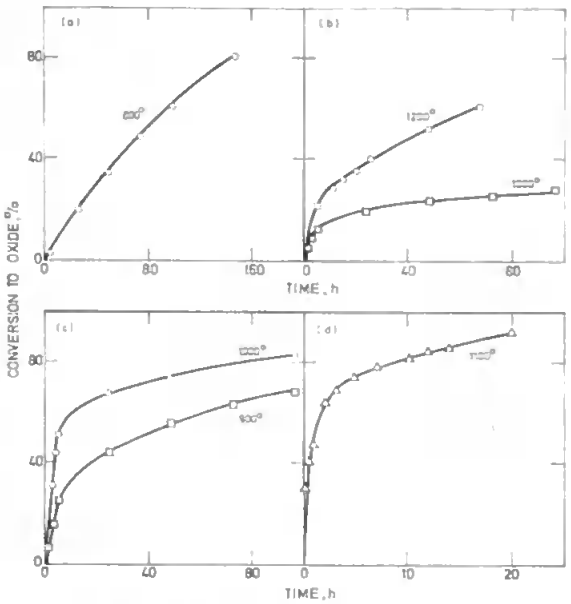

Fig. 2. *Calcination of boron, silicon and aluminium nitrides in air at different temperatures*
(a) ○——○ boron nitride at 800°C
(b) □——□ silicon nitride at 1000°C, ○——○ at 1200°C
(c) and (d) □——□ aluminium nitride at 900°C, ○——○ at 1000°C and △——△ at 1100°C
(Only a representative selection of points is shown for the sake of clarity)

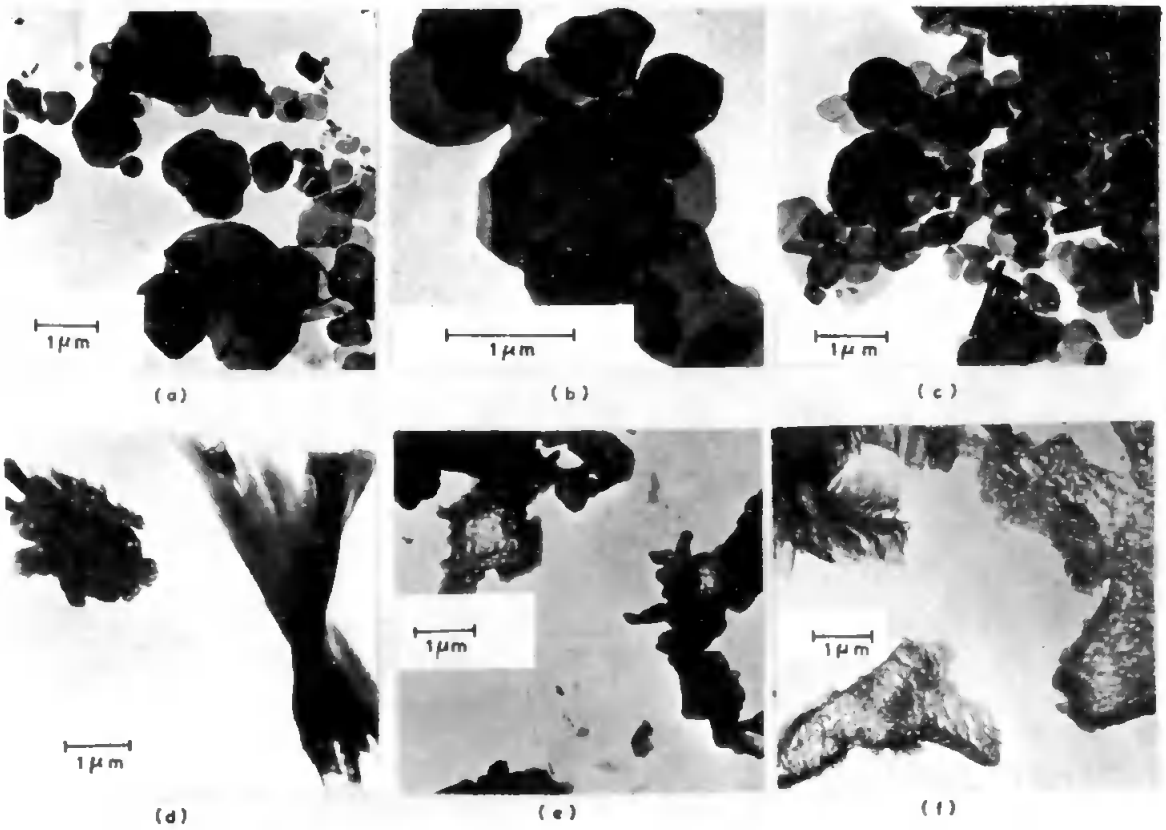

Fig. 3. *Electron micrographs of boron nitride calcined in air at* 800°C
(a) and (b) after 24 h, (c) 48 h, (d) 96 h, and (e) and (f) 144 h

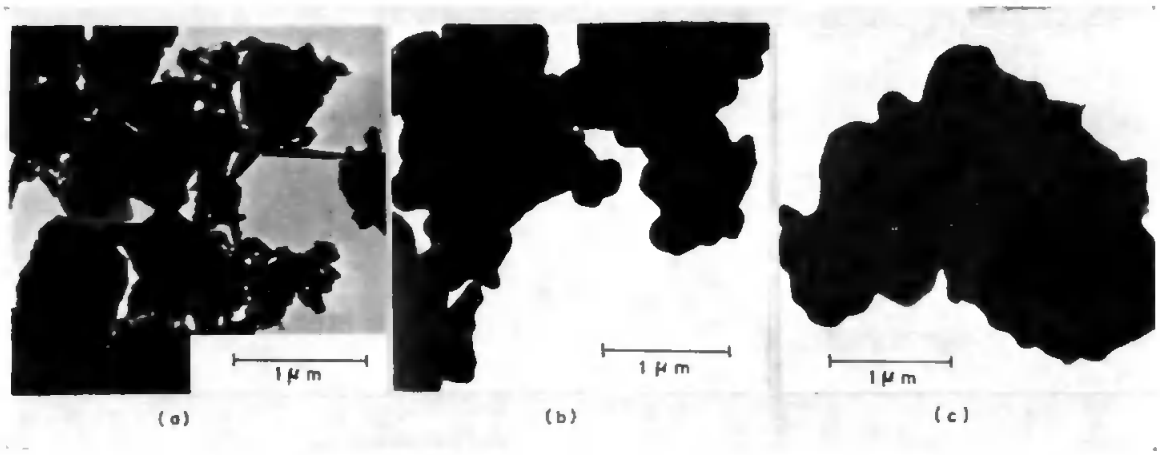

Fig. 4. *Electron micrographs of silicon nitride calcined in air at* 1200°C
(a) original sample, (b) after 5 h and (c) after 35 h

slower especially after about 80% conversion. These variations in rate are accompanied by corresponding increases and decreases in specific surface, S, in Fig. 1 (a) and (b), and in actual surface area, S', for an initial 1 g-sample of AlN illustrated by the broken-lined curve in Fig. 1 (b). Consequently, the average crystallite size of the material at first decreases and later increases, Fig. 1 (e).

Several factors may contribute to the detailed shape of the initial rate curve of an oxidation isotherm,[15] e.g. decreases in surface heterogeneity as the reaction proceeds, changes in specific surface or in local surface temperature due to heat of reaction, solubility effects, impurity concentrations, possible changes in oxide composition and electrical double layer effects. In accordance with the oxidation of coarser samples of aluminium nitride,[16] a specific amount of oxide must be formed (depending on the specific surface of the sample) before a coherent alumina layer can be produced. Meanwhile, the free nitride surfaces remain exposed to the gas phase, so that the kinetics approach linearity. When there is sufficient oxide of rational crystallite-size composition, it sinters to form surface films through which normal gaseous diffusion cannot easily occur. The reaction becomes controlled by solid-state diffusion, with the kinetics becoming parabolic and the surface area decreasing as observed after about 50% conversion in Fig. 1 (a), (b) and (d). Parabolic kinetics are characteristic also when the oxidation of aluminium produces better crystallised aluminas.[17]

The increases in S (and decreases in average crystallite size) during the acceleratory and approximately linear stages of the oxidation, Fig. 1 (a), (b) and (d), indicate that the alumina initially formed on the surface of the nitride splits off to give smaller crystallites. Any additional spalling at the nitride–oxide interface when the samples were cooled for surface area determination was negligible by comparison, since the reheated samples proceeded to give oxidation rates similar to those of samples which had been continuously heated. Thus, the extent of crystallite splitting depends generally on differences in molecular volume and type of crystal lattice compared with the original nitride (cf. Pilling–Bedworth rule for oxidised metals[18]), and also on the rate of oxide sintering as discussed in Part I.[3] Although the conversion of AlN to α-Al_2O_3 involves practically no fractional volume change,[16] nevertheless the crystal lattice change is apparently sufficient to cause a limited amount of crystallite splitting. In this instance, $(S'/S)^3$ directly represents the increases in the number of crystallites as oxidation proceeds, Fig. 1 (c), no allowance being required for molecular volume changes.[19] The maximum increases of less than twenty-fold are comparable with those found for the oxidation of TiN[2] described more fully in the next paper. They are much smaller than the increases during the oxidation and hydrolysis of Ca_3N_2, viz. 5×10^{10} and 10^{12} respectively.[1,2]

The m.p. of AlN (> 2400°) and Al_2O_3 (2050°) give Tammann temperatures (half m.p. in °K) of > 1336°K, and 1160°K, indicating that sintering of alumina should be much more extensive than that of aluminium nitride at 1000°. In the latter stages of the oxidation, the alumina appears to act as a mineraliser for the remaining aluminium nitride particles, inhibiting their further oxidation, cf. Fig. 1 (d), and moulding together the material. Changes in the average crystallite size of the aluminium nitride (assuming no appreciable sintering) and the α-Al_2O_3 are deduced from the surface-area data and shown in Fig. 1 (f). These confirm the ultimate sintering of the alumina, and the larger crystallite sizes given during the first half of the oxidation (above the broken-line) are caused probably by some of the newly-formed alumina not being detached from the nitride surface. Accordingly, the aggregate sizes of the materials (Table 1) indicate that the original nitride consists mainly of single crystallites. The alumina produced tends to promote formation of aggregates, mainly of 3—8 μm sizes, in which the individual crystallites appear to be over 0·5 μm in the later stages of the oxidation as also indicated in Fig. 1 (f). Similarly, 86% oxidation of aluminium nitride in 14 h at 1100°, Fig. 2 (d), gives alumina crystallites of 0·5—1 μm size, sintering at the higher temperature being restricted by the shorter oxidation time.

Oxidation of nitrides of boron and silicon

The boron nitride and silicon nitride oxidise at 800° and 1200° respectively, giving diboron trioxide, B_2O_3, and silicon dioxide, SiO_2 (α-cristobalite), even in the early stages. In contrast to the behaviour of aluminium nitride on oxidation, the specific surfaces of the materials initially decrease rapidly as the boric oxide (m.p. ~ 450°) and the silica (m.p. 1710°) act as mineralisers. Although the silica does not melt, it is well

above its Tammann temperature (720°) and the specific surface, *S*, falls from 1·7 to below 0·3 m^2g^{-1} when one third of the silicon nitride has been oxidised. The products tend to bond together and shrink, cf. bonding and hot pressing of boron nitride with silica glass.[20] Consequently, the rates decrease considerably for both nitrides as their oxidations become increasingly controlled by liquid- or solid-state diffusion, especially the latter, cf. Fig. 2 (a) and (b).

The original boron nitride has a flaky texture with rod-shaped and hexagonal plate-like particles. About 20% of the BN is converted to B_2O_3 after 24 h calcination at 800° in air, Fig. 2 (a), while the hexagonal plates become rounded and tend to form aggregates as in the electron micrographs in Fig. 3 (a) and (b). Further calcination continues this aggregation, cf. Fig. 3 (c) at 48 h, and after 96 h the rod-shaped particles become distorted by the newly-formed B_2O_3, cf. Fig. 3 (d). When over 80% of the BN has been oxidised after 144 h, there is sufficient B_2O_3 to crystallise out and change the appearance of the aggregates as in Fig. 3 (e) and (f). The silicon nitride particles, Fig. 4 (a), also form aggregates with rounded edges when only about 20% of the nitride has been converted to silica after 5 h calcination at 1200° in air as in Fig. 4(b). Further calcination (35 h) produces larger aggregates as in Fig. 4 (c).

Acknowledgment

The authors thank Mrs. M. A. Sheppard for her assistance in the analytical work; the University of London, Imperial Chemical Industries Ltd., and the Science Research Council for grants for apparatus and a S.R.C. Research Technicianship (for M.A.S.); the College Governors for a Research Assistantship (for N.G.C.).

John Graymore Chemistry Laboratories,
College of Technology,
Plymouth

cf. also N. G. Coles, Ph.D. thesis (C.N.A.A.).

References

[1] Glasson, D. R., & Jayaweera, S. A. A., *J. appl. Chem., Lond.*, 1968, **18**, 77
[2] Glasson, D. R., & Jayaweera, S. A. A., 'Surface phenomena of metals', *Soc. chem. Ind. Monogr.*, 1968, No. 28, p. 353 (London: The Society)
[3] Glasson, D. R., & Jayaweera, S. A. A., *J. appl. Chem., Lond.*, 1968, **18**, 65
[4] Samsonov, G. V., 'High temperature materials', 1964, Handbook 2, pp. 235, 266 (New York: Plenum)
[5] Taylor, K., *Ind. Engng Chem.*, 1955, **47**, 2506
[6] Renner, T., *Z. anorg. Chem.*, 1959, **257**, 127
[7] Collins, J., & Gerby, R., *J. Metals, N.Y.*, 1955, 7, 612
[8] Billey, M., *Annls Chim.*, 1959, **4**, 795
[9] Zagyanskiy, I. L., & Samsonov, G. V., *Zh. prikl. Khim.*, 1952, **25**, 557
[10] Samsonov, G. V., Markovskiy, L. Ya., Zhigach, A. F., & Valyashko, G. M., 'Bor, ego soedinenya i splavy', 1960 (Kiev: Akad. Nauk Ukr. SSR.); USAEC translation, 1962, No. 5032, (1), 209
[11] Podszus, E., *Z. anorg. Chem.*, 1917, **30**, 156
[12] Brunauer, S., Emmett, P. H., & Teller, E., *J. Am. chem. Soc.*, 1938, **60**, 309
[13] Gregg, S. J., *J. chem. Soc.*, 1946, p. 561
[14] Sartorius-Werke, 'Electrono-vacuum balances', 1963 (Göttingen: Sartorius-Werke, A.-G.)
[15] Gulbransen, E. A., & Andrew K. F., *J. electrochem. Soc.*, 1951, **98**, 241
[16] Cooper, C. F., George, C. M., & Hopkins, S. W. J., 'Special ceramics', *Proc. Symp. Br. ceram. Res. Ass.*, 1962, p. 49 (London: Academic Press)
[17] Sleppy, W. C., *J. electrochem. Soc.*, 1961, **108**, 1097
[18] Pilling, N. B., & Bedworth, R. E., *J. Inst. Metals*, 1923, **29**, 529
[19] Glasson, D. R., *J. appl. Chem., Lond.*, 1958, **8**, 798
[20] Carborundum Co., B.P. 1,052,295

FORMATION AND REACTIVITY OF NITRIDES

IV.* TITANIUM AND ZIRCONIUM NITRIDES

By D. R. GLASSON and S. A. A. JAYAWEERA

The reactivities of the interstitial titanium and zirconium nitrides have been compared. Samples of these nitrides have been converted to oxides by being calcined in air. Changes in phase composition, surface area, crystallite and aggregate sizes have been correlated with oxidation time and temperature.

Crystallites of rutile, TiO_2, split off from the remaining titanium nitride before they sinter, and inhibit further oxidation. Zirconium nitride oxidation is complicated by formation of tetragonal ZrO_2 at higher temperatures, particularly over 1200°, and monoclinic ZrO_2 at lower temperatures. The nitride initially forms the so-called 'amorphous' cubic ZrO_2, notably between 400—600°, which may be stabilised somewhat by the remaining cubic ZrN. Subsequently, there is a further fractional volume increase while formation of monoclinic ZrO_2 is being completed.

Introduction

The formation, hydrolysis and oxidation of the more ionic and covalent nitrides have been described in earlier papers.[1-4] This research is extended now to a further study of titanium and zirconium nitrides which are regarded generally as interstitial nitrides.[1] The thermodynamics of their formation and the relation between bonding and crystal structure have been discussed in Part I.[1] Their preparation has been described previously by the authors.[4] The titanium nitride was found to be stable up to 1000°, but the zirconium nitride showed a range of homogeneity from nearly stoicheiometric ZrN (13·3 wt.-%, 50 atom-% N) at 600° to lower nitrogen contents at temperatures up to 1800°. Thus, a typical sample of nitrided zirconium contained only 10·32 wt.-%, 42·8 atom-% N.

Most interstitial nitrides are hydrolysed less readily than the ionic and covalent nitrides, but are converted to oxides on calcining in air.[1] Hence, although the corrosion resistance of layers of titanium or zirconium nitrides on the metal surfaces is excellent, the scaling resistance in air (or oxygen) is not very good. Preliminary investigations[4] have indicated that the conversion of nitride to oxide involves splitting of the newly formed oxide layers. Changes in molecular volume and type of crystal lattice are important (cf. Pilling–Bedworth rule for oxidised metals[5]), and also the rate of oxide sintering. These variations are examined now more closely at different temperatures and calcination times.

Experimental

Procedure

Separate portions of finely divided titanium and zirconium nitrides were calcined in air for various times at each of a series of fixed temperatures. Oxidation rates were estimated from weight changes in the samples during calcination.[4] The cooled products were outgassed at 200° *in vacuo* before their specific surfaces were determined by B.E.T. procedure[6] from nitrogen isotherms recorded at −183° on an electrical sorption balance.[7,8] The deduced average crystallite sizes (equivalent spherical diameters) were compared with particle size ranges determined by optical or electron microscopy.

Phase composition identification

Samples were examined for phase composition and crystallinity using an *X*-ray powder camera and a Solus-Schall *X*-ray diffractometer with Geiger counter and Panax rate-meter. Certain samples were examined further by optical- and electron-microscopes (Philips EM-100).

Results

Fig. 1 (a), (b) and (d) shows the overall variations in specific surface, *S*, and average crystallite size during the conversion of titanium nitride to titanium dioxide (rutile) at 600° in air. These are compared with oxidation rates in Fig. 1 (c). Electron-micrographs of the titanium and zirconium nitride samples and their oxidation products are presented in Fig. 2.

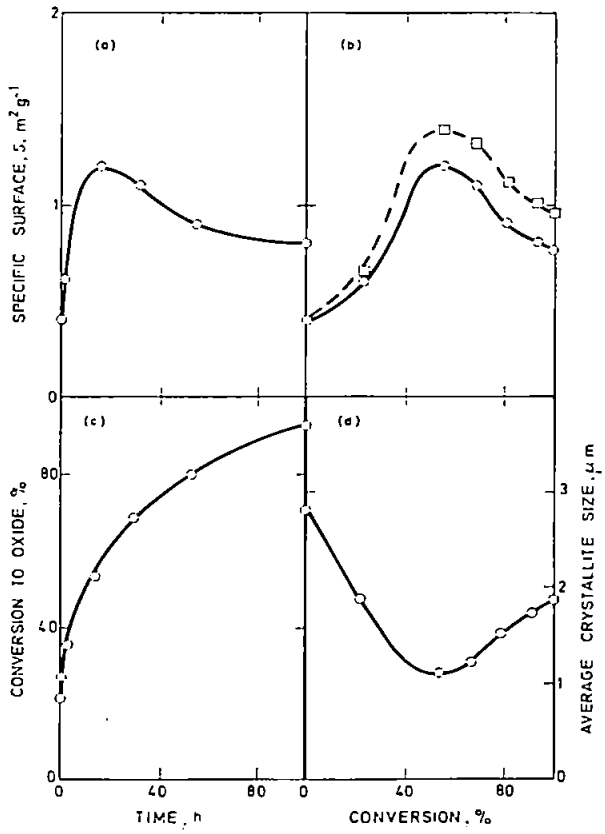

Fig. 1. *Calcination of titanium nitride in air at* 600°C

In (b), broken curve represents actual surface area (S′), for an initial one-gramme sample of titanium nitride

*Part III: preceding paper

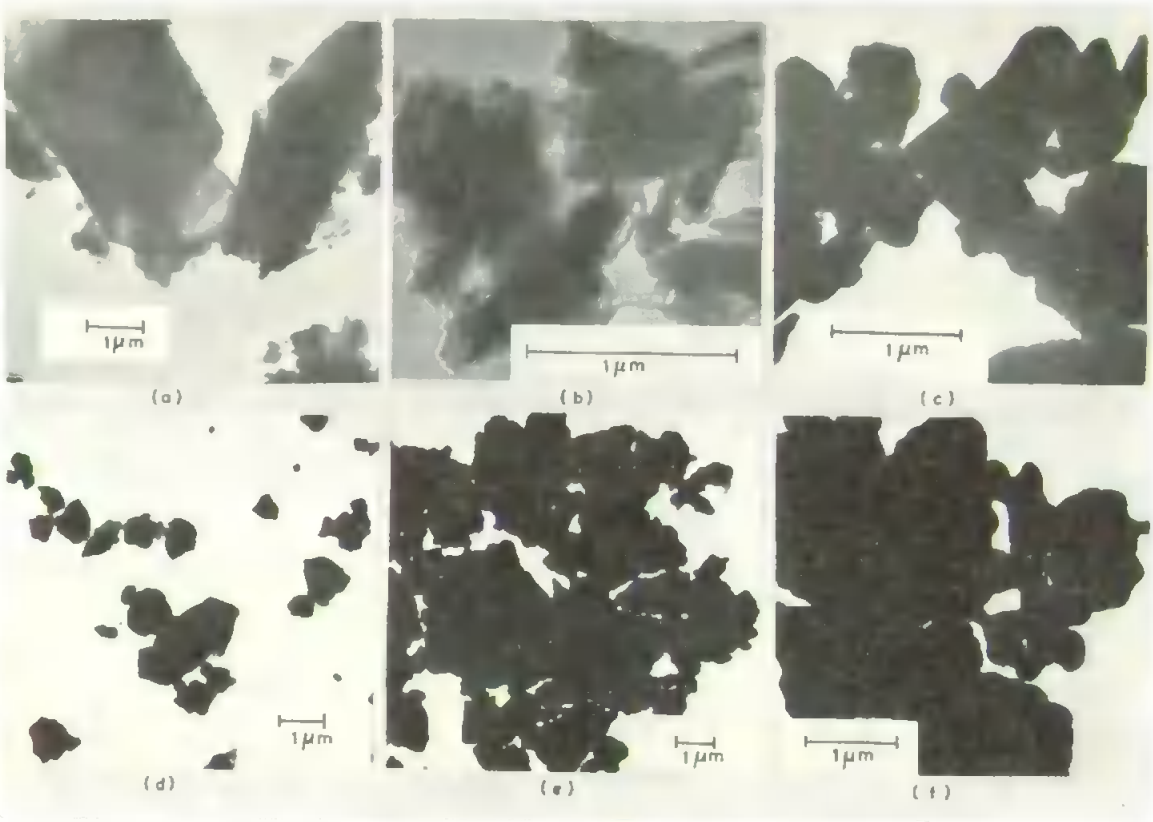

Fig. 2. *Electron micrographs of titanium and zirconium nitrides calcined in air at 600°C and 1000°C respectively*

Titanium nitride: (a) original sample; (b) after 15 h calcination; (c) after 200 h calcination

Zirconium nitride: (d) original sample; (e) after 2 h calcination; (f) after 20 h calcination

Discussion

Oxidation of titanium nitride

Titanium nitride, TiN, is converted to tetragonal TiO_2 (rutile) at 600° in air. *X*-ray powder photographs and diffractometer traces give no indications of any oxynitrides being formed at temperatures between 400—1000°. In the oxidation at 600°, Fig. 1 (c), the initial weight increase is comparatively rapid, accelerating during the first half hour before becoming approximately linear and then parabolic,[9] as found for aluminium nitride.[3] The titanium dioxide *X*-ray patterns are given only after about a quarter of the total weight increases are recorded at 600°, but rutile patterns are detected after only 7% oxidation at 500°. The longer calcination time (5 h) at the lower temperature evidently permits crystallisation of the rutile, while at higher temperatures, TiN has a limited solubility in TiO as discussed in Part I.[1] The lattice constant of TiN can remain unchanged from TiN to $TiN_{0\cdot6}O_{0\cdot4}$ when the binary compounds are sintered at 1700°, and this may retard crystallisation of rutile at higher temperatures.

The variations in rate of titanium nitride oxidation at 600° are accompanied by corresponding increases and decreases in specific surface, *S*, in Fig. 1 (a) and (b) and in actual surface area, *S'*, for an initial 1 g-sample of titanium nitride, illustrated by the broken-lined curve in Fig. 1 (b). Consequently, the average crystallite size of the material at first decreases and later increases, Fig. 1 (d). Factors contributing to the detailed shape of the initial oxidation rate curves have been summarised in the previous paper[3] and apply similarly to aluminium and titanium nitrides. When there is sufficient titanium dioxide of rational crystallite size composition, it sinters to form surface films through which normal gaseous diffusion cannot easily occur. The reaction becomes controlled by solid-state diffusion, with the kinetics becoming parabolic and the surface area decreasing, as observed after about 50% conversion in Fig. 1 (a), (b) and (c).

When the titania crystallises out from the nitride matrix, during the acceleratory and approximately linear stages of the oxidation, it evidently splits off to give smaller crystallites as *S* and *S'* increase more rapidly in Fig. 1 (b). Any additional spalling at the nitride-oxide interface when the samples were cooled for surface area determination was negligible by comparison, since the reheated samples proceeded to give oxidation rates similar to those of samples which had been continuously heated. Thus, the crystallite splitting results mainly from changes in type of crystal structure (cubic F-type to tetragonal) and a volume increase (0·630 of the original volume) as the nitride is converted to the less dense oxide.

The maximum increase in the number of crystallites, calculated from $(S'/S)^3$ and allowing for molecular volume changes,[10] is about twenty-fold, similar to that found for the aluminium nitride oxidation at 1000°. The splitting apparently facilitates release of nitrogen, since the material ultimately (after 200 h) reaches constant weight corresponding to the calculated weight-loss for complete conversion of nitride to TiO_2.

The m.p. of TiN (2930°) and TiO_2 (1920°) give Tammann temperatures (half m.p. in °K) of 1600° K and 1096 °K, indicating very little crystal lattice diffusion at 600°, but limited sintering promoted by surface diffusion should be possible for TiO_2 but not TiN at this temperature, cf. one-third m.p. = 460°C and 800°C respectively. This is confirmed by decreases in surface area and increases in average crystallite size during the later stages of the titanium nitride oxidation (Fig. 1 (a), (b) and (d)), i.e., as TiN is consumed by oxidation, its crystallite size must decrease while that of the oxide increases. Longer calcination (up to 200 h) causes very little additional sintering. In contrast, there is extensive sintering during the oxidation of titanium nitride at 1000° in air, giving a solid mass of TiO_2, mainly formed within 2 h.[4] It is even greater than sintering of TiO_2, promoted by crystal lattice diffusion at temperatures above 1000°, which has been reported recently by one of the authors for samples from other sources.[11] The titania from the TiN must be produced in a more compact form, possibly also giving a more suitable grain size composition for sintering. Electron micrographs also indicate fragmentation and subsequent sintering of material during the oxidation of titanium nitride, cf. Fig. 2 (a), (b) and (c).

Oxidation of zirconium nitride

Zirconium nitride, Fig. 2 (d), is converted to zirconium dioxide, Fig. 2 (e), which subsequently sinters at 1000° in air, Fig. 2 (f); at this temperature, any initial crystallite splitting is hidden by the more extensive oxide sintering which gives denser and more rounded aggregates. The oxidation of this nitride is complicated by the formation of tetragonal ZrO_2[12] at higher temperatures, particularly over 1200°, and monoclinic ZrO_2[12,13] at lower temperatures.

When samples of zirconium nitride containing some free zirconium metal are calcined in air, the metal oxidises rapidly at temperatures of 350—400°. The nitride requires correspondingly higher oxidising temperatures, and initially forms the so-called 'amorphous' cubic ZrO_2,[14] notably between 400° and 600° (cf. cubic ZrO_2 from Zr alkoxides decomposed in nitrogen at 300—400°,[14] which may be stabilised somewhat by the remaining cubic ZrN in the present work). *X*-ray diffractometer traces show an additional reflection at 2·94—5 Å, some reinforcement of the 2·54 Å spacing and displacement and broadening of the 1·81 and 1·54 Å spacings of monoclinic ZrO_2 towards the shorter distances of 1·80 and 1·53 Å of the cubic form. At higher temperatures, 700—1000°, the additional reflection disappears and the main monoclinic ZrO_2 reflections at 3·16 and 2·84 Å develop more rapidly. The conversion of the cubic F-ZrN (a = 4·56 Å) to cubic F-ZrO_2 (a = 5·09 Å) involves a fractional volume increase of 0·367 (of the initial volume) which further increases to 0·521 when formation of monoclinic ZrO_2 is completed.

Acknowledgments

The authors thank Mr. I. Ali and Mrs. M. A. Sheppard for their assistance in the analytical work; the University of London, Imperial Chemical Industries Ltd., and the Science Council for grants for apparatus and a S.R.C. Research Technicianship (for M.A.S.); the College Governors for a Research Assistantship (for I.A.).

John Graymore Chemistry Laboratories,
College of Technology,
Plymouth

cf. also I. Ali,
Ph.D. thesis (C.N.A.A.).

References

[1] Glasson, D. R., & Jayaweera, S. A. A., *J. appl. Chem., Lond.*, 1968, **18**, 65
[2] Glasson, D. R., & Jayaweera, S. A. A., *J. appl. Chem. Lond.*, 1968, **18**, 77
[3] Coles, N. G., Glasson, D. R., & Jayaweera, S. A. A., *J. appl. Chem., Lond.*, 1969, **19**, 178
[4] Glasson, D. R., & Jayaweera, S. A. A., 'Surface phenomena of metals', *Soc. chem. Ind. Monogr.*, 1968, No. 28, p. 353 (London: The Society)
[5] Pilling, N. B., & Bedworth, R. E., *J. Inst. Metals*, 1923, **29**, 529
[6] Brunauer, S., Emmett, P. H., & Teller, E., *J. Am. chem. Soc.*, 1938, **60**, 309
[7] Gregg, S. J., *J. chem. Soc.*, 1946, p. 561
[8] Sartorius-Werke, 'Electrono-vacuum balances', 1963 (Göttingen: Sartorius-Werke, A.-G.)
[9] Münster, A., *Z. elektrochem.*, **63**, 807
[10] Glasson, D. R., *J. appl. Chem., Lond.*, 1958, **8**, 798
[11] Glasson, D. R., Johnson, J. S., & Sheppard, M. A., *J. appl. Chem., Lond.*, 1969, **19**, 46
[12] Lynch, C. T., Vahldiek, F. W., & Robinson, L. B., *J. Am. ceram. Soc.*, 1961, **44**, 147
[13] McCullough, J. D., & Trueblood, K. N., *Acta crystallogr.*, 1959, **12**, 507
[14] Mazdiyasni, K. S., & Lynch, C. T., 'Special ceramics', *Proc. symp. Br. ceram. Res. Ass.*, 1964, p. 115 (London: Academic Press)

ERRATUM

In the paper by Marson, *J. appl. Chem.*, 1969, **19**, page 97, left hand column, line 12:

for '$S(\mu g/ml \text{ of } Cu^+) = 6{\cdot}357 \times 10^4 \log_{10} (4{\cdot}03 - pH)$'
read '$S(\mu g/ml \text{ of } Cu^+) = 6{\cdot}357 \times 10^{8{\cdot}03 - pH}$'

With the Compliments of the Author